VOLUME 2 (1956/57) No. 4

NUCLEAR PHYSICS

MONTHLY JOURNAL DEVOTED TO THE EXPERIMENTAL AND THEORETICAL STUDY OF ATOMIC NUCLEI, NUCLEAR FIELDS AND THE FUNDAMENTAL ASPECTS OF COSMIC RADIATION

EDITOR: L. ROSENFELD - MANCHESTER

D. A. TIDMAN, A quantum theory of refractive index, Čerenkov radiation and the energy loss of a fast charged particle 289

S. T. MA, Contact and core interactions according to Dirac's relativistic theory of the electron 347

V. Z. BLANK and D. V. SHIRKOV, Improvement of quantum electrodynamics perturbation theory with help of the renormalization group 356

J. ERÖ and L. KESZTHELYI, Cross section of the $I^{127}(\gamma, n)I^{126}$ reaction 371

R. K. SHELINE, The possible existence of rotational levels in Al^{28} 382

V. M. KELMAN, V. A. ROMANOV, R. YA. METSKHVARISHVILI and V. A. KOLYUNOV, Investigation of internal conversion lines in the β-spectrum of a mixture of Eu^{152} and Eu^{154} isotopes 395

B. S. DZHELEPOV, N. N. ZHUKOVSKY, V. G. NEDOVESOV, I. F. UCHEVATKIN and V. G. CHUMIN, The gamma spectrum of Sb^{124} 408

(continued on p. 3 of cover)

NORTH - HOLLAND PUBLISHING COMPANY - AMSTERDAM

December 1956

EDITORIAL BOARD

AUSTRIA:	B. Karlik (Vienna), H. Thirring (Vienna)
BELGIUM:	M. de Hemptinne (Louvain), J. Verhaeghe (Ghent)
CANADA:	G. Volkoff (Vancouver)
DENMARK:	C. Møller (Copenhagen), S. Rozental (Copenhagen)
EGYPT & ARAB COUNTRIES:	F. El Bedewi (Alexandria), M. G. Nooh (Cairo)
FINLAND:	L. Simons (Helsinki)
FRANCE:	A. Berthelot (Saclay), S. Gorodetzky (Strasbourg), F. Joliot (Paris)
GERMANY (FED. REP.):	W. Gentner (Freiburg i. B.), J. H. D. Jensen (Heidelberg)
GERMANY (DEM. REP.):	G. Hertz (Leipzig)
GREAT BRITAIN:	S. Devons (Manchester)
HUNGARY:	L. Janossy (Budapest)
INDIA:	H. Bhabha (Bombay), B. Peters (Bombay), R. Ramanna (Trombay)
IRISH REPUBLIC:	J. McConnell (Maynooth)
ISRAEL:	G. Racah (Jerusalem)
ITALY:	E. Amaldi (Rome)
JAPAN:	S. Kikuchi (Tokyo), S. Tomonaga (Tokyo)
NETHERLANDS:	H. Brinkman (Groningen), S. R. de Groot (Leiden)
NORWAY:	E. Hylleraas (Oslo), A. Lundby (Oslo), H. Wergeland (Trondheim)
POLAND:	L. Infeld (Warsaw)
PORTUGAL:	J. M. Araújo (Porto), J. R. de Almeida Santos (Coimbra)
SOUTH AMERICA:	G. Beck (Saõ Paulo), J. Leite Lopes (Rio de Janeiro)
SPAIN:	J. M. Otero (Madrid), C. Sanchez del Rio (Madrid)
SWEDEN:	O. Klein (Stockholm), K. Siegbahn (Uppsala), I. Waller (Uppsala)
SWITZERLAND:	P. Huber (Basel), P. Scherrer (Zürich)
U.S.S.R.:	M. A. Markov (Moscow), I. S. Shapiro (Moscow), D. V. Skobeltzyn (Moscow)
YUGOSLAVIA:	I. Supek (Zagreb)
U.S.A. & MEXICO:	V. Weisskopf (Cambridge, Mass.)
AUSTRALIA & NEW ZEALAND:	H. Messel (Sydney), M. L. Oliphant (Canberra)

CONTRIBUTIONS may be sent to the Editor, Professor L. Rosenfeld, Dept. of Theoretical Physics, The University, Manchester, either directly, or preferably through the intermediary of one of the members of the Editorial Board of the country or region in which the author is working. They may be written in English, French or German.

BOOKS FOR REVIEW should be sent to Professor Rosenfeld.

NUCLEAR PHYSICS is published in monthly issues. The subscription price of a volume of 700 pages is fl 57.00; 114s; $ 15.00. Postfree.

SUBSCRIPTIONS should be sent to the publishers, NORTH-HOLLAND PUBLISHING COMPANY, P.O.Box 103, Amsterdam or to any subscription-agent. Subscriptions for U.S.A. are to be sent exclusively to INTERSCIENCE PUBLISHERS, INC., 250 Fifth Avenue, New York 1, N.Y.

Printed in the Netherlands.

Nuclear Physics **2** (1956/57) 289—346; *North-Holland Publishing Co., Amsterdam*

A QUANTUM THEORY OF REFRACTIVE INDEX, ČERENKOV RADIATION AND THE ENERGY LOSS OF A FAST CHARGED PARTICLE

D. A. TIDMAN

The F.B.S. Falkiner Nuclear Research and Adolph Basser Computing Laboratories, School of Physics †, *The University of Sydney, Sydney*

Received 4 May 1956

Abstract: A quantum theory of the three related subjects of refractive index, Čerenkov radiation, and the excitation and ionization of atoms in a polarisable medium is developed.

The classical theory of the electromagnetic field in a medium of extended dipoles is first written in hamiltonian form. This makes obvious a canonical transformation related to refractive index which enables one to express the total field in the medium as a superposition of oscillators. A similar transformation is made on the quantised radiation field variables, which takes account of the modified time dependence of the field due to its interaction with the medium.

The processes of Čerenkov radiation and the ionization and excitation of atoms in a polarisable medium are then treated. The partition of the total energy loss between these different primary processes is obtained directly. This is done by making a perturbation expansion on the basis of physical-photon states for processes caused by the passage of a fast charged particle through the medium. For the case in which the reaction of the medium on the particle is neglected we obtain formulae which agree with those obtained previously by other authors i.e., in the first approximation the quantum theory frequently gives the same result as the classical theory for these processes.

1. Introduction

In the passage of a fast charged particle through matter many collision processes involving the atomic electrons take place. These can be divided into two classes, namely those in which the collision with an electron can be considered as an individual event involving just one bound electron, and those in which it is important to consider that a large number of electrons are present in the medium. This latter class of processes i.e., collective processes, are frequently of physical interest. The emission of Čerenkov radiation by a charged particle moving faster than the phase velocity of light in a

† Also supported by the Nuclear Research Foundation within the University of Sydney.

medium is an example of an emission process which is entirely collective. Also, although it is frequently an adequate approximation to treat the excitation or ionization of atoms in a medium as a series of individual collisions involving only the elementary systems of a particle plus one atom, the rest of the medium sometimes has an important effect on these collisions at high energies. This occurs when the radiation part of the field of the particle becomes important.

The ionizing collision of a particle with a single free atom was first treated classically by Bohr [1]) and on quantum mechanics by Bethe [2]) and Bloch [3]). They gave an energy loss from the ionization and excitation of atoms in a medium, which increased logarithmically in the high energy region as the velocity of the particle approached the velocity of light. The reason for this increase is easily seen by considering the electromagnetic field of a relativistic charged particle moving through free space. One can represent the field adequately for many purposes by a spectrum of "equivalent photons" [4]). The number of equivalent photons representing the field outside a radius d about the path of the particle increases indefinitely as the velocity of the particle approaches the velocity of light, for any value of d. This leads to the possible excitation of an atom at ever increasing distances away from the particle as the energy of the particle increases. The relativistic rise in the energy loss formulae of Bethe and Bloch is due to this expanding range of action of the particle if one treats the atoms in the medium as independent of each other.

The possibility that a screening effect due to polarisation of the medium reduces the ionization loss was first suggested by Swann [5]), and Fermi [6]) in 1940 was the first to make quantitative calculations on this. He used classical electromagnetic theory for a continuous dielectric represented by just one type of dispersion oscillator. The energy loss was calculated from the flux of the Poynting vector over the surface of a cylinder about the path of the particle. Fermi found the important result that the total energy loss reached a plateau value at high energies, part of which was made up of a flow of radiation at large distances from the path of the particle. This latter contribution was the Čerenkov radiation. The classical theory of Čerenkov radiation had previously been worked out by Frank and Tamm [7]).

The ionization plateau is a purely electromagnetic effect which

can be thought of as deriving from scattering of the radiation part of the field by the medium, these scattered amplitudes then causing destructive interference along the path of the particle so limiting its range of action. This is the most important collective effect taking place in the medium at high energies. Space charge effects deriving from the electrostatic interaction of the electrons are unimportant except at low energies when the collision time of the particle with an electron is so long that the actual displacement of the electron during the collision is important.

Numbers of authors have since elaborated on Fermi's theory of the energy loss but none have changed its classical nature. Halpern and Hall [8]) developed Fermi's treatment for media in which the atoms were more accurately represented by a superposition of dispersion oscillators of different frequencies.

The partition of the energy loss calculated from the Poynting vector between the processes of excitation, ionization and Čerenkov radiation has been the subject of a paper by Huybrechts and Schönberg [9]). They found that in a perfectly transparent medium the relativistic increase of the energy loss beyond the minimum should be due exclusively to the emission of Čerenkov radiation. This was also discussed by Messel and Ritson [10]) and agrees with previous results obtained by A. Bohr [11]). The result is however contrary to experimental evidence which is that the ionization loss behaves like the total energy loss, i.e., there is a relativistic rise beyond the minimum. To explain this using Fermi's theory one needs to assume a strong absorption of the Čerenkov radiation.

Rather than assume this, Schönberg [12]) modified the Fermi calculation of the energy loss. He calculated the Poynting flux for the case in which the medium was represented as a continuous dielectric except for a cylinder with its axis along the path of the particle and with radius of order 10^{-4} cm, which was removed. The reason given for this was that it would not be valid to describe the medium as a continuous dielectric for losses involving small impact parameters, whereas the Poynting flux at large distances from the path of the particle depends on the polarisation close to the track of the particle. In this way Schönberg obtained agreement with the experimental results of Gosh, Jones and Wilson [13]) for the ionization loss of mesons in oxygen.

This problem was further discussed by G. N. Fowler and G. M. D. B. Jones [13a]). These authors pointed out that since the main

interaction term between atoms in condensed media is the electrostatic interaction one should not expect the dielectric character of the medium as such to be affected over the region suggested by Schönberg. They showed that the contribution to the dielectric constant due to the continuous spectrum of states of the atomic electrons should be included, and that this gives rise to a heavily damped Čerenkov radiation, which is entirely absorbed within a distance of about 10^{-4} cm from the track of the particle.

More recently Sternheimer [14]) likewise obtained agreement with experimental results without making the type of modification of Fermi's theory attempted by Schönberg. He considered in detail the reabsorption of Čerenkov radiation in the proximity of the track and its subsequent inclusion as primary ionization.

At about the same time Budini [15]) also made calculations in which the classical Poynting vector was used to calculate an equivalent photon spectrum for the continuous dielectric. This could then be used together with quantal photo-absorption cross-sections to calculate the excitation and ionization loss. The energy loss to Čerenkov radiation was also obtained. His results are in agreement with those of Sternheimer and both these authors showed the importance of considering the breadths of the spectroscopic lines of the medium.

Related directly to the problem of a quantal treatment of the polarisation phenomena in the above energy loss processes is the quantum theory of a refracting medium. This has been discussed by a number of authors, though not in a form suitable for our requirements. A phenomenological quantum theory of the Maxwell equations for a continuous dielectric was published in 1948 by Jauch and Watson [16]). In this theory, the dielectric properties of the medium were characterized by a dielectric constant which was not derived from an atomic model, without which one cannot give unambiguous foundation to the method of quantization used.

Most recently a further quantum theory of Čerenkov radiation and refractive index was put forward by Neamtan [17]), which had the advantage that the medium was not assumed to be continuous. None of these authors attempted a quantum theory of the polarisation effect on the excitation and ionization of atoms in the medium.

In view of the lack of any single method of dealing with these related problems we decided to adopt a different approach which enables us to treat quantally the effect of polarisation of a medium

on a large number of processes. This is described in two parts. In Part I we describe a quantum theory of refractive index and in Part II some processes caused by a fast charged particle passing through the medium are treated.

PART I: QUANTUM THEORY OF REFRACTIVE INDEX

2. Summary of Method

We first write in Hamiltonian form the equations of the classical electromagnetic field in interaction with a medium of extended induced dipoles. The corresponding theory of a polarisable medium expressed in the form of integral equations can be found in Born's "Optik" [18]). It is then found that a transformation

$$\begin{aligned} q_\lambda &= \mu_\lambda^{-1} Q_\lambda \\ p_\lambda &= \mu_\lambda P_\lambda \end{aligned} \tag{2.1}$$

of the canonical variables q_λ and p_λ of the radiation field enables one to express the total field in the medium as a superposition of oscillators with the correct time dependence of the field in the refracting medium. μ_λ is the classical index of refraction. The transformed oscillators can be excited by the passage of a fast charged particle through the medium and we obtain by this method the Čerenkov radiation process.

The basic property of this classical model is that the medium is treated as passive, i.e., with a behaviour completely determined by the electromagnetic field. It has no internal degrees of freedom of its own and so cannot for example become excited. The altered time dependence of the radiation field is thus due only to scattering by the medium.

In the quantal case we apply a canonical transformation of the same form to the Hamiltonian, H, of a radiation field in interaction with a medium of atoms, the difference now being that $\mu_\lambda(\tilde{\nu}_\lambda)$ is defined by a frequency $\tilde{\nu}_\lambda$ in the interacting system rather than the wavelength λ as in our simple classical model. We then demand that our new zero-order system, which we take as transformed radiation oscillators and medium, has the correct time dependence, i.e., that corresponding to the interacting system of radiation and medium. This means that the eigenvalues of our zero-order Hamiltonian correspond to those of H diagonalised, in our case by the perturbation method. This condition fixes the parameter $\mu_\lambda(\tilde{\nu}_\lambda)$ in the transfor-

mation and is shown to provide us with a quantal definition of refractive index.

The canonical variables of the transformed oscillators enable us to define quanta of the total field in the medium and we call these "physical photons". They are photons which in matter have a self energy deriving from polarisation of the medium. These quanta have the energy momentum relation

$$|\bar{P}_\lambda| = \frac{\mu_\lambda \bar{E}_\lambda}{c} \tag{2.2}$$

where μ_λ is the quantal refractive index, $\bar{P}_\lambda$ the momentum and $\bar{E}_\lambda$ the energy of a physical photon.

The same transformation is then applied to the Hamiltonian of a fast charged particle passing through a medium of atoms. Processes involving the particle are then expanded in a perturbation series on the basis of physical photon states instead of free photon states. We find that as a consequence of the energy momentum relation (2.2) the particle can radiate physical photons in first order. This process corresponds to Čerenkov radiation.

In higher order processes, such as the simultaneous emission of two physical photons or the excitation and ionization of atoms in the medium, we have to consider radiation damping theory since real first order processes exist. We find that another consequence of the relation (2.2) is the screening effect which gives rise to a plateau in the energy loss to ionization and excitation by a relativistic particle.

3. Classical Theory of Radiation in a Polarizable Medium

3(a) CLASSICAL THEORY OF REFRACTIVE INDEX IN HAMILTONIAN FORM

It has long been realised that Maxwell's equations for the electromagnetic field in a refracting medium could be derived from equations for the field in free space with a distribution of microscopic charges and currents present. Lorentz used this idea to derive an expression for the refractive index in terms of the density of atoms in the medium and their polarizability. He considered a medium made up of a distribution of point dipoles with induced dipole moments given by

$$\mathbf{p}_i = \alpha \mathbf{E}(\mathbf{r}_i) \tag{3.1}$$

where α is the polarisability and $\mathbf{E}(\mathbf{r}_i)$ the electric field at the dipole

excluding its own field. The field $\mathbf{E}$ responsible for the dipole moment is called the acting field. Neglecting magnetic dipoles the acting field $\mathbf{E}'$ in the medium can then be expressed in terms of a contribution $\mathbf{E}_e$ from external sources and a sum of contributions from the other dipoles in the medium taken at the appropriately retarded times.

Treating the dipole distribution as continuous we have an integral equation for $\mathbf{E}'$,

$$\mathbf{E}'(\mathbf{r}, t) = \mathbf{E}_e(\mathbf{r}, t) + \int_v N(\mathbf{r}')\nabla \wedge \nabla \wedge \frac{\mathbf{p}(t')}{R}\, d\tau' \tag{3.2}$$

where $\mathbf{p} = \alpha\mathbf{E}'$, $t' = t - R/c$, $R = |\mathbf{r} - \mathbf{r}'|$, and the integral extends over the volume of the medium excluding a small volume around the point $\mathbf{r}$ in which ∇ operates. $N(\mathbf{r}')$ is the mean density of dipoles in the medium at the point $\mathbf{r}'$. We then substitute a plane wave solution

$$\mathbf{E}'(\mathbf{r}, t) = \mathbf{E}'_0 e^{i(\mathbf{K}_\lambda \cdot \mathbf{r} - \nu t)}$$

in eq. (3.2), where ν is the frequency and $\mathbf{K}_\lambda$ the wave number of the wave. Taking $v \to 0$ after performing the integral one obtains in the usual way for the refractive index of the medium

$$\mu = \frac{c|\mathbf{K}_\lambda|}{\nu} = \left[\frac{1 + \frac{8\pi}{3}\alpha N}{1 - \frac{4\pi}{3}\alpha N}\right]^{\frac{1}{2}} \tag{3.3}$$

This result, i.e., the Lorentz-Lorenz result, is for a homogeneous medium with a dipole density N.

We now require to express a model of a refracting medium in Hamiltonian form. We start by considering the scalar and vector potentials ϕ_i and $\mathbf{A}_i$ of a point dipole situated at $\mathbf{r}_i$ with moment $\mathbf{p}_i(\mathbf{r}, \mathbf{r}_i, t) = \mathbf{p}'_i(t)\delta(\mathbf{r} - \mathbf{r}_i)$.

We can represent the dipole by the appropriate charge and current distribution in the inhomogeneous wave equations,

$$\begin{aligned} \frac{1}{c^2}\ddot{\mathbf{A}}_i - \nabla^2\mathbf{A}_i &= \frac{4\pi}{c}\mathbf{j} = \frac{4\pi}{c}\dot{\mathbf{p}}'_i(t)\delta(\mathbf{r} - \mathbf{r}_i) \\ \frac{1}{c^2}\ddot{\phi}_i - \nabla^2\phi_i &= 4\pi\varrho = -4\pi\mathbf{p}'_i(t)\ \mathrm{grad}\ \delta(\mathbf{r} - \mathbf{r}_i) \end{aligned} \tag{3.4}$$

where $\delta(\mathbf{r} - \mathbf{r}_i)$ are the Dirac δ functions, and the dot indicates

differentiation with respect to the time. The potentials deriving from these are the usual ones for a point dipole and satisfy the Lorentz relation.

Now consider the dipole moments $\mathbf{p}_i$. We cannot write an equation of the same form as (3.1), namely $\mathbf{p}_i = \alpha\mathbf{E}(\mathbf{r}_i)\delta(\mathbf{r}-\mathbf{r}_i)$ in the inhomogeneous wave equations with $\mathbf{E}$ the acting electric field since such an induced point dipole leads to a classical infinite self energy of a worse type than that for a point charge. Further we cannot exclude from $\mathbf{E}(\mathbf{r}_i)$ that part of the electric field due to the ith dipole and find simple differential equations for $\mathbf{E}$. Instead we will construct a model in which we have a medium of extended dipoles with dipole moments determined by the total electric field in their neighbourhood †. This model can be described by differential equations which give potentials without singularities. Thus we write by analogy with (3.1)

$$\mathbf{p}_i(\mathbf{r}, \mathbf{r}_i, t) = p_i\mathbf{E}(\mathbf{r}, t)U_i(\mathbf{r}-\mathbf{r}_i) \tag{3.5}$$

where $U_i(\mathbf{r}-\mathbf{r}_i)$ is a source function which is appreciably different from zero only in the neighbourhood of $\mathbf{r}_i$. Since $\mathbf{E}(\mathbf{r}, t)$ is the total electric field at the point $\mathbf{r}$, such an extended dipole has an effect on its own moment. This will be our model of a polarisable atom. It has no internal degrees of freedom but only an electric moment determined by the electric field.

With $\mathbf{p}_i$ defined by (3.5) the potentials of our smeared out dipoles, namely

$$\begin{aligned}\phi_i(\mathbf{r}, t) &= \int \mathrm{d}\tau' \left\{ \frac{\mathbf{p}_i(\mathbf{r}', \mathbf{r}_i, t') \cdot (\mathbf{r}-\mathbf{r}')}{|\mathbf{r}-\mathbf{r}'|^3} + \frac{\dot{\mathbf{p}}_i(\mathbf{r}', \mathbf{r}_i, t')(\mathbf{r}-\mathbf{r}')}{c|\mathbf{r}-\mathbf{r}'|^2} \right\} \\ \mathbf{A}_i(\mathbf{r}, t) &= \int \mathrm{d}\tau' \frac{\dot{\mathbf{p}}_i(\mathbf{r}', \mathbf{r}_i, t')}{c|\mathbf{r}-\mathbf{r}'|},\end{aligned} \tag{3.6}$$

can be derived from the inhomogeneous wave eqs. (3.4) with the charge and current distributions

$$\begin{aligned}\varrho_i &= -p_i\mathbf{E}\,\mathrm{grad}\,U_i(\mathbf{r}-\mathbf{r}_i) - p_iU_i(\mathbf{r}-\mathbf{r}_i)\,\mathrm{div}\,\mathbf{E} \\ \mathbf{j}_i &= p_i\dot{\mathbf{E}}\,U_i(\mathbf{r}-\mathbf{r}_i).\end{aligned} \tag{3.7}$$

These are gauge invariant since they involve only $\mathbf{E}$, $\dot{\mathbf{E}}$ and div $\mathbf{E}$,

† *Editor's note.* This assumption excludes the possibility of taking into account the so-called Lorentz field, which is just the difference between the acting field and the total field in the medium. The validity of the theory is thus restricted to media of small polarizability. In particular, it will not yield the Lorenz-Lorentz expression (3.3) for the refractive index, but only the approximate relation (3.18).

and they also satisfy the continuity condition

$$\dot{\varrho}_i + \operatorname{div} \mathbf{j}_i = 0.$$

For a medium consisting of a large number of such dipoles we have for the potentials $\mathbf{A}$ and ϕ,

$$\begin{aligned} \frac{1}{c^2}\ddot{\mathbf{A}} - \nabla^2 \mathbf{A} &= \frac{4\pi}{c} \sum_i \mathbf{j}_i(\mathbf{r}, t) \\ \frac{1}{c^2}\ddot{\phi} - \nabla^2 \phi &= 4\pi \sum_i \varrho_i(\mathbf{r}, t). \end{aligned} \tag{3.8}$$

These are the differential equations which we want to express in Hamiltonian form. They describe a medium of dipoles whose moments are determined by the potentials. The medium is "passive" in this respect i.e., it has no internal degrees of freedom of its own and is represented just by the polarisability law (3.5). Thus many effects which take place in real media, such as the excitation of atoms or plasma oscillations will not be contained in this model.

We find for the Lagrangian density of the system which corresponds to the above equations

$$L' = -\frac{1}{16\pi} \sum_{\mu,\nu} \left(\frac{\partial A_\mu}{\partial x_\nu} - \frac{\partial A_\nu}{\partial x_\mu} \right)^2 + \tfrac{1}{2} \sum_i p_i U_i(\mathbf{r} - \mathbf{r}_i)\, \mathbf{E}^2(\mathbf{r}) \tag{3.9}$$

where Greek indices denote the four-vectors $A_\mu \equiv (\mathbf{A}, i\phi)$ or $x_\mu \equiv (\mathbf{r}, ict)$. We require the Lagrangian of the system integrated over all space, which can then be expressed in terms of canonical variables dependent only on time. This is more relevant to our later discussion of the quantal case. Write

$$L(t) = \int L'(\mathbf{r}, t)\, \mathrm{d}\tau.$$

We expand the potentials in the usual way into a set of orthogonal eigenwaves of the homogeneous wave equation.

Now the vector potential can always be divided into two parts, the transverse part which has a divergence equal to zero, and a longitudinal part which can be written as the gradient of a scalar field. We thus use

$$\mathbf{A} = \sum_\gamma q_\gamma(t) \mathbf{A}_\gamma(\mathbf{r}) + \sum_\sigma q_\sigma(t) \mathbf{A}_\sigma(\mathbf{r}) \tag{3.10}$$

$$\nabla \cdot \mathbf{A}_\gamma = 0$$

$$\nabla \wedge \mathbf{A}_\sigma = 0$$

with the normalisation

$$\int \mathbf{A}_\gamma \mathbf{A}_\mu \mathrm{d}\tau = 4\pi c^2 \delta_{\gamma\mu}.$$

The scalar potential ϕ is expanded in the same way

$$\phi = \sum_\sigma a_\sigma(t)\,\phi_\sigma(\mathbf{r}) \tag{3.11}$$

Different eigenwaves labelled with different subscripts may have the same wavelengths due to the possible sine and cosine modes and different polarisations.

By multiplying (3.8) by $\mathbf{A}_\gamma$, $\mathbf{A}_\sigma$ and ϕ_σ respectively and integrating over the normalization volume we obtain the following differential equations for the variables q_γ, q_σ and a_σ:

$$\begin{aligned}
\ddot{q}_\gamma + \nu_\gamma^2 q_\gamma &= -\frac{1}{c^2}\sum_i \sum_{\gamma'} \ddot{q}_{\gamma'}\alpha^i_{\gamma\gamma'} - \frac{1}{c^2}\sum_i \sum_\sigma \ddot{q}_\sigma \alpha^i_{\sigma\gamma} - \frac{1}{c^2}\sum_i \sum_\sigma \dot{a}_\sigma \nu_\sigma \alpha^i_{\sigma\gamma} \\
\ddot{q}_\sigma + \nu_\sigma^2 q_\sigma &= -\frac{1}{c^2}\sum_i \sum_{\sigma'} \dot{a}_{\sigma'}\nu_{\sigma'}\alpha^i_{\sigma\sigma'} - \frac{1}{c^2}\sum_i \sum_{\sigma'} \ddot{q}_{\sigma'}\alpha^i_{\sigma\sigma'} - \frac{1}{c^2}\sum_i \sum_\gamma \ddot{q}_\gamma \alpha^i_{\gamma\sigma} \\
\ddot{a}_\sigma + \nu_\sigma^2 a_\sigma &= -\frac{1}{c^2}\sum_i \sum_{\sigma'} a_{\sigma'}\nu_{\sigma'}\nu_\sigma \alpha^i_{\sigma\sigma'} - \frac{1}{c^2}\sum_i \sum_{\sigma'} \dot{q}_{\sigma'}\nu_\sigma \alpha^i_{\sigma\sigma'} - \frac{1}{c^2}\sum_i \sum_\gamma \dot{q}_\gamma \nu_\sigma \alpha^i_{\sigma\gamma}
\end{aligned} \tag{3.12}$$

where we have made use of the Lorentz relation $\nu_\sigma q_\sigma = \dot{a}_\sigma$ and used the notation

$$\alpha^i_{\gamma\gamma'} = p_i \int U_i(\mathbf{r}-\mathbf{r}_i)\mathbf{A}_\gamma(\mathbf{r})\mathbf{A}_{\gamma'}(\mathbf{r})\,\mathrm{d}\tau. \tag{3.13}$$

The Lagrangian L for these differential equations becomes,

$$\begin{aligned}
L(t) &= \frac{1}{2}\sum_\gamma (\dot{q}_\gamma^2 - \nu_\gamma^2 q_\gamma^2) + \frac{1}{2}\sum_\sigma (\dot{q}_\sigma^2 - \nu_\sigma^2 q_\sigma^2) - \frac{1}{2}\sum_\sigma (\dot{a}_\sigma^2 - \nu_\sigma^2 a_\sigma^2) \\
&+ \frac{1}{2c^2}\sum_i \sum_{\sigma,\sigma'} a_\sigma \nu_c a_{\sigma'}\nu_{\sigma'}\alpha^i_{\sigma\sigma'} + \frac{1}{c^2}\sum_i \sum_{\sigma,\sigma'} a_\sigma \nu_\sigma \dot{q}_{\sigma'}\alpha^i_{\sigma\sigma'} \\
&+ \frac{1}{2c^2}\sum_i \sum_{\gamma,\gamma'} \dot{q}_\gamma \dot{q}_{\gamma'}\alpha^i_{\gamma\gamma'} + \frac{1}{2c^2}\sum_i \sum_{\sigma,\sigma'} \dot{q}_\sigma \dot{q}_{\sigma'}\alpha^i_{\sigma\sigma'} \\
&+ \frac{1}{c^2}\sum_i \sum_{\gamma,\sigma} \dot{q}_\sigma \dot{q}_\gamma \alpha^i_{\sigma\gamma} + \frac{1}{c^2}\sum_i \sum_{\sigma,\gamma} a_\sigma \nu_\sigma \dot{q}_\gamma \alpha^i_{\sigma\gamma}
\end{aligned} \tag{3.14}$$

and the canonical momenta to the variables q_γ, q_σ and a_σ are

$$\begin{aligned}
p_\gamma &= \frac{\partial L}{\partial \dot{q}_\gamma} = \dot{q}_\gamma + \frac{1}{c^2}\sum_i \sum_{\gamma'} \dot{q}_{\gamma'}\alpha^i_{\gamma\gamma'} + \frac{1}{c^2}\sum_i \sum_\sigma a_\sigma \nu_\sigma \alpha^i_{\sigma\gamma} + \frac{1}{c^2}\sum_i \sum_\sigma \dot{q}_\sigma \alpha^i_{\sigma\gamma} \\
p_\sigma &= \frac{\partial L}{\partial \dot{q}_\sigma} = \dot{q}_\sigma + \frac{1}{c^2}\sum_i \sum_{\sigma'} \dot{q}_{\sigma'}\alpha^i_{\sigma\sigma'} + \frac{1}{c^2}\sum_i \sum_{\sigma'} a_{\sigma'}\nu_{\sigma'}\alpha^i_{\sigma\sigma'} + \frac{1}{c^2}\sum_i \sum_\gamma \dot{q}_\gamma \alpha^i_{\sigma\gamma} \\
b_\sigma &= -\dot{a}_\sigma.
\end{aligned} \tag{3.15}$$

The Hamiltonian of the system, which is to be expressed as a function only of the variables q_γ, q_σ and a_σ and their momenta, is defined as

$$H = \sum_\gamma p_\gamma \dot{q}_\gamma + \sum_\sigma p_\sigma \dot{q}_\sigma + \sum_\sigma b_\sigma \dot{a}_\sigma - L$$

The general expression for H is lengthy and will not be given since we are interested in a simpler case. We assume that the dipoles are distributed randomly and that a large number are contained in the volume of integration. The positions of the dipoles are to be completely uncorrelated. The derivation of the general Hamiltonian and its simplification under these conditions is straightforward and one finds

$$H = \frac{1}{2}\sum_\gamma \left[\frac{p_\gamma^2}{1+\frac{1}{c^2}\sum_i \alpha_{\gamma\gamma}^i} + \nu_\gamma^2 q_\gamma^2 \right] \tag{3.16}$$

and $H(\sigma) = 0$. That $H(\sigma)$, i.e., the part dependent on the longitudinal variables, should average out to zero is to be expected for this model. We have no charge density over large volumes and as stated before cannot describe many of the effects which take place in real media.

In eq. (3.16) Σ_i sums over all the dipoles in a unit volume. There may be several distinct species of dipole and the equation still holds provided each is distributed randomly.

Now consider the Hamiltonian (3.16). Using Hamilton's equations we have

$$\ddot{q}_\gamma + \frac{\nu_\gamma^2}{\left(1+\frac{1}{c^2}\sum_i \alpha_{\gamma\gamma}^i\right)} q_\gamma = 0$$

i.e.

$$q_\gamma(t) = |q_\gamma| \exp\left(\frac{-i\nu_\gamma t}{\mu_\gamma}\right)$$

where

$$\mu_\gamma = \left(1+\frac{1}{c^2}\sum_i \alpha_{\gamma\gamma}^i\right)^{1/2}. \tag{3.17}$$

Hence μ_γ is the refractive index of the medium of dipoles for the wavelength $\lambda = (2\pi c/\nu_\gamma)$. We can compare this with the Lorentz-Lorenz result (3.3) by replacing the source functions $U_i(\mathbf{r}-\mathbf{r}_i)$

by constant dipole densities over the medium. Write

$$p_i U_i(\mathbf{r}-\mathbf{r}_i) = \alpha.$$

Then

$$\sum_i \alpha^i_{\gamma\gamma} = 4\pi N\alpha c^2$$

if there is only one species of dipoles, where N is the number of dipoles per unit volume. Thus μ_γ becomes

$$\mu_\gamma = (1+4\pi\alpha N)^{\frac{1}{2}}. \tag{3.18}$$

For $|\mu_\gamma-1| \ll 1$ this result agrees with the expression (3.3). It differs from (3.3) in general because in our calculations we allowed dipoles to overlap. The average field acting on a dipole is thus that obtained by averaging the total electric field in the medium over the volume of space both inside and outside of dipoles. We could describe the more physical case in which dipoles are not allowed to overlap by introducing the appropriate hard sphere type of short range correlations in their positions.

The Hamiltonian can now be written as

$$\tfrac{1}{2}\sum_\lambda (p_\gamma^2+\nu_\gamma^2 q_\gamma^2)-\tfrac{1}{2}\sum_\gamma \left(\frac{\mu_\gamma^2-1}{\mu_\gamma^2}\right) p_\gamma^2. \tag{3.19}$$

Thus in addition to the free field Hamiltonian we have a polarization energy

$$H_{\text{pol}} = -\tfrac{1}{2}\sum_\gamma \left(\frac{\mu_\gamma^2-1}{\mu_\gamma^2}\right) p_\gamma^2. \tag{3.20}$$

We can express the total Hamiltonian (3.19) as a superposition of oscillators which include the polarization energy of the medium by making the canonical transformation

$$q_\gamma = \mu_\gamma^{-1} Q_\gamma \tag{3.21}$$
$$p_\gamma = \mu_\gamma P_\gamma$$

so that

$$H = \tfrac{1}{2}\sum_\gamma (P_\gamma^2+\tilde{\nu}_\gamma^2 Q_\gamma^2) \tag{3.22}$$

where

$$\tilde{\nu}_\gamma = \mu_\gamma^{-1}\nu_\gamma. \tag{3.23}$$

The variables Q_γ have the correct time dependence of the field in the refracting medium, namely

$$\ddot{Q}_\gamma+\tilde{\nu}_\gamma^2 Q_\gamma = 0.$$

We have thus expressed the complete field in the medium by a set of independent oscillators and the effect of the medium on the free radiation field, which was represented by a simple scattering term H_{pol}, has been transformed away.

Suppose we had started with a more general type of classical model, i.e., a medium of scattering centres which had degrees of freedom of their own. We would write a Hamiltonian

$$H(t) = H_R(t) + H_M(t) + H_{RM}(t)$$

where $H_R(t)$ is due to the radiation, $H_M(t)$ to the medium, and $H_{RM}(t)$ involves the variables of both the radiation and the medium. The state of the medium is specified by all the coordinates M, say, and that of the radiation by R. In general $H_{RM}(t)$ will contribute a time dependence to $H(t)$ which is due to the medium scattering the radiation and in turn the radiation changing the state of the medium. Now under what conditions can we expect to be able to replace $H_{RM}(t)$ by a term dependent only on the radiation variables and possibly certain averages over the variables M? Only if the most important effect of $H_{RM}(t)$ on the time dependence of the system is due to its effect on the state of the radiation field i.e., if the medium can be assumed to be in a stationary state. This would in some cases allow certain averages to be carried out over the variables of the medium thus making it possible to express H_{RM} in terms of the variables R only. Certain of these averages can be given physical meaning and the refractive index is one of them.

The model we described in this section is a particularly simple case of this procedure. We have excluded degrees of freedom M from the start and instead assumed a simple polarisability law for the atoms. The possibility of the medium changing its state was excluded from the model from the beginning.

The above classical considerations suggest a useful approach to the quantum theory of radiation in interaction with a medium of real atoms. We shall make a similar transformation to the above on the canonical variables of the quantised radiation field. The parameter μ_γ occurring in the transformation is then fixed by a physical condition which gives a quantal definition of refractive index. The condition will however be on the frequency $\tilde{\nu}_\gamma$ of the transformed oscillator rather than its wavelength, so that the refractive index will be defined by $\tilde{\nu}_\gamma$. It then turns out to be useful to attach physical significance to the transformed oscillators rather than to the free

oscillators and use them to form a basis for a "zero-order system" in perturbation theory. They can be thought of as photons with modified propagation properties due to the medium and as far as this goes the medium has been treated as "passive" i.e., giving rise to a scattering without changing its state as in the preceding classical theory. Starting with this new zero-order system the Hamiltonian is capable, under certain conditions, of solution in principle to any required accuracy (including the calculation of damping effects) by the perturbation method just as in the more usual case.

Before going on to discuss this we first apply this model to the classical theory of Čerenkov radiation produced by a fast charged particle passing through the medium of dipoles.

3(b). CLASSICAL THEORY OF A FAST CHARGED PARTICLE PASSING THROUGH THE MEDIUM OF DIPOLES

Suppose we have a charged particle passing with a velocity $\mathbf{v}$ through the medium of dipoles. Then in the inhomogeneous wave equation we have an additional charge $eZ\delta(\mathbf{r}-\mathbf{r}_p)$ and current $eZ\mathbf{v}\delta(\mathbf{r}-\mathbf{r}_p)$, where $\mathbf{r}_p$ is the position of the particle. In this § we shall assume a medium of randomly distributed dipoles from the beginning to simplify the calculations. Expanding the field amplitudes as before we now find for the time dependence of the quantities q_γ,

$$\left(1+\frac{1}{c^2}\sum_i \alpha^i_{\gamma\gamma}\right)\ddot{q}_\gamma+\nu_\gamma^2 q_\gamma=\frac{eZ}{c}\,\mathbf{v}\cdot\mathbf{A}_\gamma(\mathbf{r}_p). \tag{3.24}$$

The canonical momenta of the system are unaltered, i.e., given by eqs. (3.15). Thus the Hamiltonian of the system becomes

$$H^1=\frac{1}{2}\sum_\gamma(p_\gamma^2+\nu_\gamma^2 q_\gamma^2)-\frac{1}{2}\sum_\gamma\left(\frac{\mu_\gamma^2-1}{\mu_\gamma^2}\right)p_\gamma^2-\frac{eZ}{c}\,\mathbf{v}\cdot\mathbf{A}(\mathbf{r}_p)$$

$$+\frac{1}{2}\frac{eZ\phi_\sigma}{\nu_\sigma}\left[\frac{p_\sigma-\frac{1}{c^2}\sum_i a_\sigma\nu_\sigma\alpha^i_{\sigma\sigma}}{1+\frac{1}{c^2}\sum_i\alpha^i_{\sigma\sigma}}\right]+\frac{1}{2}eZ\phi(\mathbf{r}_p).$$

We know that when a relativistic charged particle passes through a medium the range of action of its field is screened by polarization of the medium. This is due to a large number of scattering and interference processes taking place along the path of the particle. The result of these is a deficiency of energy H_{pol} actually in the form

of electromagnetic field amplitudes at any one time, compared with what we would have if the particle were passing through free space. Under certain conditions these interference processes may lead to a flow of radiation away from the path of the particle and this can be identified with Čerenkov radiation.

Applying the canonical transformation (3.21) to the Hamiltonian and using Hamilton's equations we find

$$\ddot{Q}_\gamma + \tilde{\nu}_\gamma^2 Q_\gamma = \frac{eZ}{\mu_\gamma c} \mathbf{v}\, \mathbf{A}_\gamma(\mathbf{r}_p). \tag{3.25}$$

We could of course for this particular problem have written (3.25) down immediately from eq. (3.24). The particle gives rise to a term on the right hand side of the equation which we can think of as forcing the oscillators of the total field in the refracting medium.

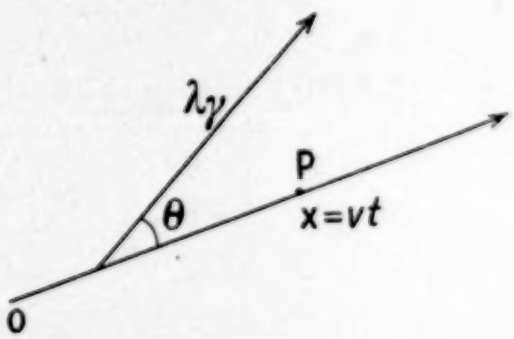

Suppose P is moving along the x axis in such a way that $x = 0$ when $t = 0$ and consider the excitation of a mode γ which propagates at an angle θ to the x axis.

Write

$$\mathbf{A}_\gamma(\mathbf{r}_p) = \mathbf{e}_\gamma \sqrt{8\pi c^2} \cos(vtK_\gamma \cos\theta).$$

Substituting in (3.25)

$$\ddot{Q}_\gamma + \tilde{\nu}_\gamma^2 Q_\gamma = b_\gamma \cos \nu_0 t \tag{3.26}$$

where

$$b_\gamma = \frac{eZv \cos\psi}{c\mu_\gamma} \sqrt{8\pi c^2}, \qquad \nu_0 = vK_\gamma \cos\theta$$

and ψ is the angle between the polarisation $\mathbf{e}_\gamma$ and $\mathbf{v}$.

The energy given per second to these oscillators is

$$W_\gamma(t) = 1/t \int_0^t \mathrm{d}t\, \ddot{Q}_\gamma b_\gamma \cos \nu_0 t$$

and if for convenience we take t so that it covers an integral number of vibrations ν_0 we have

$$W_\gamma(t) = \frac{b_\gamma^2 \tilde{\nu}_\gamma}{2t(\tilde{\nu}_\gamma^2 - \nu_0^2)} \left[\frac{1 - \cos(\tilde{\nu}_\gamma - \nu_0)t}{(\tilde{\nu}_\gamma - \nu_0)} + \frac{1 - \cos(\tilde{\nu}_\gamma + \nu_0)t}{(\tilde{\nu}_\gamma + \nu_0)} \right]. \quad (3.27)$$

We next sum over the two directions of polarisation for the cosine mode of wavelength $\lambda_\gamma = \lambda_{\gamma'}$. Choose two orthogonal states of polarisation corresponding to $\mathbf{e}_\gamma$ parallel and $\mathbf{e}_{\gamma'}$ perpendicular to the plane of $\mathbf{v}$ and $\mathbf{K}_\lambda$. Then $\cos\psi = 0$ for perpendicular polarisation and $\cos\psi = \sin\theta$ for parallel polarisation. Therefore $\sum W_\gamma(t)$ is given by (3.27) with $\cos\psi = \sin\theta$ and the radiation is polarised in the plane of $\mathbf{v}$ and its direction of propagation.

Now the density of oscillators in the medium is given by

$$\varrho(\tilde{\nu}_\gamma)\mathrm{d}\tilde{\nu}_\gamma \mathrm{d}\Omega = \frac{u_\gamma}{U_\gamma} \frac{\mu_\gamma^3 \tilde{\nu}_\gamma^2 \mathrm{d}\tilde{\nu}_\gamma \mathrm{d}\Omega}{(2\pi c)^3} \quad (3.28)$$

where $\mathrm{d}\Omega = \mathrm{d}(\cos\theta)\mathrm{d}\phi$ is the element of solid angle into which they propagate and the group velocity U_γ is related to the phase velocity u_γ by

$$U_\gamma = \frac{\mathrm{d}\left(\frac{u_\gamma}{\lambda_\gamma}\right)}{\mathrm{d}\left(\frac{1}{\lambda_\gamma}\right)}. \quad (3.29)$$

Thus if we now integrate $\sum W_\gamma$ over the solid angle we find for total energy radiated per second

$$E_\gamma(\tilde{\nu}_\gamma)\mathrm{d}\tilde{\nu}_\gamma = \frac{\mathrm{d}\tilde{\nu}_\gamma}{t} \int_{-1}^{+1} \frac{\mathrm{d}(\cos\theta) 2\pi \tilde{\nu}_\gamma^2 \mu_\gamma^3 u_\gamma}{(2\pi c)^3 U_\gamma} W(t).$$

Most of the contribution to this integral occurs when $\tilde{\nu} \approx \nu_0$, i.e.

$$\cos\theta_0 = \frac{\nu_0}{vK_\gamma} = \frac{c}{v\mu_\gamma}. \quad (3.30)$$

Thus if (3.30) has a solution we can approximate the integral by extending the range of integration to $\theta = \pm\infty$, which gives

$$E_\gamma \mathrm{d}\tilde{\nu}_\gamma = \frac{e^2 Z^2 u_\gamma v \tilde{\nu}_\gamma \sin^2\theta_0 \mathrm{d}\tilde{\nu}_\gamma}{2c^2 U_\gamma}.$$

Finally multiplying by 2 to account for the sine mode as well as the cosine mode we find for the total energy radiated per second,

of wavelength $\lambda = \lambda_\gamma$, say,

$$E_\lambda \mathrm{d}\bar{\nu}_\lambda = \bar{\nu}_\lambda v \frac{e^2 Z^2}{c^2} \frac{u_\lambda}{U_\lambda} \left(1 - \frac{c^2}{v^2 \mu_\lambda^2}\right) \mathrm{d}\bar{\nu}_\lambda. \tag{3.31}$$

This is radiated mainly along the cone given by equation (3.30). It is thus to be identified with Čerenkov radiation. The result (3.31) agrees with the result obtained by authors [7]) using the more usual method of calculating the Poynting flux vector inside the medium at large distances from the path of the particle.

4. Quantum Theory of Refractive Index

4(a). RADIATION DAMPING THEORY

We begin by making a few observations on the usual quantum theory of a radiation field in interaction with a medium of atoms. Consider the Hamiltonian operator of this system. We have in Coulomb gauge

$$H = H_M + H_R + H_{MR} \tag{4.1}$$

with

$$H_M = \sum_i (c\alpha_i \mathbf{p}_i + mc^2 \beta_i + e_i \phi(\mathbf{r}_i)) + \frac{1}{2} \sum_{i \neq k} \frac{e_i e_k}{r_{ik}}$$

$$H_R = \tfrac{1}{2} \sum_\lambda n_\lambda (\bar{p}_\lambda^2 + \nu_\lambda^2 \bar{q}_\lambda^2)$$

$$H_{MR} = -\sum_i e c \boldsymbol{\alpha}_i \mathbf{A}(\mathbf{r}_i)$$

where $\mathbf{A}$ is the transverse vector potential, $\phi(\mathbf{r}_i)$ the scalar potential deriving from the atomic nuclei, $\mathbf{p}_i$ the momentum of the ith electron, $\bar{q}_\lambda = q_\lambda + q_\lambda^*$, and $(\boldsymbol{\alpha}_i, \beta_i)$ the Dirac matrices.

The radiation field has been expanded into plane waves represented by exponential functions:

$$\mathbf{A} = \sum_\lambda (q_\lambda \mathbf{A}_\lambda + q_\lambda^* \mathbf{A}_\lambda^*)$$

$$\mathbf{A}_\lambda = \mathbf{e}_\lambda \sqrt{4\pi c^2}\, \mathrm{e}^{i\mathbf{K}_\lambda \cdot \mathbf{r}}, \qquad |\mathbf{K}_\lambda| = \frac{\nu_\lambda}{c}. \tag{4.2}$$

The behaviour of the physical system is then described by a state function ϕ satisfying

$$(H_M + H_R + H_{MR})\phi = i\hbar\dot{\phi}.$$

Eigenfunctions of $H_0 = H_M + H_R$ describing the zero-order system will be written in the usual way $|A;\ n_1 \cdots n_\lambda \cdots\rangle$ where

n_λ is the number of radiation oscillators in the excited state λ and A is some quantum state of the medium †. The eigenvalue of H_0 for the above state is $E_A+\sum_\lambda n_\lambda \hbar\nu_\lambda$ where E_A is the energy of the medium in state A.

In doing perturbation theory we first require to add a mass operator H_s to H_0 and subtract it from the interaction to ensure that the electron masses are the observable ones. We further require to account for the shifts in the energy eigenvalues of the zero-order system due to the interaction and this will now be discussed. This means that we should start with a zero-order system which has the correct time dependence.

Consider first the medium in the absence of radiation. The interaction H_{MR} produces a perturbed state corresponding to the state $|A;\ 0\cdots 0\rangle$, which has a shifted eigenvalue which we shall write as $E_A+\varepsilon_0^L$; ε_0^L is simply the self energy of the medium in the absence of radiation.

Next consider the general state ϕ of the medium with radiation present, say $|A;\ n_1\cdots n_\lambda\cdots\rangle$. Suppose we want to calculate the perturbed state ϕ' corresponding to ϕ and the energy eigenvalue belonging to ϕ'. In this case in general we have the complication that real transitions of the system may be possible. For example a photon may be absorbed by an atomic electron. This real excitation of the medium however happens infrequently enough for us to be able to treat the system as if it were in a stationary state ϕ' with eigenvalues displaced from those of the state ϕ. The radiation field in the medium will have modified propagation properties due to a large number of coherent scattering and interference processes, i.e., as far as the stationary state ϕ' goes the medium is just a passive scatterer. This scattering proceeds through the *virtual* excitation of the medium and modifies the time dependence of the stationary state ϕ thus giving rise to the displaced eigenvalue. Frequencies for which a real absorption is possible have the strongest interaction with the medium and suffer the greatest modification of their propagation properties.

The eigenvalue of ϕ' differs from that of ϕ by the self energy

† We have assumed the medium to be in one particular state A. In fact this will only be the case at zero temperature. More generally the medium in the absence of radiation should be represented by an incoherent superposition of possible excited states, with statistical weights proportional to $\exp(-E/kT)$, where T is the temperature of the medium.

of the system in the state ϕ which we write as

$$\varepsilon_\phi^L = \varepsilon_\phi + \varepsilon_0^L. \tag{4.3}$$

ε_ϕ is that part of the self energy of the system due to the real photons and will be called the polarisation energy of the medium. Thus we further require to add to H_0 and subtract from the interaction an operator H_L which accounts for the energy shifts ε_ϕ^L, i.e. write

$$K_0+K = (H_0+H_s+H_L)+(H_{RM}-H_s-H_L) \tag{4.4}$$

where H_L is defined so that the interaction K produces no further shift in the energy eigenvalues of K_0.

We shall be interested in calculating the energies ε_ϕ^L, and in Part II the transition probabilities when a fast charged particle passes through the medium. For this we use the theory given in a paper by Arnous and Heitler [19]) on Line Breadth Phenomena, though the theory in this section is standard radiation damping theory insofar as we do not require the refinement discussed by these authors.

It is convenient to use the interaction representation $\psi(t) = e^{itK_0}\phi(t)$ and the state of the system at time t can then be expressed in terms of that at t_0 by

$$\psi(t) = S(t)\psi(t_0);$$

$S(t)$ has both a diagonal part S_d and a non-diagonal part S_{nd} which it is convenient to separate. There are several ways of expressing this and we shall use the symmetrical form

$$S(t) = \frac{i}{2\pi}\int_{-\infty}^{\infty} dE\, e^{\frac{-i(E-K_0)t}{\hbar}} [N_d+N_d U_{nd} N_d]\, e^{\frac{it_0(E-K_0)}{\hbar}} \tag{4.5}$$

where N_d is a typical diagonal resonance denominator

$$N_d = \left(E-K_0+\frac{i\hbar}{2}\Gamma(E)\right)^{-1} \tag{4.6}$$

and U_{nd} is a non-diagonal amplitude responsible for transitions. $\Gamma(E)$ is a diagonal operator whose real part plays the role of a line breadth and complex part that of a self energy.

Explicit expansions for Γ and U_{nd} in terms of the perturbing Hamiltonian K were obtained by Arnous and Heitler. They are

$$\frac{1}{2i}\Gamma = \{K+KNK_{nd}+KN(K_{nd}NK_{nd})_{nd}+\ldots\}_d \tag{4.7}$$

and

$$U_{\mathrm{nd}} = \{K+K_{\mathrm{nd}}NK_{\mathrm{nd}}+[K_{\mathrm{nd}}N(K_{\mathrm{nd}}]_{\mathrm{nd}}NK_{\mathrm{nd}})_{\mathrm{nd}}+\ldots\}_{\mathrm{nd}}. \quad (4.8)$$

We now are in a position to calculate the self energy ε_ϕ^L for any particular state φ. To do this we simply use the condition that H_L be such that K produces no further shift in the eigenvalues of K_0, i.e., that the imaginary part of Γ vanishes. This gives to second order

$$\varepsilon_\phi^L = \mathrm{Re}\left\{\langle\phi|H_{MR}-H_s|\phi\rangle+\sum_\alpha \frac{\langle\phi|H_{MR}|\alpha\rangle\langle\alpha|H_{MR}|\phi\rangle}{E_\varphi+\varepsilon_\phi^L-E_\alpha-\varepsilon_\alpha^L+\frac{i\hbar}{2}\gamma_\alpha}\right\} \quad (4.9)$$

where γ_α is the real part of the matrix element of Γ for the state $|\alpha\rangle$ i.e., the total transition probability from the state $|\alpha\rangle$ to all other states.

Using the above damping theory we could attempt to go ahead and calculate the effects of the polarisation energies ε_ϕ on the various radiation processes which can take place in matter. However we shall show how they are related to the refractive index of the medium. This is done by making a canonical transformation of the variables $\bar{q}_\lambda$ and $\bar{p}_\lambda$, of the radiation field similar to the one used in the classical theory. The parameter μ_λ in the transformation is then defined on such a way that the transformation "renormalises" the state of the medium with one photon present, i.e., accounts for the polarisation energy ε_ϕ.

4(b) CANONICAL TRANSFORMATION

Consider an as yet undefined c-number $\mu_\lambda(\bar{\nu}_\lambda)$ which is a unique function of the frequency $\bar{\nu}_\lambda = c\mu_\lambda^{-1}\lambda^{-1}$. For a given wavelength λ there may correspond several possible frequencies $\bar{\nu}_\lambda^i$ satisfying the above relation. Thus we start by splitting up the Hamiltonian H of the radiation field as follows

$$H_R = \sum_\lambda \sum_i n_\lambda^i(\bar{p}_\lambda^2+\nu_\lambda^2\bar{q}_\lambda^2)$$

and apply the following canonical transformation to the variables of the radiation oscillator in the ith sum

$$\begin{aligned}\bar{q}_\lambda &= \mu_\lambda^{-1}(\bar{\nu}_\lambda^i)\,\bar{Q}_\lambda^i \\ \bar{p}_\lambda &= \mu_\lambda(\bar{\nu}_\lambda^i)\,\bar{P}_\lambda^i.\end{aligned} \quad (4.10)$$

Then

$$H = (H_M+\overline{H}_R+H_S)+(\overline{H}_{MR}+H_{\text{pol}}-H_s) \tag{4.11}$$

is the transformed Hamiltonian, where

$$\begin{aligned}
\overline{H}_R &= \tfrac{1}{2}\sum_\lambda \sum_i n_\lambda^i (\bar{P}_\lambda^{i2}+\bar{\nu}_\lambda^{i2}\overline{Q}_\lambda^{i2}) \\
H_{\text{pol}} &= \tfrac{1}{2}\sum_\lambda \sum_i n_\lambda^i (\mu_\lambda^2(\bar{\nu}_\lambda^i)-1)\bar{P}_\lambda^{i2} \\
\overline{H}_{RM} &= -\sum_j \sum_\lambda \sum_i e\alpha_j \mu_\lambda^{-1} n_\lambda^i (\overline{Q}_\lambda^i \mathbf{A}_\lambda+\overline{Q}_\lambda^{i*}\mathbf{A}_\lambda^*) \\
\bar{\nu}_\lambda &= \nu_\lambda \mu_\lambda^{-1}(\bar{\nu}_\lambda^i)
\end{aligned} \tag{4.12}$$

and the commutation relations for the transformed variables are

$$\begin{aligned}
[\bar{P}_\lambda^i, \overline{Q}_\lambda^i] &= -i\hbar \\
[Q_\lambda^i, Q_\lambda^{i*}] &= \frac{\hbar\mu_\lambda(\bar{\nu}_\lambda^i)}{2\bar{\nu}_\lambda}.
\end{aligned} \tag{4.13}$$

From now on we shall replace the sums $\sum_\lambda\sum_i n_\lambda^i$ by $\sum_\lambda \bar{n}_\lambda$ where $\bar{n}_\lambda$ will be understood as the number of transformed oscillators of a given frequency $\bar{\nu}_\lambda$, and denote eigenfunctions of

$$(H_M+\overline{H}_R+H_s) \text{ by } |A;\ \bar{n}_1 \cdots \bar{n}_\lambda \ldots\rangle.$$

The Hamiltonian (4.11) is of course still exact. In order to do perturbation theory with it we must calculate a level shift operator $\overline{H}_L$ in just the same way as we calculated H_L. We write

$$\overline{H} = (H_M+\overline{H}_R+H_s+\overline{H}_L)+(\overline{H}_{RM}+H_{\text{pol}}-H_s-\overline{H}_L) = \overline{H}_0+\overline{H} \tag{4.14}$$

and define $\overline{H}_L$ so that the eigenvalues of $\overline{H}_0$ are the correct shifted values appropriate to the interacting system of medium and transformed oscillators.

We next impose a condition which fixes μ_λ. Consider the two states, one with no transformed oscillators excited and one with one transformed oscillator in the excited state λ; i.e. the states $|A;\ \bar{0}-\bar{0}-\bar{0}\rangle$ and $|A;\ \bar{0}-\bar{1}_\lambda-\bar{0}\rangle$. Then the eigenvalues of $\overline{H}_0$ for these states are $E_A+\bar{\varepsilon}_0^L$ and $E_A+\hbar\bar{\nu}_\lambda+\bar{\varepsilon}_\lambda^L$ respectively, where

$$\begin{aligned}
\bar{\varepsilon}_0^L &= \langle A;\ \bar{0}-\bar{0}|\overline{H}_L|A;\ \bar{0}-\bar{0}\rangle \\
\bar{\varepsilon}_\lambda^L &= \langle A;\ \bar{0}-\bar{1}_\lambda-\bar{0}|\overline{H}_L|A;\ \bar{0}-\bar{1}_\lambda-\bar{0}\rangle.
\end{aligned} \tag{4.15}$$

The quantity $(\bar{\varepsilon}_\lambda^L-\bar{\varepsilon}_0^L)$ is the level shift due to the excited transformed oscillator, i.e., that part of the self energy of the system due to the

oscillator. We shall demand that this vanishes, i.e., that $\bar{\varepsilon}_\lambda^L = \bar{\varepsilon}_0^L$. This means that in the case of one transformed oscillator excited the canonical transformation is adjusted so that the self energy of the system due to the oscillator is absorbed into the energy of the oscillator. Unlike the untransformed oscillators which behave like particles of zero rest mass, the transformed ones will be seen to behave like particles with a non-zero rest mass.

Now the eigenvalue of the transformed Hamiltonian $\overline{H}$ diagonalised by the perturbation method carried to infinite order should equal that of H diagonalised in the same way, provided the perturbation expansion converges, i.e., for the states $|A;\ 0{-}0{-}0\rangle$ and $|A;\ 0{-}1_\lambda{-}0\rangle$ we have

$$E_A + \bar{\varepsilon}_0^L = E_A + \varepsilon_0^L$$

and

$$E_A + \hbar\bar{\nu}_\lambda + \bar{\varepsilon}_\lambda^L = E_A + \hbar\nu_\lambda + \varepsilon_\lambda^L .$$

Using the condition $\bar{\varepsilon}_0^L = \bar{\varepsilon}_\lambda^L$ we get

$$\mu_\lambda(\bar{\nu}_\lambda) = \frac{\hbar\nu_\lambda}{\hbar\nu_\lambda + \varepsilon_\lambda} \tag{4.16}$$

where

$$\varepsilon_\lambda = \varepsilon_\lambda^L - \varepsilon_0^L .$$

Eq. (4.16) serves as our definition of μ_λ. In the case in which we consider frequencies not in resonance with excited states of the medium eq. (4.16) is similar to a definition of refractive index given by Neamtan [17]). It differs insofar as we have defined the refractive index for a given frequency in the interacting system, which as we shall see later leads to the exact Sellmeyer-Drude dispersion relation.

The zero-order system described by eigenfunctions of $\overline{H}_0$ now has the correct time dependence of the interacting system of radiation and medium. The canonical transformation has accounted for that part of the time dependence which is due to virtual transitions involving the real photon. For both the states of zero or one transformed oscillator excited $\overline{H}_L$ gives merely the self energy $\bar{\varepsilon}_0^L$ of the medium in the absence of radiation.

We now show that eq. (4.16) is the quantal definition of the refractive index for a single oscillator excited. To see this consider the time dependence of the operators Q_λ^*. Using

$$\dot{Q}_\lambda^* = \frac{i}{\hbar}[\overline{H},\ Q_\lambda^*] \tag{4.17}$$

we find

$$\langle A;\ \bar{0}\ldots\bar{1}_\lambda\ldots\bar{0}|\ddot{Q}_\lambda^*|A;\ \bar{0}\ldots\bar{0}\ldots\bar{0}\rangle + \tilde{\nu}_\lambda^2\langle A;\ \bar{0}\ldots\bar{1}_\lambda\ldots\bar{0}|Q_\lambda^*|\bar{0}\ldots\bar{0}\ldots\bar{0}\rangle = 0 \quad (4.18)$$

with

$$\tilde{\nu}_\lambda = c/\lambda\mu_\lambda.$$

From (4.18) we see that μ_λ is to be identified with the refractive index of a single photon. The definition is general for gases and liquids and it should also be possible to calculate μ_λ for crystalline media. In this case the polarisation energy ε_λ would be a function of both the direction of propagation $\mathbf{K}_\lambda$ of the wave and its direction of polarisation $\mathbf{e}_\lambda$.

It should be noted that in general the propagation properties of a photon in the medium depend on the intensity of the radiation present. Thus for a particular state with several oscillators excited say $|A;\ \bar{n}_1-\bar{n}_\lambda-\rangle$ one could define the refractive index by an equation similar to (4.16) in which $\hbar\nu_\lambda+\varepsilon_\lambda$ is replaced by the energy required to excite one more oscillator in the above state, i.e.,

$$\hbar\nu_\lambda+\langle A;\ n_1\ldots n_\lambda+1\ldots|H_L|A;\ \ldots n_\lambda+1\ldots\rangle - \langle A;\ \ldots n_\lambda\ldots|H_L|A;\ \ldots n_\lambda\ldots\rangle$$

One then obtains similarly to (4.18)

$$\langle A;\ \ldots\overline{n_\lambda+1}\ldots|\ddot{Q}_\lambda^*|A;\ \bar{n}_1\ldots\bar{n}_\lambda\ldots\rangle + \tilde{\nu}_\lambda^2\langle A;\ \ldots\overline{n_\lambda+1}\ldots|Q_\lambda^*|A;\ \ldots\bar{n}_\lambda\ldots\rangle = 0$$

This however would involve redefinition of μ_λ for different states and would be of little use in our canonical transformation. For states with more than one oscillator excited the energy required to excite one more oscillator in the state λ will differ from $\hbar\nu_\lambda+\varepsilon_\lambda$ only by terms of the fourth order in perturbation theory, i.e., corresponding to terms non-linear in the field in classical theory. In most of the processes we later consider we use states in which there is at most one oscillator excited. Such states will be involved in the lowest order contribution to these processes so that it is convenient to define the refractive index of a single quantum the way we have done here.

Excited states of the oscillators $\overline{H}_R$ will be called "physical photons". They are photons which have a self energy due to the polarisation of the medium in which they propagate. We have for

the energy $\overline{E}_\lambda$ and momentum $\overline{P}_\lambda$ of a "physical photon" of frequency $\bar{\nu}_\lambda$

$$\overline{E}_\lambda = \hbar\bar{\nu}_\lambda = \hbar\nu_\lambda + \varepsilon_\lambda \tag{4.19}$$

and

$$|\overline{\mathbf{P}}_\lambda| = \frac{\mu_\lambda \overline{E}_\lambda}{c}. \tag{4.20}$$

The momentum is obtained as follows. The momentum operator $\mathbf{P}$ in the untransformed system corresponding to the Hamiltonian (4.1) is

$$\mathbf{P} = \sum_\lambda 2cn_\lambda \nu_\lambda \mathbf{K}_\lambda q_\lambda q_\lambda^* + \sum_i \mathbf{p}_i$$

where $\mathbf{p}_i$ is the momentum of the ith electron. In the transformed variables $\mathbf{P}$ becomes

$$\mathbf{P} = \sum \bar{n}_\lambda \overline{\mathbf{P}}_\lambda + \sum_i \mathbf{p}_i$$

where

$$\overline{\mathbf{P}}_\lambda = 2c\bar{\nu}_\lambda \overline{\mathbf{K}}_\lambda Q_\lambda^* Q_\lambda, \qquad |\overline{\mathbf{K}}_\lambda| = \frac{\bar{\nu}_\lambda}{c}.$$

Now consider the commutators

$$[\overline{\mathbf{P}}_\lambda, Q_\lambda^*] = \hbar\overline{\mathbf{K}}_\lambda Q_\lambda^* \mu_\lambda$$
$$[\overline{\mathbf{P}}_\lambda, Q_\lambda] = -\hbar\overline{\mathbf{K}}_\lambda Q_\lambda \mu_\lambda .$$

Taking matrix elements of these we find

$$\{\langle A;\ \bar{0}-\bar{1}_\lambda-|\overline{\mathbf{P}}_\lambda|A;\ -\bar{1}_\lambda \ldots\rangle - \langle A;\ \bar{0}-\bar{0}-\bar{0}|\overline{\mathbf{P}}_\lambda|A;\ \bar{0}-\bar{0}-\bar{0}\rangle - \hbar\overline{\mathbf{K}}_\lambda\mu_\lambda\} \cdot \langle A;\ \bar{0}-\bar{1}_\lambda-|Q_\lambda^*|A;\ \bar{0}-\bar{0}-\bar{0}\rangle = 0 \tag{4.21}$$

and

$$\{\langle A;\ \bar{0}-\bar{1}_\lambda-\bar{0}|\overline{\mathbf{P}}_\lambda|A;\ \bar{0}-\bar{1}_\lambda-\bar{0}\rangle - \langle A;\ \bar{0}-\bar{0}-\bar{0}|\overline{\mathbf{P}}_\lambda|A;\ \bar{0}-\bar{0}-\bar{0}\rangle + \hbar\overline{\mathbf{K}}_\lambda\mu_\lambda\} \cdot \langle A;\ \bar{0}-\bar{0}-\bar{0}|Q_\lambda|A;\ \bar{0}-\bar{1}_\lambda-\bar{0}\rangle = 0. \tag{4.22}$$

Consider for example (4.21). The operator Q_λ^* has a nonvanishing matrix element for the creation of a "physical photon" of wavelength λ. Thus the curly bracket must be zero which means that the momentum changes by $+\hbar\overline{\mathbf{K}}_\lambda\mu_\lambda$ in the creation of the "physical photon" i.e.,

$$|\overline{\mathbf{P}}_\lambda| = \frac{\hbar\bar{\nu}_\lambda}{c}\mu_\lambda \tag{4.23}$$

from which eq. (4.20) follows.

We next show that the quantum definition (4.16) of the refractive

index gives the usual expression when we calculate it for a gas. A similar calculation for the particular case of frequencies displaced from any resonances has been made by Neamtan [17]).

5. Refractive Index of a Gas

In order to calculate the refractive index we first require the polarisation energy ε_λ. In the following calculations the self energy terms H_s will be left out. They only cancel infinite sums of matrix elements which are easily recognised as self energies and which will be dropped from the terms where they occur.

The first approximation we make is to use a non-relativistic Hamiltonian for the interaction between the medium and radiation since the electrons have small momenta in the rest frame of the medium. We write

$$\begin{aligned} H_{RM} &= \sum_i \frac{e_i^2}{2mc^2}\mathbf{A}^2(\mathbf{r}_i) - \sum_i \frac{e_i}{mc}\mathbf{p}_i\mathbf{A}(\mathbf{r}_i) \\ &= H_{RM}^{(2)} + H_{RM}^{(1)} \end{aligned} \tag{5.1}$$

where the suffix (2) stands for the perturbation involving emission or absorption of 2 quanta at a time and (1) for one at a time. $\sum_i$ sums over all the electrons in the medium.

Suppose we start with the medium in state A and an oscillator of wavelength λ excited. Then to second order the polarisation energy is

$$\varepsilon_\lambda = \varepsilon_\lambda^{(2)} + \varepsilon_\lambda^{(1)} \tag{5.2}$$

where, from eq. (4.9),

$$\begin{aligned} \varepsilon_\lambda^{(2)} &= \langle A;\, 1_\lambda | H_{MR}^{(2)} | A;\, 1_\lambda\rangle - \langle A;\, 0_\lambda | H_{MR}^{(2)} | A;\, 0_\lambda\rangle \\ \varepsilon_\lambda^{(1)} &= \mathrm{Re}\left\{ \sum_\phi \frac{\langle A;\, 1_\lambda | H_{MR}^{(1)} | \phi\rangle \langle \phi | H_{MR}^{(1)} | A;\, 1_\lambda\rangle}{E_A + \hbar\nu_\lambda + \varepsilon_\lambda^L - E_\phi - \varepsilon_\phi^L + \frac{i\hbar}{2}\gamma_\phi} \right. \\ &\quad \left. - \sum_\psi \frac{\langle A;\, 0_\lambda | H_{MR}^{(1)} | \psi\rangle \langle \psi | H_{MR}^{(1)} | A;\, 0_\lambda\rangle}{E_A + \varepsilon_0^L - E_\psi - \varepsilon_\psi^L + \frac{i\hbar}{2}\gamma_\psi} \right\}. \end{aligned} \tag{5.3}$$

We have written $|A;\, 1_\lambda\rangle$ for $|A;\, 0 \ldots 1_\lambda \ldots 0\rangle$, and $|\phi\rangle$ and $|\psi\rangle$ are general states.

Consider first $\varepsilon_\lambda^{(2)}$. Using the well known matrix elements of the q_λ's we find

$$\varepsilon_\lambda^{(2)} = \frac{2\pi\hbar}{\nu_\lambda} \sum_i \frac{e_i^2}{m}. \tag{5.4}$$

We next require $\varepsilon_\lambda^{(1)}$. From eqs. (5.1) and (5.3) we have

$$\begin{aligned}\varepsilon_\lambda^{(1)} = 4\pi c^2 \operatorname{Re}\Bigg\{ &\sum_B \frac{|\langle B;\ 0_\lambda| \sum_i \frac{e_i}{mc} \mathbf{p}_i \mathbf{e}_\lambda q_\lambda e^{i\mathbf{K}_\lambda \cdot \mathbf{r}} |A;\ 1_\lambda\rangle|^2}{E_A + \hbar\nu_\lambda + \varepsilon_\lambda - E_B + \frac{i\hbar}{2}\gamma_B} \\ &+ \sum_B \frac{|\langle B;\ 2_\lambda| \sum_i \frac{e_i}{mc} \mathbf{p}_i \mathbf{e}_\lambda q_\lambda^* e^{-i\mathbf{K}_\lambda \cdot \mathbf{r}} |A;\ 1_\lambda\rangle|^2}{E_A - \hbar\nu_\lambda + \varepsilon_\lambda - E_B - \varepsilon_{2\lambda} + \frac{i\hbar}{2}\gamma_{B2\lambda}} \\ &- \sum_B \frac{|\langle B;\ 1_\lambda| \sum_i \frac{e_i}{mc} \mathbf{p}_i \mathbf{e}_\lambda q_\lambda^* e^{-i\mathbf{K}_\lambda \cdot \mathbf{r}} |A;\ 0_\lambda\rangle|^2}{E_A - E_B - \hbar\nu_\lambda - \varepsilon_\lambda + \frac{i\hbar}{2}\gamma_{B1\lambda}} \Bigg\}\end{aligned} \tag{5.5}$$

where B is some excited state of the medium and $\varepsilon_{2\lambda}$ the polarisation energy with two oscillators excited.

Now the small line breadths $\gamma_{B1\lambda}$ and $\gamma_{B2\lambda}$ in the last two terms of (5.5) are only of importance when the real part of the energy denominators vanish. This never happens for these terms so that the line breadths can be neglected. Also the polarisation energy $\varepsilon_{2\lambda}$ deriving from two oscillators excited in the medium differs from twice the polarisation of either one excited only by terms of the fourth order. Therefore the energy denominators of the last two terms of (5.5) can be written as both equal to $(E_A - E_B - \hbar\nu_\lambda - \varepsilon_\lambda)$. Then using the matrix elements of the q_λ's, $\varepsilon_\lambda^{(1)}$ becomes

$$\begin{aligned}\frac{2\pi\hbar}{\nu_\lambda} \operatorname{Re}\Bigg\{ &\sum_B \frac{|\langle B| \sum_i \frac{e_i}{m} \mathbf{p}_i \cdot \mathbf{e}_\lambda e^{i\mathbf{K}_\lambda \cdot \mathbf{r}} |A\rangle|^2}{E_A - E_B + \hbar\bar{\nu}_\lambda + \frac{i\hbar}{2}\gamma_B} \\ &+ \sum_B \frac{|\langle B| \sum_i \frac{e_i}{m} \mathbf{p}_i \cdot \mathbf{e}_\lambda e^{-i\mathbf{K}_\lambda \cdot \mathbf{r}} |A\rangle|^2}{E_A - E_B - \hbar\bar{\nu}_\lambda} \Bigg\}\end{aligned} \tag{5.6}$$

where we have written $\hbar\tilde{\nu}_\lambda = \hbar\nu_\lambda + \varepsilon_\lambda$. The only line breadth of importance is γ_B which is the spontaneous emission probability for the excited state B of the medium.

We now make two approximations. The first will be that the medium is of low density. This enables us to neglect the direct interaction between different atoms so that the above matrix elements will be different from zero only if B represents a state in which only that atom to which the ith electron belongs has been excited. Sums $\sum_B$ over such matrix elements will then be replaced by a sum $\sum_n$ over excited states Ψ_n of a single atom.

The second approximation is to treat the atoms as fixed and assume the wavelength λ to be much greater than an atomic radius. Thus the exponentials $\exp(i\mathbf{K}_\lambda \cdot \mathbf{r}_i)$ will be replaced by their values at the positions of the centre of the atom to which the ith electron belongs. We then find by combining $\varepsilon_\lambda^{(1)}$ and $\varepsilon_\lambda^{(2)}$

$$\mu_\lambda^{-1} = \mathrm{Re}\left\{ 1 + \frac{2\pi}{\nu_\lambda^2} \sum_{j,k} \frac{e_k^2}{m} + \frac{2\pi}{\nu_\lambda^2} \sum_n |\langle \Psi_0 | \sum_k \frac{e_k}{m} \mathbf{e}_\lambda \cdot \mathbf{p}_k | \Psi_n \rangle|^2 \right.$$
$$\left. \times \left[\frac{|\sum_j \mathrm{e}^{-i\mathbf{K}_\lambda \cdot \mathbf{R}_j}|^2}{E_0 - E_n - \hbar\tilde{\nu}_\lambda} + \frac{|\sum_j \mathrm{e}^{i\mathbf{K}_\lambda \cdot \mathbf{R}_j}|^2}{E_0 - E_n + \hbar\tilde{\nu}_\lambda + \frac{i\hbar}{2}\gamma_n} \right] \right\} \tag{5.7}$$

where $\mathbf{R}_j$ is the position of the jth atom, Σ_j sums over atoms in a unit volume and Σ_k over the electrons in a single atom. E_0 and E_n are energy eigenvalues of the atomic states Ψ_0 and Ψ_n and γ_n is the spontaneous emission probability for the state Ψ_n.

The expression (5.7) can be simplified by making use of the sum rule for oscillator strengths f_{n0}, namely

$$\sum_n f_{n0} = \frac{2m}{\hbar} \sum_n \tilde{\nu}_{n0} |\langle \Psi_0 | \mathbf{e}_\lambda \cdot \mathbf{r}_k | \Psi_n \rangle|^2 = 1 \tag{5.8}$$

where $\hbar\tilde{\nu}_{n0} = E_n - E_0$. This sum rule is true for hydrogen-like atoms where we do not have to worry about forbidden transitions to levels already filled.

If we further assume a random distribution of atoms in the medium and average over the phases for the sums $\sum_j$ in (5.7) we find by making use of (5.8) the expression

$$\mu_\lambda^{-1} = 1 - \frac{4\pi N}{\hbar} \sum_n \frac{\tilde{\nu}_{n0}(\tilde{\nu}_{n0}^2 - \tilde{\nu}_\lambda^2) |\sum_k e_k \langle \Psi_0 | \mathbf{e}_\lambda \cdot \mathbf{r}_k | \Psi_n \rangle|^2}{(\tilde{\nu}_{n0}^2 - \tilde{\nu}_\lambda^2)^2 + \frac{\gamma_n^2}{4}(\tilde{\nu}_{n0} + \tilde{\nu}_\lambda)^2} \tag{5.9}$$

where N is the number of atoms in a unit volume. Finally, since we are dealing with a medium of low density we can write approximately $\mu_\lambda = 2-\mu_\lambda^{-1}$.

The Lorenz-Lorentz correction is missing from formula (5.9), though of course not from the definition of μ_λ. This is because we simplified the matrix elements by assuming the atoms to be located at completely uncorrelated positions, as in our classical treatment above.

The expression (5.9) agrees with the Sellmeyer-Drude dispersion formula where we have only one species of atom. Although we have only calculated μ_λ for a gas the definition (4.16) is general and could under certain conditions be applied to solids. The above calculation of the refractive index is more general than that of Neamtan [17]) in that (5.9) applies in the region of maximum dispersion when $\tilde{\nu}_\lambda \approx \tilde{\nu}_{n0}$.

Consider under what conditions it is valid to derive the refractive index by the perturbation method we have used here. We would expect to obtain an accurate result provided $|\mu_\lambda - 1| \ll 1$. We can examine this condition in a little more detail. At worst the refractive index (5.9) rises in the resonance regions to a maximum value μ_M where

$$\mu_M - 1 \approx \pi N \frac{e^2}{\hbar c} \frac{\hbar}{mc} c^2 \frac{f_{n0}}{\gamma_n \tilde{\nu}_{n0}}.$$

Using the expression for the spontaneous emission probability given in Part II the condition becomes

$$Nv \ll 1 \tag{5.10}$$

where

$$v = \frac{\pi}{2} \frac{f_{n0}}{\Sigma_{n'} \lambda_{nn'}^{-2} \lambda_{n0}^{-1} f_{nn'}}.$$

The sum $\Sigma_{n'}$ extends over all states $\Psi_{n'}$ of energy lower than E_n to which a transition is possible, $f_{nn'}$ is the corresponding oscillator strength for the transition, and the wavelength $\lambda_{nn'}$ is $\hbar c (E_n - E_{n'})^{-1}$. The quantity Nv represents the number of atoms in the small volume v. Due to the sum over n' we may however satisfy the condition (5.10) over a range of wavelengths larger than the mean interatomic distance. It should be noted of course that the further displaced we are from the resonance regions the more easily satisfied are the conditions for a perturbation calculation of μ_λ.

The condition (5.10) is also made less stringent at normal temperatures by the collision and Doppler broadening of the line breadth γ_n.

PART II: ČERENKOV RADIATION AND ENERGY LOSS OF FAST CHARGED PARTICLES

1. Introduction

In the first part we discussed the excitation of a transverse physical photon oscillator in a medium, and the quantum theory of refractive index. We now consider the perturbations caused by the passage of a fast charged particle through the interacting system of atoms. In most of the particular processes which we consider the transverse part of the field of the particle will play a dominant role. Thus although a medium can undergo longitudinal plasma oscillations, we shall neglect the possibility of these excitations and the resulting screening of the Coulomb interaction between the medium and the particle in this treatment. These latter effects have been treated on quantum mechanics by a number of other authors [20]).

We begin by applying the canonical transformation to physical photons to the system in which a fast charged particle is present in the medium, and then make some general considerations of the possible transitions involving the physical photon field, of which this system is capable. The particular processes of the first and second order contributions to Čerenkov radiation are then discussed in §§ 3 and 4, and the cross-section for the ionization and excitation of atoms in the medium in § 5. In the remaining sections we are concerned with the energy loss of the particle in the medium. Throughout these calculations it is frequently important to consider the line breadths of the various states of the system consisting of medium and particle and physical photons, and in calculating these we make use of standard radiation damping theory [19]).

2. The Passage of a Fast Charged Particle through a Polarisable Medium

Consider a fast charged particle passing through a medium of atoms. In the notation of Part I the Hamiltonian for the system

can be written

$$H = (H_M+H_R+H_P)+(H_{PR}+H_{MR}+H_e) \tag{2.1}$$

where H_P is the Hamiltonian for the particle, H_{PR} the interaction between the particle and radiation and H_e the Coulomb interaction between the particle and atomic electrons and nuclei in the medium.

We now apply the canonical transformation discussed in Part I with μ_λ defined by eq. (4.16) (I) to the above Hamiltonian. The transformed Hamiltonian is then

$$\overline{H} = (H_M+\overline{H}_R+H_P)+(\overline{H}_{MR}+\overline{H}_{PR}+H_e+H_{\text{pol}}) = \overline{H}_0+\overline{H}_i \tag{2.2}$$

where

$$\overline{H}_R = \tfrac{1}{2}\sum_\lambda \bar{n}_\lambda (\bar{P}_\lambda^2+\tilde{\nu}_\lambda^2 \bar{Q}_\lambda^2)$$

and

$$H_{\text{pol}} = \tfrac{1}{2}\sum_\lambda \bar{n}_\lambda(\mu_\lambda^2-1)\,\bar{P}_\lambda^2 .$$

Now the zero-order system defined by the eigenfunctions of $\overline{H}_0$ will not in general have the correct eigenvalues of the interacting system of medium, particle and radiation due to virtual processes involving the particle which have not been accounted for by our transformation. Thus we also add to $\overline{H}_0$ a diagonal level shift operator $\overline{H}'_L$ which accounts for this additional shift in the energy eigenvalues of the zero-order system due to the interaction, i.e., write

$$\overline{H} = \overline{K}_0+\overline{K} = (\overline{H}_0+\overline{H}'_L)+(\overline{H}_i-\overline{H}'_L) \tag{2.3}$$

where $\overline{H}'_L$ is defined so that the imaginary part of the line breadth operator Γ for the system vanishes. There is then no further displacement of the energy eigenvalues of $\overline{K}_0$ due to the interaction $\overline{K}$.

For the eigenfunctions and eigenvalues of $\overline{K}_0$ we shall use the usual notation

$$\begin{aligned}\langle A;\, p;\, -\bar{n}_\lambda-|\overline{K}_0|\, A;\, p;\, -\bar{n}_\lambda-\rangle &= E_A+E_p+\sum_\lambda \bar{n}_\lambda \hbar\bar{\nu}_\lambda \\ &\quad +\langle A;\, p;\, -\bar{n}_\lambda-|\overline{H}'_L|A;\, p;\, -\bar{n}_\lambda-\rangle\end{aligned} \tag{2.4}$$

where p denotes the state of the particle and $\bar{n}_\lambda$ is the number of physical photons in the excited state λ. The zero-order system described by eigenfunctions of $\overline{K}_0$ is one in which the frame in which the medium is at rest is a preferred one. μ_λ is the refractive

index for radiation of frequency $\tilde{\nu}_\lambda$ in the rest frame of the medium.

The interacting system of medium+particle+physical photons is in general capable of making a large number of real transitions from any particular state say ϕ, and in this sense the state ϕ can be considered as a highly excited state with its appropriate line breadth. We shall be concerned in particular with transitions which start from a state with no transformed oscillators excited, namely $|A; p; \bar{0}-\bar{0}\rangle$, and finish in some other state. The general expressions for the probability amplitude $S(t)$, the line breadth operator Γ, the resonance denominator N, and the transition probability are then given by expressions identical to those of eqs. (4.5), (4.6), (4.7) and (4.8) of Part I where one simply uses the new interaction Hamiltonian $\overline{K}$ in these formulae.

Consider some of the lowest order transitions which are possible from the state $|A; p; \bar{0}-\bar{0}\rangle$. The first one of interest is that in which a real physical photon is emitted by the particle without excitation of the medium, namely,

$$|A; p_1; \bar{0}-\bar{0}-\bar{0}\rangle \to |A; p_2; \bar{0}-\bar{1}_\lambda-\bar{0}\rangle. \tag{2.5}$$

The real emission of ordinary photons in free space by a charged particle is impossible. This is simply because for a particle of finite rest mass any change in its energy and momentum, say (E_1-E_2) and $(\mathbf{p}_1-\mathbf{p}_2)$, involved in a real process must satisfy

$$\frac{E_1-E_2}{c|\mathbf{p}_1-\mathbf{p}_2|} < 1. \tag{2.6}$$

For photon emission this ratio is equal to one. However under certain circumstances the process (2.5) can take place and satisfy (2.6) due to the energy-momentum relation for physical photons. The transition (2.5) will be identified with the lowest order Čerenkov process. In fact the process of Čerenkov radiation will be seen to derive from a series of terms corresponding to all those transitions in which the interaction between the medium and the physical photon radiation is not involved, even in intermediate states. Thus for example we shall also consider the second-order contribution

$$|A; p_1; \bar{0}-\bar{0}-\bar{0}-\bar{0}\rangle \to |A; p_2; \bar{0}-\bar{1}_\lambda-\bar{1}_{\lambda'}-\bar{0}\rangle. \tag{2.7}$$

The second type of process we shall be interested in is that corresponding to the excitation or ionization of atoms in the

medium, namely

$$|A;\ p_1;\ \bar{0}-\bar{0}\rangle \rightarrow |A^*;\ p_2;\ \bar{0}-\bar{0}\rangle. \tag{2.8}$$

Now consider the initial and final states involved in these processes. One can derive a transition probability which is independent of time from the probability amplitude $S(t)$ only for the case in which the line breadths of the initial and final states can be neglected. Their lifetimes must be long compared with the time taken by the emission or excitation process involved. This is usually the case. Suppose the initial state consisting of simply a particle passing through an unexcited medium in the absence of radiation has a lifetime $\bar{\gamma}^{-1}$. This is determined mainly by collisions in which the medium becomes excited by the particle, so that $\bar{\gamma}^{-1}$ is the mean "intercollision time". It means that inside the medium one cannot measure the energy of the particle to within an uncertainty $\Delta E = \hbar\bar{\gamma}$ due to the reaction of the medium on the particle. However the matrix elements for these transitions are functions of the energy E of the particle and the energy transfers ε involved in the collision under consideration. If these are large compared with ΔE then we expect this uncertainty to be unimportant. We shall make a rough estimate of this.

Suppose $\mathrm{d}E/\mathrm{d}x$ is the average energy loss for a fast charged particle passing through a medium and I the average ionization potential for the atomic collisions. Then using an approximate formula due to Bloch [3]), namely

$$I = 13.5Z \text{ eV}$$

where Z is the atomic charge of the atoms in the medium, we can write

$$\Delta E \approx \frac{\hbar\beta c}{13.5Z}\frac{\mathrm{d}E}{\mathrm{d}x} \quad (E \text{ in eV}). \tag{2.9}$$

For a typical example we refer to the measurements of the energy loss of mesons in Argon at N.T.P. by Parry, Rathgeber and Rouse [21]). They find a value for $\mathrm{d}E/\mathrm{d}x$ which rises to a maximum of about 3 keV/cm as the velocity of the mesons approach the velocity of light. Using $I = 234$ eV we then have $\Delta E = 2.10^{-4}$ eV. This is much less than the energy transfers we shall be considering and also considerably greater than the typical magnitudes of natural line breadths of excited atomic states. It should be noted of course

that this figure is only a rough estimate of ΔE. For a more exact calculation one should consider the distribution of energy loss to energy transfers of different magnitudes.

3. Quantum Theory of Čerenkov Radiation

Single Emission

The particle can now under certain conditions radiate physical photons in first order and we shall identify this process with the lowest order contribution to Čerenkov radiation. We consider the special case of a charged particle of spin 1/2, although any particle with a coupling to the electromagnetic field will give rise to a similar process.

Consider the field of virtual physical photons in the neighbourhood of the particle. Suppose those of wavelength λ occur at most a distance $d(\lambda)$ from the path of the particle. Then a physical photon emitted at an angle θ to the path of the particle can only have the point of its emission localised to within $\Delta x_1 = d(\lambda)(\sin\theta)^{-1}$. Until it has emerged from this region of the field we cannot say that it was a real emission.

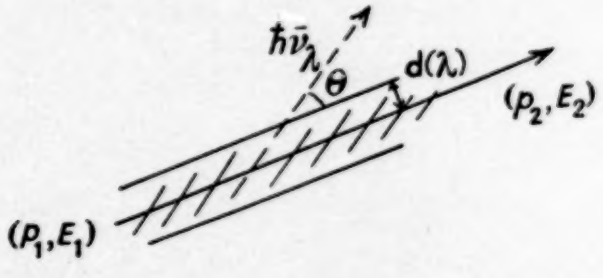

Suppose Δx_c is the mean distance between successive emissions of physical photons of wavelength λ. Then if $\Delta x_c \gg \Delta x_1$, we can find a Δx such that

$$\Delta x_c \gg \Delta x \gg \Delta x_1 \tag{3.1}$$

i.e. we can construct wavepackets to describe the emitted physical photons such that successive emissions will not interfere with each other. We will assume (3.1) and justify it later. Also since $\Delta x \gg \Delta x_1$, i.e. greater than the region of the field in which the physical photon is produced then the probability for its emission will be insensitive to the value of Δx. Thus we can let $\Delta x \to \infty$ and use plane wave functions for our physical photons. The pro-

bability calculated for the emission of such a "plane wave quantum" will be the same as that for a wave packet satisfying (3.1). This is because the range of wave numbers in our packet will be small compared with those present in the field around the particle, thus the uncertainty in momentum arising from the width of the packet will affect the emission probability less than the field itself.

Consider the process (2.5). We require the transition probability

$$\omega = \frac{2\pi}{\hbar} |U_{fi}|^2_{\mathrm{av}} \delta(E_i - E_f) \tag{3.2}$$

where

$$U_{fi} = \langle A;\ p_2;\ \bar{1}_\lambda | (\overline{K} + \overline{K}_{\mathrm{nd}} N \overline{K}_{\mathrm{nd}} + \ldots)_{\mathrm{nd}} | A;\ p_1;\ \bar{0} \rangle \tag{5.3}$$

which in lowest order from (2.3) and with

$$\overline{H}_{\mathrm{PR}} = -eZ \sum_\lambda \bar{n}_\lambda \mu_\lambda^{-1} \boldsymbol{\alpha} (Q_\lambda \mathbf{A}_\lambda + Q_\lambda^* \mathbf{A}_\lambda^*) \tag{3.4}$$

for a Dirac particle is

$$U_{fi} = -Ze\mu_\lambda^{-1} \langle A;\ p_2;\ \bar{1}_\lambda | \boldsymbol{\alpha} Q_\lambda^* \mathbf{A}_\lambda^* | A;\ p_1;\ \bar{0} \rangle.$$

We make use of the plane wave functions $u_1 \exp(-i\mathbf{p}_1 \cdot \mathbf{r}/\hbar)$ and $u_2 \exp(-i\mathbf{p}_2 \cdot \mathbf{r}/\hbar)$ for the initial and final states of the particle, where $\mathbf{p}_1$ and $\mathbf{p}_2$ are the momenta of the particle. Also using the matrix element

$$\langle \bar{1}_\lambda | Q_\lambda^* | \bar{0} \rangle = \sqrt{\frac{\hbar}{2\bar{\nu}_\lambda}} \tag{3.5}$$

U_{fi} becomes

$$-\frac{Ze}{\mu_\lambda} \left(\frac{2\pi\hbar c^2}{\bar{\nu}_\lambda} \right)^{\frac{1}{2}} (u_2^* \mathbf{e}_\lambda \boldsymbol{\alpha} u_1)$$

where $\mathbf{e}_\lambda$ is the polarisation vector of the physical photon. This expression is the lowest order matrix element for emission of a physical photon by the particle inside the medium. It differs from a similar expression used by Neamtan [17]) by a factor μ_λ^{-1}.

For the transition probability ω we require the sum over final spins and average over initial spins of the particle for positive energy states, i.e.,

$$|U_{fi}|^2_{\mathrm{av}} = \frac{Z^2 e^2}{\mu_\lambda^2} \frac{2\pi\hbar c^2}{\bar{\nu}_\lambda} \sum (u_2^* \mathbf{e}_\lambda \boldsymbol{\alpha} u_1)\ (u_1^* \boldsymbol{\alpha} \mathbf{e}_\lambda u_2).$$

Since $E_1 \approx E_2 \gg h\bar{\nu}_\lambda$ we make the approximation $E_1 = E_2 = E$ and $\mathbf{p}_1 = \mathbf{p}_2 = \mathbf{p}$. Then if ψ is the angle between $\mathbf{e}_\lambda$ and $\mathbf{p}$ the above expression simplifies to

$$|U_{fi}|^2_{\text{av}} = \frac{Z^2e^2}{\mu_\lambda^2}\,\frac{2\pi\hbar c^2}{\tilde{\nu}_\lambda}\,\frac{c^2p^2\cos^2\psi}{E^2}. \tag{3.6}$$

We now choose two orthogonal states of polarisation for the physical photon with $\mathbf{e}_\lambda$ perpendicular and parallel to the plane of $\mathbf{p}_1$ and $\mathbf{K}_\lambda$. Then $\cos^2\psi = 0$ for perpendicular polarisation and $\cos^2\psi = \sin^2\theta$ for parallel polarisation, where θ is the angle between $\mathbf{p}_1$ and $\mathbf{K}_\lambda$. Thus summing over the directions of polarisation (3.6) gives

$$\frac{Z^2e^2}{\mu_\lambda^2}\,\frac{2\pi\hbar c^2}{\tilde{\nu}_\lambda}\,\frac{v^2\cos^2\theta}{E^2} \tag{3.7}$$

where v is the velocity of the particle. We obtain the result then that the radiation is polarised with its electric vector in the plane defined by its direction of propagation and the path of the particle.

We have from the frequency-wavelength relation $\tilde{\nu}_\lambda = c\lambda^{-1}\mu_\lambda^{-1}$ the following expression for the density of final states for the physical photons:

$$\varrho(\tilde{\nu}_\lambda)\mathrm{d}\tilde{\nu}_\lambda = \frac{\mu_\lambda^3\tilde{\nu}_\lambda^2\mathrm{d}\nu_\lambda}{2\pi^2c^3}\,\frac{u_\lambda}{U_\lambda} \tag{3.8}$$

where the group velocity U_λ is obtained from the phase velocity u_λ,

$$U_\lambda = \frac{\mathrm{d}\left(\frac{u_\lambda}{\lambda}\right)}{\mathrm{d}\left(\frac{1}{\lambda}\right)}. \tag{3.9}$$

This gives the density of states per unit volume per unit range of angular frequency. Dispersion can sometimes be neglected.

Now the change in the energy of the particle in the emission process is approximately

$$E_1 - E_2 \approx \mu_\lambda v\,\frac{\hbar\tilde{\nu}_\lambda}{c}\cos\theta. \tag{3.10}$$

Hence the total number of emissions per second in the frequency interval $\mathrm{d}\tilde{\nu}_\lambda$ is given by

$$N(\tilde{\nu}_\lambda)\mathrm{d}\tilde{\nu}_\lambda = \mathrm{d}\tilde{\nu}_\lambda \int \frac{2\pi}{\hbar}\,|U_{fi}|^2_{\text{av}}\,\varrho(\tilde{\nu}_\lambda)\,\frac{\mathrm{d}\Omega}{4\pi}\,\delta\left(\frac{hv\mu_\lambda}{c}\cos\theta - h\tilde{\nu}_\lambda\right) \tag{3.11}$$

where $\mathrm{d}\Omega$ is the element of solid angle $\mathrm{d}\phi\mathrm{d}(\cos\theta)$. The integral (3.11) is non-vanishing if θ_0 exists such that

$$\cos\theta_0 = \frac{c}{v\mu_\lambda} \tag{3.12}$$

and becomes

$$N(\tilde{\nu}_\lambda)\,\mathrm{d}\tilde{\nu}_\lambda = Z^2\frac{v}{c}\frac{u_\lambda}{U_\lambda}\frac{e^2}{\hbar c}\sin^2\theta_0\cdot\mathrm{d}\tilde{\nu}_\lambda = Z^2\frac{v}{c}\frac{u_\lambda}{U_\lambda}\frac{e^2}{hc}\left(1-\frac{c^2}{v^2\mu_\lambda^2}\right)\mathrm{d}\tilde{\nu}_\lambda. \tag{3.13}$$

This expression gives the first order contribution to the number of physical photons emitted per second by the particle in the frequency interval $\mathrm{d}\tilde{\nu}_\lambda$ along a cone about the particle making an angle with its path of $\cos^{-1}(c/v\mu_\lambda)$. The radiation is also polarised in the plane of its direction of propagation and the path of the particle and is thus identified as Čerenkov radiation.

The energy radiated per second is

$$E(\tilde{\nu}_\lambda)\mathrm{d}\tilde{\nu}_\lambda = v\tilde{\nu}_\lambda\frac{u_\lambda}{U_\lambda}\frac{Z^2e^2}{c^2}\left(1-\frac{c^2}{v^2\mu_\lambda^2}\right)\mathrm{d}\tilde{\nu}_\lambda \tag{3.14}$$

which agrees with the classical expression. Before discussing this result we will first work out the emission probability for pairs of physical photons.

Double Emission

Since the real first order radiation process exists we expect the second order process, namely the simultaneous emission of two physical photons to show the effects of a resonance. The result of calculation is that there is a resonance in the emission probability for two physical photons with a width given by the probability for absorption of the physical photons by atomic electrons in the state $|A;\,p;\,\bar{0}-\bar{1}_\lambda-\bar{0}\rangle$ in which the particle is present. The resonance occurs in such a way that both physical photons tend to be emitted as if they were separate real emissions, i.e., along the Čerenkov cones appropriate to each frequency. Thus Čerenkov radiation as observed and defined by the angle – frequency relation with which it is emitted is contributed to by all the processes in which the particle simultaneously emits n physical photons without involving the interaction between the medium and physical photons even in intermediate states. Processes in which this interaction is involved are of a different type, for example Bremsstrahlung.

Consider the matrix element corresponding to the process of double emission. This is given by

$$U_{fi} = \langle A;\ p_2;\ \bar{1}_\lambda,\ \bar{1}_{\lambda'} | (\overline{K} + \overline{K}_{\mathrm{nd}} N \overline{K}_{\mathrm{nd}} + \ldots)_{\mathrm{nd}} | A;\ p_1;\ \bar{0},\ \bar{0} \rangle \quad (3.15)$$

where λ and λ' are the wavelengths of the physical photons with frequencies $\tilde{\nu}_\lambda$ and $\tilde{\nu}_{\lambda'}$, and we have abbreviated the states.

The contribution to this matrix element deriving from processes involving the interaction $\overline{H}_{MR}$ (i.e. incoherent processes) is negligible in the region where we later find a resonance, i.e., to radiation emitted along the Čerenkov cones. The only nondiagonal part of $\overline{K}$ which is effective in the second order term (3.15) is thus $(\overline{H}_{PR} + H_{\mathrm{pol}})$. However H_{pol} is an operator which merely changes the number of physical photons by 0 or ± 2 without operating on the particle state. It can only lead to virtual processes. Therefore the matrix element for the simultaneous emission of two physical photons becomes

$$\langle A;\ p_2;\ \bar{1}_\lambda,\ \bar{1}_{\lambda'} | \overline{H}_{PR} N \overline{H}_{PR} | A;\ p_1;\ \bar{0},\ \bar{0} \rangle.$$

We split this into two parts by writing

$$U_{fi} = U_{fi}^{(1)} + U_{fi}^{(2)}$$

with

$$U_{fi}^{(1)} = \frac{Z^2 e^2}{\mu_\lambda \mu_{\lambda'}} \langle p^2; \bar{1}_\lambda, \bar{1}_{\lambda'} | \alpha Q_\lambda^* \mathbf{A}_\lambda^* | p'; \bar{0}, \bar{1}_{\lambda'} \rangle \langle A; p'; \bar{0}, \bar{1}_{\lambda'} | N | A; p'; \bar{0}, \bar{1}_{\lambda'} \rangle \cdot \langle p'; \bar{0}, \bar{1}_{\lambda'} | \alpha Q_{\lambda'}^* \mathbf{A}_{\lambda'}^* | p_1; \bar{0}, \bar{0} \rangle \quad (3.16)$$

and

$$U_{fi}^{(2)} = \frac{Z^2 e^2}{\mu_\lambda \mu_{\lambda'}} \langle p_2; \bar{1}_\lambda, \bar{1}_{\lambda'} | \alpha Q_{\lambda'}^* \mathbf{A}_{\lambda'}^* | p; \bar{0}, \bar{1}_\lambda \rangle \langle A; p; \bar{0}, \bar{1}_\lambda | N | A; p; \bar{0}, \bar{1}_\lambda \rangle \cdot \langle p; \bar{0}, \bar{1}_\lambda | \alpha Q_\lambda^* \mathbf{A}_\lambda^* | p; \bar{0}, \bar{0} \rangle. \quad (3.17)$$

These matrix elements can be represented by two interaction diagrams corresponding to the two orders in which the physical

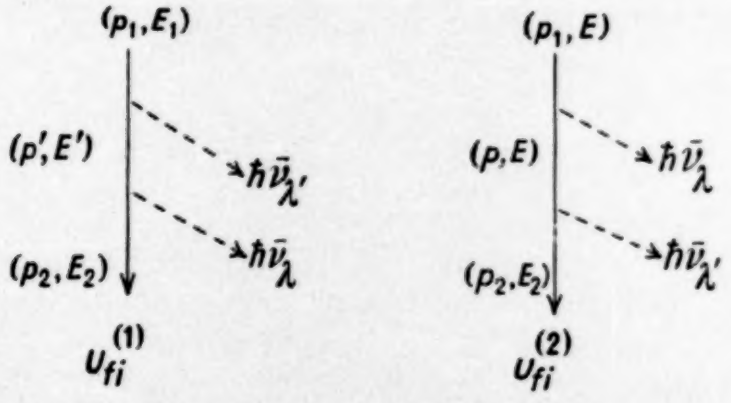

photons can be emitted. $(\mathbf{p}', E')$ and $(\mathbf{p}, E)$ are the momentum and energies for the intermediate states of the particle.

Now consider the matrix elements of the resonance denominators N. We require for example in (3.17),

$$\langle A;\ p;\ \bar{0},\ \bar{1}_\lambda|\left(E_i-\overline{K}_0+\frac{i\Gamma}{2}\right)^{-1}|A;\ p;\ \bar{0},\ \bar{1}_\lambda\rangle \qquad (3.18)$$

where E_i is the initial energy of the system i.e.,

$$E_i = E_A+E_1+\langle A;\ p_1;\ \bar{0}\ldots\bar{0}|\overline{H}'_L|A;\ p_1;\ \bar{0}\ldots\bar{0}\rangle \qquad (3.19)$$

and $\overline{H}'_L$ was defined so that the imaginary part of Γ vanishes. We have for the real part of the resonance denominator (3.18)

$$(E_1-E-\hbar\bar{\nu}_\lambda)-\Delta \qquad (3.20)$$

where Δ is the small energy shift

$$\langle A;\ p;\ \bar{0},\ \bar{1}_\lambda|\overline{H}'_L|A;\ p;\ \bar{0},\ \bar{1}_\lambda\rangle-\langle A;\ p;\ \bar{0},\bar{0}|\overline{H}'_L|A;\ p_1;\ \bar{0},\bar{0}\rangle.$$

Note that Δ is a small shift in addition to that arising from the interaction between the radiation field and the medium, this latter having already been accounted for by the canonical transformation. Using the condition $\mathrm{Im}\,(\Gamma)=0$ together with the definition of μ_λ one can show that, neglecting the reaction of the medium on the particle, Δ is to second order just the difference in the self energy of the particle in its field of virtual physical photons with none and one real physical photon present, i.e., an addition to the polarisation energy deriving from the particle. Since there is only one particle in comparison with the number of electrons per unit volume the additional shift Δ will be neglected. Using plane wave functions as in the previous case of single emission one then obtains for the matrix element U_{fi}

$$U_{fi}=\frac{4\pi e^2c^2Z^2}{\mu_\lambda\mu_{\lambda'}}\left(\frac{\hbar^2}{4\bar{\nu}_\lambda\bar{\nu}_{\lambda'}}\right)^{\frac{1}{2}}\left\{\frac{(u_2^*\boldsymbol{\alpha}\mathbf{e}_{\lambda'}u)(u^*\boldsymbol{\alpha}\mathbf{e}_\lambda u_1)}{E_1-E-\hbar\bar{\nu}_\lambda+\frac{i\hbar}{2}\bar{\gamma}_\lambda}\right.$$
$$\left.+\frac{(u_2^*\boldsymbol{\alpha}\mathbf{e}_\lambda u')(u'^*\boldsymbol{\alpha}\mathbf{e}_{\lambda'}u_1)}{E_1-E'-\hbar\bar{\nu}_{\lambda'}+\frac{i\hbar}{2}\bar{\gamma}_{\lambda'}}\right\} \qquad (3.21)$$

where $\bar{\gamma}_\lambda$ is given by the real part of Γ, i.e., the total transition probability out of the state $|A;\ p;\ \bar{0},\ \bar{1}_\lambda\rangle$, and $\bar{\gamma}_{\lambda'}$ out of the state $|A;\ p';\ \bar{1}_{\lambda'},\ \bar{0}\rangle$. We require to average the square of this matrix element over the initial spins and sum over the final spins of the particle for positive energy states. If we make the approximation

$p_1 = p_2 = p = p'$ in the numerator of (3.21) but not in the resonance denominator this reduces to

$$|U_{fi}|^2_{\text{av}} = \left(\frac{\pi e^2 Z^2}{\mu_\lambda \mu_{\lambda'}}\right)^2 \frac{2\hbar^2 c^4 p^4}{\tilde{\nu}_\lambda \tilde{\nu}_{\lambda'} E^4} \cos^2\psi_1 \cos^2\psi_2 \left[\frac{1}{(E_1 - E - \hbar\tilde{\nu}_\lambda)^2 + \frac{\hbar^2\tilde{\gamma}_\lambda^2}{4}} + \frac{1}{(E_1 - E' - \hbar\tilde{\nu}_{\lambda'})^2 + \frac{\hbar^2\tilde{\gamma}_{\lambda'}^2}{4}}\right] \quad (3.23)$$

where

$$\mathbf{p}\,\mathbf{e}_\lambda = p\cos\psi_1\,, \qquad \mathbf{p}\,\mathbf{e}'_\lambda = p\cos\psi_2.$$

If for the physical photon λ we now choose two orthogonal states of polarisation with $\mathbf{e}_\lambda$ in the plane of and perpendicular to the vectors $\mathbf{K}_\lambda$ and $\mathbf{p}$, we have $\cos\psi_1 = 0$ for perpendicular polarisation and $\cos\psi_1 = \sin\theta_1$ for parallel polarisation. Similarly the second physical photon leaves the particle at an angle θ_2 with its polarisation in the plane of its direction of propagation and the path of the particle.

Now consider the delta function which occurs in calculating the transition probability from the matrix element U_{fi}. Using elementary mechanics as in eq. (3.10) we have for the energy change of the system

$$\frac{\hbar v}{c}(\tilde{\nu}_\lambda \mu_\lambda \cos\theta_1 + \tilde{\nu}_{\lambda'} \mu_{\lambda'} \cos\theta_2) - \hbar\tilde{\nu}_\lambda - \hbar\tilde{\nu}_{\lambda'}. \quad (3.24)$$

Therefore the number of such pair emissions per second in which one physical photon has a frequency between $\tilde{\nu}_\lambda$ and $\tilde{\nu}_\lambda + \mathrm{d}\tilde{\nu}_\lambda$ and the other between $\tilde{\nu}_{\lambda'}$ and $\tilde{\nu}_{\lambda'} + \mathrm{d}\tilde{\nu}_{\lambda'}$ is

$$\mathrm{d}\tilde{\nu}_\lambda \mathrm{d}\tilde{\nu}_{\lambda'} \int \frac{\mathrm{d}\Omega_1}{4\pi} \frac{\mathrm{d}\Omega_2}{4\pi} \frac{2\pi}{\hbar} |U_{fi}|^2_{\text{av}} \varrho(\tilde{\nu}_\lambda)\varrho(\tilde{\nu}_{\lambda'}) \delta\left[\frac{\hbar v}{c}(\tilde{\nu}_\lambda \mu_\lambda \cos\theta_1 + \tilde{\nu}_{\lambda'} \mu_{\lambda'} \cos\theta_2) - \hbar(\tilde{\nu}_\lambda + \tilde{\nu}_{\lambda'})\right]$$

where the physical photons are emitted into the elements of solid angle

$$\mathrm{d}\Omega_1 = \mathrm{d}\phi_1\,\mathrm{d}(\cos\theta_1), \quad \mathrm{d}\Omega_2 = \mathrm{d}\phi_2\,\mathrm{d}(\cos\theta_2).$$

Consider the energy denominators in the expression $|U_{fi}|^2_{\text{av}}$. Momentum is conserved in the emission of each physical photon. Therefore

$$E_1 - E - \hbar\tilde{\nu}_\lambda \approx \hbar\tilde{\nu}_\lambda \left(\frac{cp_1 \mu_\lambda \cos\theta_1}{E_1} - 1 \right). \tag{3.25}$$

If we now write

$$x = \frac{h\nu\mu_\lambda \cos\theta_1}{c} \tilde{\nu}_\lambda - h\tilde{\nu}_\lambda \tag{3.26}$$

and

$$y = \frac{h\nu\mu'_\lambda \cos\theta_2}{c} \tilde{\nu}_{\lambda'} - h\tilde{\nu}_{\lambda'}$$

the integral becomes

$$N(\tilde{\nu}_\lambda, \tilde{\nu}_{\lambda'}) = \int \mathrm{d}x\, \mathrm{d}y\, \delta(x+y)\, \frac{v^2 e^4 Z^4}{2\pi\hbar} \frac{u_\lambda}{U_\lambda} \frac{u_{\lambda'}}{U_{\lambda'}} \sin^2\theta_1(x) \sin^2\theta_2(y) \left[\left(x^2 + \frac{\tilde{\gamma}_\lambda^2}{4} \right)^{-1} + \left(y^2 + \frac{\tilde{\gamma}_{\lambda'}^2}{4} \right)^{-1} \right]. \tag{3.27}$$

Thus if there exist values of θ_1, θ_2, $\tilde{\nu}_\lambda$, $\tilde{\nu}_{\lambda'}$ such that $x+y=0$ we can extend the range of integration for the above integral to $\pm\infty$ and also take the factors $\sin^2\theta_1$ and $\sin^2\theta_2$ outside with their values at $x = y = 0$. This is because the major contribution to (3.27) is at $x = 0$. Also it is easily shown that the change in $\sin^2\theta_1(x)$ for x changing by $\pm\tilde{\gamma}_\lambda$ is of order $\tilde{\gamma}_\lambda/\tilde{\nu}_\lambda$ i.e., very small. Hence from (3.26) we see that

$$\cos\theta_1 = \frac{c}{v\mu_\lambda}, \qquad \cos\theta_2 = \frac{c}{v\mu_{\lambda'}}, \tag{3.28}$$

and

$$N(\tilde{\nu}_\lambda, \tilde{\nu}_{\lambda'})\mathrm{d}\tilde{\nu}_\lambda \mathrm{d}\tilde{\nu}_{\lambda'} = Z^4\beta^2 \left(\frac{e^2}{\hbar c} \right)^2 \left(1 - \frac{c^2}{v^2\mu_\lambda^2} \right) \left(1 - \frac{c^2}{v^2\mu_{\lambda'}^2} \right) \frac{\tilde{\gamma}_\lambda + \tilde{\gamma}_{\lambda'}}{\tilde{\gamma}_\lambda \tilde{\gamma}_{\lambda'}} \frac{u_\lambda}{U_\lambda} \frac{u_{\lambda'}}{U_{\lambda'}} \mathrm{d}\tilde{\nu}_\lambda \mathrm{d}\tilde{\nu}_{\lambda'}. \tag{3.29}$$

This gives the total number of pair emissions per second in which one physical photon lies in the frequency interval $\mathrm{d}\tilde{\nu}_\lambda$ and the other in the interval $\mathrm{d}\tilde{\nu}_{\lambda'}$. From (3.28) we see that each physical photon is emitted as if it were an independent real emission. This second order process will therefore be identified as a further contribution to Čerenkov radiation. One can see that the process of emission of any number of physical photons without involving the medium will give rise to Čerenkov radiation.

Consider the line breadth $\bar{\gamma}_\lambda$ occurring in the above formula. This is given by the real part of the line breadth operator Γ which was defined by eq. (4.7) of Part I. For the state $|A; \mathfrak{p}; \bar{0}, \bar{1}_\lambda\rangle$ this is given mainly by the probability for the medium to absorb the physical photon, for frequencies in the neighbourhood of an excitation frequency of the medium. In fact we require $\bar{\gamma}_\lambda$ in this region of frequencies. Thus we shall write

$$\begin{aligned}\bar{\gamma}_\lambda &= \langle A; \mathfrak{p}; \bar{1}_\lambda| \operatorname{Re} \Gamma |A; \mathfrak{p}; \bar{1}_\lambda\rangle \\ &\approx \bar{\gamma} + \sum_n \frac{\bar{\gamma}|\langle A^*; \mathfrak{p}; \bar{0}|H_{MR}|A; \mathfrak{p}; \bar{1}_\lambda\rangle|^2}{(E_0 - E_n + h\bar{\nu}_\lambda)^2 + \dfrac{\hbar^2\bar{\gamma}^2}{4}}\end{aligned} \tag{3.30}$$

where E_0 and E_n are the ground state and excited state energies of the atom in the medium involved in the absorption. $\bar{\gamma}$ is formally the total transition probability out of the state $|A^*; \mathfrak{p}; \bar{0}\rangle$. It should be noted however that this is made up mainly of processes involving further excitation of the medium by the particle and is thus nearly the same as the line breadth of the state $|A; \mathfrak{p}; \bar{0}\rangle$ which represents the reaction of the medium on the particle as discussed with eq. (2.9). This is true even when one considers the collision and Doppler broadening of the spontaneous emission probability γ_n of the excited state $|A^*\rangle$.

The second i.e. absorption term is the dominant term of the expression (3.30) for $\bar{\nu}_\lambda$ close to the excitation frequency $\bar{\nu}_{n0}$. Thus we also neglect interference terms in (3.30) between absorption and the processes represented by $\bar{\gamma}$. Using the oscillator strengths f_{n0} defined by (5.8) (I) we thus find

$$\bar{\gamma}_\lambda \approx \bar{\gamma} + \frac{\pi N}{\mu_\lambda^2}\frac{e^2}{\hbar c}\frac{\hbar}{mc}\sum_n \frac{c^2\bar{\gamma} f_{n0}}{(\bar{\nu}_{n0} - \bar{\nu}_\lambda)^2 + \frac{1}{4}\bar{\gamma}^2} \tag{3.31}$$

for the line breadths to be used in eq. (3.29).

4. Discussion of the Čerenkov Calculations

We stated at the beginning of section 3 that a real first order emission process was possible for a fast charged particle passing through a medium of atoms. This derives from the coherent scattering of the field of the particle by the medium, and the particle could be said to radiate insofar as the physical photon emerged from a screened distance $d(\lambda)$ around the path of the particle.

In fact $d(\lambda)$ extends over many interatomic distances and the emission is in a real sense a collective process. The physical photon was also emitted along a cone making an angle θ to the direction of motion of the particle given by

$$\cos\theta = \frac{c}{\mu_\lambda v}$$

and polarised in the plane defined by its direction of propagation and the path of the particle. It was thus identified as Čerenkov radiation.

The fact that the interference is coherent and leads to emission along this cone is expressed in the quantal matrix element for this process in terms of the conservation of energy and momentum. Conservation is only possible by virtue of the relation $\overline{E}_\lambda = c\mu_\lambda^{-1}|\overline{P}_\lambda|$ for physical photons.

In our calculations we made use of plane wave physical photons. This is correct provided eq. (3.1) holds, i.e., $\Delta x_e \gg \Delta x_1$. In § 7 on the excitation and ionization of atoms in the medium it is shown that the loss of energy to the continuous ionized states takes place within a cylinder of radius at Čerenkov threshold

$$d(\lambda_i) = \frac{\beta c}{\tilde{\nu}_i}\left(\frac{2\tilde{\nu}_i}{\tilde{\gamma}_\lambda}\right)^{\frac{1}{2\mu^4}}$$

where $\tilde{\nu}_i$ is the ionization frequency of the atomic state and $\tilde{\gamma}_\lambda(\tilde{\nu}_i)$ is given by (3.31). By integrating (3.13) over a range of frequencies $\tilde{\nu}_i \pm \tilde{\gamma}_\lambda(\tilde{\nu}_i)$, over which we can assume μ to be slowly varying, the condition (3.1) for the ionization frequencies becomes

$$\sin\theta \gg Z^2\frac{e^2}{\hbar c}\left(1-\frac{1}{\mu^2(\tilde{\nu}_i)}\right)\left(\frac{2\tilde{\gamma}_\lambda}{\tilde{\nu}_i}\right)^{\frac{1}{2\mu^4}}$$

for the use of plane waves to be valid. This is satisfied except for very small values of θ, i.e., when the radiation is emitted down the path of the particle.

Now consider the higher order processes involving the emission of physical photons by the particle in which the medium interaction $\overline{H}_{MR}$ is not involved. The matrix element for the simultaneous emission of n physical photons contains a product of energy denominators for the intermediate states. These denominators resonate if their real parts vanish. This will occur when all the physical photons emerge as if they were independent real first

order emissions. Thus the bulk of the radiation of this n^{th} order type will emerge along the Čerenkov cones appropriate to each frequency, i.e., as if each conserved energy and momentum independently. We therefore identify Čerenkov radiation in general as the physical photon radiation emitted by the particle in which the interaction between the medium and the physical photon radiation is not involved — even in intermediate states.

Processes involving the medium will be of a different type, for example Bremsstrahlung. The contribution to the radiation along the Čerenkov cone arising from such incoherent processes is negligible — at least compared to the first two orders of the Čerenkov process. One could work out by quantum mechanics the effects of polarisation on many of these other processes and in the next section we consider the case of ionization and excitation of atoms in the medium.

The integrated contribution of the second order term (3.29) to the emission of, say, physical photons $h\bar{\nu}_\lambda$ due to pair emissions with physical photons $h\bar{\nu}_{\lambda'}$ will be much smaller than the first order contribution. This is simply because $\bar{\gamma}_\lambda$ and $\bar{\gamma}_{\lambda'}$ are absorption breadths given by (3.30) whereas the integral (e.g. for radiation from discrete states) extends over a range of frequencies corresponding to a spontaneous emission breadth which is much smaller. This is true even though the emission breadth, which is of importance in the resonance region for the refractive index, is broadened by other effects such as collision broadening etc. We thus expect the series of contributions tho Čerenkov radiation to converge very rapidly.

5. Excitation and Ionization of Atoms in the Medium

We now consider the transition

$$|A;\, p_1;\, \bar{0}-\bar{0}\rangle \to |A^*;\, p_2;\, \bar{0}-\bar{0}\rangle \tag{5.1}$$

in which A represents the ground state of the medium and A^* an excited state corresponding to one atom excited or ionized. As before the operator responsible for transitions is given by

$$(\overline{K}+\overline{K}_{\text{nd}}N\overline{K}_{\text{nd}}+\ldots)_{\text{nd}}$$

which gives to second order the matrix element

$$M = \langle A^*;\ p_2;\ \bar{0}|(H_c)_{\rm nd}|A;\ p_1;\ \bar{0}\rangle$$
$$+ \sum_{\phi} \langle A^*; p_2; \bar{0}|\bar{H}_{MR}|\phi\rangle\langle\phi|N|\phi\rangle\langle\phi|\bar{H}_{PR}|A; p_1; \bar{0}\rangle \qquad (5.2)$$
$$+ \sum_{\psi} \langle A^*; p_2; \bar{0}|H_{PR}|\psi\rangle\langle\psi|N|\psi\rangle\langle\psi|\bar{H}_{MR}|A;\ p_1;\ \bar{0}\rangle.$$

We again consider a fast charged particle of spin 1/2 so that H_{PR} is given by (3.4). The interaction between physical photons and electrons in the medium is given by

$$\bar{H}_{MR} = -e\sum_{\lambda}\sum_{i} \alpha_i \bar{n}_\lambda \mu_\lambda^{-1} (Q_\lambda^* \mathbf{A}_\lambda^* + Q_\lambda \mathbf{A}_\lambda) \qquad (5.3)$$

and the Coulomb interaction between the particle and electrons

$$H_c = \sum_i \frac{Ze^2}{r_{iP}}. \qquad (5.4)$$

Consider the collision of the fast charged particle with the particular atom in the medium which is involved in the excitation of the state A^*. Suppose that the electron changes its state from ψ_0 to ψ_n which have energies E_0 and E_n and that the particle changes its energy from E_1 to E_2. Then drawing as before a dotted line to represent a physical photon and a heavy line for an atomic electron we can draw interaction diagrams for the three matrix elements which contribute to the transition probability ω:

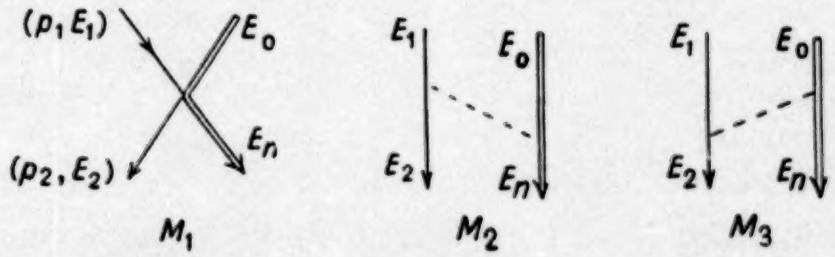

(Coulomb term) (particle emits) (particle absorbs)

The rest of the medium apart from the atom under consideration does not take part in the non-diagonal matrix elements except through the constant μ_λ. It does however enter into the diagonal resonance denominators N and determines their line breadths as will be seen later. It is through μ_λ and the line breadths of the intermediate states that the physical effects of the rest of the medium on this individual collision will be understood.

We have from eqs. (5.2) to (5.4)

$$M_1 = \langle \Psi_n; p_2; \bar{0} \left| \frac{Ze^2}{r_{ep}} \right| \Psi_0; p_1; \bar{0} \rangle \tag{5.5}$$

$$M_2 = Ze^2 \sum S \frac{1}{\mu_\lambda^2} \langle \Psi_n; p_2; \bar{0} | \alpha_e Q_\lambda \mathbf{A}_\lambda | \Psi_0; p_2; \bar{1}_\lambda \rangle \langle A; p_2; \bar{1}_\lambda | N | A; p_2; \bar{1}_\lambda \rangle \cdot \langle \Psi_0; p_2; \bar{1}_\lambda | \alpha Q_\lambda^* \mathbf{A}_\lambda^* | \Psi_0; p_1; \bar{0} \rangle \tag{5.6}$$

$$M_3 = Ze^2 \sum S \frac{1}{\mu_\lambda^2} \langle \Psi_n; p_2; \bar{0} | \alpha Q_\lambda \mathbf{A}_\lambda | \Psi_n; p_1; \bar{1}_\lambda \rangle \langle A^*; p_1; \bar{1}_\lambda | N | A^*; p_1; \bar{1}_\lambda \rangle \cdot \langle \Psi_n; p_1; \bar{1}_\lambda | \alpha_e Q_\lambda^* \mathbf{A}_\lambda^* | \Psi_0; p_1; \bar{0} \rangle \tag{5.7}$$

where Σ sums the polarisations of the physical photon in the intermediate state and α_e is the Dirac matrix for the atomic electron. S sums over the physical photons of different energies with the same momentum $\hbar\lambda^{-1} = \bar{P}_\lambda$. It sometimes happens that although for a unique energy we always have a unique momentum for physical photons a momentum does not always define a unique energy. This follows from the energy-momentum relation for physical photons.

It should be noted that μ_λ for our non-crystalline medium is independent of the direction of polarisation of the physical photon and so can be taken outside the summation Σ. We require then the transition probability

$$\omega = \frac{2\pi}{\hbar} |M|^2_{\text{av}} \delta(E_0 + E_1 - E_n - E_2) \tag{5.8}$$

with $M = M_1 + M_2 + M_3$.

Consider the resonance denominators in the above matrix elements. We have

$$\langle A; p_2; \bar{1}_\lambda | N | A; p_2, \bar{1}_\lambda \rangle = \left(\varepsilon_n - \hbar\bar{\nu}_\lambda + \frac{i\hbar}{2} \bar{\gamma}_\lambda \right)^{-1} \tag{5.9}$$

and

$$\langle A^*; p_1; \bar{1}_\lambda | N | A^*; p_1; \bar{1}_\lambda \rangle = -(\varepsilon_n + \hbar\bar{\nu}_\lambda)^{-1} \tag{5.10}$$

where $\varepsilon_n = E_1 - E_2 = E_n - E_0$ and $\bar{\gamma}_\lambda$ is the real part of the operator Γ for the state $|A; p_2; \bar{1}_\lambda\rangle$, which is given by equation (3.31). The line breadths are only of importance when the real part of the resonance denominator vanishes. Since this cannot happen for the matrix element M_3 we have neglected the corresponding line breadth in (5.10). The additional small shift Δ

in the energy eigenvalues, which was discussed for the second order Čerenkov process has also been neglected.

For the initial and final states of the particle P of charge eZ we use plane wave functions as in the case of Čerenkov radiation. Then

$$M_1 = Ze^2 \int \Psi_n^*(\mathbf{r}_e)\Psi_0(\mathbf{r}_e)u_2^* u_1^* \frac{e^{-\frac{i}{\hbar}(\mathbf{p}_2-\mathbf{p}_1)\mathbf{r}_p}}{|\mathbf{r}_p-\mathbf{r}_e|}\,d\tau_p\,d\tau_e \qquad (5.11)$$

where $\mathbf{r}_p$ and $\mathbf{r}_e$ are the position vectors of the particle and electron respectively. Using the matrix elements of Q_λ and Q_λ^*, the matrix elements M_2 and M_3 for which momentum is conserved at the particle vertex become

$$\begin{aligned} M_2 &= 2\pi c^2 e^2 ZS \frac{\hbar}{\bar{\nu}_\lambda \mu_\lambda^2} \\ &\left(\varepsilon_n - \hbar\bar{\nu}_\lambda + \frac{i\hbar}{2}\bar{\gamma}_\lambda\right)^{-1} \sum (u_2^* \mathbf{e}_\lambda \boldsymbol{\alpha} u_1) \int \Psi_n^* \boldsymbol{\alpha}_e \mathbf{e}_\lambda e^{\frac{i}{\hbar}(\mathbf{p}_1-\mathbf{p}_2)\cdot\mathbf{r}_e} \Psi_0\,d\tau_e \\ M_3 &= -2\pi c^2 e^2 ZS \frac{\hbar}{\bar{\nu}_\lambda \mu_\lambda^2} \\ &(\varepsilon_n + \hbar\bar{\nu}_\lambda)^{-1} \sum (u_2^* \mathbf{e}_\lambda \boldsymbol{\alpha} u_1) \int \Psi_n^* \boldsymbol{\alpha}_e \mathbf{e}_\lambda e^{\frac{i}{\hbar}(\mathbf{p}_1-\mathbf{p}_2)\cdot\mathbf{r}_e} \Psi_0\,d\tau_e. \end{aligned} \qquad (5.12)$$

We now require to perform the sum Σ over polarisations. This is done in the usual way choosing two orthogonal states of polarisation along axes perpendicular to $\bar{\mathbf{P}}_\lambda = \mathbf{p}_1 - \mathbf{p}_2$. The total matrix element M then reduces to

$$\begin{aligned} Me^{\frac{-i\bar{\mathbf{P}}_\lambda \mathbf{R}_e}{\hbar}} &= \frac{4\pi\hbar^2 Ze^2 (u_2^* u_1) I'}{P_\lambda^2} + 2\pi c^2 e^2 ZS \frac{\hbar}{\bar{\nu}_\lambda \mu_\lambda^2}\left[\left(\varepsilon_n - \hbar\bar{\nu}_\lambda + \frac{i\hbar}{2}\bar{\gamma}_\lambda\right)^{-1}\right. \\ &\left. + (\varepsilon_n + \hbar\bar{\nu}_\lambda)^{-1}\right]\left[(u_2^* \boldsymbol{\alpha}\mathbf{I} u_1) - \frac{\varepsilon_n (u_2^* u_1)}{cP_\lambda^2}\bar{\mathbf{P}}_\lambda \cdot \mathbf{I}\right] \end{aligned} \qquad (5.13)$$

where $\mathbf{R}_e$ is the position of the nucleus to which the electron under consideration is bound. $\mathbf{R}_e$ is constant during the collision since the recoil of the atom as a whole is negligible. The integrals I' and $\mathbf{I}$ are thus dependent only on $\bar{\mathbf{P}}_\lambda$ and the states Ψ_n and Ψ_0 and are given by

$$I' = \int \Psi_n^* e^{\frac{i\bar{\mathbf{P}}_\lambda}{\hbar}(\mathbf{r}_e - \mathbf{R}_e)} \Psi_0\,d\tau$$

$$\mathbf{I} = \int \Psi_n^* \boldsymbol{\alpha}_e e^{\frac{i\bar{\mathbf{P}}_\lambda}{\hbar}\cdot(\mathbf{r}_e - \mathbf{R}_e)} \Psi_0\,d\tau.$$

Eq. (5.13) gives the matrix element for the collision and so far

we have not made any important approximations. However in general M is complicated and one has to consider special cases. We will assume $\varepsilon_n \ll mc^2$ so that the atomic electron can be treated non-relativistically. Then in the above expression the Dirac velocity operator $\boldsymbol{\alpha}_e$ can be replaced by $\mathbf{P}_e/mc$ where $\mathbf{P}_e$ is the momentum of the electron. The result is the same as if we had started with the non-relativistic interaction $\overline{H}_{\mathrm{MR}}$.

For the transition probability in which the particle changes its state from momentum $\mathbf{p}_1$ to $\mathbf{p}_2$ of either spin and the electron from state Ψ_0 to Ψ_n, we require to average M^2 over the initial spins and sum over the final spins of the particle. This we write as $|M|^2_{\mathrm{av}}$:

$$\frac{|M|^2_{\mathrm{av}}}{16\pi^2\hbar^4 Z^2 e^4} = \frac{|\mathbf{I}'|^2}{P_\lambda^4} + \mathrm{SS}' \frac{c^4}{\mu_\lambda^2(\tilde{\nu}_\lambda)\mu_\lambda^2(\tilde{\nu}'_\lambda)} (\varepsilon_n + \hbar\tilde{\nu}_\lambda)^{-1}(\varepsilon_n + \hbar\tilde{\nu}'_\lambda)^{-1} \cdot \left(\varepsilon_n - \hbar\tilde{\nu}_\lambda + \frac{i\hbar}{2}\tilde{\gamma}_\lambda(\tilde{\nu}_\lambda)\right)^{-1}\left(\varepsilon_n - \hbar\tilde{\nu}'_\lambda - \frac{i\hbar}{2}\tilde{\gamma}_\lambda(\tilde{\nu}'_\lambda)\right)^{-1} \left|\frac{c\mathbf{p}_1 \cdot \mathbf{I}}{E_1} - \frac{\varepsilon_n \overline{\mathbf{P}}_\lambda \cdot \mathbf{I}}{cP_\lambda^2}\right|^2 . \tag{5.14}$$

The effects of retardation of the interaction are contained in the second term which is a function of both the quantum refractive index μ_λ and the line breadths $\tilde{\gamma}_\lambda$. This term is responsible for the indefinately increasing radius of action of a fast charged particle if one neglects consideration of polaristion effects. The first term in (5.14) represents the instantaneous electrostatic interaction between the particle and the atomic electron and should of course contain the static dielectric constant. However this screening of the Coulomb interaction should appear in the higher order terms of the perturbation expansion we have used and as stated in the introduction will be neglected in this paper.

In order to obtain the cross-section from the transition probability we require the density of final states for the particle. This is given by

$$\varrho(p_2)\mathrm{d}E_2\,\mathrm{d}\Omega = \frac{E_2}{(2\pi\hbar c)^3}\frac{P_\lambda \mathrm{d}P_\lambda \mathrm{d}E_2 \mathrm{d}\phi}{p_1} \tag{5.15}$$

where $\mathrm{d}\Omega$ is an element of solid angle along the direction $\mathbf{p}_2$ which makes angles (θ, ϕ) with $\mathbf{p}_1$ and a plane through $\mathbf{p}_1$. The cross-section for excitation of the state Ψ_n thus becomes

$$\sigma = \frac{8\pi}{\beta^2}\frac{Z^2e^4}{c^3}\int_{P_{\min}}^{P_{\max}} \mathrm{d}P_\lambda P_\lambda \left\{\frac{|I'|^2}{P_\lambda^4} + \mathrm{SS}' \frac{c^4}{\mu_\lambda^2(\tilde{\nu}_\lambda)\mu_\lambda^2(\tilde{\nu}'_\lambda)} (\varepsilon_n + \hbar\tilde{\nu}_\lambda)^{-1}(\varepsilon_n + \hbar\tilde{\nu}'_\lambda)^{-1} \cdot \left(\varepsilon_\lambda - \hbar\tilde{\nu}_\lambda + \frac{i\hbar}{2}\tilde{\gamma}_\lambda(\tilde{\nu}_\lambda)\right)^{-1}\left(\varepsilon_n - \hbar\tilde{\nu}'_\lambda - \frac{i\hbar}{2}\tilde{\gamma}_\lambda(\tilde{\nu}'_\lambda)\right)^{-1} \left|\frac{c\mathbf{p}_1}{E_1} - \frac{\varepsilon_n \overline{\mathbf{P}}_\lambda}{cP_\lambda^2}\right|^2 |I_z|^2\right\} \tag{5.16}$$

where I_Z represents the component of the vector $\mathbf{I}$ along the direction defined by the vector $c\mathbf{p}_1/E_1 - \varepsilon_n \overline{\mathbf{P}}_\lambda / cP_\lambda^2$ and

$$P_{\min} = p_1 - p_2 \approx \frac{\varepsilon_n}{v}, \qquad P_{\max} = p_1 + p_2$$

where v is the velocity of the particle.

Consider the integrals I' and I_Z. If R is a length of order the extension of the wave function Ψ_0 for the electron and $\hbar P_\lambda^{-1} \gg R$ then these integrals can be written approximately [22])

$$\begin{aligned} I' &\approx \frac{i\overline{\mathbf{P}}_\lambda}{\hbar} \cdot \int \Psi_v^* \mathbf{r} \Psi_0 \, \mathrm{d}\tau = \frac{iP_\lambda}{\hbar} x_{n0} \\ I_Z &\approx \frac{i\varepsilon_n}{c\hbar} x_{n0} \end{aligned} \tag{5.17}$$

since the wave functions Ψ_0 and Ψ_n will be assumed spherically symmetric. If on the other hand we have $\hbar P_\lambda^{-1} \ll R$ the integrals I' and I_Z become very small due to the rapidly oscillating function in the integrands. Thus provided in our expression (5.16) for the cross-section the lower limit $P_{\min}$ satisfies $\hbar P_{\min} \gg R$ we can approximate the expression by substituting the above values for I' and I_Z and cutting off the range of integration at $P_{\max} = \hbar R^{-1}$. Since $\varepsilon_n \ll E_1$ we also have

$$\left| \frac{c\mathbf{p}_1}{E_1} - \frac{\varepsilon_n \overline{\mathbf{P}}_\lambda}{cP_\lambda^2} \right|^2 = \beta^2 - \frac{\varepsilon_n^2}{c^2 P_\lambda^2} \tag{5.18}$$

so that finally our cross-section becomes

$$\sigma = \frac{8\pi}{\beta^2} |x_{n0}|^2 Z^2 \left(\frac{e^2}{\hbar c}\right)^2 \int_{\frac{\varepsilon_n}{\beta c}}^{\frac{\hbar}{R}} \mathrm{d}P_\lambda \left\{ \frac{1}{P_\lambda} + \mathrm{SS}' \frac{c^2 p_\lambda \tilde{\nu}_n^2}{\hbar^2 \mu_\lambda^2(\tilde{\nu}_\lambda) \mu_\lambda^2(\tilde{\nu}_\lambda')} \left(\beta^2 - \frac{\varepsilon_n^2}{c^2 p_\lambda^2}\right) A(\tilde{\nu}_\lambda, \tilde{\nu}_\lambda') \right\} \tag{5.19}$$

where

$$A(\tilde{\nu}_\lambda, \tilde{\nu}_\lambda') = \frac{(\tilde{\nu}_n^2 - \tilde{\nu}_\lambda^2)(\tilde{\nu}_n^2 - \tilde{\nu}_\lambda'^2) + \tilde{\nu}_n^2 \tilde{\gamma}(\tilde{\nu}_\lambda) \tilde{\gamma}(\tilde{\nu}_\lambda')}{[(\tilde{\nu}_n^2 - \tilde{\nu}_\lambda^2)^2 + \tilde{\nu}_n^2 \tilde{\gamma}_\lambda^2(\tilde{\nu}_\lambda)][(\tilde{\nu}_n^2 - \tilde{\nu}_\lambda'^2)^2 + \tilde{\nu}_n^2 \tilde{\gamma}_\lambda^2(\tilde{\nu}_\lambda')]}$$

and $\tilde{\nu}_\lambda$ is a function of P_λ and S sums over all the possible frequencies of a physical photon of momentum P_λ. We have also multiplied the factors $(\varepsilon_n + h\tilde{\nu}_\lambda)$ through in the denominators of (5.16) to obtain (5.19) and written $(\varepsilon_n + h\tilde{\nu}_\lambda)\tilde{\gamma}_\lambda \approx 2\varepsilon_n \tilde{\gamma}_\lambda$. This is a valid approximation since these line breadths are only of importance in the region $\varepsilon_n \approx h\tilde{\nu}_\lambda$. The above cross-section for excitation of the atomic

Ψ_n is a good approximation if $\varepsilon_n \beta^{-1} c^{-1} \ll \hbar R^{-1}$. It corresponds to the contribution from collisions with large impact parameters.

6. Derivation of the Energy Loss

In order to do a consistently quantum mechanical calculation all through we should substitute the quantum refractive index into the expression (5.19). However the dependence of μ_λ and $\bar{\gamma}_\lambda$ on P_λ is the main source of complication in the integral for the cross-section and we shall have to make some further approximations. Before doing this we first derive a quantity of more interest, namely the energy loss of the particle to ionizing and exciting collisions with atoms in the medium.

Using the oscillator strengths f_{n0} and the fact that the second term of the integrand (5.19) converges rapidly at the upper limit we have for the energy loss to distant collisions,

$$\left(\frac{\mathrm{d}E}{\mathrm{d}x}\right)_{\mathrm{d}} = \frac{4\pi}{\beta}\frac{Z^2 e^4 N}{mc^2}\sum_n f_{n0}\left\{\log\frac{\hbar\beta c}{R\varepsilon_n} + \mathrm{SS}'\int_{\frac{\varepsilon_n}{\beta c}}^{\infty}\frac{c^2 P_\lambda \bar{\nu}_n^2 \,\mathrm{d}P_\lambda}{\hbar^2 \mu_\lambda^2(\bar{\nu}_\lambda)\mu_\lambda^2(\bar{\nu}'_\lambda)}\left(\beta^2 - \frac{\varepsilon_n^2}{c^2 P_\lambda^2}\right) A(\bar{\nu}_\lambda, \bar{\nu}'_\lambda)\right\} \qquad (6.1)$$

If we require the total energy loss including collisions in which the electron gets an amount of energy greater than $\hbar\beta c R^{-1}$ then we must add on the close-collision loss. Close collisions give a negligible cross-section but due to the large energy transfers usually involved they contribute an important energy loss. The approximation of the integrals I' and I_Z to obtain (5.19) is just that of neglecting the close-collision cross-section.

We will treat the electrons as free in the usual way in order to calculate the energy loss to close collisions. The bulk of these collisions derive from the longitudinal matrix element in (5.14) into which neither μ_λ or $\bar{\gamma}_\lambda$ enters. These collisions involve very short collision times. It is interesting to note that although by this procedure we justifiably neglect the effect of the medium on the close collision cross-section we do not neglect the effect of polarisation close to the track on the field, and thus the energy loss, at large distances. We shall assume that the maximum energy transfer ε_M we are interested in is considerably less than mc^2. Then neglecting spin,

$$\left(\frac{dE}{dx}\right)_c = \frac{2\pi Z^2 e^4 N}{mc^2\beta^2} \log \frac{2\varepsilon_M mR^2}{\hbar^2}. \qquad (6.2)$$

It should be noted that there are three important lengths in this problem. They are the atomic radius R, the interatomic distance D and the wavelength of a physical photon λ. It is valid to describe a medium by a refractive index for wavelengths λ greater than the interatomic distance D. Thus we expect our treatment of the energy loss to be correct for energy transfers ε_n such that

$$\lambda_n = \frac{\hbar c}{\varepsilon_n} > D$$

where λ_n is the wavelength of the virtual physical photons which contribute most to the excitation of the state Ψ_n. Typical values for a solid give then $\varepsilon_n < 1000$ eV which covers the range of excitations and ionizations of interest. For energy transfers greater than this amount we approach first the region where we may neglect polarisation effects and then the region $\lambda_n < R$ where it soon becomes valid to treat the electrons as free.

Consider the general expression (6.1). The sum $\sum_n$ is to be understood as a sum over the discrete excited states and an integral over the continuous ionized states of the atom. The physical effects of the medium on the collision loss are described by the quantal refractive index μ_λ and the line breadths $\bar{\gamma}_\lambda$. The line breadth is made up of the total transition probability out of the state $|A; p; \bar{1}_\lambda\rangle$. Basically then the problem of evaluating the integral (6.1) becomes one of finding suitable expressions for $\bar{\gamma}_\lambda$ and μ_λ. There are a large number of special cases which one could consider. We shall first consider the simple case of completely neglecting the collective effects of the medium, i.e., derive the Bethe-Bloch [2, 3]) formula as a limiting case, and then in section 7 consider some approximations to obtain the energy loss in a medium.

Consider the case where $\mu_\lambda = 1$ and $\bar{\gamma}_\lambda = 0$. The physical photons then become ordinary photons and the sum S reduces to the single frequency corresponding to a particular momentum of a photon. The integral in (6.1) then simplifies directly and using the simple sum rule

$$\sum_{n \neq 0} f_{0n} = 1$$

the total energy loss becomes

$$\left(\frac{\mathrm{d}E}{\mathrm{d}x}\right) = \left(\frac{\mathrm{d}E}{\mathrm{d}x}\right)_{\mathrm{d}} + \left(\frac{\mathrm{d}E}{\mathrm{d}x}\right)_{\mathrm{c}} = \frac{2\pi}{\beta^2}\frac{Z^2e^4N}{mc^2}\left\{\log\frac{2mc^2\beta^2\varepsilon_{\mathrm{M}}}{I^2(1-\beta^2)} - \beta^2\right\} \quad (6.3)$$

where the average ionization potential I is defined by

$$\log I = \sum_n f_{0n}\log\varepsilon_n .$$

7. Discussion of the Energy Loss to Excitation and Ionization

In order to evaluate the expression (6.1) for the distant collision energy loss we require the integral

$$I_n = \mathrm{SS}'\int_{\substack{\varepsilon_n \\ \beta c}}^{\infty} \frac{c^2 P_\lambda \tilde{\nu}_n^2 \,\mathrm{d}P_\lambda}{\hbar^2 \mu_\lambda^2(\tilde{\nu}_\lambda)\mu_\lambda^2(\tilde{\nu}'_\lambda)}\left(\beta^2 - \frac{\varepsilon_n^2}{c^2P_\lambda^2}\right) A(\tilde{\nu}_\lambda, \tilde{\nu}'_\lambda). \quad (7.1)$$

This integral is in general complicated. In order to discuss it we shall make various approximations appropriate to the physical processes of excitation or ionization, though in some cases it would be preferable to do a numerical integration of the above more exact expression.

For complex atoms the sum S extends over a large number of possible frequencies for a given momentum P_λ. However only those in the neighbourhood of the excitation frequency $\tilde{\nu}_n$ for the state being considered are of importance for the integral I_n due to the resonance denominators in the expressions $A(\tilde{\nu}_\lambda, \tilde{\nu}'_\lambda)$.

Discrete Levels

Consider the excitation of a discrete state Ψ_e. We require, in the integrand of I_e for the excitation of this state, the refractive index and line breadth accurately only in the neighbourhood of the excitation frequency $\tilde{\nu}_e$. Thus the refractive index will be split into two parts as follows

$$\mu_\lambda - 1 \approx 2\pi N\frac{e^2}{\hbar c}\frac{\hbar}{mc}\frac{c^2 f_e(\tilde{\nu}_e^2 - \tilde{\nu}_\lambda^2)}{(\tilde{\nu}_e^2-\tilde{\nu}_\lambda^2)^2+\gamma_e^2\tilde{\nu}_e^2} + (\mu(\tilde{\nu}_e) - 1). \quad (7.2)$$

The maximum value of μ_λ which we write as μ_{Me} is given by

$$\mu_{\mathrm{Me}} - 1 = \pi N\frac{e^2}{\hbar c}\frac{\hbar}{mc}\frac{c^2 f e}{\gamma_e\tilde{\nu}_e} + (\mu - 1). \quad (7.3)$$

It should be noted that the spontaneous emission breadth γ_e may be considerably broadened at normal temperatures by other processes such as collision broadening etc., thus by γ_e we shall in future mean this broadened line breadth.

Now in the collision momentum was conserved at the particle vertex and the energy of the physical photon in the intermediate state was

$$\hbar\tilde{\nu}_\lambda = \frac{cP_\lambda}{\mu_\lambda}. \tag{7.4}$$

In the diagram we have drawn a curve of the energy-momentum relation (7.4) to show the range of integration over P_λ in the integral I_e for the two cases of $\mu(\tilde{\nu}_e) > 1$ and $\mu(\tilde{\nu}_e) < 1$. At some critical value P_c of the momentum the physical photon energies become three valued for a given momentum. This occurs when

$$P_\lambda > P_c = \frac{\varepsilon_e \mu_{Me}}{c}.$$

The range of integration $\infty > P_\lambda > \varepsilon_e/\beta c$ reaches this value of P_λ when β increases to the point where it is first possible for the particle to emit Čerenkov radiation corresponding to the level Ψ_e. The three roots for the frequency we then write as $\tilde{\nu}_1(P_\lambda)$, $\tilde{\nu}_2(P_\lambda)$ and $\tilde{\nu}_3(P_\lambda)$ where only the root $\tilde{\nu}_1(P_\lambda)$ exists below Čerenkov threshold. The sum S in the integral (7.1) then extends over these three roots.

Next consider the line breadth $\bar{\gamma}_\lambda(\tilde{\nu}_\lambda)$ which is the total transition probability out of the state $|A; \not{p}; \overline{1}_\lambda\rangle$. It is made up of a large number of possible processes which constitute the active effect of the medium on the individual collision. We use the expression (3.30) for $\bar{\gamma}_\lambda$ which in the neighbourhood of the resonance frequency $\tilde{\nu}_e$ can be written

$$\bar{\gamma}_\lambda \approx \bar{\gamma} + \frac{\bar{\gamma}\gamma_e \tilde{\nu}_e(\mu_{Me}-1)}{(\tilde{\nu}_e - \tilde{\nu}_\lambda)^2 + \dfrac{\bar{\gamma}^2}{4}}. \tag{7.5}$$

The absorption term is dominant for $\tilde{\nu}_\lambda \approx \tilde{\nu}_e$. $\bar{\gamma}$ represents the reaction breadth of the medium on the particle and will be assumed independent of the frequency $\tilde{\nu}_\lambda$ though of course it may depend on β.

The general expression we now require is the integral (7.1) in which the sum S over the A functions extends over the three frequencies $\tilde{\nu}_1$, $\tilde{\nu}_2$ and $\tilde{\nu}_3$ and with the line breadth (7.5) and refractive index (7.2) used in the integrand. Consider first the terms $A(\tilde{\nu}_1, \tilde{\nu}_1)$, $A(\tilde{\nu}_2, \tilde{\nu}_2)$ and $A(\tilde{\nu}_3, \tilde{\nu}_3)$ and the ranges of frequency in the integration of these three quantities. The momentum range is

$$\varepsilon_e \beta^{-1} c^{-1} \leqq P_\lambda \leqq \infty$$

and the corresponding frequency ranges,

$$\left.\begin{aligned} \bar{\nu}_e - \gamma_1 < \bar{\nu}_1 < \bar{\nu}_e - \frac{\gamma_e}{2} \\ \bar{\nu}_e - \frac{\gamma_e}{2} < \bar{\nu}_2 < \bar{\nu}_e - \gamma_2 \end{aligned}\right\} \quad \text{above Čerenkov threshold}$$

$$\bar{\nu}_e + \gamma_3 < \bar{\nu}_3 < \infty \qquad \text{above and below Čerenkov threshold,}$$

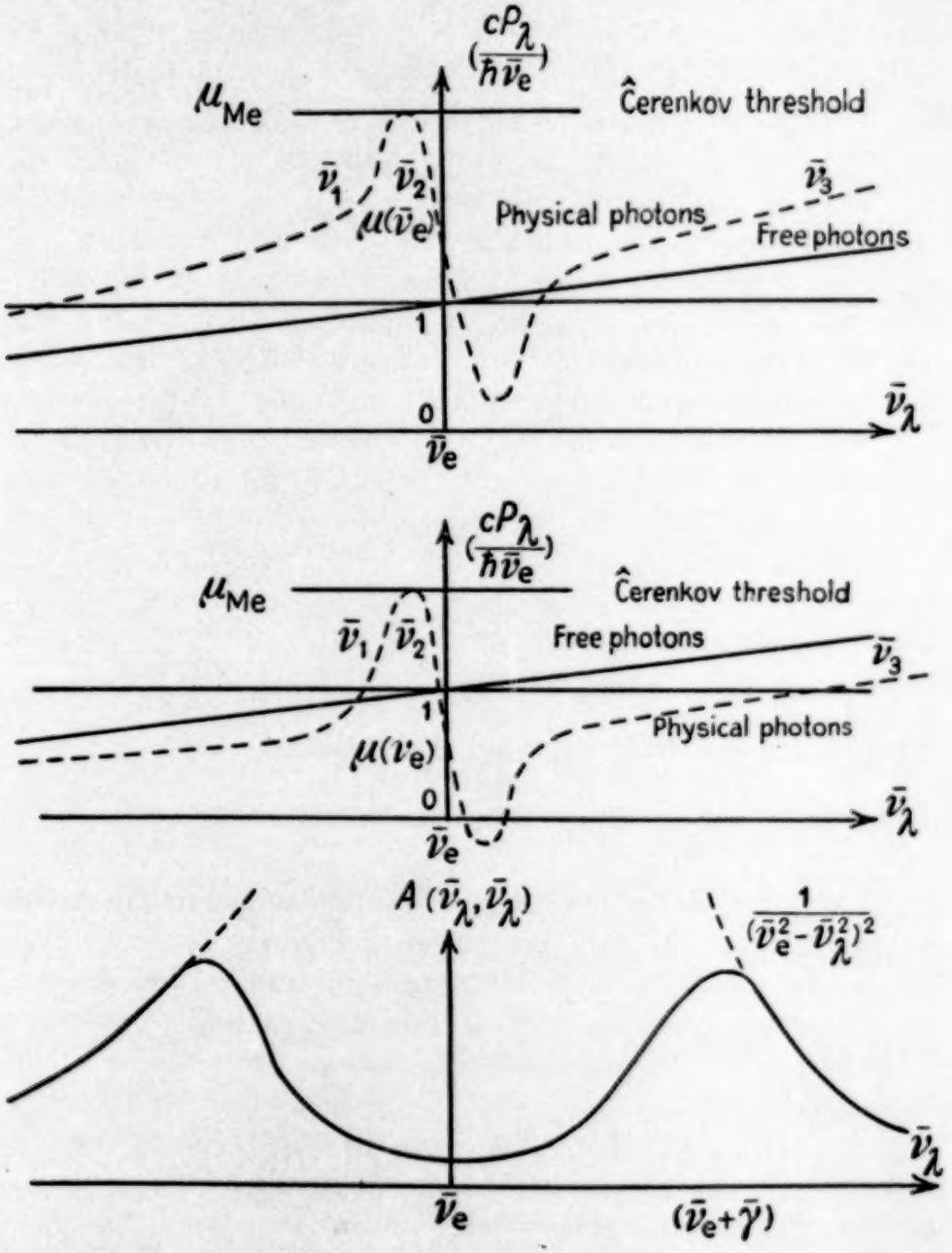

where γ_1 and γ_3 are given by

$$\begin{aligned} 2\gamma_1 &= -\tilde{\nu}_e\left(\frac{1}{\beta}-\mu\right)+\left[\left(\frac{1}{\beta}-\mu\right)^2\tilde{\nu}_e^2+4(\mu_{Me}-1)\gamma_e\tilde{\nu}_e\right]^{\frac{1}{2}} \\ 2\gamma_3 &= \tilde{\nu}_e\left(\frac{1}{\beta}-\mu\right)+\left[\left(\frac{1}{\beta}-\mu\right)^2\tilde{\nu}_e^2+4(\mu_{Me}-1)\gamma_e\tilde{\nu}_e\right]^{\frac{1}{2}} \end{aligned} \tag{7.6}$$

for $\gamma_1, \gamma_3 > \gamma_e$.

The resonance denominator function

$$A(\tilde{\nu}_\lambda, \tilde{\nu}_\lambda) = [(\tilde{\nu}_e^2-\tilde{\nu}_\lambda^2)^2+\tilde{\nu}_e^2\tilde{\gamma}_\lambda^2(\tilde{\nu}_\lambda)]^{-1}$$

is also shown in the diagram. Provided the reaction breadth $\tilde{\gamma}$ of the medium on the particle is larger than the spontaneous emission breadth γ_e then A has an "absorption-well" of breadth $\tilde{\gamma}$ about the frequency $\tilde{\nu}_e$. Frequencies inside this well will contribute very little to the excitation of the state Ψ_e.

By further examining the A functions we note the following. First the root $\tilde{\nu}_2$ always lies in the centre of the absorption-well so that $A(\tilde{\nu}_2, \tilde{\nu}_2)$ is small compared with either $A(\tilde{\nu}_1, \tilde{\nu}_1)$ or $A(\tilde{\nu}_3, \tilde{\nu}_3)$ in the regions where these functions are large. In fact the frequencies $\tilde{\nu}_2$ come off almost exclusively as Čerenkov radiation. Further the relative magnitude of $A(\tilde{\nu}_1, \tilde{\nu}_1)$ and $A(\tilde{\nu}_3, \tilde{\nu}_3)$ are always considerably different for the same value of P_λ except for a very small range of P_λ. Thus neglect of the interference term $A(\tilde{\nu}_1, \tilde{\nu}_3)$ should be unimportant. Expressed as a frequency integral I_e will therefore be written as approximately

$$\begin{aligned} I_e \approx &\int_{\tilde{\nu}_e-\gamma_1-\tilde{\gamma}}^{\tilde{\nu}_e-\tilde{\gamma}} \frac{\tilde{\nu}_e^2\tilde{\nu}_1^2\,d\tilde{\nu}_1}{\mu_\lambda^3(\tilde{\nu}_1)}\left(\beta^2-\frac{\tilde{\nu}_e^2}{\tilde{\nu}_1^2\mu_\lambda^2(\tilde{\nu}_1)}\right)\left(\mu_\lambda+\tilde{\nu}_1\frac{d\mu_\lambda}{d\tilde{\nu}_1}\right)(\tilde{\nu}_e^2-\tilde{\nu}_1^2)^{-2} \\ &+\int_{\tilde{\nu}_e+\tilde{\gamma}+\gamma_3}^{\infty} \frac{\tilde{\nu}_e^2\tilde{\nu}_3\,d\tilde{\nu}_3}{\mu_\lambda^3(\tilde{\nu}_3)}\left(\beta^2-\frac{\tilde{\nu}_e^2}{\tilde{\nu}_3\mu_\lambda^2(\tilde{\nu}_3)}\right)\left(\mu_\lambda+\tilde{\nu}_3\frac{d\mu_\lambda}{d\tilde{\nu}_3}\right)(\tilde{\nu}_e^2-\tilde{\nu}_3^2)^{-2} \end{aligned} \tag{7.7}$$

where we have cut out the range of heavily damped frequencies in the integration. This is a very good approximation in the case $\gamma_3 \gg \tilde{\gamma}$ and $\mu(\tilde{\nu}_e) < 1$ since in this case the range of integration never enters the absorption breadth region of the A functions. It is however only approximate in the case where the medium reaction $\tilde{\gamma}$ is important.

Next consider the dispersion terms in (7.7). We can neglect dispersion provided $\tilde{\nu}_\lambda\, d\mu_\lambda/d\tilde{\nu}_\lambda \ll 1$ for the smallest value of $|\tilde{\nu}_e-\tilde{\nu}_\lambda|$ in the range of integration. This condition gives

$$(\mu_{\mathrm{Me}}-1)\left(\frac{\bar{\gamma}}{\bar{\nu}_e}+\frac{1}{\mu}-1\right)^{-2}\left(\frac{\gamma_e}{\bar{\nu}_e}\right)\ll 1 \quad \text{for } \mu(\bar{\nu}_e)<1$$
$$(\mu_{\mathrm{Me}}-1)\frac{\bar{\nu}_e\gamma_e}{\bar{\gamma}^2}\ll 1 \qquad \text{for } \mu(\bar{\nu}_e)>1 \tag{7.8}$$

For the first case this is nearly always satisfied. The more stringent condition for $\mu > 1$ is not satisfied in all cases so that in this case neglect of disperion may not always be justified.

Writing I_e for the contribution to the integral (7.7) which derives from the Čerenkov frequencies we then find finally for the distant collision energy loss to excitation of discrete states Ψ_e,

$$\left(\frac{\mathrm{d}E}{\mathrm{d}x}\right)_{\mathrm{d}}^{\mathrm{ext}}=\frac{4\pi}{\beta^2}\frac{Z^2e^4N}{mc^2}\sum_e f_{e0}\left\{\log\frac{\beta c}{\mathrm{R}\bar{\nu}_e}+I_e\right\} \tag{7.8}$$

where $I_e = I+I_c$

$$I=\frac{\bar{\nu}_e^2\beta^2(1-\mu^{-2}\beta^{-2})}{2\mu^2\omega(2\bar{\nu}_e+\omega)}+\frac{1}{2\mu^4}\log\frac{(\bar{\nu}_e+\omega)^2}{\omega(2\bar{\nu}_e+\omega)} \tag{7.9}$$

$$I_c=\frac{\beta^2}{4\mu^2}\left(1-\frac{1}{\beta^2\mu^2}\right)\left(\frac{\bar{\nu}_e}{\bar{\gamma}}-\frac{\bar{\nu}_e}{\omega_c}\right)+\frac{1}{2\mu^4}\log\frac{\bar{\gamma}}{\omega_c},$$

$$\text{and } \omega=\bar{\gamma}+\bar{\nu}_e\left(\frac{1}{\beta\mu}-1\right)_+,\ \omega_c=\bar{\gamma}-\bar{\nu}_e\left(\frac{1}{\beta\mu}-1\right)_-.$$

The $+$ or $-$ signs outside the brackets for the quantities ω and ω_c mean: take positive or negative values only for the brackets and otherwise zero.

The term I_c represents a contribution to the primary excitation from Čerenkov frequencies sufficiently displaced from $\bar{\nu}_e$ not to be highly damped by the absorption well around the frequency $\bar{\nu}_e$. These frequencies are in the region where the refractive index is due mainly to possible excited states other than Ψ_e for the medium.

We now consider the expression (7.8) for the two cases of $\mu(\bar{\nu}_e)$ greater or less than unity.

$\mu(\bar{\nu}_e) < 1$

This is the case in which the reaction breadth $\bar{\gamma}$ of the medium on the particle is usually of no importance, i.e., $\omega \approx (1/\beta\mu-1)\bar{\nu}_e$. If this is so the expression for the energy loss to the excitation of states Ψ_e reduces to

$$\frac{4\pi}{\beta^2}\frac{Z^2e^4N}{mc^2}f_{e0}\left\{\log\frac{\beta c}{R\tilde{\nu}_e(1-\beta^2\mu^2)^{1/2\mu^4}}-\frac{\beta^2}{2\mu^2}\right\}. \qquad (7.10)$$

Since $\mu(\tilde{\nu}_e)$ will not be much different from unity this expression is in close agreement with a formula given by Budini [15]) for the excitation loss, which he obtained by calculating the field of the fast charged particle classically. We would expect such an agreement in this case since it corresponds to that in which the line breadth $\tilde{\gamma}$ can be neglected. This is assumed from the beginning in a classical theory which represents the particle by a stationary current and charge distribution.

The important effect in producing a plateau in the energy loss (7.10) for $\beta \to 1$ is the passive effect of the medium represented by $\mu(\tilde{\nu}_e)$ i.e. that part of the refractive index due to all the possible excitation frequencies other than $\tilde{\nu}_e$. In this sense the interference between levels in the medium is important for the saturation of the energy loss.

$\mu(\tilde{\nu}_e) > 1$

If $\mu(\tilde{\nu}_e)$ is sufficiently greater than unity then we have to consider the contribution I_c from virtual Čerenkov frequencies displaced from the heavily damped region $(\tilde{\nu}_e \pm \tilde{\gamma})$. In simplifying the expression (7.8) for this case we may use $\tilde{\gamma} \ll \tilde{\nu}_e$ which as stated earlier is the condition that it be valid to treat the excitation as a stationary state problem. We may not however assume anything about the relative magnitude of $(1-1/\mu)\tilde{\nu}_e$ and $\tilde{\gamma}$.

The distant collision energy loss to excitation of an atomic state Ψ_e then becomes

$$\frac{4\pi}{\beta^2}\frac{Z^2e^4N}{mc^2}f_{e0}\left\{\log\frac{\beta c}{R\tilde{\nu}_e}+\frac{\beta^2}{4\mu^2}\left(1-\frac{1}{\beta^2\mu^2}\right)\left(\frac{1}{\omega}-\frac{1}{\omega_c}+\frac{1}{\tilde{\gamma}}\right)\tilde{\nu}_e+\frac{1}{2\mu^4}\log\frac{\tilde{\nu}_e\tilde{\gamma}}{2\omega\omega_c}\right\} \qquad (7.11)$$

Ionization

We also require the contribution to the energy loss deriving from the ionization of atoms in the medium. This is obtained from the integral I_i where

$$I_i = SS'\int_{\frac{\varepsilon_i}{\beta c}}^{\infty}\frac{c^2\,dP_\lambda P_\lambda\tilde{\nu}_i^2}{\hbar^2\mu_\lambda^2(\tilde{\nu}_\lambda)\mu_\lambda^2(\tilde{\nu}'_\lambda)}\left(\beta^2-\frac{\varepsilon_i^2}{c^2P_\lambda^2}\right)A(\tilde{\nu}_\lambda, \tilde{\nu}'_\lambda).$$

In this case we have the advantage that the refractive index $\mu_\lambda(\tilde{\nu}_\lambda)$

and line breadth $\bar{\gamma}_\lambda(\bar{\nu}_\lambda)$ are usually slowly varying with $\bar{\nu}_\lambda$ for frequencies in the region of the ionization frequency $\bar{\nu}_i$. Provided they are approximately constant over the interval

$$\bar{\nu}_i - \bar{\gamma}_\lambda(\bar{\nu}_i) < \bar{\nu}_\lambda < \bar{\nu}_i + \bar{\gamma}_\lambda(\bar{\nu}_i)$$

we may use the values of μ_λ and $\bar{\gamma}_\lambda$ at the frequency $\bar{\nu}_\lambda = \bar{\nu}_i$ in the above integral.

If we further use the condition that the line breadth $\bar{\gamma}_\lambda(\bar{\nu}_i)$, which from eq. (3.30) includes the absorption breadth, be much less than the ionization frequency $\bar{\nu}_i$ we find

$$\left(\frac{dE}{dx}\right)_d^{ion} = \frac{4\pi}{\beta^2}\frac{Z^2e^4N}{mc^2}\int f_{i0}\,\varrho(\varepsilon_i)d\varepsilon_i\left\{\log\frac{\beta c}{R\bar{\nu}_i} + \frac{(\beta^2\mu^2-1)}{\mu^4}\left(\frac{\varepsilon_i}{2\hbar\bar{\gamma}_\lambda}\right)\left(\frac{\pi}{2}-\tan^{-1}\frac{2\bar{\nu}_i}{\bar{\gamma}_\lambda}\left(\frac{1}{\beta\mu}-1\right)\right)\right. \tag{7.12}$$
$$\left. -\frac{(1+\beta\mu)}{8\mu^4}\log\frac{\mu^2\beta^2\bar{\gamma}_\lambda^2}{4\bar{\nu}_i^2}\left[1+\frac{4\bar{\nu}_i^2}{\bar{\gamma}_\lambda^2}\left(\frac{1}{\beta\mu}-1\right)^2\right]\right\}$$

where the principal value of the inverse tangent is taken and $\varrho(\bar{\nu}_i)$ is the density of ionized states Ψ_i.

Consider the case in which it is possible to produce Čerenkov radiation in the region of the ionization frequency $\bar{\nu}_i$. Then at Čerenkov threshold, namely $\beta\mu(\bar{\nu}_i) = 1$ the above expression for the distant collision energy loss to ionizations Ψ_i reduces to

$$\frac{4\pi}{\beta^2}\frac{Z^2e^4N}{mc^2}f_{i0}\left\{\log\frac{\beta c}{R\bar{\nu}_i}+\frac{1}{2\mu^4}\log\frac{2\bar{\nu}_i}{\bar{\gamma}_\lambda}\right\} \tag{7.13}$$

which gives a range of action at Čerenkov threshold of

$$d(\lambda_i) = \frac{\beta c}{\bar{\nu}_i}\left(\frac{2\bar{\nu}_i}{\bar{\gamma}_\lambda}\right)^{\frac{1}{2\mu^4}}. \tag{7.14}$$

There is a further increase in the primary ionization beyond this point up to a plateau value.

In conclusion, we have obtained various particular expressions from the general integral (7.1) for the primary excitation and ionization energy losses, together with eqs. (3.13) and (3.29) which give the first and second order probabilities for the emission of Čerenkov radiation from the immediate neighbourhood of the particle. To obtain the energy loss to these processes the numerical integration of these various equations will sometimes be preferable to approximate analytic methods since we will not always be able

to satisfy the conditions under which the approximations are good ones.

Apart from being quantal the method used in these calculations has the advantage that the distribution of the energy loss between the different primary processes is obtained automatically. In previous classical electromagnetic theories making use of the Poynting flux vector to obtain the total energy loss the problem of partitioning this loss between the different processes is more complicated.

I would like to thank Dr. J. M. Blatt, Dr. M. R. Schafroth and Mr. J. E. Moyal, together with many other members of the School of Physics for stimulating discussions. I am also indebted to the University of Sydney Research Committee for the provision of a research grant. Finally I would like to thank Professor Messel for the excellent research facilities provided in the School of Physics.

Note added in proof: I am grateful to Dr. U. Fano for communicating preprints of related calculations in which he considers the excitations of the transverse and longitudinal collective oscillations of a medium, using a method related to Tomonaga's [23]) treatment of collective motion.

References

1) N. Bohr, Phil. Mag. **25** (1913) 10, **30** (1915) 581
2) H. A. Bethe, Ann. d. Phys. **5** (1930) 325, Zeitschr. f. Phys. **76** (1932) 293
3) F. Bloch, Ann. d. Phys. **5** (1933a) 285, Zeitschr. f. Phys. **81** (1933b) 363
4) E. J. Williams, Proc. Roy. Soc. A **139** (1933) 163, Dan. mat.-fys. Medd. **13** No. 4 (1935), C. F. v. Weizsäcker, Ann. d. Phys. **5** (1933) 869
5) W. F. G. Swann, J. Franklin Inst. **226** (1938) 598
6) E. Fermi, Phys. Rev. **57** (1940) 485
7) I. Frank and I. Tamm, C. R. Acad. Sci. USSR **14** (1937) 109
8) O. Halpern and H. Hall, Phys. Rev. **57** (1940) 459
9) M. Huybrechts and M. Schönberg, Nuovo Cimento **9** No. 9 (1952) 1
10) H. Messel and D. M. Ritson, Phil. Mag. **7** (1950) 1129
11) A. Bohr, Dan. mat.-fys. Medd. **24** No. 19 (1948)
12) M. Schönberg, Nuovo Cimento **9** No. 4 (1952) 1
13) S. G. Gosh, G. M. D. B. Jones and J. G. Wilson, Proc. Phys. Soc. A **65** (1952) 68
13a) G. N. Fowler and G. M. D. B. Jones, Proc. Phys. Soc. A **66** (1953) 597
14) R. M. Sternheimer, Phys. Rev. **91** (1953) 256
15) P. Budini, Nuovo Cimento **10** (1953) 1
16) T. M. Jauch and K. M. Watson, Phys. Rev. **74** (1948) 950, **74** (1948) 1485, **75** (1949) 1249
17) S. M. Neamtan, Phys. Rev. **92** (1953) 1362, **94** (1954) 327
18) M. Born, "Optik", (1933) 313
19) E. Arnous and W. Heitler, Proc. Roy. Soc. A **220** (1953) 290
W. Heitler, The Quantum Theory of Radiation, 3rd. Edition, Oxford (1954)
20) D. Bohm and D. Pines, Phys. Rev. **82** (1951) 625, **85** (1952) 338, **92** (1953) 609
21) J. K. Parry, H. D. Rathgeber and J. L. Rouse, Proc. Phys. Soc. A **66** (1953) 541
22) N. F. Mott and H. S. Massey, The Theory of Atomic Collisions, Oxford (1933).
23) S. Tomonaga, Progr. Theor. Phys. **13** (1955) 467

Nuclear Physics **2** (1956/57) 347—355; *North-Holland Publishing Co., Amsterdam*

CONTACT AND CORE INTERACTIONS ACCORDING TO DIRAC'S RELATIVISTIC THEORY OF THE ELECTRON

S. T. MA

The F.B.S. Falkiner Nuclear Research and Adolph Basser Computing Laboratories, School of Physics †, *The University of Sydney*

Received 25 August 1956

Abstract: This article deals with the contact and core interactions between a Dirac electron and an atomic nucleus. It is shown that improvement of a well known approximate two-component form of the Dirac equation changes the repulsive contact interaction into a core interaction. The role played by the exact form of the core interaction in the determination of stationary states is analysed and compared with that of the hard core in the meson theory of nuclear forces.

1. Introduction

In the present article we are concerned with the two-component Pauli forms of Dirac's relativistic equation for the electron with special emphasis on the contact and core interactions between an electron and an atomic nucleus. There is a well-known equation for the two large components of the Dirac wave function which contains approximate relativistic corrections to the non-relativistic Hamiltonian [1, 2, 3, 4]). Among the relativistic corrections there are a spin-orbit interaction and a repulsive contact interaction which depends only on the value of the wave function at the origin. The contact interaction was first found by Darwin in a non-hermitian form, but it has real expectation values and the relativistic corrections lead to results in agreement with experiment. An alternative method of obtaining a two-component equation by unitary transformation has more recently been developed by Foldy and Wouthuysen [5, 6]). It has the advantage of producing a Hamiltonian which is automatically hermitian and independent of the eigenvalue of the stationary state. However, it will be seen below that the hermitian contact interaction of ref. [5, 6]) may also be derived by a slight modification of the elimination method and,

† Also supported by the Nuclear Research Foundation within the University of Sydney.

furthermore, the elimination method yields in a simple way closed expressions which will be useful for our purpose.

As has often been emphasized [7, 8, 9]), there is some similarity between the elimination method used in the Dirac theory and the elimination method used in the meson theory of nuclear forces. In the case of a two-nucleon system the latter consists in eliminating all states except those in which two nucleons and no mesons are present. The result derived from the pseudo-scalar theory by perturbation method contains in the lowest approximation a tensor force whose potential varies as $1/r^3$, and also a contact interaction, both of which have counterparts in the Dirac theory that are similar in mathematical form. In the past the $1/r^3$ tensor interaction was considered inadmissible because of the mathematical difficulty it led to. The trend of recent development is to avoid this difficulty by introducing a hard core in the nuclear interaction which is repulsive enough to make the wave functions vanish at small distances [10]). Lévy has found in quantum field theory indications for a hard core by a more accurate treatment of the repulsive contact interaction [11]). Lévy's work has been commented upon in ref. [10]) and elsewhere [12, 13]).

The nuclear interaction derived by perturbation method is generally recognized to be uncertain at very small distances. It is therefore of interest to analyse a similar problem which can be dealt with exactly. It has long been known that the spin orbit interaction in the Dirac theory, which varies as $1/r^3$ according to the approximate treatment, varies only as $1/r$ at small distances when it is treated exactly. Improvement in the calculation of relativistic corrections modifies also the repulsive contact interaction and changes it into a core interaction. The simplicity of the problem makes it possible to analyse without approximations the role played by the core interaction in the determination of stationary states. In view of the mathematical similarity, it is felt that what one learns from the Dirac theory of the electron may provide useful clues to the more intricate theory of nuclear forces.

2. The Contact Interaction

Consider the Dirac equation for an electron in a time-independent electrostatic field A_0,

$$E\psi = (\boldsymbol{\alpha}\cdot\mathbf{p}+\beta m+V)\psi,$$

where E is the energy of a stationary state of positive energy, V is the potential energy $-eA_0$, and $c = \hbar = 1$. Let φ be the spinor formed by the two large components of ψ, where we use the terms "large" and "small" with reference to the numerical magnitude at a large distance from the origin. Elimination of the small components leads to the equation

$$(E-m-V)\varphi = \boldsymbol{\sigma}\cdot\mathbf{p}(1/D)\boldsymbol{\sigma}\cdot\mathbf{p}\varphi \tag{2}$$

where

$$D = E+m-V. \tag{3}$$

Let $E_N = E-m$ be the non-relativistic energy. Eq. (2) has then the approximate form

$$E_N\varphi = [(p^2/2m)+V+W]\varphi, \tag{4}$$

where

$$W = -(1/4m^2)\boldsymbol{\sigma}\cdot\mathbf{p}(E_N - V)\boldsymbol{\sigma}\cdot\mathbf{p}. \tag{5}$$

The operator W may be written

$$W = -(1/4m^2)(E_N-V)p^2-(ie/4m^2)\boldsymbol{\sigma}\cdot\boldsymbol{\mathcal{E}}\,\boldsymbol{\sigma}\cdot\mathbf{p}. \tag{6}$$

The first term on the right-hand side of eq. (6) may be interpreted as the relativistic correction to the kinetic energy. The second term may be separated into two parts, V_s and V_c, where

$$V_s = (e/4m^2)\boldsymbol{\sigma}\cdot(\boldsymbol{\mathcal{E}}\times\mathbf{p}) \tag{7}$$

is the spin-orbit interaction and

$$V_c = -(ie/4m^2)\boldsymbol{\mathcal{E}}\cdot\mathbf{p} \tag{8}$$

is the contact interaction found by Darwin. Though the operator W is hermitian, as one immediately sees from eq. (5), the interaction (8) is not hermitian. If we derive from eq. (4) by successive approximations a Hamiltonian which is independent of the eigenvalue E_N, the result is also non-hermitian.

A hermitian contact interaction has been derived by the method of unitary transformation discussed in the Appendix. However, it may also be derived by a modification of the elimination method which consists in symmetrizing the expression (6) for W and the alternative expression

$$W = -(1/4m^2)p^2(E_N-V)+(ie/4m^2)\boldsymbol{\sigma}\cdot\mathbf{p}\boldsymbol{\sigma}\cdot\boldsymbol{\mathcal{E}}. \tag{9}$$

This gives

$$W = -(1/8m^2)\{(E_N-V)p^2+p^2(E_N-V)\}-(ie/8m^2)[\boldsymbol{\sigma}\cdot\boldsymbol{\mathcal{E}},\boldsymbol{\sigma}\cdot\mathbf{p}]. \tag{10}$$

The two terms on the right-hand side of eq. (10) are both hermitian operators. In the case of a central field, the second term may also be written V_s+V_c, with V_s given by eq. (7), but

$$V_c = (e/8m^2)\nabla\cdot\boldsymbol{\mathcal{E}}, \tag{11}$$

which is the result of ref [5, 6]).

When the field is due to an atomic nucleus of charge Ze, we obtain from eqs. (11), (7)

$$V_c = (\pi Ze^2/2m^2)\delta(\mathbf{r}), \tag{12}$$

which shows clearly the repulsive contact interaction, and

$$V_s = (Ze^2/4m^2 r^3)\,\boldsymbol{\sigma}\cdot\mathbf{l}, \tag{13}$$

where $\mathbf{l}$ is the orbital angular-momentum operator. The relativistic displacement of the energy levels of hydrogen-like atoms is given by the expectation value

$$\langle W\rangle = \left(\int\varphi^* W\varphi\,\mathrm{d}\tau\right) / \left(\int\varphi^*\varphi\,\mathrm{d}\tau\right). \tag{14}$$

It has been shown in ref. [3, 4]) that eq. (14) gives the correct fine structure, and that the contact interaction plays an important part in the relativistic displacement of the S-levels. The contact interaction plays also an important part in the radiative displacement of energy levels (the Lamb shift), which may be expressed as the combined effect of contact and spin-orbit interactions between the electron and the atomic nucleus [14]). Investigations on the contact interaction between two electrons may be found in a recent paper by Wu and Tauber [15]) and earlier references given there.

As will be seen in the Appendix, extension of the unitary transformation of Foldy and Wouthuysen to a higher approximation does not change the contact interaction in the case of an electrostatic field. We return therefore to the closed two-component form of the Dirac equation obtained by the elimination method, eq. (2).

3. The Core Interaction

The exact equation (2) may also be written in the form of Eq. (4) with

$$W = (1/2m)\,\boldsymbol{\sigma}\cdot\mathbf{p}\,[(E_N-V)/D]\,\boldsymbol{\sigma}\cdot\mathbf{p}. \tag{15}$$

As in the previous section, the operator W may be expressed in various ways. To see how the repulsive contact interaction goes

over into a core interaction, it is most convenient to adopt the symmetrized form, namely

$$W = -(1/4m)\{p^2[(E_N-V)/D] + [(E_N-V)/D]\,p^2\} - (ie/2)[\boldsymbol{\sigma}\cdot\boldsymbol{\xi}/D^2,\ \boldsymbol{\sigma}\cdot\mathbf{p}]. \quad (16)$$

For a central field,

$$-(ie/2)[\boldsymbol{\sigma}\cdot\boldsymbol{\xi}/D^2, \boldsymbol{\sigma}\cdot\mathbf{p}] = (e/D^2)\,\boldsymbol{\sigma}\cdot(\boldsymbol{\xi}\times\mathbf{p}) + (e^2/D^3)\,|\boldsymbol{\xi}|^2 + (e/2D^2)\,\boldsymbol{\Delta}\cdot\boldsymbol{\xi}. \quad (17)$$

When the field is due to an electric charge Ze, the right-hand side of eq. (17) may again be written as V_s+V_c with

$$V_s = (Ze^2/D^2r^3)\boldsymbol{\sigma}\cdot\mathbf{l}, \quad (18)$$

$$V_c = Z^2e^4/D^3r^4. \quad (19)$$

The last term in eq. (17) makes no contribution.

It can now be seen that a slight improvement in approximation changes the contact interaction into a core interaction. The expressions for V_c and V_s given by eqs. (12) and (13) of the previous section may be obtained from the left-hand side of eq. (17) by making the approximation $D = 2m$. If the approximation is made in eqs. (18) and (19), we obtain the same result for V_s but

$$V_C = Z^2e^4/8m^3r^4. \quad (20)$$

Except in the case of the S-states where V_s vanishes, V_s makes a much larger contribution for large r but V_c is predominant for small r.

Let us consider next eq. (4) in conjunction with eq. (16) without approximations. The operator that operates on φ in the right-hand side of eq. (4) depends then on the energy E_N but, for a state of known energy, it may be considered as a Hamiltonian in a restricted sense. The first term on the right-hand side of eq. (16) may again be interpreted as the relativistic correction to the kinetic energy, and the other term as the sum of a modified spin-orbit interaction and a core interaction whose space integral

$$\int V_c\,d\tau = 2\pi Ze^2/(E+m)^2 \quad (21)$$

is nearly the same as that of the contact interaction (12). Eqs. (13) and (20) are still approximately valid for large r, but we have for small r

$$V_c = 1/Ze^2r, \quad (22)$$

$$V_s = V_c\,\boldsymbol{\sigma}\cdot\mathbf{l}, \quad (23)$$

as a result of the increase of the expression D in the denominators. Thus the interactions V_c and V_s vary much slower at small distances than the approximate formulas indicate. This effect of the increase of D resembles the effect of radiation damping on scattering cross-sections [16]), though we are here dealing with a different problem.

Let l be quantum number associated with the orbital angular momentum of the wave function φ,

$$j = l \pm \tfrac{1}{2} \tag{24}$$

the quantum number associated with the total angular momentum, and let

$$k = \mp(j+\tfrac{1}{2}) \tag{25}$$

for the two eigenvalues of j. Let $u(r)/r$ be the radial factor of φ. The function u satisfies the differential equation

$$u''+(Ze^2/Dr^2)u'+[E+Ze^2/r)^2-m^2-(k(k+1)/r^2) \\ +(kZe^2/Dr^3)]\,u = 0. \tag{26}$$

The coefficients of u' and u in eq. (26) vary as $1/r$ and $1/r^2$ respectively for small r. Hence the singularity at the origin is regular according to Fuchs' theorem, and there exist regular solutions of the form

$$u = r^\varrho(c_0+c_1 r+c_2 r^2+\cdots). \tag{27}$$

The indicial equation of eq. (26) is the well known relation

$$\varrho^2 = k^2-Z^2 e^4. \tag{28}$$

The core interaction is essential for this indicial equation. Without it, an additional term -1 would appear in the right-hand side, and the behaviour of the wave functions would be quite different. However, the core is not hard enough to make the wave function vanish at the origin for all the states. In fact we know from eq. (28) that φ is infinitely large at the origin for the states $j = \frac{1}{2}$.

Like the modification of the spin-orbit interaction, the modification of the contact interaction into the core interaction has an important bearing on the expectation values. In the calculation of $\langle W\rangle$ mentioned in § 2, the expectation values of the contact interaction are usually obtained by using the two component form of Schrödinger's non-relativistic wave functions. If the exact wave functions φ of the Dirac theory are used instead, the results will be infinite for the states $j = \frac{1}{2}$. The explanation of this apparently paradoxical

situation is that one really should calculate the expectation values of the core interaction (19) rather than those of the contact interaction, and then the difference between the relativistic and non-relativistic wave functions become far less significant. In the case of the Lamb shift, improvement in the approximation also changes the contact interaction, the modification of which is beyond the scope of the present work.

Finally, it should be noted that the interactions discussed in this article are phenomenological in the sense that they determine the apparent probability amplitude φ instead of the true probability amplitude ψ. Furthermore, we have assumed that the electron is negatively charged. In the case of a positive electron in the field of an atomic nucleus, the contact interaction is attractive, and the closed form of the two-component equation is complicated by the fact that the expression D in the denominators vanishes at the critical distance $Ze^2/(E+m)$.

Appendix

The Method of Unitary Transformation

In the case of an electron in a time-independent field, the Foldy-Wouthuysen transformation is expressed by the equations

$$U^{-1}HU = H_{\mathrm{T}}, \tag{29}$$

$$\psi = U\psi_{\mathrm{T}}, \tag{30}$$

where H is the Hamiltonian, H_{T} the transformed Hamiltonian, and the unitary matrix U is chosen such that H_{T} is an even matrix of the form

$$H_{\mathrm{T}} = \begin{pmatrix} H^{(+)} & 0 \\ 0 & H^{(-)} \end{pmatrix}. \tag{31}$$

The connection between the method of elimination and that of unitary transformation, which has been dealt with in ref. [8, 9]), may be stated as follows. Let ξ be a two-component eigenspinor of $H^{(+)}$ satisfying the equation

$$H^{(+)}\xi = E\xi. \tag{32}$$

Then the spinor

$$\psi_{\mathrm{T}} = \begin{pmatrix} \xi \\ 0 \end{pmatrix} \tag{33}$$

satisfies the equation

$$H_{\mathrm{T}}\psi_{\mathrm{T}} = E\psi_{\mathrm{T}}, \tag{34}$$

and the spinor ψ given by eq. (30) satisfies the equation

$$H\psi = E\psi. \tag{35}$$

From eqs. (30) and (33) we obtain for the two large components of ψ the equation

$$\varphi = U_{++}\,\xi, \tag{36}$$

where U_{++} is a submatrix of U. The spinor φ satisfies the equation

$$H_e^{(+)}\varphi = E\varphi, \tag{37}$$

with

$$H_e^{(+)} = U_{++}H^{(+)}U_{++}^{-1}. \tag{38}$$

There is thus a set of eigenspinors ψ, ψ_T, φ, ξ associated with the same eigenvalue E. Since the submatrix U_{++} is not unitary, the similarity transformation (38) does not guarantee that $H_e^{(+)}$ is hermitian.

For an electromagnetic field described by the potentials $(A_0, \mathbf{A})$,

$$H = \beta m + \boldsymbol{\alpha}\cdot\boldsymbol{\pi} + V, \tag{39}$$

with $\boldsymbol{\pi} = \mathbf{p} + e\mathbf{A}$. Put

$$U = 1 + U_1 + U_2 + \cdots, \tag{40}$$

$$H_T = \beta m + H_0 + H_1 + \cdots, \tag{41}$$

with the suffixes 0, 1, etc. denoting the powers of $1/m$. In ref [5, 6]) the transformed Hamiltonian was calculated up to H_2. Extending to terms of order $(1/m)^3$, we obtain

$$U_1 = -(1/2m)\beta\boldsymbol{\alpha}\cdot\boldsymbol{\pi}, \tag{42}$$

$$U_2 = (ie/4m^2)\boldsymbol{\alpha}\cdot\boldsymbol{\mathscr{E}} - (1/8m^2)(\boldsymbol{\alpha}\cdot\boldsymbol{\pi})^2, \tag{43}$$

$$U_3 = (3/16m^3)\beta(\boldsymbol{\alpha}\cdot\boldsymbol{\pi})^3 + (ie/16m^3)\beta[\boldsymbol{\alpha}\cdot\boldsymbol{\mathscr{E}},\ \boldsymbol{\alpha}\cdot\boldsymbol{\pi}], \tag{44}$$

and

$$H_0 = V, \tag{45}$$

$$H_1 = (1/2m)\beta(\boldsymbol{\alpha}\cdot\boldsymbol{\pi})^2, \tag{46}$$

$$H_2 = -(ie/8m^2)[\boldsymbol{\alpha}\cdot\boldsymbol{\mathscr{E}},\ \boldsymbol{\alpha}\cdot\boldsymbol{\pi}], \tag{47}$$

$$H_3 = -(1/8m^3)\beta(\boldsymbol{\alpha}\cdot\boldsymbol{\pi})^4. \tag{48}$$

From eqs. (41) and (45)—(48) we obtain, up to terms of order $(1/m)^3$,

$$H^{(+)} = m + V + (1/2m)(\boldsymbol{\sigma}\cdot\boldsymbol{\pi})^2 - (ie/8m^2)[\boldsymbol{\sigma}\cdot\boldsymbol{\mathscr{E}},\ \boldsymbol{\sigma}\cdot\boldsymbol{\pi}] - (1/8m^3)(\boldsymbol{\sigma}\cdot\boldsymbol{\pi})^4 + \cdots, \tag{49}$$

which is a familiar expression.

Note added in proof

The total relativistic correction in eq. (17) may be written $V_s+V_c+V_k$, where V_s and V_c are given by eqs. (18), (19) and

$$V_k = -(1/4m)[p^2, (E_N-V)/D]_+ \tag{50}$$

is interpreted in this article as the correction to the kinetic energy.

After this paper was submitted, a paper by J. Werle [17]) became available to the writer. In the case of a Dirac electron in an electrostatic field A_0, the "effective potential" discussed by Werle is the sum of the potential energy $V = -eA_0$ and an attraction $-(1/2m)V^2$, which may be obtained from V_k by making the approximations $(p^2/2m) = E_N-V = -V$ and $D = 2m$. Thus Werle is mainly concerned with the correction V_k, while we are mainly concerned with the correction V_c.

References

1) C. G. Darwin, Proc. Roy. Soc. A **118** (1928) 654
2) W. Pauli, Handbuch der Physik, Vol. 24, Part 1 (Springer, 1933)
3) H. A. Bethe, Handbuch der Physik, Vol. 24, Part 1 (Springer, 1933)
4) E. U. Condon and G. H. Shortley, The Theory of Atomic Spectra (Cambridge University Press, 1935)
5) L. L. Foldy and S. A. Wouthuysen, Phys. Rev. **78** (1950) 29
6) L. L. Foldy, Phys. Rev. **87** (1952) 688
7) D. Feldman, Proceedings of the Fourth Annual Rochester Conference on High Energy Nuclear Physics (1954)
8) N. Fukuda, K. Sawada and M. Taketani, Prog. Theor. Phys. **12** (1954) 156
9) S. Ôkubo, Prog. Theor. Phys. **12** (1954) 603
10) S. S. Schweber, H. A. Bethe and F. de Hoffmann, Mesons and Fields, Vol. 2 (Row, Peterson and Co., 1955)
11) M. M. Lévy, Phys. Rev. **88** (1952) 725
12) A. Klein, Phys. Rev. **90** (1953) 1101
13) K. A. Brueckner and K. M. Watson, Phys. Rev. **92** (1953) 1023
14) W. Heitler, The Quantum Theory of Radiation (Oxford, 1954)
15) T. Y. Wu and G. E. Tauber, Phys. Rev. **100** (1955) 1767
16) W. Heitler and H. W. Peng, Proc. Camb. Phil. Soc. **38** (1942) 296
17) J. Werle, Acta Phys. Polonica **14** (1955) 233

Nuclear Physics **2** (1956/57) 356—370; *North-Holland Publishing Co., Amsterdam*

IMPROVEMENT OF QUANTUM ELECTRODYNAMICS PERTURBATION THEORY WITH HELP OF THE RENORMALIZATION GROUP

V. Z. BLANK

Physical Faculty, Moscow State University

D. V. SHIRKOV

Steklov Mathematical Institute, the USSR Academy of Sciences, Moscow

Received 25 July 1956

Abstract: It is shown that the renormalization group technique previously used to improve perturbation theory formulas for the Green functions can also be effectively used to improve the vertex part formulas. A survey of results for Green functions is presented as well.

1. Introduction

The renormalization group method was used [1]) (see also ref. [2])) to obtain asymptotic expressions for the photon (D) and electron (G) Green functions of quantum electrodynamics in the infrared and ultraviolet regions. However, all the calculations in ref. [1]) and [2]) were carried through in the special case of a purely transverse form of the photon Green function:

$$D \to D^{\mathrm{tr}}_{mn}(k) = -\frac{d(k^2)}{k^2}\left(g^{mn} - \frac{k_m k_n}{k^2}\right). \tag{1}$$

The results were subsequently extended by Logunov [3]) to the more general case when

$$D_{mn}(k) = -\frac{d(k^2)}{k^2}\left(g^{mn} - \frac{k_m k_n}{k^2}\right) + \frac{d_l^0}{k^2}\cdot\frac{k_m k_n}{k^2}. \tag{2}$$

The renormalization group method, however, can also be utilized to investigate a larger variety of problems, such as for example, to improve the expressions for the vertex function Γ^n.

With this aim in mind we shall briefly review the main results obtained up to the present time with help of the renormalization group technique in quantum electrodynamics (section 2) and then consider the problem of determining various asymptotic expressions for the vertex part.

2. The Green Functions D and G

In accord with ref. [3]) the equations defining the multiplicative renormalization group in quantum electrodynamics for $d_l^0 \neq 0$ have the form †

$$\begin{aligned} &G \to zG, \quad \Gamma \to z^{-1}\Gamma, \quad D \to z_3 D, \\ &e^2 \to z_3^{-1} e^2, \quad d_l^0 \to z_3 d_l^0, \end{aligned} \tag{3}$$

G, D and Γ being the expressions obtained by the standard subtraction procedure; they do not contain the usual divergences; z and z_3 are finite constants.

The electron function $G(k)$ can be represented in the form

$$G(k) = \frac{s_1(k^2)\hat{k} + s_2(k^2)m}{m^2 - k^2}. \tag{4}$$

Thus, with the help of formulas (2) and (4) D and G which are functions of the 4-momentum k have been expressed in terms of scalar functions d, s_1 and s_2 each of which depends only on a single scalar argument.

In distinction to D and G, the vertex part Γ depends on two independent 4-momenta and hence cannot be represented in such simple form. In view of the relative complexity of function Γ only Green functions D and G have been considered up to the present.

According to (3) some finite arbitrary multiplicative constants are involved in functions d and $s = s_1, s_2$. These constants can be fixed by the normalization conditions. Namely, we transfer the arbitrary factor in the function $d(k^2)$ to the argument of function d, assuming that d is normalized so that

$$d = 1 \quad \text{for} \quad k^2 = \lambda^2, \tag{5}$$

λ^2 playing the role of the square of the normalization momentum.

Evidently, normalization to unity is possible only for values of λ^2 for which the usual photon function d^0 (normalized to $k^2 = 0$) is real and positive. This is a result of the circumstance that renormalization of the function d is carried out by the same quantity z_3 which renormalizes the square of the charge and hence must be real and positive.

In conformity with second order perturbation theory formulas the condition that d^0 be real for $k^2 = \lambda^2$ requires that

$$\lambda^2 < 4m^2. \tag{6}$$

† d_l^0 will be considered a constant.

It is well known that account of higher orders in perturbation theory modifies this condition to

$$\lambda^2 < 0. \tag{7}$$

Thus, from the condition that d is a real function it follows that the normalization momentum obeys condition (7). In some cases, however, such as when calculating the infrared asymptotic behaviour of the electron Green function (in this case it is sufficient to consider only the first term in the expansions of d in powers of e^2) condition (6) may be valid.

It should be noted that, in general, restriction (7) is not essential because when domains in momentum space are considered in which the Green functions are complex, one has but to consider separately their real and imaginary parts.

From considerations of homogeneity in momentum space it now follows that the functions d, s_1 and s_2 have the form

$$f\left(\frac{k^2}{\lambda^2},\ \frac{m^2}{\lambda^2},\ e^2\right) \tag{8}$$

and, according to (5),

$$d\left(1,\ \frac{m^2}{\lambda^2},\ e^2\right) = 1. \tag{9}$$

Introducing representation (8) into (3) and taking into account (9) we obtain for d and $s = s_1,\ s_2$ the functional equations

$$e^2 d(x, y, e^2) = e^2 d(t, y, e^2) d\left(\frac{x}{t},\ \frac{y}{t},\ e^2\, d(t, y, e^2)\right), \tag{10}$$

$$s(x, y, e^2, e^2 d_l^0) = s(t, y, e^2, e^2 d_l^0) \cdot \frac{s\left(\frac{x}{t},\ \frac{y}{t},\ e^2 d(t, y, e^2),\ e^2 d_l^0\right)}{s\left(1,\ \frac{y}{t},\ e^2 d(t, y, e^2),\ e^2 d_l^0\right)}. \tag{11}$$

Here

$$x = \frac{k^2}{\lambda^2},\ y = \frac{m^2}{\lambda^2},\ t = \frac{\lambda_1^2}{\lambda^2}. \tag{12}$$

Equations (10) and (11) are renormalization group functional equations which describe the simultaneous transformation of all three arguments of functions d, s_1 and s_2.

Considering these equations as equations for the unknown func-

tions d and s one may attempt to determine d and s from equations (10) and (11).

As was shown by Ovsiannikov [4]) the general solutions of equations (10) and (11) have the form

$$H(y, e^2) = H\left(\frac{y}{x},\ e^2 d(x, y, e^2)\right) \tag{13}$$

and (for $d_i^0 = 0$)

$$s(x, y, e^2) = P(y, e^2) Q\left(\frac{y}{x}, e^2 d(x, y, e^2)\right), \tag{14}$$

the function $e^2 d$ in the second argument of Q being one of the solutions of equation (13); H, P and Q are arbitrary functions of two arguments. Thus, equations (10) and (11) are not sufficient to find the concrete form of the quantum electrodynamics Green functions because along with the desired solutions there are irrelevant solutions which satisfy these equations.

We therefore shall seek those solutions of group equations (10) and (11) which, under certain conditions change over to some explicitly known expressions for the Green functions. Such is, for instance, the case when e^2 is small. We require that for any values of the arguments x and y the solutions d and s of equations (10) and (11) in the limit of small e^2 should take the form

$$d(x, y, e^2) = 1 + e^2 d_1(x, y) + e^4 d_2(x, y) + \ldots, \tag{15}$$

$$s(x, y, e^2, e^2 d_i^0) = 1 + e^2 s_1(x, y) + e^2 d_i^0 s_1^i(x, y) + e^4 \ldots, \tag{16}$$

where the functions $d_1, d_2, \ldots; s_1, s_1^i, \ldots$ are determined from the usual perturbation theory.

In order to find the solutions which obey the correspondence requirement in the limit of small e^2 we change from (10) and (11) to differential Lie equations.

Differentiating with respect to x equation (10) and the logarithm of equation (11) and putting $t = x$ we get

$$\frac{\partial e^2 d(x, y, e^2)}{\partial x} = \frac{e^2 d(x, y, e^2)}{x} \cdot \varphi\left(\frac{y}{x}, e^2 d(x, y, e^2)\right) \tag{17}$$

and

$$\frac{\partial \ln s(x, y, e^2, e^2 d_i^0)}{\partial x} = \frac{1}{x} \psi\left(\frac{y}{x}, e^2 d(x, y, e^2),\ e^2 d_i^0\right) \tag{18}$$

where

$$\varphi(y, e^2) = \left[\frac{\partial}{\partial \xi} d(\xi, y, e^2)\right]_{\xi=1} \tag{19}$$

and

$$\psi(y, e^2, e^2 d_i^0) = \left[\frac{\partial}{\partial \xi} \ln s(\xi, y, e^2, e^2 d_i^0)\right]_{\xi=1}. \tag{20}$$

By substituting into (19) and (20) expressions (15) and (16) obtained from perturbation theory for d and s we automatically ensure that the correspondence condition for $e^2 \to 0$ will be satisfied.

It should be noted that use in (19) and (20) of expansions for d and s which are valid for $e^2 \ll 1$ yields the result that expressions for φ and ψ which are power series expansions in the "invariant charges" $e^2 d$ and $e^2 d_i^0$ will be substituted in (17) and (18). Thus, the region of validity of the solutions of equations (29) and (30) will be restricted by the condition of smallness of the "invariant charge"

$$e^2 d \ll 1. \tag{21}$$

It is likewise clear that practically only equation (17) will have to be solved, since for a given d function s can be found from (18) by simple quadratures

$$\ln \frac{s(x, y, e^2, e^2 d_i^0)}{s(x_0, y, e^2, e^2 d_i^0)} = \int_{x_0}^{x} \frac{dz}{z} \psi\left(\frac{y}{z}, e^2 d(z, y, e^2), e^2 d_i^0\right). \tag{22}$$

Equation (17) can particularly easily be solved if the second order perturbation expression for φ is employed. In this case the integration can be completely performed in explicit form.

Indeed, since

$$d(x, y, e^2) = 1 + \frac{e^2}{2\pi^2} \int_0^1 \alpha(1-\alpha) \ln \left| \frac{y - \alpha(1-\alpha)x}{y - \alpha(1-\alpha)} \right| d\alpha + \ldots$$

$$= 1 + e^2 \left[f\left(\frac{x}{y}\right) - f\left(\frac{1}{y}\right) \right]$$

we get

$$\varphi(y, e^2) = e^2 \left[\frac{\partial}{\partial \xi} f\left(\frac{\xi}{y}\right)\right]_{\xi=1};$$

thus,

$$\frac{\partial e^2 d(x, y, e^2)}{\partial x} = \frac{(e^2 d)^2}{x} \left[\frac{\partial}{\partial \xi} f\left(\frac{x\xi}{y}\right)\right]_{\xi=1}$$

and hence

$$d(x, y, e^2) = \left\{1-e^2\int_1^x \frac{dz}{z}\left[\frac{\partial}{\partial\xi} f\left(\frac{z\xi}{y}\right)\right]_{\xi=1}\right\}^{-1} = \frac{1}{1-e^2\left[f\left(\frac{x}{y}\right)-f\left(\frac{1}{y}\right)\right]}. \quad (23)$$

If function φ has been determined to higher order terms equation (17) cannot be integrated in general form. We therefore confine our attention to the most important, ultraviolet, asymptotic case when $x \gg y$.

In this case the variable y drops out and we obtain [1, 2])

$$d^{-1}(x, e^2) = 1-\frac{e^2}{12\pi^2}\ln x+\frac{3e^2}{16\pi^2}\ln\left(1-\frac{e^2}{12\pi^2}\ln x\right)+e^4\ldots \quad (24)$$

Consider now the electron Green function. We shall first examine the region of large momentum values. In this case, as before, the variable y drops out and, by changing the integration variable, formula (22) can be reduced to the form

$$\ln\frac{s(x, e^2, e^2 d_l^0)}{s(1, e^2, e^2 d_l^0)} = \int_{e^2}^{e^2 d(x, e^2)} \frac{dz}{z\varphi(z)}\psi(z, e^2 d_l^0). \quad (25)$$

Here $\varphi(z)$ and $\psi(z, e^2 d_l^0)$ have been obtained from (19) and (20) by omitting the variable y.

Using perturbation theory to determine ψ we can express the latter as a series in powers of $e^2 d_l^0$ and z. Substituting in (25) the corresponding expansion of φ^{-1} and performing the integration we arrive at the formula

$$\ln\frac{s(x, e^2, e^2 d_l^0)}{s(1, e^2, e^2 d_l^0)} = Ad_l^0(1-d^{-1}(x, e^2)) + B\ln d(x, e^2)+Ce^2(d(x, e^2)-1)+\ldots \quad (26)$$

in which the coefficients $A, B, C, \ldots$ have the form of power series expansions in the "longitudinal invariant charge" $e^2 d_l^0$:

$$a_0+a_1 e^2 d_l^0+a_2(e^2 d_l^0)^2+\ldots. \quad (27)$$

In particular, using only second order perturbation theory to determine functions φ and ψ we obtain the familiar formulas first derived by Landau, Abrikosov and Khalatnikov [5])

$$\ln\frac{s_1(x, e^2, e^2 d_l^0)}{s_1(1, e^2, e^2 d_l^0)} = \frac{e^2 d_l^0}{16\pi^2}\ln x, \quad (28)$$

$$\ln \frac{s_2(x, e^2, e^2 d_l^0)}{s_2(1, e^2, e^2 d_l^0)} = \frac{e^2 d_l^0}{16\pi^2} \ln x + \frac{9}{4} \ln \left(1 - \frac{e^2}{12\pi^2} \ln x\right). \qquad (29)$$

The well known infrared singularity of the electron Green function for $k^2 \approx m^2$ can be investigated in a similar manner with the help of formula (22). The relevant study carried out in ref. [1, 2]) was based on second order perturbation theory. The result is as follows:

$$s_1(k^2) = s_2(k^2) \approx \left(\left| 1 - \frac{k^2}{m^2} \right| \right)^{-\alpha(e_0^2)} \qquad (30)$$

where

$$\alpha(e_0^2) = \frac{e_0^2}{4\pi} \cdot \frac{3 - d_l^0}{2\pi} \qquad (31)$$

and

$$\frac{e_0^2}{4\pi} = \frac{1}{137}.$$

3. Asymptotic Investigation of the Vertex Part

In distinction to the Green function the vertex operator has a comparatively complex matrix structure and depends on two four-dimensional momentum vectors. In the general case it can be decomposed into products of various numbers of Dirac matrices. Since it is the asymptotic expression for the vertex operator in the infrared and ultraviolet regions that will be deduced below we shall confine our attention from the very beginning to the term in Γ^n which is proportional to the matrix γ^n. Evidently this term is a scalar function of three independent scalar arguments p^2, q^2, k^2 $(p - q = k)$:

$$\Gamma^n = \gamma^n \Gamma(p^2, q^2; k^2).$$

According to (3) multiplicative renormalization for function Γ reduces to the transformation

$$\Gamma \to z^{-1}\Gamma. \qquad (32)$$

As can be seen from (32) function Γ has been determined with an accuracy to an arbitrary constant z. In the usual manner we transfer this arbitrariness to the argument of the function Γ and introduce the square of an auxiliary momentum λ^2 and change to dimensionless arguments:

$$\Gamma\left(\frac{p^2}{\lambda^2}, \frac{q^2}{\lambda^2}, \frac{k^2}{\lambda^2}, \frac{m^2}{\lambda^2}, e^2, e^2 d_l^0\right). \tag{33}$$

We first consider Γ as a function of p^2, the other variables being fixed. Substituting (33) in (32) and excluding the constant z we arrive at an equation which is similar to (11):

$$\frac{\Gamma(x, y, z, u, e^2, e^2 d_l^0)}{\Gamma(t, y, z, u, e^2, e^2 d_l^0)} = \frac{\Gamma\left(\frac{x}{t}, \frac{y}{t}, \frac{z}{t}, \frac{u}{t}, e^2 d(t, u, e^2), e^2 d_l^0\right)}{\Gamma\left(1, \frac{y}{t}, \frac{z}{t}, \frac{u}{t}, e^2 d(t, u, e^2), e^2 d_l^0\right)} \tag{34}$$

where

$$x = \frac{p^2}{\lambda^2}, y = \frac{q^2}{\lambda^2}, z = \frac{k^2}{\lambda^2}, u = \frac{m^2}{\lambda^2}, t = \frac{\lambda_1^2}{\lambda^2}.$$

Differentiating the logarithm of equation (34) with respect to x and putting $t = x$ we get

$$\frac{\partial}{\partial x} \ln \Gamma(x, y, z, u, e^2, e d_l^0) = \frac{1}{x}\left[\frac{\partial}{\partial \xi} \ln \Gamma\left(\xi, \frac{y}{x}, \frac{z}{x}, \frac{u}{x}, e^2 d(x, u, e^2), e^2 d_l^0\right)\right]_{\xi=1}. \tag{35}$$

The solution of equation (35) has the form

$$\ln \frac{\Gamma(x, y, z, u, e^2, e^2 d_l^0)}{\Gamma(x_0, y, z, u, e^2, e^2 d_l^0)} = \int_{x_0}^{x} \frac{dx'}{x'}\left[\frac{\partial}{\partial \xi} \ln \Gamma\left(\xi, \frac{y}{x'}, \frac{z}{x'}, \frac{u}{x'}, e^2 d(x', u, e^2), e^2 d_l^0\right)\right]_{\xi=1}. \tag{36}$$

Considering now $\Gamma(x_0, y, z, \ldots)$ as a function of y and then $\Gamma(x_0, y_0, z, \ldots)$ as a function of z we obtain the final formula

$$\begin{aligned}\ln \frac{\Gamma(x, y, z, u, e^2, e^2 d_l^0)}{\Gamma(x_0, y_0, z_0, u, e^2, e^2 d_l^0)} &= \int_{x_0}^{x} \frac{dx'}{x'}\left[\frac{\partial}{\partial \xi} \ln \Gamma\left(\xi, \frac{y}{x'}, \frac{z}{x'}, \frac{u}{x'}, e^2 d(x', u, e^2), e^2 d_l^0\right)\right]_{\xi=1} \\ &+ \int_{y_0}^{y} \frac{dy'}{y'}\left[\frac{\partial}{\partial \xi} \ln \Gamma\left(\frac{x_0}{y'}, \xi, \frac{z}{y'}, \frac{u}{y'}, e^2 d(y', u, e^2), e^2 d_l^0\right)\right]_{\xi=1} \\ &+ \int_{z_0}^{z} \frac{dz'}{z'}\left[\frac{\partial}{\partial \xi} \ln \Gamma\left(\frac{x_0}{z'}, \frac{y_0}{z'}, \xi, \frac{u}{z'}, e^2 d(z', u, e^2), e^2 d_l^0\right)\right]_{\xi=1}.\end{aligned} \tag{37}$$

A different order of integration, of course, can be used in (37). As will be demonstrated below this order can be uniquely determined in each particular case from considerations of correspondence to perturbation theory.

The right hand side of (37) can be considerably simplified if second order perturbation theory is used to determine Γ (which enters (37)).

We then have

$$\Gamma(x, y, z, u, e^2, e^2 d^0) = 1+e^2\left[\Lambda_t\left(\frac{x}{u}, \frac{y}{u}, \frac{z}{u}\right)-\tilde{\Lambda}_t(u)\right] + e^2 d_l^0\left[\Lambda_l\left(\frac{x}{u}, \frac{y}{u}, \frac{z}{u}\right)-\tilde{\Lambda}_l(u)\right]. \tag{38}$$

Of course (38) is valid only if

$$e^2\Lambda_t\left(\frac{x}{u}, \frac{y}{u}, \frac{z}{u}\right) \ll 1, \qquad e^2 d_l^0\Lambda_l\left(\frac{x}{u}, \frac{y}{u}, \frac{z}{u}\right) \ll 1, \tag{39}$$

which imposes certain restrictions on the arguments of functions Λ_t and Λ_l. These restrictions should be taken into account when determining Γ in the right hand side of (37).

Consider a concrete case, that of the ultraviolet asymptotic region when

$$|k^2| \gg |p^2|, \ |q^2| \gg m^2$$

or

$$|z| \gg |x|, \ |y| \gg |u|. \tag{40}$$

The corresponding second order perturbation theory calculations were performed by Abrikosov [6]) and Sudakov [7]) who obtained

$$\Lambda_l = 0, \ \Lambda_t\left(\frac{x}{u}, \frac{y}{u}, \frac{z}{u}\right) = -\frac{1}{8\pi^2}\ln\left|\frac{z}{x}\right|\ln\left|\frac{z}{y}\right|. \tag{41}$$

Here, as in similar cases previously encountered, the "mass" variable u has dropped out.

In order to find the asymptotic behaviour of Γ we change the order of integration in formula (37) and write it as follows:

$$\ln \frac{\Gamma(x, y, z, u, e^2, e^2 d_l^0)}{\Gamma(x_0, y_0, z_0, u, e^2, e^2 d_l^0)} = I_1(x, y, z, e^2, e^2 d_l^0 | z_0) + I_2(x, y, z_0, e^2, e^2 d_l^0 | x_0) + I_3(x_0, y, z_0, e^2, e^2 d_l^0 | y_0), \tag{42}$$

$$I_1 = \int_{z_0}^{z} \frac{dz'}{z'} \left[\frac{\partial}{\partial \xi} \ln \Gamma\left(\frac{x}{z'}, \frac{y}{z'}, \xi, e^2 d(z', e^2), e^2 d_l^0 \right) \right]_{\xi=1}, \tag{43}$$

$$I_2 = \int_{x_0}^{x} \frac{dx'}{x'} \left[\frac{\partial}{\partial \eta} \ln \Gamma\left(\eta, \frac{y}{x'}, \frac{z_0}{x'}, e^2 d(x', e^2), e^2 d_l^0 \right) \right]_{\eta=1}, \tag{44}$$

$$I_3 = \int_{y_0}^{y} \frac{dy'}{y'} \left[\frac{\partial}{\partial \zeta} \ln \Gamma\left(\frac{x_0}{y'}, \zeta, \frac{z_0}{y'}, e^2 d(y', e^2), e^2 d_l^0 \right) \right]_{\zeta=1}. \tag{45}$$

Assuming x_0, y_0, z_0 to be quantities of the same order of magnitude we can make use of usual perturbation theory to compute I_3. This gives

$$I_3 = \frac{e^2}{8\pi^2} \ln \frac{z_0}{x_0} \int_{y_0}^{y} \frac{dy'}{y'} d(y', e^2) = \frac{3}{2} \ln \frac{z_0}{x_0} \ln \frac{d(y, e^2)}{d(y_0, e^2)}. \tag{46}$$

As usual the applicability of this formula is restricted by the condition of validity of invariant perturbation theory

$$e^2 d(y, e^2) \ll 1 \tag{47}$$

or

$$1 - \frac{e^2}{12\pi^2} \ln y \gg e^2.$$

We now proceed to calculate I_2. The second argument of function Γ in the right hand side of (44) for $x' = O(x_0)$ may turn out to considerably exceed unity. On the other hand the first and third arguments cannot appreciably exceed unity. Therefore, in order to determine Γ which enters I_2 we make use of an equation similar to (36) obtained after integration over y:

$$\ln \frac{\Gamma(\bar{x}, y, \bar{z}, e^2)}{\Gamma(\bar{x}, y_0, \bar{z}, e^2)} = I_3(\bar{x}, y, \bar{z}, e^2 | y_0). \tag{48}$$

Here $\bar{x}$ and $\bar{z}$ cannot be much larger than unity and the region of variation of y is restricted only by condition (47). Inserting (48) into (44) and taking into account (41) we find

$$I_2(x, y, z_0, e^2|x_0)$$

$$= \frac{e^2}{8\pi^2} \ln \frac{z_0}{y_0} \int_{x_0}^{x} \frac{dx'}{x'} d(x', e^2) - \frac{3}{2} \int_{x_0}^{x} \frac{dx'}{x'} \ln \frac{d\left(\frac{y}{x'}, e^2 d(x', e^2)\right)}{d\left(\frac{y_0}{x'}, e^2 d(x', e^2)\right)} \tag{49}$$

$$= \frac{3}{2} \ln \frac{z_0}{y_0} \ln \frac{d(x, e^2)}{d(x_0, e^2)} - \frac{3}{2} \ln \frac{x}{x_0} \ln \frac{d(y, e^2)}{d(y_0, e^2)}.$$

This formula is valid if condition (47) for variables x and y is satisfied.

We now compute I_1. A scrutiny of the arguments of function Γ' in the right hand side of (43) shows that in order to determine Γ, use should be made of an equation of the same type as (48), the right hand side of which contains the sum I_2+I_3. Computations yield the expression

$$\begin{aligned} I_1(x, y, z, e^2|z_0) = {} & 3\left(\ln \frac{z}{z_0} - \frac{12\pi^2}{e^2} \ln \frac{d(z, e^2)}{d(z_0, e^2)}\right) \\ & + \frac{3}{2} \ln \frac{z}{z_0} \left[\ln \frac{d(x, e^2)}{d(x_0, e^2)} + \ln \frac{d(y, e^2)}{d(y_0, e^2)}\right] \\ & + \frac{3}{2} \ln x_0 y_0 \ln \frac{d(z, e^2)}{d(z_0, e^2)}. \end{aligned} \tag{50}$$

Before writing down the final form of the right hand side of (42) it seems pertinent to point out the following. Although (50) is symmetric with respect to x and y, the sums (46) and (49) do not possess this property. The reason for this is that non-symmetrical assumptions relating to x and y were made in determining I_3 and I_2. In view of symmetry of the initial formulas (40) and (41) we shall perform the corresponding symmetrization. This gives

$$\begin{aligned} \ln \frac{\Gamma(x, y, z, e^2)}{\Gamma(x_0, y_0, z_0, e^2)} = {} & 3\left[\ln \frac{z}{z_0} - \frac{12\pi^2}{e^2} \ln \frac{d(z, e^2)}{d(z_0, e^2)}\right] + \frac{3}{2} \ln x_0 y_0 \ln \frac{d(z, e^2)}{d(z_0, e^2)} \\ & + \frac{3}{2}\left[\ln \frac{z}{x_0} \ln \frac{d(y, e^2)}{d(y_0, e^2)} + \ln \frac{z}{y_0} \ln \frac{d(x, e^2)}{d(x_0, e^2)}\right] \\ & + \frac{3}{4}\left[\ln \frac{x_0}{x} \ln \frac{d(y, e^2)}{d(y_0, e^2)} + \ln \frac{y_0}{y} \ln \frac{d(x, e^2)}{d(x_0, e^2)}\right]. \end{aligned} \tag{51}$$

This formula is valid on the following conditions:

$$1 - \frac{e^2}{12\pi^2} \ln z \gg e^2, \tag{52}$$

$$\ln z > \ln x, \ \ln y \geqq \ln x_0, \ \ln y_0, \ \ln z_0.$$

Moreover, $z_0, x_0, y_0 \gg 1$, $\ln x_0 = O(\ln y_0)$, and $\ln z_0$ cannot considerably exceed $\ln x_0$, $\ln y_0$.

It should also be noted that for

$$e^2 \ln z \ll 1$$

we arrive at the formula

$$\ln \frac{\Gamma(x, y, z, e^2)}{\Gamma(x_0, y_0, z_0, e^2)} = -\frac{e^2}{8\pi^2} \left\{ \ln \frac{z}{x} \ln \frac{z}{y} - \ln \frac{z_0}{x_0} \ln \frac{z_0}{y_0} \right\} \tag{53}$$

which was previously obtained by Sudakov [7]) by summation of a series of significant Feynman diagrams and by Blank [8]) who obtained an approximate solution of the Schwinger equation by the proper time technique.

In another ultraviolet case, when

$$p^2 = q^2 \gg k^2, m^2 \tag{54}$$

perturbation theory yields

$$\Lambda_i = 0, \ \Lambda_i \left(\frac{x}{u}, \frac{x}{u}, \frac{z}{u} \right) = -\frac{1}{(4\pi)^2} \ln \frac{x}{u} \tag{55}$$

and hence

$$\frac{\Gamma(x, x, z, u, e^2, e^2 d_i^0)}{\Gamma(x_0, x_0, z_0, u, e^2, e^2 d_i^0)} = \left(\frac{x}{x_0} \right)^{-\frac{e^2 d_i^0}{16\pi^2}}. \tag{56}$$

We now turn our attention to the infrared limit and consider the case when

$$p^2 = q^2 \to m^2, \qquad k^2 < 0. \tag{57}$$

The corresponding second order perturbation theory computations were carried out by Abrikosov [6]) who obtained

$$\Lambda_i \left(\frac{x}{u}, \frac{z}{u} \right) = \frac{1}{8\pi^2} \ln \left| \frac{u}{x-u} \right|, \tag{58}$$

$$\Lambda_t\left(\frac{x}{u}, \frac{z}{u}\right) = \varphi\left(\frac{z}{u}\right) + \psi\left(\frac{z}{u}\right) \ln\left|\frac{u}{x-u}\right|, \tag{59}$$

where

$$\varphi\left(\frac{z}{u}\right) = \frac{1-\dfrac{2u}{z}}{\sqrt{1-\dfrac{4u}{z}}}\left\{\ln\left|1-\frac{z}{2u}\right|\right\}^2, \tag{60}$$

$$\psi\left(\frac{z}{u}\right) = 4\frac{\dfrac{u}{z}-\dfrac{1}{2}}{\sqrt{1-\dfrac{4u}{z}}} \ln\left(1-\frac{4u}{z}+\frac{|z|}{2u}\sqrt{1+\frac{4u}{|z|}}\right)-1. \tag{61}$$

Integrating, we get

$$\ln\frac{\Gamma(x, z, u, e^2, e^2 d_i^0)}{\Gamma(x_0, z_0, u, e^2, e^2 d_i^0)} = \frac{e^2}{8\pi^2}\ln\left|\frac{x_0-u}{x-u}\right| \Phi\left(\frac{z}{u}, \frac{z_0}{u}, u\right) + \frac{e^2}{8\pi^2}\Psi\left(\frac{z}{u}, \frac{z_0}{u}, \frac{x_0}{u}, u\right). \tag{62}$$

Here

$$\Psi\left(\frac{z}{u}, \frac{z_0}{u}, \frac{x_0}{u}, u\right) = \int_{z_0}^{z} d(z', u, e^2)\left[\frac{\partial\varphi\left(\dfrac{z'}{u}\right)}{\partial z'} + \ln\left|\frac{u}{x_0-u}\right|\frac{\partial\psi\left(\dfrac{z'}{u}\right)}{\partial z'}\right] dz', \tag{63}$$

$$\Phi\left(\frac{z}{u}, \frac{z_0}{u}, u\right) = \int_{z_0}^{z} d(z', u, e^2)\frac{\partial\psi\left(\dfrac{z'}{u}\right)}{\partial z'}\,dz' + f\left(\frac{z_0}{u}\right) - 1 + d_i^0. \tag{64}$$

Let us examine in greater detail the infrared singularity exponent

$$\Phi\left(\frac{z}{u}, \frac{z_0}{u}, u\right).$$

To compute the integral in the right hand side of (64) we note that in the case under consideration function d has the same form as (23), the function $f(t)$ which enters (23), being proportional to $\psi(t)$ in the region of large values of t. In view of this circumstance one may write (with an accuracy to small terms of the order e^2)

$$\int_{z_0}^{z} \frac{dz'}{1-e^2\left[f\left(\frac{z'}{u}\right)-f\left(\frac{1}{u}\right)\right]} \cdot \frac{\partial\psi\left(\frac{z'}{u}\right)}{\partial z'} \approx \int_{z_0}^{z} \frac{dz'}{1-\frac{e^2}{24\pi^2}\psi\left(\frac{z'}{u}\right)} \cdot \frac{\partial\psi\left(\frac{z'}{u}\right)}{\partial z'}$$
$$= \frac{24\pi^2}{e^2} \ln \frac{1-\frac{e^2}{24\pi^2}\psi\left(\frac{z_0}{u}\right)}{1-\frac{e^2}{24\pi^2}\psi\left(\frac{z}{u}\right)}. \tag{65}$$

Inserting this expression into (64) and taking into account the smallness of $(e^2/24\pi^2)\psi(z_0/u)$ we find for the infrared singularity exponent β

$$\Gamma(p^2, p^2, k^2, m^2, e^2, e^2 d_1^0) \approx \left|\frac{m^2}{p^2-m^2}\right|^{\beta\left(\frac{k^2}{m^2}\right)} \tag{66}$$

the following expression:

$$\beta\left(\frac{k^2}{m^2}\right) = \frac{e^2 d_1^0}{8\pi^2} - 3 \ln \left|1-\frac{e^2}{24\pi^2}\psi\left(\frac{k^2}{m^2}\right)\right|. \tag{67}$$

In the limiting case of large k^2, when

$$\frac{e^2}{12\pi^2}\ln\frac{k^2}{m^2} \text{ is } O(1),$$

we obtain

$$\beta\left(\frac{k^2}{m^2}\right) = \frac{e^2 d_1^0}{8\pi^2} + 3 \ln d\left(\frac{k^2}{m^2}, e^2\right). \tag{68}$$

On the other hand, for

$$\frac{e^2}{12\pi^2}\ln\frac{k^2}{m^2} \ll 1,$$

when

$$\frac{e^2}{24\pi^2}\psi\left(\frac{k^2}{m^2}\right) \ll 1,$$

we get the result

$$\beta\left(\frac{k^2}{m^2}\right) = \frac{e^2}{8\pi^2}\left[d_1^0 + \psi\left(\frac{k^2}{m^2}\right)\right], \tag{69}$$

previously obtained by Abrikosov [6]) by summation of a series of the significant Feynman diagrams. Going over to the limit $k^2 \to 0$ in (69) we obtain the formula

$$\beta(0) = \frac{e^2}{8\pi^2}(d_l^0 - 3) \tag{70}$$

which in virtue of the Ward identity is found to agree with the main term in (31).

We have examined here the main asymptotic expressions for the vertex part when Γ^n was assumed proportional to the matrix γ^n. If higher orders in e^2 are taken into account it may be necessary to consider components of Γ^n which possess a different matrix structure. However from the present investigation it follows that the corresponding consideration can be extended to these cases.

It is also evident that the renormalization group technique may be applied to more complex functions such as those which correspond, for example, to various types of scattering processes.

In conclusion the authors express their deep appreciation to N. N. Bogolyubov for a number of invaluable suggestions.

References

1) N. N. Bogolyubov and D. V. Shirkov, Doklady Akad. Nauk USSR **103** (1955) 203, 391
2) N. N. Bogolyubov and D. V. Shirkov, JETP (USSR) **30** (1956) 77; Nuovo Cimento **3** (1956) 845
3) A. A. Logunov, JETP (USSR) **30** (1956) 793
4) L. V. Ovsiannikov, Doklady Akad. Nauk USSR **109** (1956) no. 6
5) L. D. Landau, A. A. Abrikosov and I. M. Khalatnikov. Doklady Akad. Nauk USSR **95** (1954) 773; **96** (1954) 261
6) A. A. Abrikosov, JETP (USSR) **30** (1956) 96
7) V. V. Sudakov, JETP (USSR) **30** (1956) 87
8) V. Z. Blank, Doklady Akad. Nauk USSR **107** (1956) 383

Nuclear Physics **2** (1956/57) 371—381; *North-Holland Publishing Co., Amsterdam*

CROSS SECTION OF THE $I^{127}(\gamma, n)I^{126}$ REACTION

J. ERÖ and L. KESZTHELYI

Central Research Institute for Physics, Department of Atomic Physics, Budapest

Received 23 July 1956

Abstract: A NaI(Tl) scintillation crystal was irradiated with the gamma radiation of the Li(p, γ) reaction. From the number of scintillations during the irradiation, and from the activity of the I^{126} isotope after the irradiation the cross section of the I^{127} (γ, n)I^{126} reaction was determined. Our measurements give $\sigma(\gamma, n) = 125 \pm 6$ mb. Combining this with the results of other measurements in which neutrons were counted, we got the value $\sigma(\gamma, 2n) = 30 \pm 20$ mb for the $I^{127}(\gamma, 2n)I^{125}$ reaction. The ratio of the K capture of the I^{126} isotope to the total number of disintegrations has also been determined. It was found to be 0.51 ± 0.03.

1. Introduction

The (γ, n) reaction of the I^{127} nucleus was investigated by several authors. McDaniel *et al.* [1]) produced the reaction with the radiation of the Li(p, γ)Be reaction, while Montalbetti *et al.* [2]) and Nathans and Halpern [3]) made their experiments with the bremsstrahlung of a betatron. All these authors observed the reactions by counting the neutrons. Their results for the cross section at 17.6 MeV energy are inaccurate owing to the many corrections that were necessary. For instance Montalbetti *et al.* have found a value almost twice as great as the other two authors. Further, we have to consider that at 17.6 MeV energy also the (γ, 2n) reaction will exist, therefore only the sum $\sigma_+ = \sigma(\gamma, n) + 2\sigma(\gamma, 2n)$ could be measured. Here $\sigma(\gamma, n)$ and $\sigma(\gamma, 2n)$ are the cross sections of the (γ, n) and (γ, 2n) reactions respectively. However, when comparing the results with the theoretical values given by the sum-rule, we must know the cross section of each reaction separately [4, 5]). The aim of our measurements was therefore to determine the (γ, n) cross section independently and to achieve a higher accuracy than was obtained in the earlier experiments.

2. The Experimental Method

The cross section was measured on the I nuclei of a NaI(Tl) scintillation crystal. The source of γ quanta was the Li^7(p, γ)Be^8

reaction. During the irradiation we counted the number of γ quanta producing fast electrons in the crystal with a photomultiplier. After the irradiation we measured by the same method the activity of the I^{126} nuclei produced in the crystal by the (γ, n) reactions. By this method a greater accuracy may be obtained because there is no need to take into account any geometrical and self absorptional corrections when determining the γ flux and the activity.

Let σ_e be the cross section of producing electrons by γ quanta in a NaI molecule, σ_n be the cross section of the reaction (γ, n) of the I^{127} nuclei. If there are n_e fast electrons produced per sec, then the number of I^{126} nuclei created is

$$n_I = \frac{\sigma_n}{\sigma_e} n_e. \tag{1}$$

The number of I^{126} nuclei in a given time t is

$$N_I(t) = \frac{\sigma_n}{\sigma_e} e^{-\lambda t} \int_{-\infty}^{t} n_e(\tau) e^{\lambda \tau} \, d\tau$$

where λ is the disintegration constant.

Taking into account that the activity is $Y_0 = \lambda N_I$ we can determine the cross section from the activity of the irradiated crystal:

$$\sigma_n = \sigma_e \frac{Y_0(t)}{\lambda e^{-\lambda t} \int_{-\infty}^{t} n_e(\tau) e^{\lambda \tau} \, d\tau}. \tag{2}$$

In order to determine σ_n, we have to know the disintegration constant λ, the cross section of producing fast electrons σ_e, the number of electrons produced by the quanta in the crystal $n_e(\tau)$, and the disintegration rate of I^{126} nuclei after activation Y_0.

3. The Experiment

3.1. IRRADIATION

The $Li^7(p, \gamma)Be^8$ reaction was produced by an 800 kV Cockroft-Walton generator [6]). Thick LiOH and metallic Li targets were bombarded with an unanalysed hydrogen ion beam of about 200 uA intensity, accelerated to 500 keV. The irradiated NaI crystal had a volume of 3 cm^3 and the scintillations, produced by the gamma quanta in the crystal were counted by an RCA 5819 photomultiplier. We had also another counting arrangement for

the monitoring of the γ flux. We performed two sets of irradiations, each in several periods of 6—7 hours.

3.2. DETERMINATION OF ν_e

The amplitudes of the pulses produced by the high-energy γ quanta in the crystal are very different: in the spectrum of pulses there may be found all values from the greatest amplitude, belonging to the maximal energy, to to the smallest one [7]). The total number

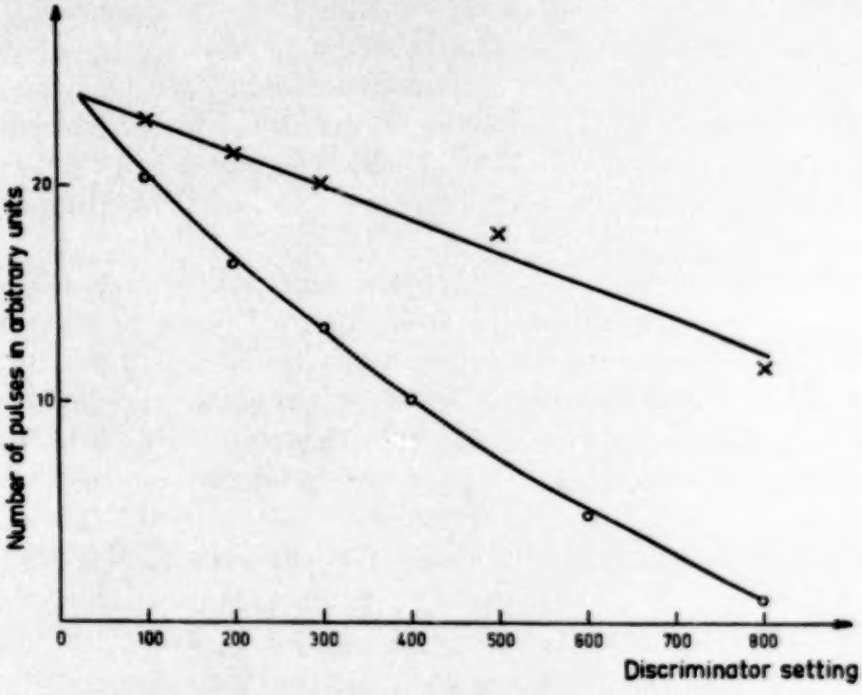

Fig. 1. The number of pulses produced by the high energy radiation vs. discriminator setting.

of the scintillations is obtainable from the extrapolation to zero value of the integral amplitudo spectrum [8]). During the irradiation we several times measured this spectrum with different amplifications. Fig. 1 shows curves of that type. The zero point of the discriminator is given by the intersection of the two curves. The number of pulses at this extrapolated point is determined with an accuracy of cca 3 %. During these measurements, as we have mentioned above, the flux was monitored by another arrangement.

The number of scintillations does not directly give the number of electrons produced in the crystal. A fraction of scintillations was caused by electrons produced in the material between target and

crystal. Thus the extrapolated number of pulses n_0 is divided into two parts:

$$n_0 = n_e + n_t.$$

Here n_e is the number of electrons produced in the crystal and n_t means the number of electrons coming from outside. To determine n_e we must measure n_t and subtract it from n_0. We solved our problem with the following simplifying assumptions: the secondary electrons are flying in the direction of the primary quanta, and the other electrons scattered from the surroundings can be neglected. This assumption is permissible, as 90 percent of the electrons created by pair production and Compton-effect, will travel within 10°.

We measured these secondary electrons with two thinwalled GM-counters connected in coincidence. Between the two GM-tubes we placed an 8 mm thick Pb sheet with a circular aperture 1 cm² large.

Before the determination of n_t, we made three control measurements. First we measured the absorption of the electrons coming from the material between target and GM-tubes. We got for the half value absorption thickness 6.5 ± 0.5 mm, in agreement with the value 6.4 ± 0.2 mm measured by Tangen [9]). This means that the electrons investigated were really produced by the gamma radiation of the Li(p, γ) reaction.

Secondly we measured the number of electrons passing through the circular aperture against the distance between target and aperture. We found this to be quadratic (fig. 2) within 5 %. Thus, according to our assumptions, we may consider the source of electrons a point source. We found a quadratic relation also by counting the pulses of the scintillation crystal.

Finally we determined the efficiency of the two GM-tubes with the well-known "three GM-tubes" method. These were 82 % and 80 % respectively.

After these measurements we placed the scintillation crystal and the aperture of the coincidence arrangement at the same distance from the target, and measured the ratio of the number of coincidences to the number of scintillation pulses n_0. Taking into account the efficiency of the tubes, we obtained the value

$$n_t/n_0 = 0.32 \pm 0.02.$$

From this result we may determine the number of electrons produced in the crystal:

$$n_e = n_0 \cdot (0.68 \pm 0.014).$$

Using a crystal of greater thickness, the correction made above may be considerably smaller, in accurate measurements, however, one must take it into consideration.

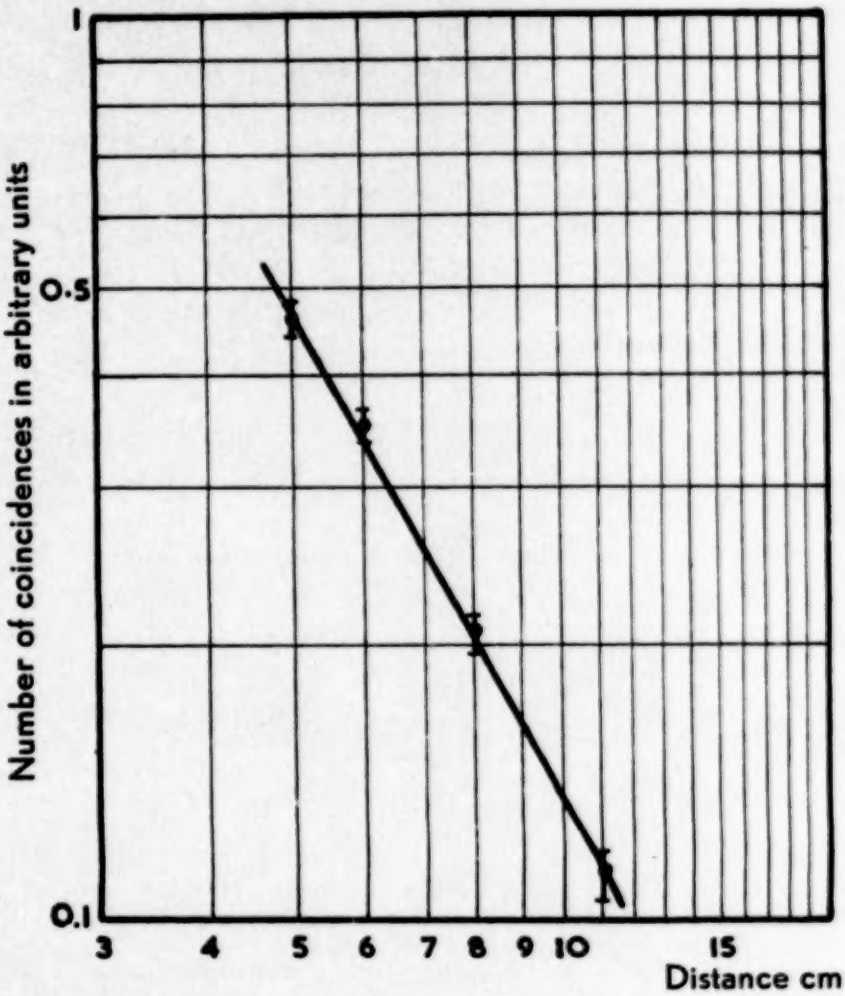

Fig. 2. The number of pulses of the coincidence arrangement vs. distance.

Knowing n_e, we might calculate the integral N_{eff} in the denominator of eq. (2). In the two runs we got $N_{eff}^{(1)} = (1.05 \pm 0.02) \times 10^8$ and $N_{eff}^{(2)} = (3.16 \pm 0.06) \times 10^8$ respectively.

3.3. DETERMINATION OF THE ACTIVITY

The scintillation counter measuring the activity of the irradiated crystal was surrounded by a 5 cm thick Pb sheet in order to reduce the background. In previous measurements during several weeks we determined the average number of background pulses at different discriminator voltages. This amounted to 10 % of the number of

pulses of the actived crystal and its fluctuation was about 10 % including the statistical error.

It is possible that besides the I^{126} nuclei also other radioactive isotopes were being produced.

The 17.6 MeV γ radiation may produce also the reaction $I^{127}(\gamma, 2n)I^{125}$. The I^{125} nuclei disintegrate with electron capture, and the maximal energy delivered by most of the disintegrations is 35.4 keV [10]). This low energy escaped our observation, because of the high discriminator setting (see below). The Na^{22} nuclei produced also by the γ irradiation disintegrate with a half life of 2.6 years, and so a considerable amount of activity was not produced.

In the bombarding ion beam there were also few deuterons which released neutrons from the Li target. Measuring the neutron flux, we came to the conclusion that the number of I^{126} nuclei produced by neutrons is negligible (smaller than 1 % of those created by the (γ, n) reaction.) By the neutrons, also I^{128} and Na^{24} nuclei were produced, but these had disintegrated before our activity measurement.

Although these considerations convince that the measured activity originates from the I^{126} nuclei, we yet made a control measurement for the disintegration constant of the activity of the crystal, which resulted in $\lambda = (5.95 \pm 0.27) \times 10^{-7}$ sec^{-1}, in good agreement with the value $\lambda = (6.04 \pm 0{,}14) \times 10^{-7}$ sec^{-1} measured by Livingood and Seaborg [11]).

The I^{126} nuclei disintegrate with β^- or β^+ emission or with electron capture processes [12]). Thus the amplitude spectrum of scintillations in the crystal consists of two parts: the continuous spectrum and the K and L lines. The energies of the discrete lines are 31.2 and 4.8 keV respectively. We get pulses in these lines only at those disintegrations, in which the high-energy γ-radiation in coincidence with the electron capture is not absorbed in the crystal.

The activity of the crystal was too small, and therefore at the energies of the K and L lines the background pulses predominated over the pulses of disintegrations. In this way we could measure directly only the number of pulses in the continuous spectrum Y_1, with a rather high discriminator setting. At the same time the small activity of the I^{125} should not be measured.

In order to determine the disintegration rate Y_0 of I^{126} it was necessary to know the ratio of the number of pulses in the continuous

spectrum to that in the K+L lines. Koerts *et al.* have determined [12]) that 48 % of the disintegrations occur with K and 6 % with L capture. 4 % of the capture processes are followed by 750 keV and 650 keV gamma radiations, while 28.7 % only by a 650 keV radiation. We calculated the probability of the absorption of a γ quantum in a crystal having absorption coefficient μ, supposing

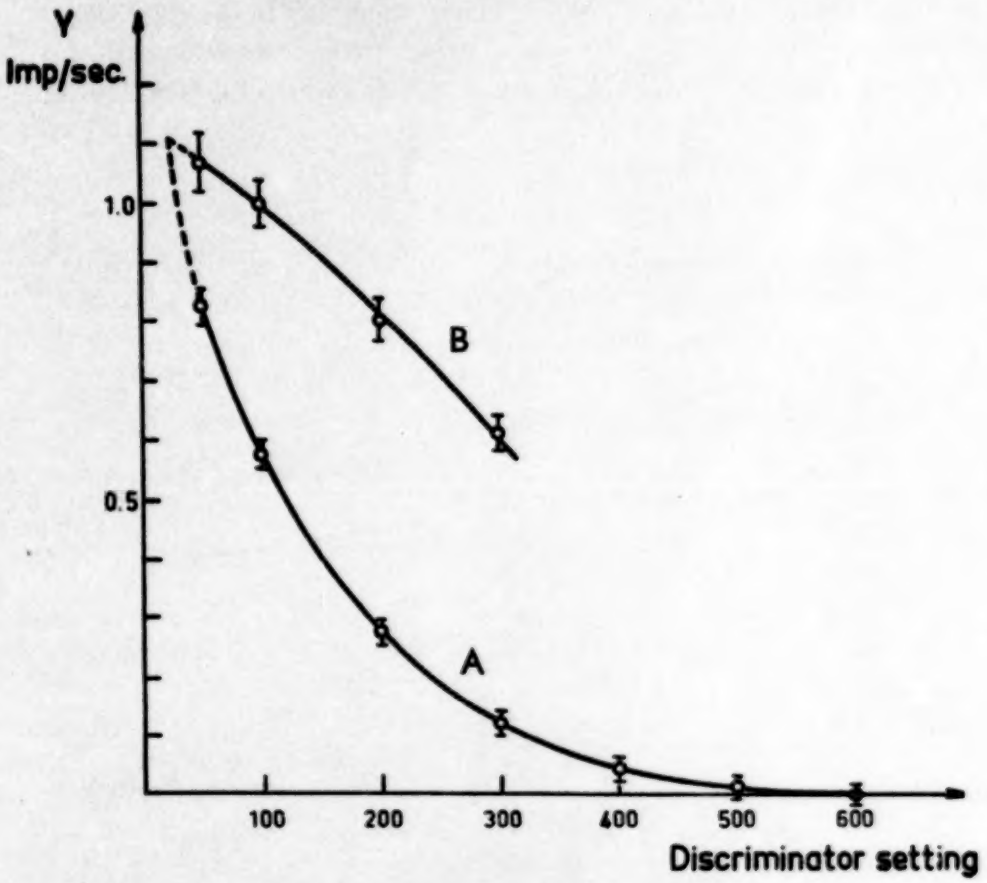

Fig. 3. The continuous part of the integral spectrum of the I^{126} disintegrations, with different amplifications.

that the source of radiation is distributed uniformly and the absorption is linear. From these calculations we concluded that 10,2 % of capture processes are followed by absorption of gamma quanta. This part of disintegrations produces pulses in the continuous spectrum, and so the ratio of all disintegrations to the continuous spectrum is $Y_0/Y_1 = 2.02 \pm 0.2$.

The number of pulses in the continuous spectrum Y_1 was determined from the integral spectrum, extrapolating it to zero discriminator voltage. This spectrum is shown in fig. 3 (curve A). Curve B

represents the low energy part of the spectrum, measured with a greater amplification. The intersection point gives the extrapolated value $Y_1^{(2)} = 1.1 \pm 0.04$ imp/sec. From the Y_1 values and from the value of Y_0/Y_1 we got $Y_0^{(1)} = 0.7 \pm 0.1$ imp/sec and $Y_0^{(2)} = 2.2 \pm 0.2$ imp/sec by the first and second irradiation respectively.

The great error of the results is caused by the inaccurate knowledge of the capture probability [12]). To avoid this uncertainty we irradiated our crystal after the (γ, n) measurements with fast neutrons from the Li(d, n)Be reaction. In this way a higher accuracy

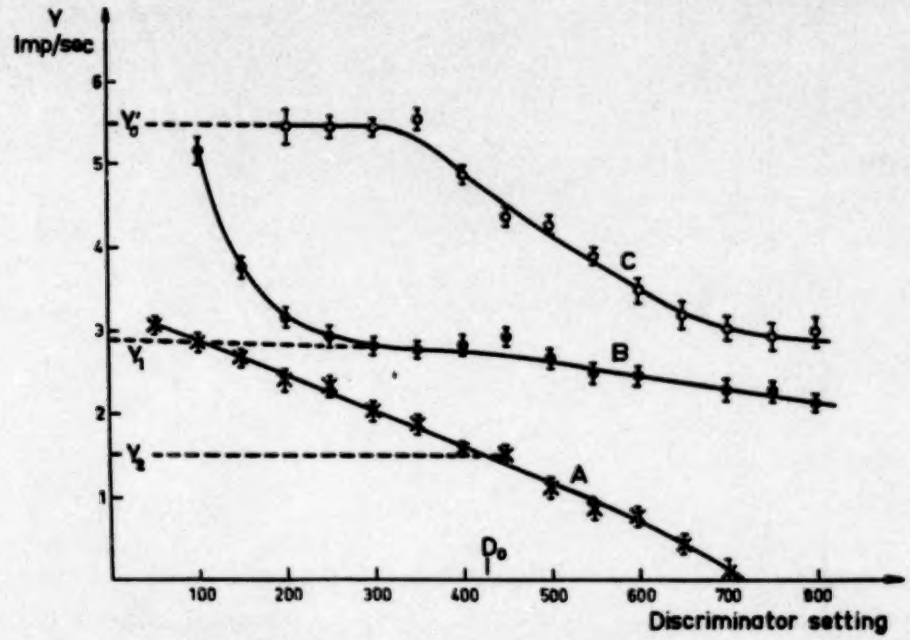

Fig. 4. The integral spectrum of the I^{126} disintegrations including K line, with different amplifications.

was obtained and we were able to measure the total spectrum (fig. 4). The three curves were measured with three different amplifications. The curve C show clearly the sloping upwards in the K line. The plateau following this slope gives, with some corrections immediately the disintegration rate of the I^{126} nuclei. The corrections are necessary, because some of the K capture X-rays will leave the crystal without absorption and the L capture X-rays were not measured. The number of X-rays quanta escaping from the crystal is in good approximation $F(4\tau_K V)$. (F surface of crystal, V its volume, τ_K the absorption coefficient of the K_α line of Te.) In our case this amounts to 2 % of the total disintegrations. Taking

into account the 6 % correction for the L capture, the whole correction to be made is 8 %.

To evaluate our (γ, n) measurements, we determined accurately the value Y_0' of this plateau and measured the counting rate Y_2 at that discriminator voltage, which served earlier as the control point in the activity measurements. After 8 % correction we got $Y_0/Y_2 = 3.89 \pm 0.15$. Thus from the values Y_2, measured by the irradiations, it was possible to determine accurately the disintegration rate in these cases: $Y_0^{(1)} = 0.73 \pm 0.03$ imp/sec and $Y_0^{(2)} = 2.27 \pm 0.1$ imp/sec respectively.

The nearly horizontal section of the curve B in fig. 4 is the low energy end of the continuous spectrum. Extrapolation of this gives the number of pulses in the continuous spectrum Y_1. With this value we may determine the Y_0/Y_1 ratio directly, and after correction, made because of absorption of γ quanta following the capture processes, we got the ratio of the K capture of the I^{126} nuclei to the total disintegrations. It is $Y_K/Y_0 = 0.51 \pm 0.03$ agreeing with the value 0.48 ± 0.04 determined from the measurements of Koerts *et al.* [12]).

3.4. DETERMINATION OF σ_e

The cross section of the NaI molecule for producing secondary electrons was determined through calculations with the help of the formula of Klein and Nishina, and through interpolation of the curve for pair production [13]). We took into consideration also the pair production on electrons. The cross section for the 17.6 MeV-radiation was 10.8×10^{-24} cm^2, agreeing well with the value $(10.7 \pm 0.11) \times 10^{-24}$ cm^2, got from measurements of Walker [14]) on Al and Sn, and converted it for Na and I respectively. For this correction we assumed, that the variation of the cross section of the Compton effect agrees with the K.N. formula, and that of the pair production will increase with Z^2. For the 14.8 MeV radiation we found $\sigma_e^{14,8} = 10.4 \times 10^{-24}$ cm^2 thus the weighted mean is [15]) $\bar{\sigma}_e = 10.7 \times 10^{-24}$ cm^2.

3.5. DETERMINATION OF σ_n

From the results of the previous sections we can at last calculate the cross section of the $I^{127}(\gamma, n)I^{126}$ reaction. At the two runs we got $\sigma(\gamma, n)^{(1)} = 123 \pm 7$ mb and $\sigma(\gamma, n)^{(2)} = 125 \pm 6$ mb.

The given error is of statistical character. Beside this, there are in our measurements some systematical errors too, because of the

inaccurate extrapolation of the discriminator curves. This error is less than the statistical one, and amounts to 3 %.

4. Discussion

The (γ, n) cross section determined in our measurements relates to the two lines of the Li(p, γ)Be reaction [15]). But from ref. [3]) we may conclude, that the value of σ_n at 14.8 MeV γ energy does not seriously differ from that measured with the 17.6 MeV gamma radiation. Therefore we may assume in good approximation that the cross section of the (γ, n) reaction is $\sigma_n = 125$ mb at both 14.8 MeV and 17.6 MeV.

Comparing our measurements with earlier results obtained by counting neutrons, we may determine the cross section of the $(\gamma,2n)$ reaction too. Mc Daniel *et al.* [1]) and Nathans and Halpern [3]) measured the cross sections $\sigma_+ = \sigma(\gamma, n)+2\sigma(\gamma, 2n)$ by observing neutrons, and found a value of 180 mb and 210 mb respectively. The error in their measurements is rather great and may be estimated to be 25 %. An average value 195 ± 40 mb seems to be correct. From this we may calculate the $\sigma(\gamma, 2n)$ cross section:

$$\sigma(\gamma, 2n) = \frac{\sigma_+ - \sigma(\gamma, n)}{2} = 30 \pm 20 \text{ mb}.$$

Heidman and Bethe [4]) calculated, that by the radiation of the Li(p, γ)Be reaction every quanta will produce 1.2 neutrons in average. This ratio may be determined from our data as follows:

$$\frac{\sigma_+}{\sigma(\gamma, n)+\sigma(\gamma, 2n)} = 1.25 \pm 0.3.$$

This value agrees well with the theory, but its error is rather large. Of course, our consideration holds only in that case, when the compound nucleus disintegrates predominantly by neutron emission.

We are indebted to Prof. K. Simonyi for his continuous interest in our work, and to Mr. J. Mráz, E. Pásztor and L. Vályi for their help and assistance in the measurements.

Note added in proof: In a recent paper [16]). L. Gavrilov and N. E. Lasareva have published data on σ_+ for several nuclei. In iodine at 17.6 MeV, $\sigma_+ = 190 \pm 20$ mb. From this we may obtain the $\sigma(\gamma, 2n)$ cross section more accurately: $\sigma(\gamma, 2n) = 27 \pm 10$ mb. Then

$$\frac{\sigma_+}{\sigma(\gamma, n)+\sigma(\gamma, 2n)} = 1.25 \pm 0.15.$$

References

1) B. C. McDaniel, R. L. Walker and M. B. Stearns, Phys. Rev. **80** (1950) 807
2) R. Montalbetti, L. Katz and J. Goldemberg, Phys. Rev. **91** (1953) 659
3) R. Nathans and J. Halpern, Phys. Rev. **93** (1954) 437
4) J. Heidman and H. A. Bethe, Phys. Rev. **84** (1951) 274
5) J. H. Carver, R. D. Edge and D. H. Wilkinson, Phys. Rev. **89** (1953) 658
6) K. Simonyi, Suppl. Nuovo Cimento **3** (1956) 345
   Mérey Imre, Magyar Fizikai Folyóirat **3** (1955) 459
   Pásztor Endre and Siegler Jánosné, Magyar Fizikai Folyóirat **3** (1955) 497
7) J. G. Campbell and A. J. F. Boyle, Austr. J. Phys. **6** (1953) 171
8) H. Casson, Phys. Rev. **89** (1953) 809
9) R. Tangen, Kgl. Norske Videnskabernes Selskab Skrifter **1** (1946)
10) G. Friedlander and W. C. Orr, Phys. Rev. **84** (1951) 484
11) J. J. Livingood and G. T. Seaborg, Phys. Rev. **54** (1938) 775
12) L. Koerts, P. Macklin, B. Farelly, R. van Lieshout and C. S.Wu, Phys. Rev. **98** (1955) 1230
13) H. A. Bethe and J. Ashkin in Segre: Experimental Nuclear Physics, Vol. I (John Wiley, New York, 1953) p. 238
14) R. L. Walker, Phys. Rev. **76** (1949) 527
15) B. C. McDaniel and R. L. Walker, Phys. Rev. **74** (1948) 315
16) L. Gavrilov and N. E. Lasareva, JETP **30** (1956) 855

Nuclear Physics **2** (1956/57) 382—394; *North-Holland Publishing Co., Amsterdam*

THE POSSIBLE EXISTENCE OF ROTATIONAL LEVELS IN Al^{28}

RAYMOND K. SHELINE †

Institute for Theoretical Physics, of the University, Copenhagen, Denmark

Received 10 September 1956

Abstract: The nine lowest levels in Al^{28} are interpreted as belonging to 4 rotational bands which in turn arise from two nuclear configurations. Experimental evidence from the beta decay of Mg^{28} and from the (d, p) stripping reaction on Al^{27}, including the spins, parities and energies of levels, the calculated moments of inertia of the bands, and the relative intensities of the beta and gamma transitions, is shown to be in excellent agreement with the interpretation. The nuclear configurations are shown to be consistent with experimental evidence and to arise naturally from the S. G. Nilsson levels for deformed nuclei. General trends in deformation in the low A region are discussed. A comparison is made between the moments of inertia of even-even, odd mass, odd-odd nuclei, and the corresponding calculated rigid moments of inertia.

1. Introduction

Evidence is accumulating that nuclear properties in the vicinity of $A \approx 25$ may be interpreted in terms of the unified model proposed by Bohr and Mottelson [1]). Thus, for example, the large measured quadrupole moments of the nuclei Na^{23} and Al^{27}, 0.10 [2, 3]) and 0.149 [4]) $\times 10^{-24}$ cm^2 respectively, can be used to determine deformations of 0.54 and 0.31 which are large enough to indicate a non-spherical equilibrium shape for nuclei in this region. There is a general lowering of the energy of the first excited states of even-even nuclei in the region $18 \leqq A \leqq 30$, as is the case in the regions $150 < A < 190$ and $A > 225$ where rotational states occur systematically, and particularly Mg^{24} has a normal rotational sequence at least as high as the second excited state. It might also be noted that the experimental value for $B(E2)$ for the Coulomb excitation of the first excited state of Na^{23} at 446 keV is 0.013×10^{-48} cm^4 [5]), approximately 25 times the single-particle value. Recently Litherland *et al.* [6–8]) have found strong indications of mirrored rotational sequences in Mg^{25} and Al^{25}. Not only are the

† Guggenheim and Fulbright research scholar on leave of absence from the Chemistry Department, Florida State University, Tallahassee, Florida.

energy, spins and moments of inertia of these sequences consistent with their rotational character, but strong K selection rules between various rotational sequences are observed in Mg^{25}. It therefore seems reasonable to look for the existence of other rotational sequences in the neighbouring nuclei.

2. Experimental Data

Although it has not been possible previously to substantiate the existence of rotational levels in an odd-odd nucleus, the wealth of data on the levels in Al^{28} makes it a particularly attractive case for study. The information available comes largely from two sources. In the first place, there is available the study of the (d, p) reaction on Al^{27}, both to observe the existence of levels [9]) in Al^{28} and in some cases to obtain information on the spins and parities of these levels by the study of the angular distribution of the protons in the stripping reaction [10]). In the second place, there is information on the first six levels of Al^{28} from the study of the decay of Mg^{28} [11]). A summary of all the available experimental information is shown in columns 1, 2, 3 and 4 of fig. 1. No new information in the region of interest is obtained from Al^{27} (n, γ) or from S^{30} (d, α) studies. Therefore this experimental information is not included in the figure or the discussion. The only discrepancy between previously published data and that indicated in fig. 1 involves the level at 974 keV. The possibility of a 0^+ assignment has not been previously considered [11]) because there was no observable beta decay to the 974 keV level. However, if the 974 keV level were a 0^+ level with a different isobaric spin than the ground state 0^+ level in Mg^{28}, then the beta transition between them would be forbidden. This isobaric spin selection rule for decays involving such low Z nuclei is fairly strong.

3. Discussion

As indicated in columns 5, 6 and 7 of fig. 1, it is suggested that the first nine states in Al^{28} may be represented as consisting of four rotational sequences with $K = 0$, 1, 2, and 3. The validity of this description of the levels of Al^{28} is supported by the following considerations.

3.1. SPINS AND PARITIES, ENERGIES AND MOMENTS OF INERTIA

It seems particularly significant that the assignment of the spins and parities of levels indicated in fig. 1 is consistent with

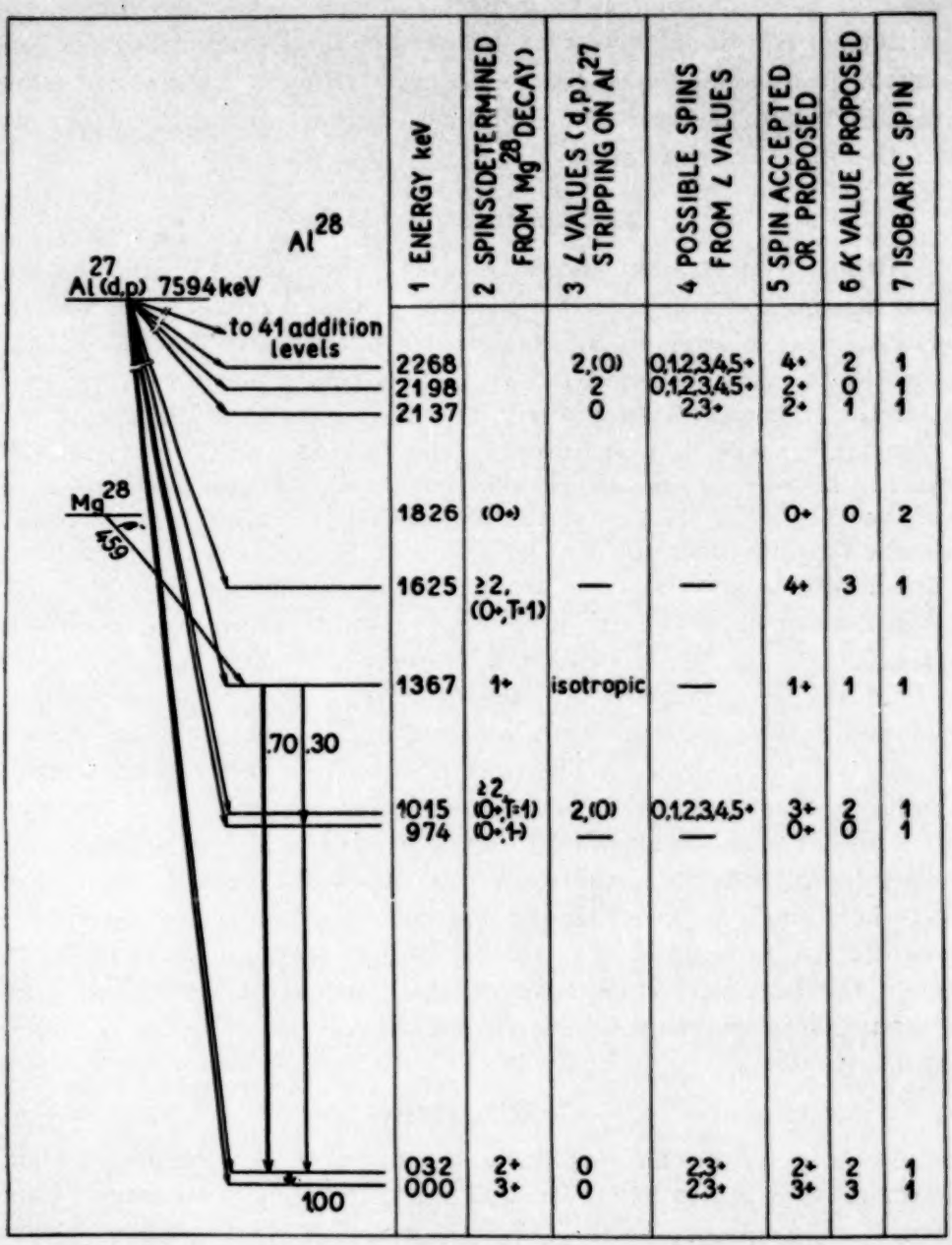
Al28
27
Al(d,p) 7594 keV
to 41 addition levels
Mg28
.70
.30
100
1 ENERGY keV
2 SPINS(DETERMINED FROM Mg28 DECAY)
3 ℓ VALUES (d,p) STRIPPING ON Al27
4 POSSIBLE SPINS FROM ℓ VALUES
5 SPIN ACCEPTED OR PROPOSED
6 K VALUE PROPOSED
7 ISOBARIC SPIN
2268 2198 2137 1826 1625 1367 1015 974 032 000
(0+) ≥2, (0+,T=1) 1+ ≥2 (0+,T=1) (0+,1-) 2+ 3+
2,(0) 2 0 — isotropic 2,(0) — 0 0
0,1,2,3,4,5+ 2,3+ — 0,1,2,3,4,5+ 2,3+
4+ 2+ 2+ 0+ 4+ 1+ 3+ 0+ 2+ 3+
2 0 1 0 3 1 2 0 2 3
1 1 1 2 1 1 1 1 1 1
LEVELS OF Al28 TO 2480 keV

Fig. 1. The levels in Al^{28} and the decay of Mg^{28}. All energies given are those of ref. [9]) with the exception of the first excited state which has been more accurately determined by measurements of the gamma ray. Recently, new measurements [17]) give slightly different energies. Also Enge has recalculated his earlier data [18]). However, these differences are within the experimental errors of approximately ± 10 keV.

all available experimental information, that the nine levels are all used in the four rotational sequences, and that there are no extraneous levels involved in the first 2.48 MeV.

The possible existence of a negative quadrupole and deformation for Si^{29} has been suggested by H. E. Gove [12]). However, the experimental determination of spin parity of the Al^{28} ground state doublet as 3^+, 2^+ indicates clearly that the deformation and quadrupole moment of Al^{28} are positive. A negative deformation would lead to a ground state doublet with either 1^+, 0^+ or 2^+, 1^+ depending on the negative deformation assumed.

The $K = 2$ band which is the only rotational sequence in Al^{28} having enough members to test the energy fit has a ratio of the second to the first excited state of 2.27; this compares well with 2.33 to be expected if there is no vibration-rotation or other perturbation correction term.

The moments of inertia calculated for each of the four bands compare very satisfactorily with the moments of inertia observed in the odd-even and even-odd Al^{25} and Mg^{25} nuclei, and with the even-even nucleus Mg^{24}. This comparison is shown in table 1.

TABLE 1

Comparison of moments of inertia $\hbar^2/2\mathcal{I}$ in the region $A \approx 25$.

The moments of inertia are calculated without assuming a vibration-rotation or other perturbation correction terms since it is not possible to include such a term for three of the four proposed rotational bands in Al^{28} or the band in Al^{25}.

Nucleus	K of Band	$\hbar^2/2\mathcal{I}$ in keV
Mg^{24}	0^+	226
Mg^{25}	$5/2^+$ †	230
Al^{25}	$5/2^+$ †	230
Al^{28}	3^+	203
Al^{28}	2^+	164
Al^{28}	0^+	204
Al^{28}	1^+	192

† The ground state rotational bands are the only ones used here although several other bands are known in which the moments of inertia $\hbar^2/2\mathcal{I}$ appear to decrease (see ref. [5], [6], [7])).

3.2. THE NUCLEAR CONFIGURATIONS GIVING RISE TO THE ROTATIONAL BANDS

Not only do the experimental data fit well into the systematics of the four rotational level sequences, but also these four sequences may be considered to result from two nuclear configurations, each

of which gives rise to two of the bands. These configurations are

$$\pi[{}_8O^{16},\ d_{5/2}(1/2^{+2},\ 3/2^{+2},\ 5/2^{+1})];$$
$$\nu[{}_8O^{16},\ d_{5/2}(1/2^{+2},\ 3/2^{+2},\ 5/2^{+2}),\ s_{1/2}(1/2^{+1})]$$

which gives rise to the ground state doublet $J = K = 3^+$ and 2^+ and

$$\pi\ [{}_8O^{16},\ d_{5/2}(1/2^{+2},\ 3/2^{+2},\ 5/2^{+0}),\ s_{1/2}(1/2^{+1})];$$
$$\nu[{}_8O^{16},\ d_{5/2}(1/2^{+2},\ 3/2^{+2},\ 5/2^{+2}),\ s_{1/2}(1/2^{+1})]$$

which gives rise to the level at $J = K = 0^+$ at 974 keV and the level at $J = K = 1^+$ at 1367 keV.

In isobaric spin notation the ground state configuration corresponds to $(\Omega = 5/2)^3$, $\Omega = 1/2$ which may be considered to be the equivalent to $\Omega = 5/2$, $\Omega = 1/2$. This will give rise to $K = J = 3^+, T = 0$ and 1, and $K = J = 2^+$, $T = 0$ and 1. This indicates that we may expect these bands in both Si^{28} and Al^{28}, but not in Mg^{28}. On the other hand if one of the $\Omega = 5/2$ particles is raised to a $\Omega = 1/2$ orbit, there is a far greater variety of potential bands arising from the configuration. These bands are indicated in table 2. It is immediately evident that 6 bands are present in Al^{28}, whereas only 1 is to be expected in Mg^{28}, namely band number 6. Band numbers 5 and 8 are the bands originating at 974 keV and 1367 keV respectively in Al^{28}.

In justification of the suggested nuclear configurations the following evidence is adduced.

A. The nuclear configurations producing the rotational bands follow very naturally from the energy levels calculated for deformed nuclei in the region of $A = 28$ by Nilsson [13]). The ground state doublet results if one fills up the levels in the Nilsson diagram in order, the thirteenth proton occupying the 5/2+ orbital and the fifteenth neutron occupying the 1/2+ orbital. The excited state configuration is very simply produced if the $d_{5/2}(5/2+)$ proton is promoted to an $s_{1/2}(1/2+)$ orbital.

The energy involved in this promotion can be estimated from the energy involved in the same transition in Al^{25} and from the mirror transition in Mg^{25} in which a neutron is promoted. This energy is 450 keV in the case of Al^{25} and 610 keV in the case of Mg^{25}. The two levels resulting from this configuration about which we are concerned in Al^{28} are at 974 and 1367 keV. Since pairing effects are of the order of several MeV in this A region, the agreement is excellent. It is known on simple coulombic considerations that

TABLE 2

Nuclear Bands Arising from the System $(\Omega = 5/2)^1$ $(\Omega = 1/2)^1$.

A convenient way of generating the bands is to consider the various combinations of Ω and isobaric spin which each pair of particles will give and then combine them. The pair of $\Omega = \pm 5/2$ particles will give $\Sigma\Omega = 5$ in only the symmetric way with $t = 0$. It can also give $\Sigma\Omega = 0$ in either a symmetric or an antisymmetric way with $t = 1$ and 0 respectively. Similarly the pair of $\Omega = \pm \frac{1}{2}$ particles can give $\Sigma\Omega = 1$, symmetric, $t = 0$ or $\Sigma\Omega = 0$ antisymmetric, $t = 1$ and symmetric $t = 0$.

Combining these possibilities, bands are obtained which are presented in the table which follows. It is well known that for a pair of particles with a symmetric wave function, $K = 0$ and $T = 0$, the sequence of spins is 0, 2, 4 . . . It is also interesting to note that it is possible to construct an antisymmetric wave function with $K = 0$ and $T = 0$ and the spin sequence 1, 3, 5 . . .

Band Number	K (Quantum Number)	Combination	T (Isobaric Spin)	Spin Sequence in the Band
1	0	sym.-sym.	0	0, 2, 4 . . .
2	0	sym.-antisym.	1	1, 3, 5 . . .
3	0	antisym.-sym.	1	1, 3, 5 . . .
4	0	antisym.-antisym.	0	0, 2, 4 . . .
5	0	antisym.-antisym.	1	0, 2, 4 . . .
6	0	antisym.-antisym.	2	0, 2, 4 . . .
7	1	sym.-sym.	0	1, 2, 3 . . .
8	1	antisym.-sym.	1	1, 2, 3 . . .
9	5	sym.-sym.	0	5, 6, 7 . . .
10	5	sym.-antisym.	1	5, 6, 7 . . .
11	6	sym.-sym.	0	6, 7, 8 . . .
12	4	sym.-sym.	0	4, 5, 6 . . .

the $K = 0$ band in Al^{28} which has the same isobaric spin as the ground state of Mg^{28} must lie approximately 4 MeV above the ground state of Al^{28}. Since the band is also a member of the configuration under discussion, the excellent agreement between the promotion energy in Al^{25} and Al^{28} may be a fortuitous coincidence. In any case no *ad hoc* assumptions are necessary as a result of poor agreement.

B. According to the single-particle model, if a single configuration results in two levels, one can expect the ratio of the cross sections for the production of these levels in a (d, p) reaction to be the ratio of the statistical weights determined from the spins of the levels. As has been previously shown [11, 14]), this is the case for the ground state doublet in Al^{28}, the ratio of the 32 keV state to the ground state cross section being 0.69, whereas the statistical

weights give the ratio 5/7 = 0.71. On the other hand, if the factor corresponding to the coupling scheme for deformed nuclei is used, one obtains a ratio of 5/6 = 0.83 which is again in good agreement with experiment. (For a discussion of stripping intensity rules in rotational structure, see ref. [15]). The ratio of the 0^+ 974 keV cross section to the 1^+ 1376 keV cross section is 0.29, whereas one would expect 0.33 from the statistical weights ratio according to the single particle model. In this second case, the reaction is not a simple capture but involves a simultaneous promotion of the proton from $d_{5/2}(5/2^+)$ to $s_{1/2}(1/2^+)$. One might hope that even in this complex capture the yield to each level might be lowered while the statistical weight factor ratio remained intact. The data seems to be suggestive of the fact that there are two sets of two levels with the desired spins which result from only two configurations. A further test of the validity of the configurations may be obtained by comparison of predicted and observed intensities of transitions occurring in the decay of Mg^{28}.

3.3. THE DECAY OF Mg^{28}

Unfortunately the decay of Mg^{28} does not provide a test of the K selection rule since there are no competing transitions with differing ΔK values. However, the decay of Mg^{28} indicated in fig. 1 may be completely understood in terms of the four rotational sequences, the factors of forbiddenness to be expected in the strong deformation limit and the isobaric spin selection rule. Thus, for example, a beta minus transition from the $T = 2$, $J = 0^+$ ground state of Mg^{28} to the $T = 1$, $J = 0^+$ 974 keV level in Al^{28} would be forbidden by the isobaric spin selection rule. This could result in a log ft value of the order of 6.5. A transition to the 974 keV level with this log ft value would probably not have been seen in the presence of the large amount of the higher energy Al^{28} beta which is in secular equilibrium with Mg^{28}. On the other hand, the decay to the 1^+ level at 1367 keV can proceed by Gamow-Teller selection rules with a somewhat reduced transition probability and is therefore the only observed beta decay in Mg^{28}. This slowing down of the transition is associated with the flip of an $s_{1/2}(1/2^+)$ nucleon from the antiparallel to the parallel position as it changes from a neutron to a proton. It is even possible to suggest the ft value by using the wave functions of S. G. Nilsson [13]). In the strong coupling limit with $\eta = 6$ there is a hindrance factor of 7.3 to the flip of the

nucleon. If this hindrance factor is multiplied by the unhindered ft value expected for Gamow-Teller transitions in this A region (≈ 5200), the value $ft \approx 38000$ is obtained. This corresponds to $\log ft = 4.58$ which must be considered in excellent agreement with the experimentally measured value, $\log ft = 4.45$, considering the nature of the assumptions.

The intensity of the various gamma transitions after the population of the single level at 1367 keV may also be understood in terms of the proposed nuclear configurations. The M1 transition, 1367 → 974 keV, represents the inverse transition from the beta decay of Mg^{28}, namely a spin flip of an $s_{1/2}(1/2^+)$ nucleon. Any E2 mixture is strictly forbidden. Therefore there should be a hindrance factor of 7.3 exactly as in the beta decay. On the other hand, the 1367 → 974 keV transition competes very well with the 1367 → 32 keV transition (3 to 7) in spite of the fact that purely from energy considerations one would expect an intensity ratio of 1 to 37. This must mean that the 1367 → 32 keV transition is considerably more forbidden even than the 1367 → 974 keV transition. Indeed this is immediately apparent when one examines the two configurations involved in the 1367 → 32 keV transition. It is a two particle transition and both the M1 and possible E2 mixture are Ω forbidden. Assuming a forbiddenness of ≈ 7 for the 1367 → 974 keV transition, the 1367 → 32 keV transition must be forbidden by a factor of ≈ 120. Such factors of forbiddenness are reasonable in the light of the configurations involved. The 1367 → ground state transition is an E2 transition with a forbidden factor of ≈ 120. It is not observed experimentally (< 0.05) and would not be expected in view of the fact that it is not enhanced by any collective character and is competing with an equally hindered M1 of approximately the same energy. A similar argument can explain the failure to populate the 1015 keV level. There is a considerable additional decrease in intensity to be expected because of the lower energy of this potential transition.

4. Conclusions

In this final section an attempt will be made to explore the general trends in deformations and moments of inertia in the region of low mass number. Since the nucleus Al^{28} is the first case in which a moment of inertia has been obtained for an odd-odd nucleus,

this moment of inertia and those of neighbouring even-even and odd mass nuclei will be compared.

4.1. GENERAL TRENDS IN DEFORMATION IN THE LOW A REGION

In view of the accumulating evidence that there is a region of considerable deformation in the vicinity of $A \approx 25$, it is of interest to determine the extent and boundaries of this region and if possible to determine the magnitude of the deformations.

Although the quadrupole moment measurements mentioned in the introduction indicate large deformations, unfortunately there are too few data to indicate the trend of deformations in this region. However, there is a general lowering of the energy of the first excited 2^+ states of all even-even nuclei in this region. The energy of these lowered first excited states can be used to calculate the square of the deformation according to the following formula:

$$\beta^2 = \frac{7.5\,\hbar^2}{E_{2+}\,AM\,R_0^2}, \tag{1}$$

where β is the deformation, A is the mass number, M is the nucleonic mass, R_0 is the radius of the nucleus in question, and E_{2+} is the energy of the first 2^+ excited state in even-even nuclei.

It has been recognized for some time that the square of the deformation determined in this way is a factor of 3—5 times too large. Therefore all the β^2 determined from formula (1) were multiplied by the factor 0.225. This factor was chosen first to give a reasonable value for the deformation of Mg^{24} (≈ 0.42) whose deformation may be estimated more directly from the measured deformations of Na^{23} (0.54) and Al^{27} (0.31), and second so that it would give reasonable deformations in the rare earth region where the deformations have been directly measured. Finally, when the condition [16])

$$E_{2+} < \frac{3\hbar^2}{0.23\,\mathscr{I}_{\mathrm{rig}}} \approx \frac{32\hbar^2}{MAR_0^2}$$

was not met, the deformation was assigned the value of zero. The radius constant $r_0 = 1.44\times10^{-13}$ cm was used throughout this low A region and is believed to be more appropriate than the value 1.2×10^{-13} cm which was used in the region of the rare earths. The deformations so determined are shown in fig. 2.

It is interesting to note the troughs in the deformations at the

closed shells, 8, 20 and 28, the possible existence of a very limited region of normally deformed nuclei in the vicinity of Ti^{46} and the existence of exceptionally strong deformations in the very light nuclei. Using the criterion of the energy of the first excited 2+ state for determination of deformations would indicate that He^6 is the most deformed even-even nucleus. This is perhaps not so surprising in view of the fact that one-third of all nucleons in the He^6 nucleus are involved in creating a deformation.

Perhaps the feature most interesting and to the point in fig. 2 is the existence of a very well defined region of strong deformation for $18 \leqq A \leqq 30$. This region of deformation rises very sharply as one adds nucleons to the completed shells of 8 protons and 8 neutrons. As in the case of He^6 this is perhaps to be expected in view of the large fractional part of all nucleons involved in the deformation when relatively few nucleons have been added after shell closure. The deformations seem to decrease more gradually as one approaches the closed shells of 20 neutrons and protons.

4.2. THE COMPARISON OF MOMENTS OF INERTIA OF EVEN-EVEN, ODD MASS AND ODD-ODD NUCLEI

In fig. 3 the moments of inertia, $\hbar^2/2\mathscr{I}$, for even-even, odd mass, odd-odd nuclei and the corresponding rigid moments of inertia are compared. It is interesting to note that the moments of inertia in this region approach more nearly to the calculated rigid moment of inertia than in any other region.

It is also interesting to note that the values of $\hbar^2/2\mathscr{I}$ are smaller in the odd-odd case than in the odd mass which in turn are smaller than in the even-even case. This is probably to be understood in the same terms that have been used to explain the higher moments of inertia in odd mass nuclei than in even-even nuclei [16]). Thus, the two unpaired particles in Al^{28} do not contribute a pairing energy to the denominator of the expression

$$J = 2\hbar^2 \sum_i \frac{|\langle 0|J_x|i\rangle|^2}{E_i - E_0},$$

where J_x is a total angular momentum of the particles about the intrinsic x-axis chosen perpendicular to the nuclear symmetry axis.

It should be indicated that the experimental data on Al^{28} are still only suggestive and that additional experimental information would be very valuable. On the other hand, since the existence of rotational levels in this region seems clearly established, it would

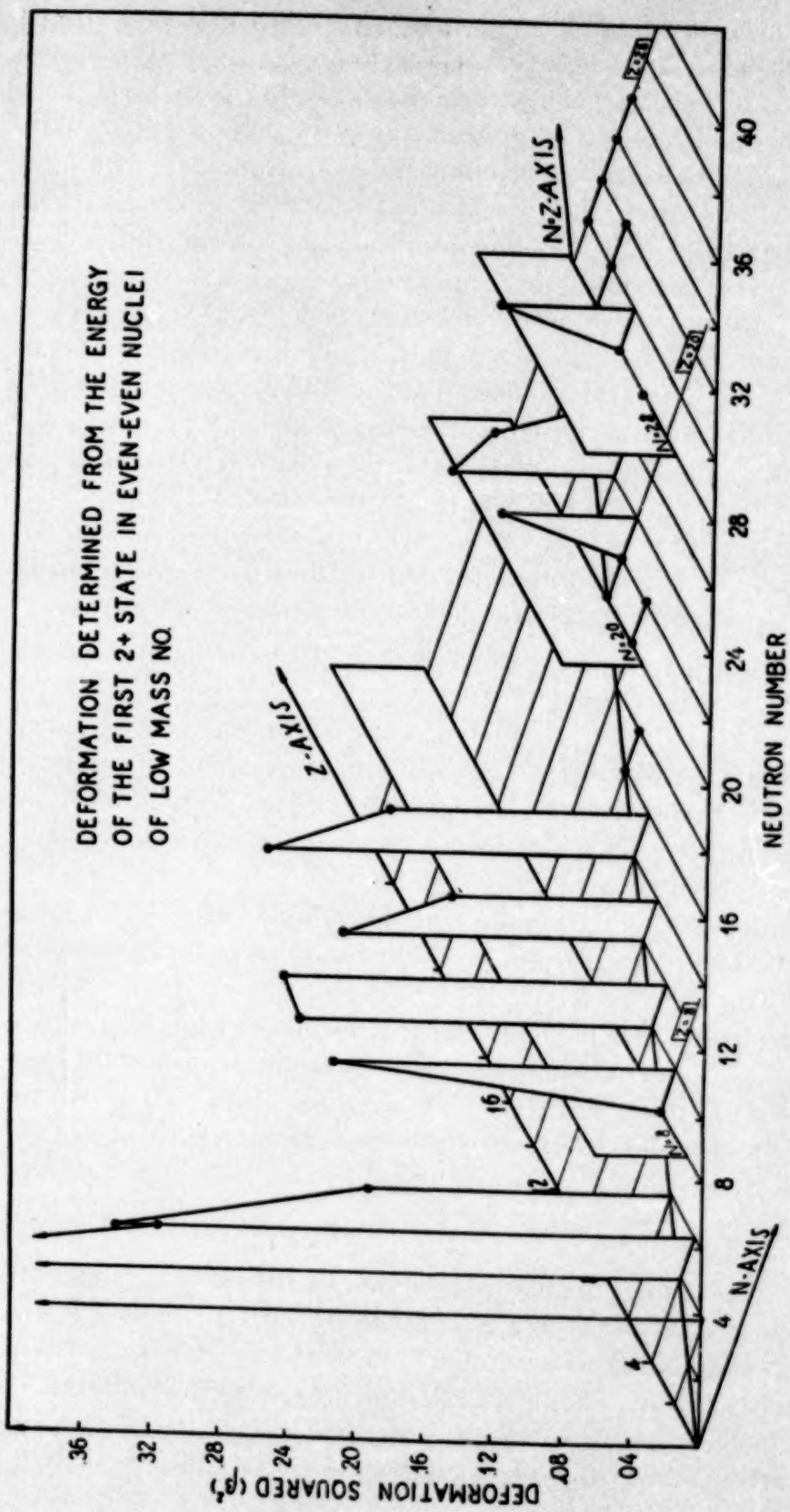

Fig. 2. Deformations determined from the energies of the first 2+ state in even-even nuclei. The text indicates the procedures used to obtain the deformations.

appear that this is the first case in which rotational levels in an odd-odd nucleus have been substantiated. It is interesting to note that these levels are exactly what would have been expected from available information about rotational levels in even-even and odd mass nuclei.

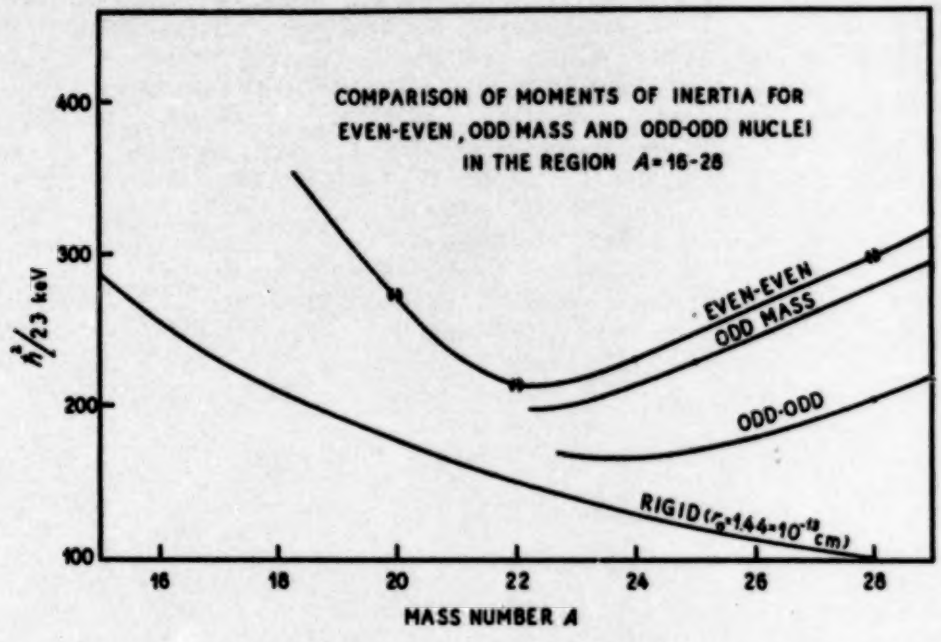

Fig. 3. Comparison of moments of inertia of even-even, odd mass and odd-odd nuclei. The points in brackets represent moments of inertia determined from the first excited 2+ states in Ne^{20}, Ne^{22} and Si^{28} where rotational sequences have not been clearly established. The single point on the odd mass line represents in reality two data, namely the moments of inertia for both Al^{25} and Mg^{25}. In no case have vibration-rotation or other perturbation correction terms been used in calculating the moments of inertia.

The author wishes to express his gratitude to Professor Niels Bohr for the kind hospitality and the ideal working conditions at the Institute for Theoretical Physics. He is especially indebted to Professor Aage Bohr and Drs. Arthur Kerman and Ben Mottelson for advice and help in interpreting the data. Finally the Fulbright and Guggenheim grants which made this work possible are gratefully acknowledged.

References

1) A. Bohr and B. R. Mottelson, Dan. Mat. Fys. Medd. **27** (1953) no. 16
2) M. L. Perl, I. I. Rabi and B. Senitzky, Phys. Rev. **98** (1955) 611
3) M. L. Perl, I. I. Rabi and B. Senitzky, Phys. Rev. **97** (1955) 838
4) J. E. Mack, Revs. Mod. Phys. **22** (1950) 64

5) G. M. Temmer and N. P. Heydenburg, Phys. Rev. **96** (1954) 426
6) A. E. Litherland, E. B. Paul, G. A. Bartholomew and H. E. Gove, Phys. Rev. **102** (1956) 208
7) A. E. Litherland, E. B. Paul, G. A. Bartholomew and H. E. Gove, Bull. Am. Phys. Soc. **1** (1956) 29
8) H. E. Gove, A. E. Litherland, E. B. Paul and G. A. Bartholomew, Bull. Am. Phys. Soc. **1** (1956) 29
9) H. A. Enge, W. W. Buechner and A. Sperduto, Phys. Rev. **88** (1952) 963
10) H. A. Enge, C. C. Anglarson and D. L. Jarrell, M. I. T. Progress Report, Laboratory for Nuclear Science, June 1956
11) R. K. Sheline, N. R. Johnson, P. R. Bell, R. Davis and F. McGowan, Phys. Rev. **94** (1954) 1642
12) H. E. Gove, private communication
13) S. G. Nilsson, Dan. Mat. Fys. Medd. **29** (1955) no. 16
14) H. A. Enge, Phys. Rev. **94** (1954) 730
15) G. R. Satchler, Phys. Rev. **97** (1955) 1416
16) A. Bohr and B. R. Mottelson, Dan. Mat. Fys. Medd. **30** (1955) no. 1
17) W. W. Buechner, M. Mazari and A. Sperduto, Phys. Rev. **188** (1956) 101
18) H. A. Enge, Naturvitenskap (1953) no. 1

Nuclear Physics **2** (1956/57) 395—407; *North-Holland Publishing Co., Amsterdam*

INVESTIGATION OF INTERNAL CONVERSION LINES IN THE β-SPECTRUM OF A MIXTURE OF Eu^{152} AND Eu^{154} ISOTOPES

V. M. KELMAN, V. A. ROMANOV, R. Ya. METSKHVARISHVILI and V. A. KOLYUNOV

Received 20 August 1956

Physico-Technical Institute of the USSR Academy of Sciences, Leningrad

Abstract: A high resolution prism β-spectrometer was employed to measure the K-shell and L- and M-subshell internal conversion lines of Sm^{152} and Gd^{154}. Internal conversion coefficient ratios for transition energies of 122 and 123.2 keV were also determined.

Energy differences between the conversion lines were measured with a high degree of precision.

1. Introduction

Several internal conversion lines are observed in the β-spectrum of a mixture of long-lived Eu^{152} and Eu^{154} isotopes; the most intensive of these lines are due to transitions of the Sm^{152} and Gd^{154} nuclei from the first excited to the ground states [1]). The energies of the first excited levels in Sm^{152} and Gd^{154} are [2]) 122 and 123.2 keV. Due to the small difference in energy the corresponding internal conversion lines for similar shells in Sm and Gd are very closely spaced with the result that it is somewhat difficult to resolve the lines.

Only by employing a high resolution β-spectrometer can one resolve the conversion electron spectra of Sm^{152} and Gd^{154} and determine the ratios of the internal conversion coefficients for the shells and subshells of each of the indicated elements. The prism β-spectrometer described in ref. [3]) was used for this purpose after improvement of its resolving power (the line half-width was 0.04 % and in some cases even 0.02 %. †) Moreover, the β-spectrometer was adjusted for precise measurement of conversion electron energy differences, this being of substantial aid in conversion line identification. The β-spectrometer was used to measure the intensity ratios and energy differences of the strongest conversion lines from Sm^{152} and Gd^{154}.

† In the present paper relative half-widths of the lines are expressed in momentum values.

The mixture of long-lived Eu^{152} and Eu^{154} isotopes was obtained hy irradiating natural europium with neutrons. After irradiation tbe europium was deposited electrolytically on a 5μ aluminium foil, a solution of europium chloride in ethyl alcohol being electrolyzed. In this way a number of sources was obtained which were 10 mm long, 1 mm wide and possessed various thicknesses. A source was chosen which was simultaneously sufficiently thin to ensure good resolution and sufficiently active. Approximately the thickness of this source was several hundredths of a milligram per cm^2.

2. Description of β-Ray Spectrometer

The prism β-spectrometer [3]) used in the present paper was modified in the following way in order to raise its resolving power.

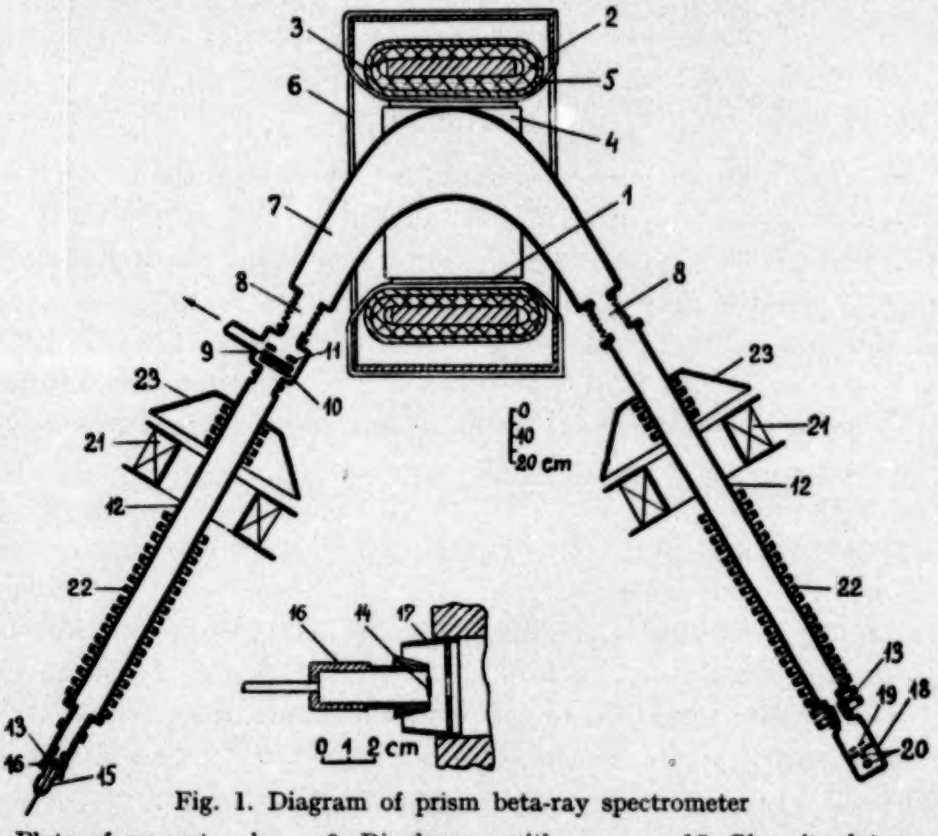

Fig. 1. Diagram of prism beta-ray spectrometer

1. Plate of magnet yoke
2. Main coil
3. Auxiliary coil arranged over the main coil
4. Auxiliary coil on plate
5. Demagnetization coil
6. Screen
7. Spectrometer chamber
8. Sylphons
9. Diaphragm with circular aperture
10. Slit diaphragm limiting vertical beam dimension
11. Slit diaphragm limiting horizontal beam dimension
12. Tube
13. Ground joint
14. Source
15. Glass insulator
16. Source holder
17. Electrode
18. Counter chamber
19. Detector slit
20. Counters
21. Magnetic lens
22. Iron rings
23. Lens screens

1. The spectrometer tube was shielded, the shield design being the same as that in Siegbahn's spectrogoniometer [4]). Iron rings and screens were mounted on the spectrometer tube 5 (fig. 1). In this way the influence of external magnetic fields on the electron motion in the tube was reduced.

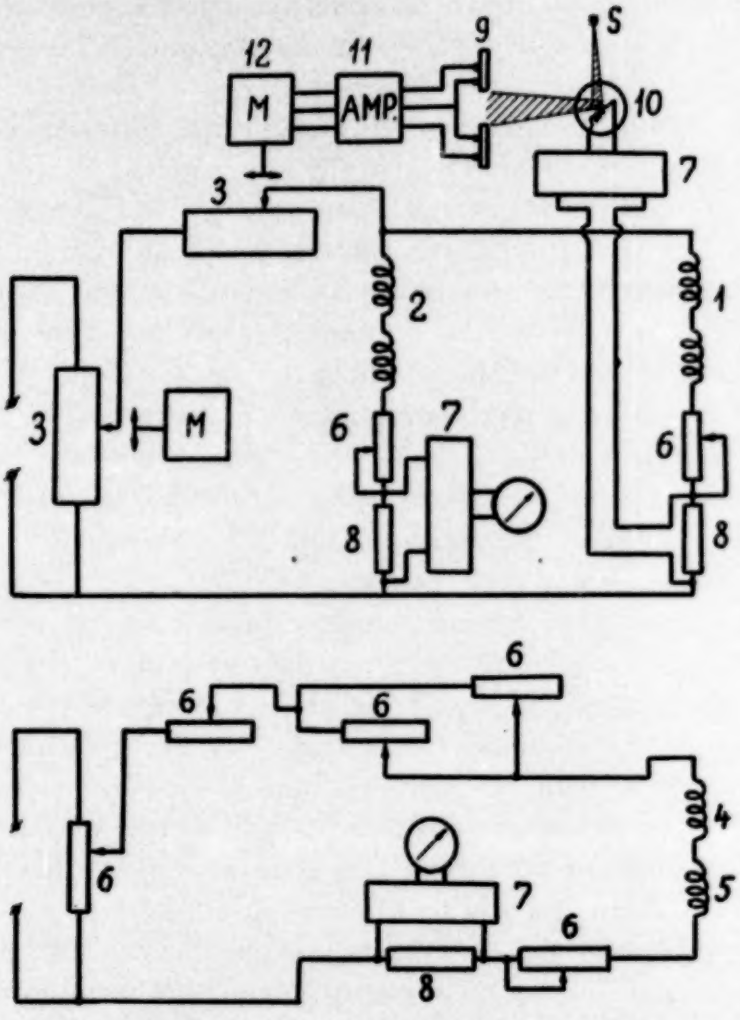

Fig. 2. Diagram of β-spectrometer power supply

1. Main coil
2. Lens coils
3. Rheocord
4. Auxiliary coil arranged over the main coil
5. Auxiliary coil on plate
6. Rheostat
7. PPTV—1 potentiometer
8. Standard resistor
9. Photocell
10. Mirror galvanometer in current stabilization circuit
11. Amplifier
12. Motor

Moreover, to some extent, the screens shielded the lens fields from the influence of the iron casing of the spectrometer deflecting magnet which could violate axial symmetry of the lens fields.

2. The straight slit of the recording arrangement was replaced by a slightly bent one, the shape of the latter being the same as that of the image of the linear source. In order to determine the shape of the image the exit slit was replaced by a photographic plate on which electrons traversing the β-spectrometer impinged. An active deposit of RdTh collected on a 10×1 mm^2 aluminium strip was the source in this case, the spectrometer being fixed on the F line.

3. The energizing circuit of the magnet and spectrometer lenses was somewhat modified. The current was supplied by an accumulator battery. Two drum type rheocords, 3, with sliding contacts were used to adjust the current in the main coil, 1 (fig. 2) and in lenses, 2; each rheocord drum was about 1 m long and about 40 cm in diameter. The ratio between the currents in the main coil and lenses and also the magnitude of the current in auxiliary coils, 4,5, was varied by using rheostats, 6. There was no need in varying this ratio or the current in the auxiliary coils when the L- and M-subshell conversion peaks were being measured. The currents were measured by the compensation method (with a PPTV-1 potentiometer, 7, and standard resistors, 8).

Stabilization of the current in the main coil and lenses was achieved with the aid of two selenium photocells, 9, which responded to the light reflected by themirr or of a sensitive galvanometer, 10, employed in the compensation circuit. A current change led to deflection of the light ray reflected from the galvanometer mirror and the current difference in the corresponding photocell after being amplified and fed to a relaysy stem, 11, actuated a motor, 12, which revolved the rheocord drum in the required direction until the light pointer returned to its original position. Any other current value could be chosen by suitably setting the resistance of the potentiometer used in the compensation circuit. The position of the light indicator was changed in this case and as a result the rheocord motor operated until the prescribed current was attained.

The electrostatic deceleration technique was used to accurately measure the energy difference of the conversion peaks. A positive voltage which could be varied step-wise was applied to the suitably insulated radioactive source (fig. 1) and all currents in the β-spectrometer coils were kept rigorously constant. The counting rate n as a function of voltage u applied to the radioactive source was then measured. From the plot $n = f(u)$ it was possible to

directly determine the conversion line separation in volts. The electric bias method was used previously by Lewis and Bowden [5]) to measure the absolute energy difference of monochromatic α-particle groups.

Siegbahn [6]) suggested that this method could be employed to accurately measure the ratio h/e.

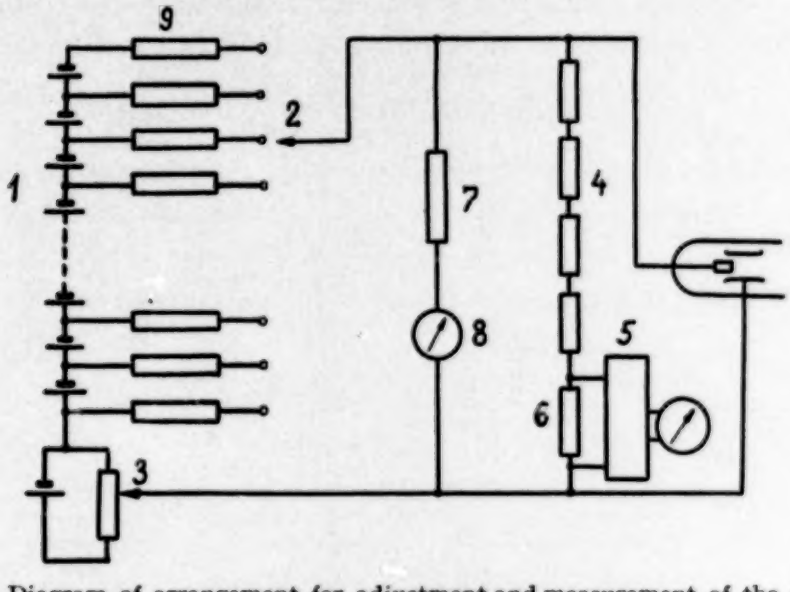

Fig. 3. Diagram of arrangement for adjustment and measurement of the voltage applied to source.

1. Dry batteries
2. Switch
3. Potentiometer
4. Wire resistor
5. PPTV–1 potentiometer
6. Standard resistor
7. Resistor
8. Microampermeter
9. Resistor

The method of applying voltage to the radioactive source is schematically illustrated in fig. 3. The voltage was supplied by dry batteries, 1, connected in series. The magnitude of the voltage was adjusted with help of switch, 2, and potentiometer, 3, and was determined by measuring the current through wire resistance, 4, which equalled $R = 3006.2$ kΩ or, in some cases 4006.1 kΩ. The current was measured by the compensation method. It was possible in this way to measure a voltage of 5 kV to within 1 V. A rough measurement of the voltage could be performed with resistor 7 and microampermeter 8.

Since it is much more convenient to measure small intervals in the β-spectrum by the electrostatic bias method than by varying the current in the main coils and lenses, this method was

also employed to measure the conversion electron spectrum with the purpose of determining the internal conversion coefficient ratios. It was preliminarily established that within the limits used in the present work the magnitude of the bias voltage did not influence the area of the conversion lines. This could be demonstrated by measuring the F line from an active RdTh deposit at various bias values and comparing the areas of the lines thus obtained. Within the statistical errors they were found to be identical.

3. L-Subshells of Sm^{152} Gd^{154} and

A section of the β-spectrum of the Eu^{152}, Eu^{154} mixture is shown in fig. 4. Electron lines due to conversion of 122 and 123.2 keV

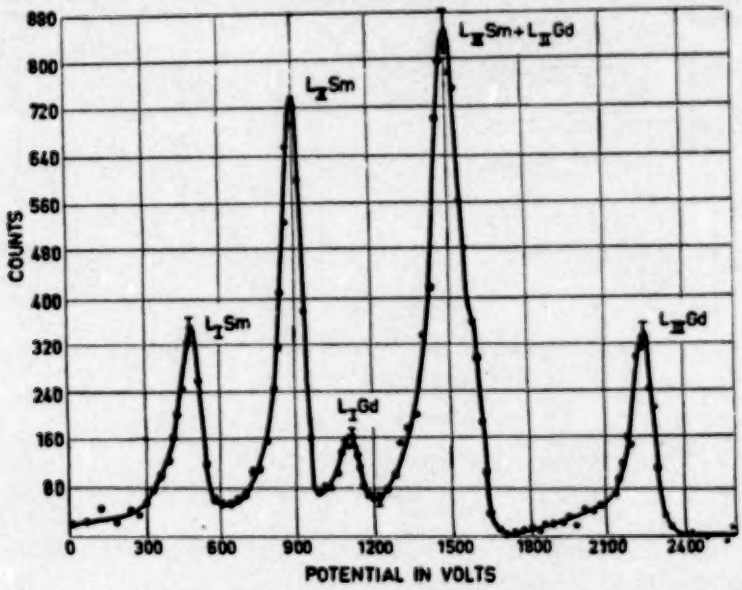

Fig. 4. Section of Eu^{152}, Eu^{154} spectrum containing Sm^{152} and Gd^{154} L-subshell internal conversion lines

γ-rays in the L-subshells of Sm^{152} and Gd^{154} are represented. The half-width of the lines is 0.05 %. The spectrum was measured under the following conditions. The source dimensions were 1×10 mm^2. The slit width of the detector was 1 mm, its length 28 mm. Slit diaphragm, 10 (fig. 1) which limited vertical spread of the beam was fully open (in the vertical direction the beam was restricted only by diaphragm 9 with a circular aperture $\varnothing$ 7 cm).

Slit diaphragm 11, which limited the horizontal spread, defined a beam 5 cm wide. The distance of the source or detector slit to the middle of the respective lens was 120 cm. The spectrometer efficiency was about 0.02 % of 4π.

Line identification was easily accomplished by measuring conversion line energy differences and comparing them with electron level energy differences deduced from X-ray measurements [7]).

Measurement of the energy difference of two conversion lines (not necessarily neighbouring lines) was achieved by first measuring one line, then directly after it the second one and finally measuring the first line again, the mean value of the two energy differences thus obtained finally being accepted. In this way drift in the deflecting magnetic field which was sometimes observed (and which, however, could introduce only small errors) was excluded. The drift was apparently due to slow variation in temperature of the spectrometer magnet. The position of the line was determined by the position of its peak.

Energy differences of the converted γ-quanta could be established with high precision by using our experimental energy differences of Sm and Gd conversion electrons and the electron energy level values presented in ref. [7]). Thus, for example, the energy difference of conversion electrons from the L_{III}Gd and L_{II}Sm subshells is 1357 ± 4 eV, whence it follows that the energy difference of γ-rays converting in Gd and Sm is 1292 eV. The error in the latter quantity depends on the accuracy of our measurements and on the accuracy of the data presented in ref. [7]).

As can be seen from the figure the L_{III}Sm and L_{II}Gd lines were not separated. Therefore the distance between these lines and other lines at first could not be determined and the distances were measured from the top of the peak of the two unseparated lines. In order to resolve lines L_{III}Sm and L_{II}Gd the resolution of the β-spectrometer was again increased as follows. An aluminium diaphragm with a 0.5 mm slit was mounted on the source and restricted in this way the width of the source. Diaphragms 10 and 11 (fig. 1) which limited the beam spread were arranged so as to form a 4×4 cm^2 square window (the efficiency of the instrument in this case was reduced to 0.01 % of 4π).

A check of the resolving power of the β-spectrometer by using lines I and Ia from an active RdTh deposit (fig. 5) showed that under the indicated conditions the instrument line half-width was 0.02 %.

Lines L_{III}Sm and L_{II}Gd measured with the aforementioned resolving power are shown in fig. 6. As can be seen the lines were partially separated. The ratio of the line areas (intensities) was

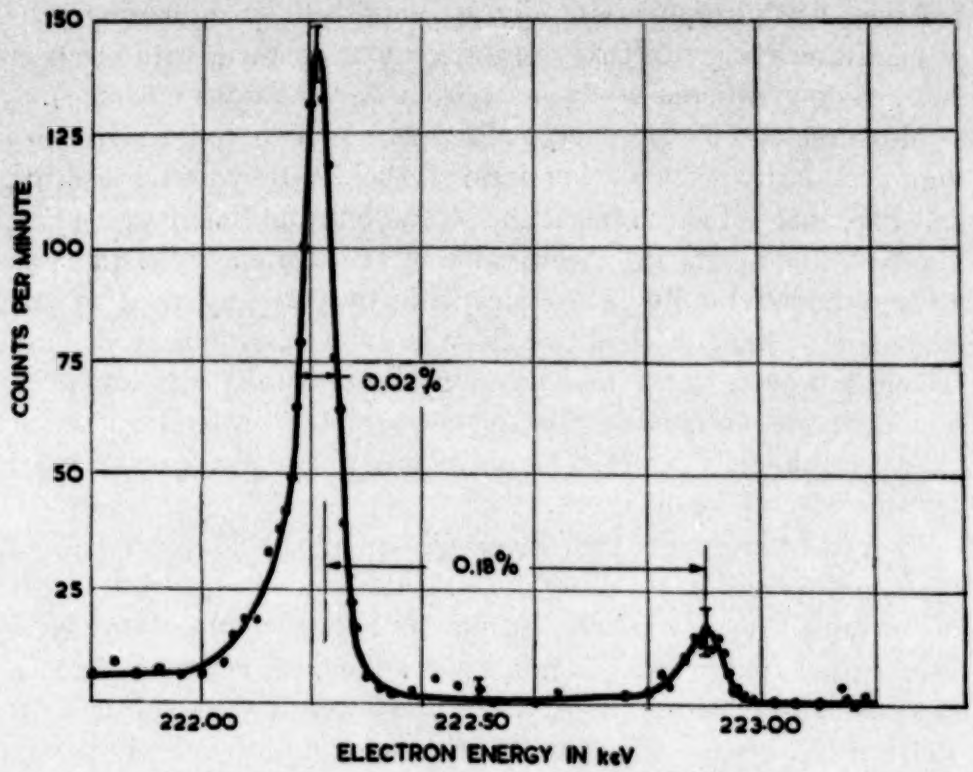

Fig. 5. Conversion lines I and Ia of active Rd TH deposit.

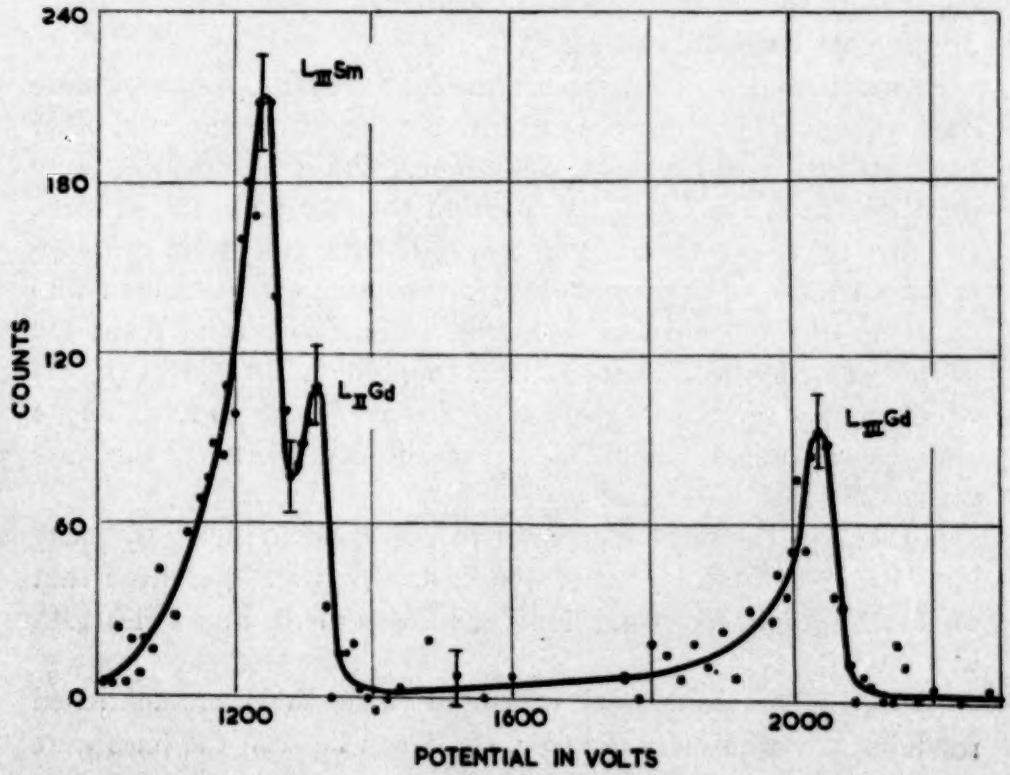

Fig. 6. Conversion lines L_{III}Sm, L_{II}Gd and L_{III}Gd measured at high resolution.

determined by graphical separation, the value $L_{III}Sm/L_{II}Gd = 1.96\pm0.05$ being obtained. The distance between the lines was 76 ± 2 V. These data were used to graphically separate lines $L_{III}Sm$ and $L_{II}Gd$ in fig. 4; after this it was possible to determine the distance between either of lines $L_{III}Sm$ or $L_{II}Gd$ and any other line and also to determine the ratios of the internal conversion coefficients for any of the L-subshells of Sm and Gd.

The electron level energy differences E obtained on basis of X-ray data presented in ref. [7]) are compared in table I with the results of our measurements.

TABLE I

	Electron level energy difference in samarium (eV)			Electron level energy difference in gadolinium (eV)		
	$E_{L_{II}}-E_{L_I}$	$E_{L_{III}}-E_{L_{II}}$	$E_{L_{III}}-E_{L_I}$	$E_{L_{II}}-E_{L_I}$	$E_{L_{III}}-E_{L_{II}}$	$E_{L_{III}}-E_{L_I}$
Hill, Church and Mihelich [7])	426	596	1022	441	691	1132
Present investigation	424 ± 2	597 ± 1	1021 ± 2	$443-\pm4$	691 ± 4	1131 ± 2

In order to measure the ratios of the Sm and Gd conversion line areas the method of measuring the conversion electron spectrum by varying the potential of the source (6 measurements) as well as the usual method of varying the current in the main coils of the lenses (4 measurements) were used.

The following area ratios were obtained by the first method: for samarium $L_{II}/L_I = 2.25\pm0.07$, $L_{III}/L_I = 2.26\pm0.07$; for gadolinium $L_{II}/L_I = 2.80\pm0.10$, $L_{III}/L_I = 2.52\pm0.07$. The second method of measuring the spectrum yielded: for samarium $L_{II}/L_I = 2.20\pm0.05$, $L_{III}/L_I = 2.07\pm0.07$; for gadolinium $L_{II}/L_I = 2.51\pm0.13$, $L_{III}/L_I = 2.30\pm0.13$. It can be seen that within the statistical errors both methods yield identical results. The values deduced from the complete set of results were as follows: for samarium $L_{II}/L_I = 2.22\pm0.04$, $L_{III}/L_I = 2.16\pm0.05$; for gadolinium $L_{II}/L_I = 2.69\pm0.08$, $L_{III}/L_I = 2.46\pm0.06$. It follows from here that the ratios of the conversion coefficients are: for samarium

$$L_I : L_{II} : L_{III} = 1 : (2.22\pm0.04) : (2.16\pm0.05)$$

and for gadolinium

$$L_I : L_{II} : L_{III} = 1 : (2.69\pm0.08) : (2.46\pm0.06).$$

The experimental internal conversion coefficient ratios were compared with the theoretical values obtained by interpolating the data of Rose cited by Siegbahn [8]). The interpolation was performed graphically. Energy interpolation was carried out by plotting the dependence of the logarithms of the conversion coefficient ratios on the logarithm of transition energy. Atomic number interpolation was carried out by plotting the dependence of the logarithm of the conversion coefficient ratio on atomic number for the given transition energies. Comparison of the theoretical values thus obtained with the experimental internal conversion coefficient ratios indicated the type of the transition which, as could be expected, was for Sm^{152} and Gd^{154} an electric quadrupole (E2) transition. For this type of transition the theoretical internal conversion coefficient ratios are the (if the transition energy, expressed in m_0c^2 units, is $k = 0.24$):

$$\text{for samarium} \quad L_I : L_{II} : L_{III} = 1 : 2.3 : 2.2;$$
$$\text{for gadolinium} \quad L_I : L_{II} : L_{III} = 1 : 2.7 : 2.5.$$

These values agree with the measured conversion coefficients ratios.

4. M-Subshells of Samarium

A part of the β-spectrum containing lines due to internal conversion electrons from the M-subshells of Sm (transition energy 122 keV) is illustrated in fig. 7. Assignments have been made by measuring the energy difference between the M-lines and also between the M-lines and the closest line of the L group, $L_{III}Gd$; the assignments are shown in the figure. Lines M_{IV} and M_V are evidently much weaker than those shown in the figure and hence could not be detected.

The ratio of the M-subshell conversion coefficients obtained in the present work was

$$M_I : M_{II} : M_{III} = 1 : (3.4 \pm 0.1) : (3.3 \pm 0.2)$$

(the mean of eight measurements). A salient feature is that conversion takes place predominantly in the M_{II} and M_{III} subshells. This fact agrees with conclusions derived on the basis of approximate computations (non-relativistic and without account of screening) of the relative M-subshell conversion coefficients [9]).

The ratio of the total L-shell conversion coefficient to the total

M-shell conversion coefficient of Sm was measured. It was found to equal $L/M = 4.5 \pm 0.1$ ($L \equiv L_I + L_{II} + L_{III}$; $M = M_I + M_{II} + M_{III}$).

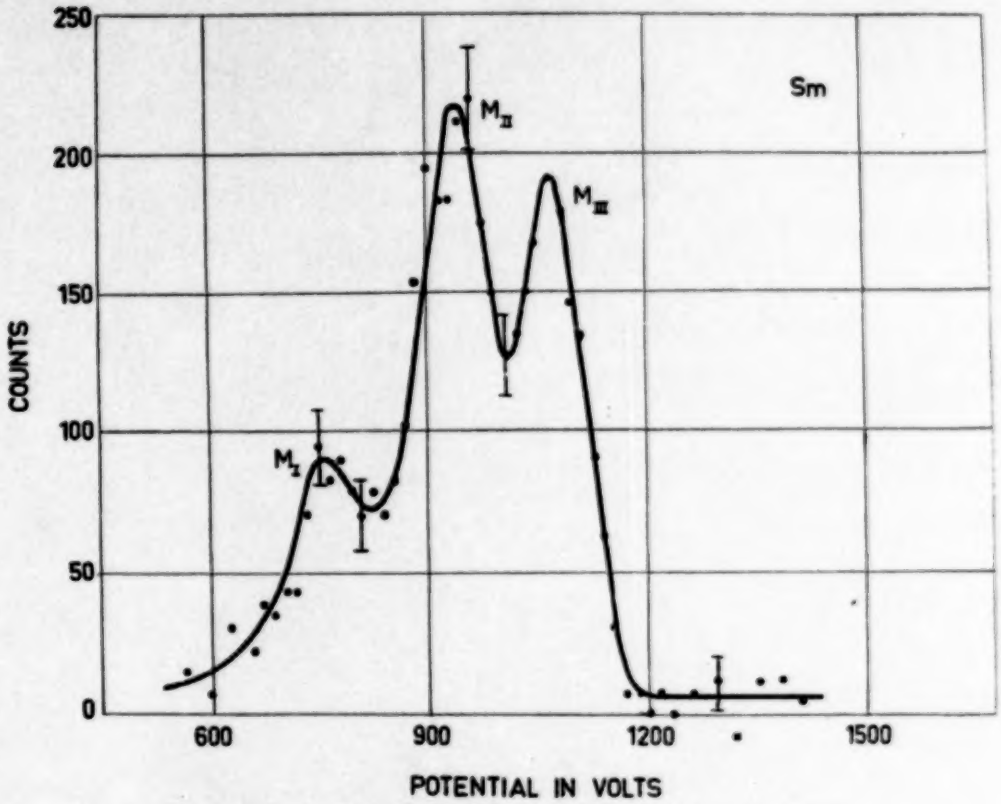

Fig. 7. Sm^{152} M-subshell internal conversion lines.

5. Measurement of K-Shell and L-Shell Conversion Coefficient Ratios for Sm and Gd

The K-lines of Sm^{152} and Gd^{154} are represented in fig. 8. The energy difference of these conversion lines as measured by applying a decelerating potential to the source was 2117 ± 1 eV.

The ratios of K-shell conversion coefficients to the total L-shell conversion coefficients for Sm and Gd were determined by utilizing the lines measured by varying the decelerating potential as well as by varying the current in the main coils. In the bias measurements of K or L-line groups the currents in the spectrometer coil were chosen in such a way as to approximately correspond to the energy of the group of lines being measured. Thus the voltage applied to the source was never large (however, it had to be large enough to ensure measurement of the spectrum within a single group).

This method of measurement requires that a correction which depends on the magnitude of the accepted energy interval (expressed in eV) be applied on changing from one group of lines to another.

If the spectrum was measured by varying the current in the main coils the dependence of counting rate on the magnitude of this

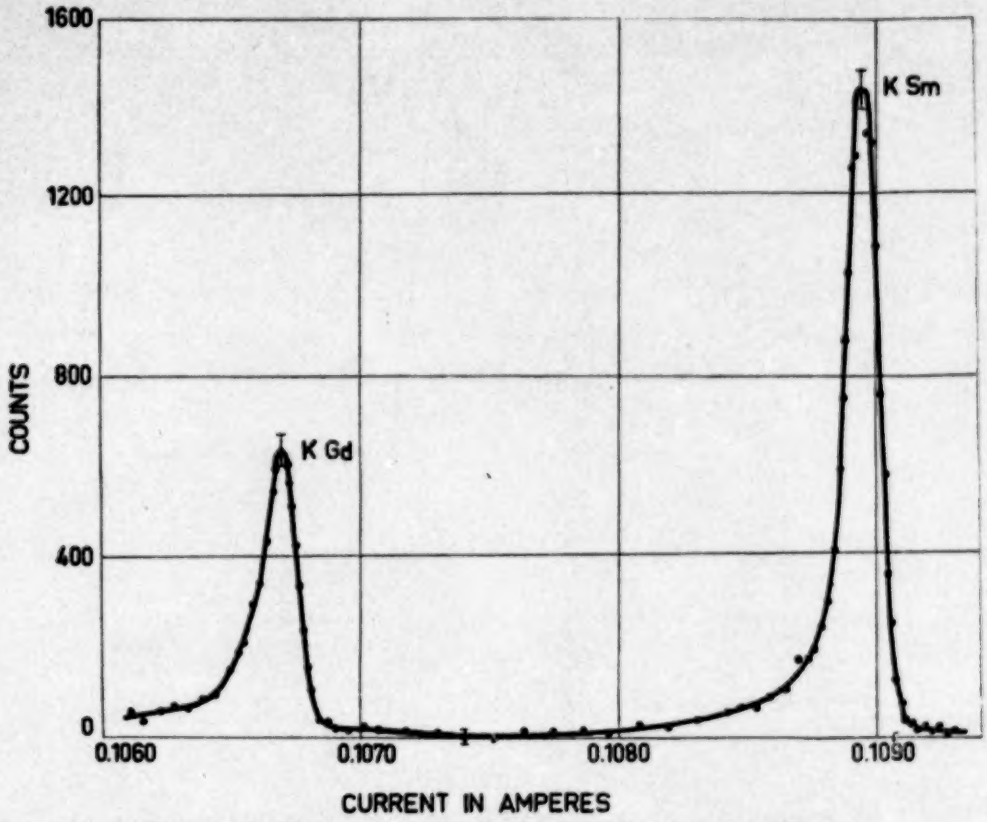

Fig. 8. Sm^{152} and Gd^{154} K-shell internal conversion lines.

current I was plotted. In this case, therefore, besides the usual correction to account for the width of the momentum interval a correction was applied to account for non linearity of dependence of the spectrometer magnetic field on I. It was an easy task to determine this correction since the momentum differences of electrons comprising different lines were known for the conversion lines under investigation.

In view of the appreciable energy difference between the K and L electrons, a correction was also applied to account for differences in absorption in the foils of the counters.

The curves presented in ref. [10]) were used to evaluate this correction. It comprised only 3 % of the K/L ratio as the thickness of the window foils of the recording arrangement was relatively

small (the counter chamber was separated from the rarefied region of the spectrometer by a 0.23 mg/cm² collodium film; the total thickness of the collodium films covering the exit aperture of the first counter and entrance aperture of the second counter was 0.1 mg/cm²).

After treatment of all the experimental results the following ratios for the conversion coefficients were obtained: for samarium (transition energy 122 keV) $K/L = 1.76 \pm 0.04$; for gadolinium (transition energy 123.2 keV) $K/L = 1.51 \pm 0.03$.

Theoretical values of the K/L ratios were obtained by using the K-shell internal conversion coefficients computed by L. A. Sliv and I. M. Band † with account of screening and finite dimensions of the nucleus. Internal conversion coefficients for the L-shell were found by interpolation of the data cited in ref. [8]). The theoretical ratios for E2 transitions and transition energy $k = 0.24$ were $K/L = 2.2$ for samarium and $K/L = 1.9$ for gadolinium.

It should be mentioned that since only a small number of L-subshell conversion coefficients were computed it was not possible to perform accurately the interpolation. On the other hand, appreciable systematic errors may be involved in the experimental K/L ratios due to the relatively large difference between the K and L electron energies. This may afford an explanation of the comparatively large discrepancy between the experimental and theoretical K/L ratios.

References

1) R. E. Slattery, D. C. Lu, and M. L. Wiedenbeck, Phys. Rev. **96** (1954) 465
2) J. M. Cork, H. B. Keller, W. C. Rutledge and A. E. Stoddard, Phys. Rev. **77** (1950) 848
3) V. M. Kelman, D. L. Kaminsky and V. A. Romanov, Izvestia Akademii Nauk SSSR, ser. phys. **18** (1954) 209
4) K. Siegbahn, Ark. f. Fys. **4** (1952) 223
5) W. B. Lewis and B. V. Bowden, Proc. Roy. Soc. A **145** (1934) 235
6) K. Siegbahn, Appl. Sci. Res. B **4** (1954) 25
7) R. D. Hill, E. L. Church and J. W. Mihelich, Rev. Sci. Inst. **23** (1952) 523
8) K. Siegbahn, Beta- and Gamma-Ray Spectroscopy (Amsterdam, 1955) p. 905
9) E. L. Church and J. E. Monahan, Phys. Rev. **98** (1955) 718
10) D. Saxon, Phys. Rev. **81** (1951) 639

† To be published.

Nuclear Physics **2** (1956/57) 408—419; *North-Holland Publishing Co., Amsterdam*

THE GAMMA SPECTRUM OF Sb^{124}

B. S. DZHELEPOV, N. N. ZHUKOVSKY, V. G. NEDOVESOV,
I. F. UCHEVATKIN and V. G. CHUMIN

V. G. Khlopin Radium Institute of the USSR Academy of Sciences, Leningrad

Received 4 May 1956

Abstract: A new determination of the gamma spectrum of Sb^{124} is described. The results, including the relative intensities of the lines, are summarized in table 1.

1. Introduction

In spite of the great number of published papers dealing with the β and γ-spectra of Sb^{124} [1–31]) the data available heretofore are not sufficient to permit one to construct a complete disintegration scheme of this isotope. The reason for this lies in the extreme complexity of the β- and γ-spectra of Sb^{124}. Five components [1–7]) have been detected in the β-spectrum. The decomposition of such a spectrum may be arbitrary to a certain degree because the shape of the elementary spectra into which the experimental curve is to be resolved remains unknown.

More than 10 γ-lines are known to exist in the γ-spectrum of Sb^{124}. None of the proposed disintegration schemes can account for all the observed γ-lines. Available $\beta-\gamma$ and $\gamma-\gamma$ coincidence data [7–10]) are not complete and sometimes seem to be inconsistent; their interpretation presents difficulties because of the fact that the energy intervals investigated in each experiment usually cover more than one γ-line.

In connection with this, before attempting to construct the complete disintegration scheme of Sb^{124} it was very important to know the relative intensities of the γ-lines.

An investigation of the γ-radiation from Sb^{124} with the use of the "ritron" [32]) was carried out in our laboratory [12]) in 1952.

Now we have undertaken a reinvestigation of the Sb^{124} gamma radiation using the so-called "elotron" [33]), i.e., a γ-spectrometer with improved focusing in which recoil electrons are employed.

2. Description of the Apparatus

Fig. 1 presents a schematic diagram of our apparatus.

Gamma quanta emitted by the source S placed in a lead collimator produce recoil electrons in the cellophane target M.

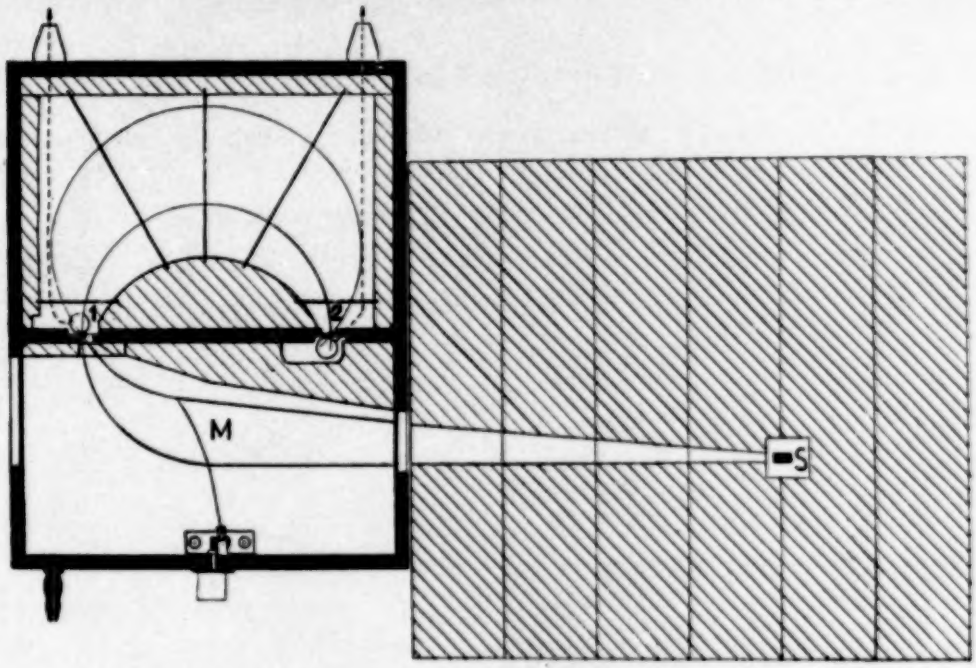

Fig. 1. Elotron. Schematic cross-section of the apparatus (horizontal plane). S: γ-rays source; M: target; 1 and 2: main slits.

Recoil electrons ejected in a small solid angle in the direction of the bombarding γ-quanta are subjected to double focusing in the magnetic field and pass through two collimating slits designated by numbers 1 and 2. Use of a bent target [34]) and of a uniform magnetic field permits one to achieve accurate focusing on the first slit of the recoil electrons travelling in the direction of the γ-quanta. Focusing on the second slit is accomplished by use of an inhomogeneous magnetic field of the type used in the "coetron" [35]) with a radius of curvature $\varrho_0 = 100$ mm. Two Geiger-Müller counters are placed directly behind the slits across the electron path; these counters have thin (1—2 μ thick) colloid film windows. The inner diameter of each counter is 15 mm. The counters were connected to a coincidence circuit with a resolving time of about 0.6 μ sec.

The beam of the focused electrons was collimated by two brass diaphragms placed at the focus points and by five aluminium ones.

The height and width of the diaphragms could be varied at will.

By the use of thin capron threads the target was attached to a duralumin frame which could be turned by means of a special rotary mechanism without any deterioration of the vacuum. The background was measured by removing the target out of the beam.

3. Apparatus Calibration

Calibration of the apparatus and the major measurements were carried out under the following conditions:

1) Distance from the source to the target—400 mm;
2) Cellophane target: surface 15×48 mm^2, thickness 2.15 mg/cm^2;
3) Apparatus entrance window thickness 2 mm (brass);
4) Size of each slit 2×15 mm^2;
5) The apparatus was filled with mixture of He and CH_4 (2 %) to a pressure of 24 cm Hg; this yielded an efficiency of electron recording of 92.45 per cent (for $E_\beta \approx 300$ keV) and 83.50 per cent (for $E_\beta \approx 1000$ keV).

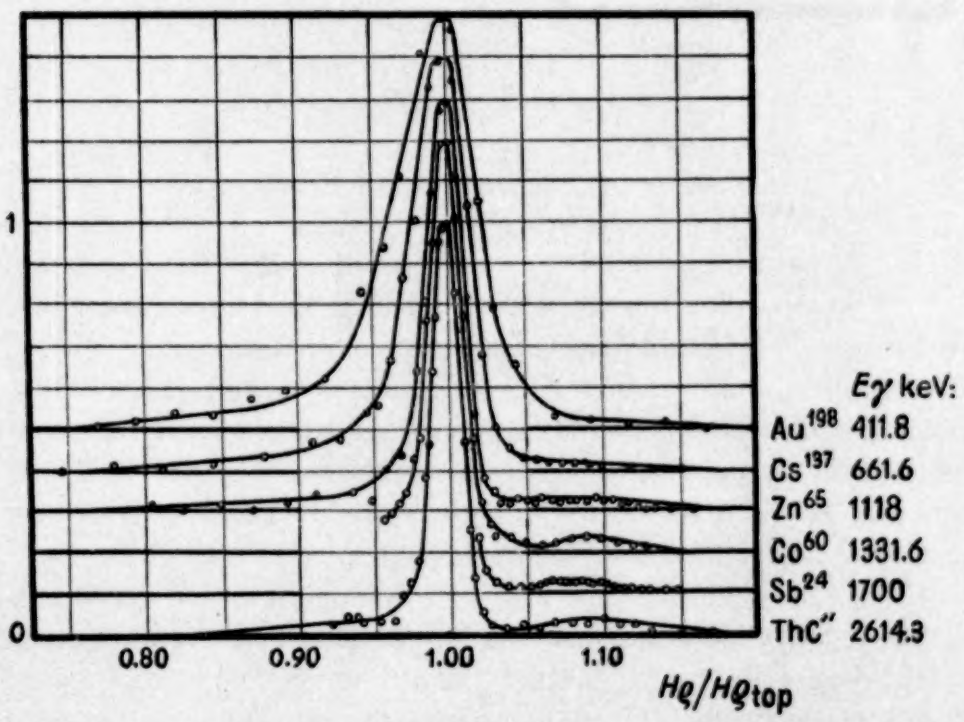

Fig. 2. Experimental calibration γ-lines obtained with the use of the elotron. All the lines are brought to equal height and for descriptive purposes displaced along the Y-axis.

X-axis: $H\varrho/H\varrho_{res}$;
Y-axis: coincidence counts in arbitrary units.

The following γ-lines were used for energy calibration and for determination of the experimental line shape:

$h\nu = 411.8$ keV — Au^{198};
$h\nu = 661.6$ keV — Cs^{137};
$h\nu = 1118$ keV — Zn^{65};
$h\nu = 1171.5$ keV — Co^{60};
$h\nu = 1331.6$ keV — Co^{60};
$h\nu = 1368$ keV — Na^{24};
$h\nu = 2614$ keV — ThC″;
$h\nu = 2753$ keV — Na^{24}.

Fig. 2 shows these lines normalized to relative coordinates and displaced along the Y-axis.

Fig. 3 presents the relation between the relative halfbreadth of a γ-line and the value of $H\varrho$. Above the 1 MeV level the magnitude of the halfbreadth constitutes 3.0—2.2 %; broadening of the lines evident in the soft region can be explained by taking into account the presence of residual gas in the apparatus.

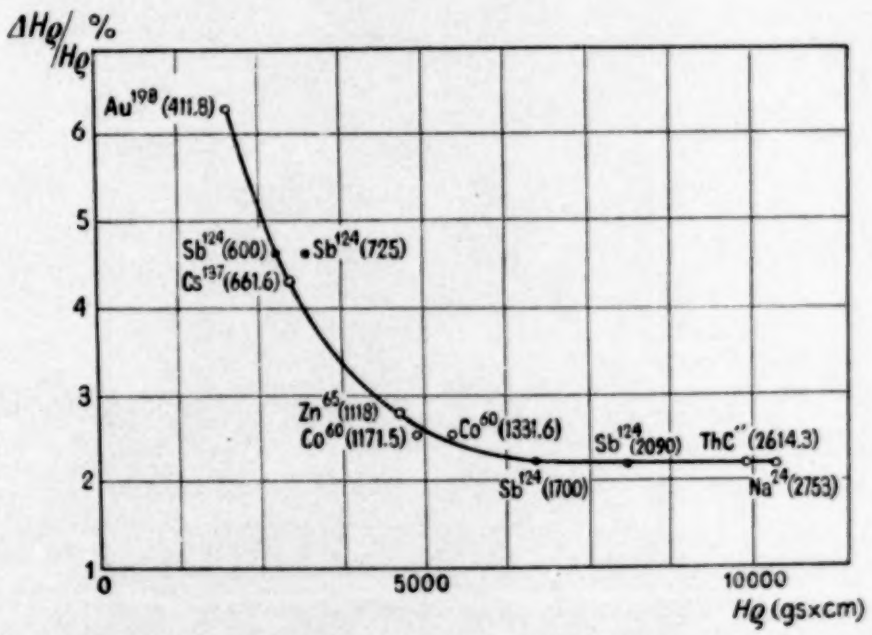

Fig. 3. Relation between $\Delta H\varrho/H\varrho$ and $H\varrho$. Circles designate the halfbreadth values of the calibration γ-lines and dots correspond to the halfbreadths of the strongest Sb^{124} γ-lines.

X-axis: $H\varrho$ (Gauss. cm);
Y-axis: Halfbreadth $\Delta H\varrho/H\varrho$.

The obtained data (fig. 2 and 3) can be used to determine by interpolation the apparatus line shape for any energy in the

400—2800 keV range. This information is used to resolve the complex γ-spectra into separate components.

The somewhat peculiar drop in the right hand part of the lines is closely connected with insufficient beam collimating before the second counter.

Some specially devised experiments showed that with the use of diaphragms the slope of the decrease could be made less steep but we did not succeed in destroying this "tail" completely.

The spectral sensitivity of the apparatus was investigated by way of studying:

a) Compton lines of Cs^{137} and Co^{60} γ-sources, their activity being defined calorimetrically by E. A. Kholnova at the VNIIM [36]);

b) Compton lines Na^{24} in the γ-spectrum of which there are two γ-lines ($h\nu = 1.38$ and 2.76 MeV) of equal intensity.

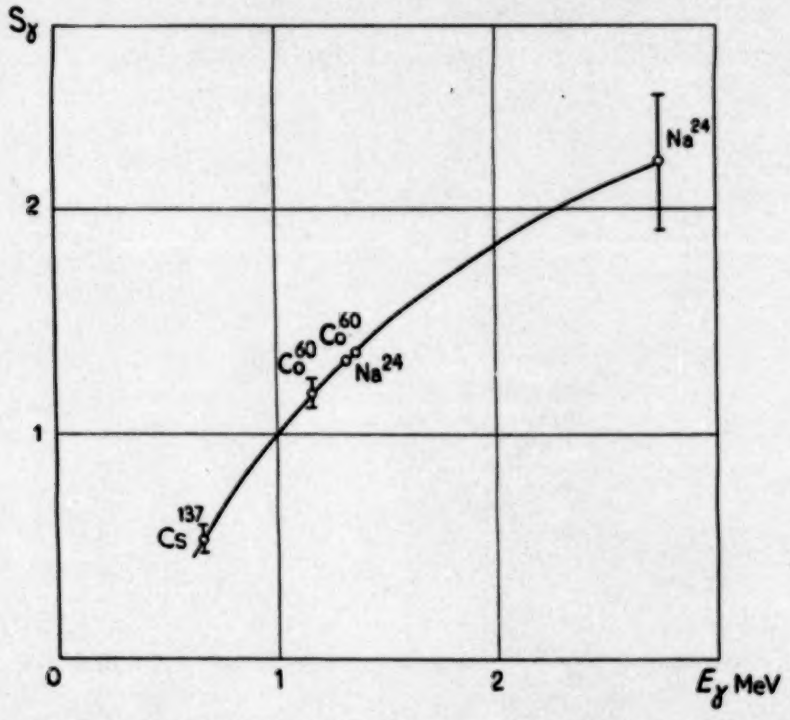

Fig. 4. Experimental elotron spectral sensitivity curve.
X-axis: γ-quanta energy E_γ;
Y-axis: spectral sensitivity S_γ.

By use of the procedure outlined above a curve for the spectral sensitivity S_γ [32]) was obtained (cf. fig. 4); the corresponding Y-axis scale was chosen so that $S_\gamma = 1$ when the energy of the γ-quanta equalled 1 MeV.

Vertical lines represent the experimental error.

4. Results

The source was a neutron-activated metallic antimony sample weighing 3 g and having radio-activity of about 4 Cu. It was placed in a glass ampule of 8 mm i.d. As all the measurements were usually performed more than two months after preparation of the source the presence of any γ-spectrum lines due to disintegration of the short-lived Sb^{122} isotope was practically excluded.

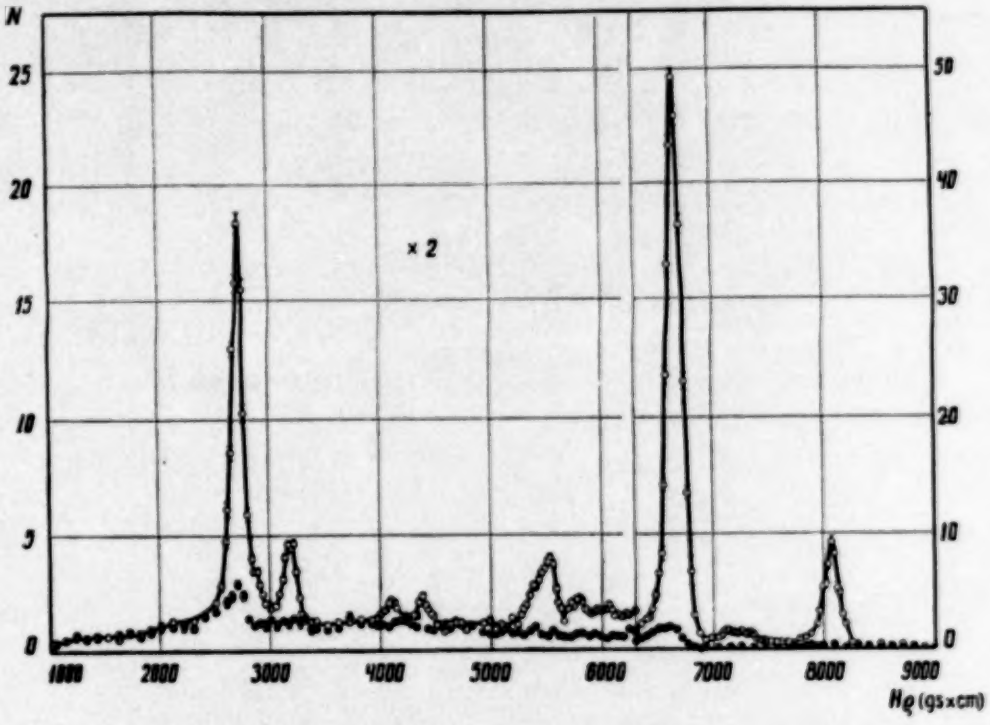

Fig. 5. experimental curve obtained during the Sb^{124} γ-spectrum investigation; background observed (with target removed from the beam).
X-axis: $H\varrho$ (Gauss · cm);
Y-axis: coincidence counts per minute.

Fig. 5 shows the experimental curve; on the Y-axis is plotted the number of coincidences per minute and on the X-axis the values of $H\varrho$. The apparatus background (designated by dots) usually showed a tendency to rise in the vicinity of the line, but generally it monotonically decreased with increasing $H\varrho$-values. The background was mainly due to the Compton effect in the gas and to electron scattering in the first part of the apparatus; the background due to random coincidences did not in any case exceed 2 counts per hour.

The statistical error is represented in the diagram by vertical

lines; the absence of a line signifies that the error was less than the diameter of the circle.

After subtracting the background the γ-spectrum was resolved into separate components with account of the relation existing between the apparatus line shape and energy as illustrated in fig. 2 and 3. An example of such resolution for $H\varrho$-values from 2000

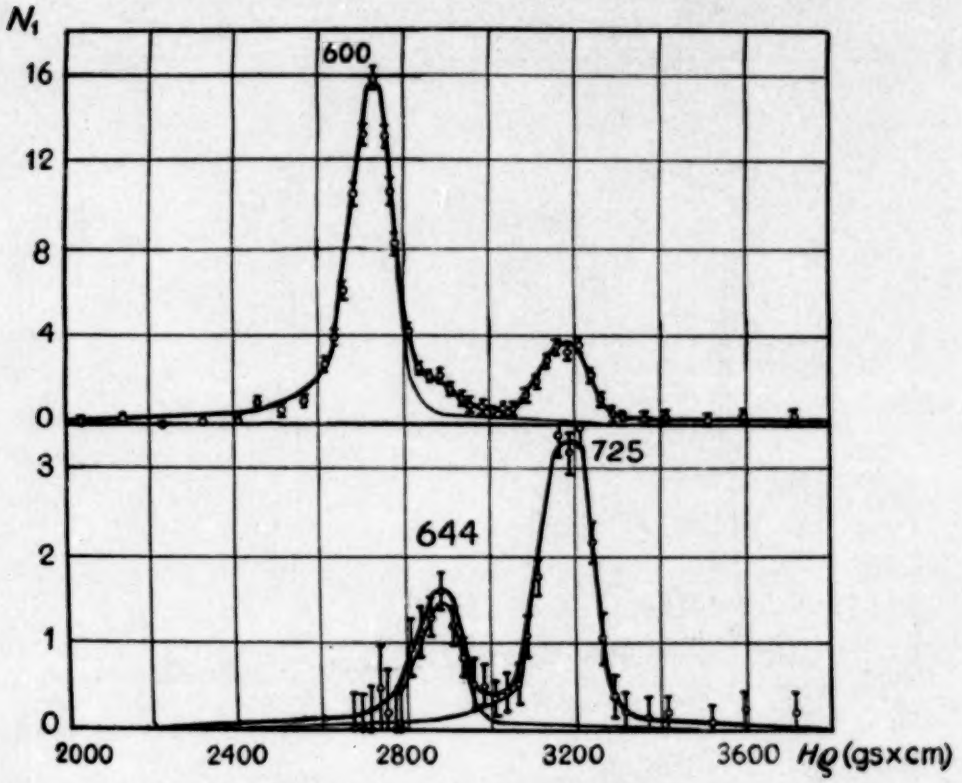

Fig. 6. Resolution of the $H\varrho$ spectrum portion from 2000 to 3800 Gauss · cm into separate lines.

X-axis: $H\varrho$ (Gauss · cm);
Y-axis: Coincidence counts per minute taking into account the observed background N_1.

to 6300 Gauss · cm is illustrated by figs. 6, 7 and 8. The thin curves refer to separate components and the thick one to their graphical sum. It is easy to see that within the limits of statistical error the integral curve follows the experimental points.

In accord with our calibration chart, the corresponding energy value expressed in keV is denoted above each of the obtained γ-lines.

In the upper portion of fig. 6 one can see a part of the experimental spectrum extending from 2000 to 3800 Gauss · cm with an

apparatus 600 keV γ-line inscribed. An excess of recoil electrons is manifest at the right of the line. The lower portion in the same figure illustrates this excess after subsequent subtraction of the line corresponding to $h\nu = 600$ keV (circles). The separation of this residual peak into two γ-lines of 644 and 725 keV energy appears to be quite unambiguous. It is noteworthy that the 725 keV γ-line is by 0.6 % broader here than it would be expected to be according to fig. 3. There are reasons to assume that this line is merely the sum of the lines corresponding to the 713 and 725 keV energy levels observed by means of conversion and photoelectron recording techniques [6]).

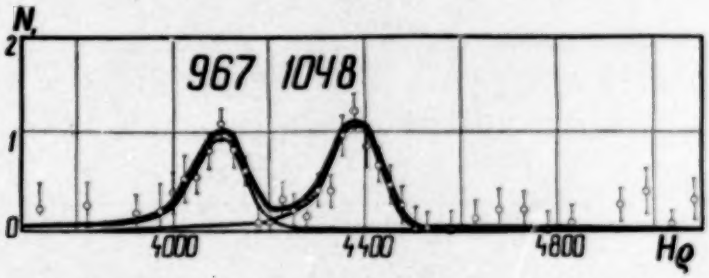

Fig. 7. The same as for Fig. 6 but for $H\varrho = 3800—4500$ Gauss · cm.

Fig. 7 illustrates a portion of the spectrum in the region between 3800 and 4500 Gauss · cm where two γ-lines of 967 and 1048 keV are plainly visible. It is highly probable that the excess above the background values observed in the region of 3400—3800 and 4600—5100 Gauss · cm is due to the presence of some comparatively weaker γ-lines.

The portion of the spectrum between 5100 and 6200 Gauss · cm is represented on the upper half of fig. 8. The thin line corresponds to the left sloping branch of the intensive γ-line 1700 keV; this branch extends approximately up to 5300 Gauss · cm. On the lower part of the drawing is depicted the residue after subsequent subtraction of the sloping branch of this line (circles). It can be quite satisfactorily resolved into 4 γ-lines corresponding to the energy values 1330, 1370, 1442 and 1525 keV. The resolution of the spectrum portion above 6300 Gauss · cm into two γ-lines of 1700 and 2090 keV is not illustrated because of complete separation of these lines. It must be noted that some appreciable excess above the background between the two most hard γ-lines is due to the peculiar form of the right sloping branch of the 1700 keV γ-line; this can easily be seen by inspecting the curve in fig. 2. In this figure this portion is

represented on such a scale that the height of the 1700 keV γ-line is equal to 1.

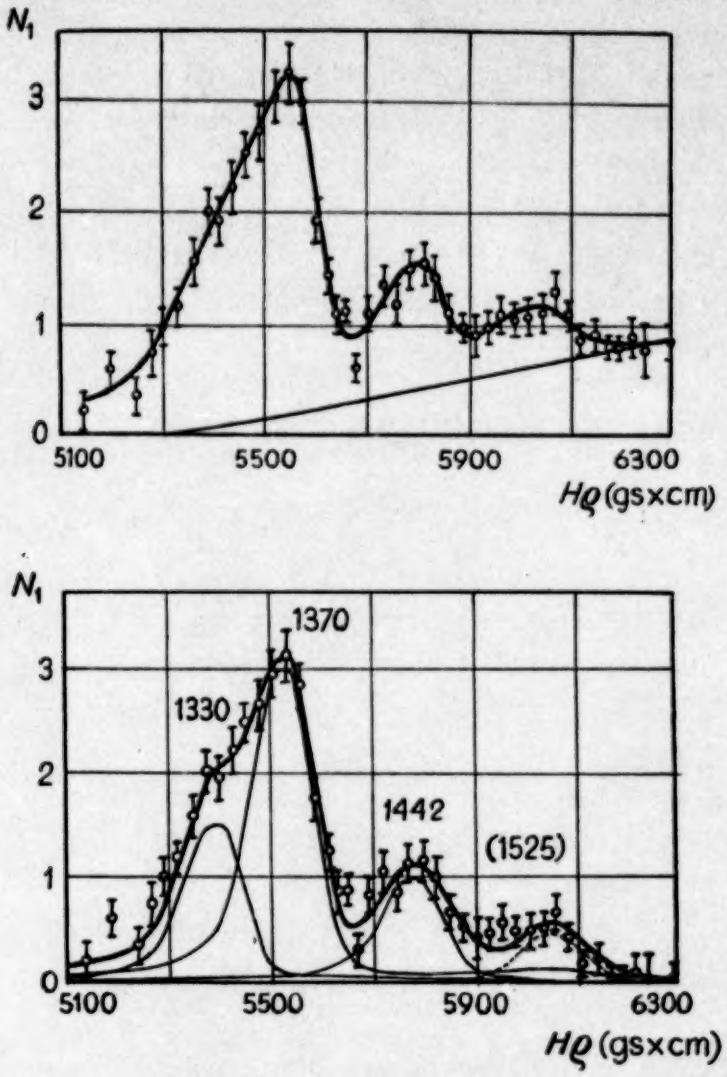

Fig. 8. The same as for Fig. 6 but for $H\varrho = 5100$—6200 Gauss · cm.

Fig. 9 represents a final version of the Sb^{124} γ-spectrum drawn in equal energy intervals after taking into account the following corrections:

a) Absorption of the γ-rays by the apparatus entrance window;
b) Self-absorption in the source;
c) Counter efficiency factor;
d) Spectral sensitivity of the apparatus.

For the sake of illustration the 800—1600 keV portion of the spectrum is depicted on a larger scale.

Table 1 contains our γ-line data including the respective spectral intensities and also the results of other workers. In addition to the previously known γ-lines corresponding to 600, 644, 725, 967,

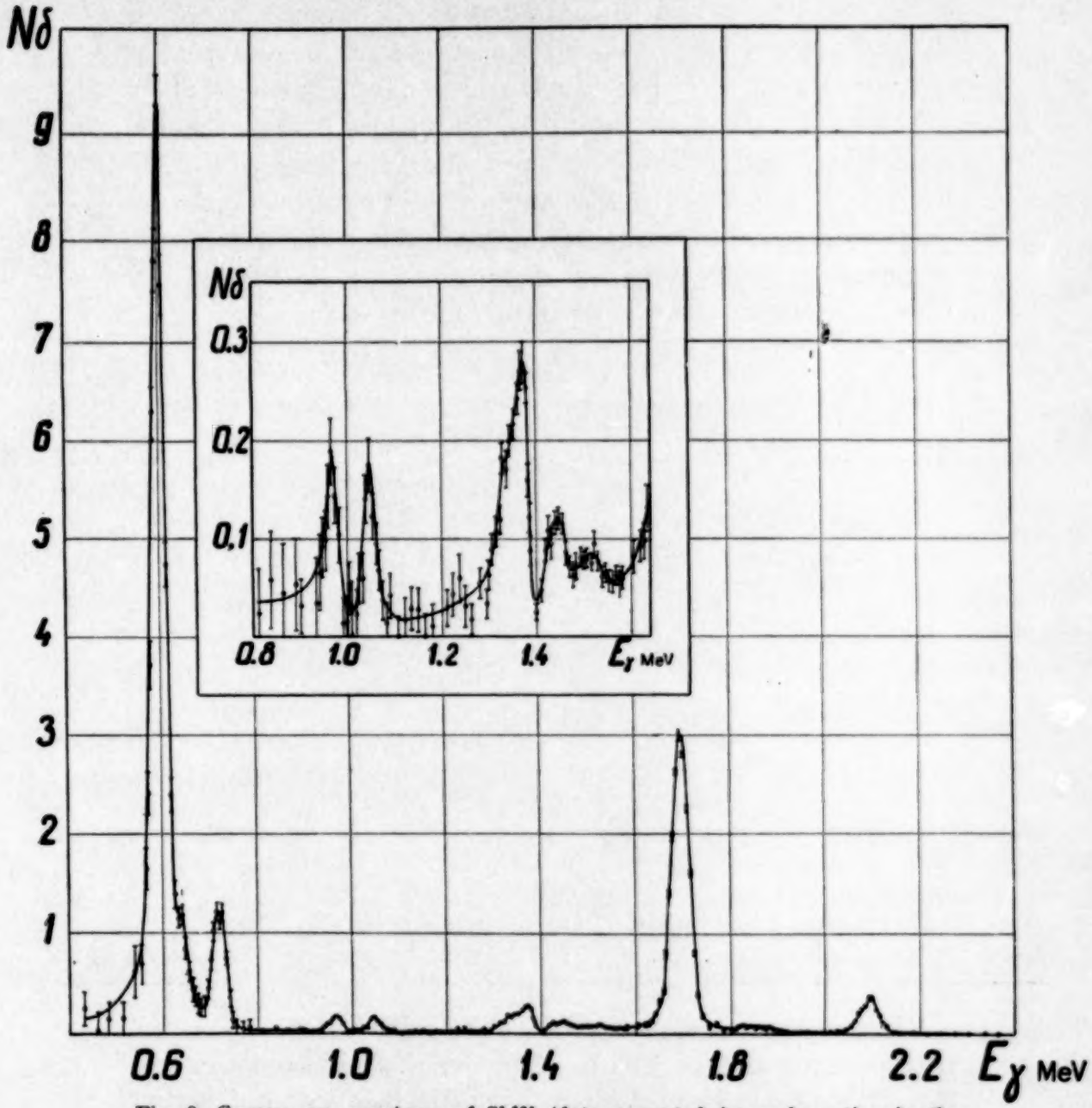

Fig. 9. Gamma ray spectrum of Sb^{124} (data corrected for γ-absorption in the apparatus entrance window and in the source itself as well as for counter efficiency and spectral sensitivity of the apparatus).
X-axis: Energy of the γ-quanta E_γ;
Y-axis: Gamma rays intensity referred to equal intervals.

1048, 1330, 1370, 1700 and 2090 keV we detected the 1442 keV γ-line; the existence of a 1525 keV γ-line is also probable.

The results of our measurements do not permit us to positively assert that these lines belong to Sb^{124} because we did not carry out an adequate radiochemical analysis. However an investigation of the source performed 80 days afterwards indicated that within the experimental errors the decrease of intensity in each part of the spectrum strictly corresponded to the 60-day half-period of Sb^{124}.

The main error in the relative intensity of the strong lines is introduced when one draws the spectral sensitivity curve ($\pm 13\%$ for the interval 600—2100 keV); in the case of weak lines one must obviously add a statistical error, an error due to the subtraction of the tails of neighbouring lines and finally an error which appears when the integral curve is separated into its components.

TABLE I

Energy values and relative intensities of the Sb^{124} γ-lines as obtained by different workers

Kern *et al.*[1]) 1948		Gromov *et al.*[12]) 1952		Lazar[11]) 1954		Zolotavin[6]) 1956		Our data 1956	
E_γ(keV)	rel. int.	E_γ(keV)	rel. int.	E_γ(keV)	rel. int.	E_γ(keV)	rel. int.	E_γ(keV)	rel. int.
603	131	597	154	603	218.8	603	194	600	232 ±30
650	11					646	12	644	20 ±4
714	34	711	19	—	—	714	7.5	725	37 ±5
						723	20		
—	—	958	6.6	990	11.8	990	5	967	5.0±0.8
—	—	1052	4.4	—	—	1047	4	1048	4.8±1.8
—	—	—	—	—	—	1298	2.5	1330	4.5±1.5
—	—	—	—	—	—	1326	4.0		
—	—	1347	17	1380	13.6	1361	6	1370	8.7±1.2
						1370			
—	—	—	—	—	—	—	—	1442	2.6±0.6
—	—	—	—	—	—	—	—	(1525)	(1.1±0.7)
1708	100	1691	100	1710	100	1691	100	1700	100
2062	8.6	2070	10	2110	21.7	2088	13	2090	14.3±1.5

We are greatly indebted to E. A. Kholnova for calorimetric measurements and to Yu. V. Kholnov, V. P. Prikhodtseva and S. A. Shestopalova for valuable discussions on the question of spectral sensitivity.

References

1) B. Kern, D. Zaffarano and A. Mitchell, Phys. Rev. **73** (1948) 1268; **73** (1948) 1142

2) C. Cook and L. Langer, Phys. Rev. **73** (1948) 1268; **73** (1948) 1149

3) E. Tomlinson, S. Ridgway and K. Gopalakrishnan, Phys. Rev. **91** (1953) 484
4) J. Moreau, Compt. Rend. **239** (1954) 800
5) T. Azuma, J. Phys. Soc. Japan **10** (1955) 167
6) A. Zolotavin, E. Grigoryev and M. Abroyan, Izv. Akad. Nauk, ser. phys. **20** (1956) 289
7) R. Moffat, N. Lazar and L. Langer, BAPS **28** (1953) 3,U13; Phys. Rev. **91** (1953) 338, 485
8) S. Almquist and S. Johansson, Nature **170** (1952) 583; Arkiv. Fys. **5** (1952) 427
9) L. Langer and J. Starner, Phys. Rev. **93** (1954) 253
10) D. Lu, W. Kelly and M. Wiedenbeck, Phys. Rev. **95** (1954) 1533
11) N. Lazar, Phys. Rev. **95** (1954) 292
12) K. Gromov, B. Dzhelepov, N. Zhukovsky, A. Silantyev and Yu. Kholnov, DAN.SSSR, ser. phys. **86** (1952) 255
13) A. Mitchell, L. Langer and P. McDaniel, Phys. Rev. **57** (1940) 1107
14) G. Klaiber and G. Scharff-Goldhaber, Phys. Rev. **61** (1942) 733
15) E. Hales and E. Jordan, Phys. Rev. **64** (1943) 202
16) P. Kruger and W. Ogle, Phys. Rev. **67** (1945) 273
17) L. Miller and L. Curtiss, Phys. Rev. **70** (1946) 983
18) W. Rall and R. Wilkinson, Phys. Rev. **71** (1947) 321
19) A. Wattenberg, Phys. Rev. **71** (1947) 497
20) W. Meyerhof and G. Scharff-Goldhaber, Phys. Rev. **72** (1947) 273
21) D. Hughes and C. Eggler, Phys. Rev. **72** (1947) 902
22) S. Jnanananda, Phys. Rev. **72** (1947) 1124
23) M. Wiedenbeck and K. Chu, Phys. Rev. **72** (1947) 1164
24) M. Scherb and C. Mandeville, Phys. Rev. **73** (1948) 1268
25) E. Jurney and A. Mitchell, Phys. Rev. **73** (1948) 1269; Phys. Rev. **73** (1948) 1153
26) I. Feister and L. Curtiss, J. Res. **NBS 40** (1948) 315
27) V. Myers and A. Wattenberg, Phys. Rev. **75** (1949) 992
28) F. Metzger, Phys. Rev. **86** (1952) 435
29) D. Hutchinson and M. Wiedenbeck, Phys. Rev. **88** (1952) 699
30) D. Alburger, Phys. Rev. **88** (1952) 1257
31) R. Maerker and R. Birkhoff, Phys. Rev. **89** (1953) 1159
32) B. Dzhelepov, N. Zhukovsky and Yu. Kholnov, Izv. AN SSSR, ser. phys. **18** (1954) 599
33) B. Dzhelepov, N. Zhukovsky, A. Karamian and G. Shestopalova, Izv. AN SSSR, ser. phys. **17** (1953) 518
34) B. Dzhelepov, DAN SSSR, ser. phys. **77** (1951) 389
35) B. Dzhelepov and A. Bashilov, Izv. AN SSSR **14** (1950) 263
36) K. Aglintsev and E. Kholnova, DAN SSSR, ser. phys. **98** (1953) 360

Nuclear Physics **2** (1956/57) 420—440; *North-Holland Publishing Co., Amsterdam*

CAUSALITY AND DISPERSION RELATIONS IN WAVE MECHANICS

E. CORINALDESI

Department of Natural Philosophy, The University of Glasgow

Received 4 June 1956

1. Introduction

As is universally known, the analysis of scattering data is a problem which may not always admit of a unique solution. It consists in deriving the scattering amplitude $f(\theta)$, or, what is the same, the phase shifts, to which $f(\theta)$ is connected by the equation †

$$f(\theta) = \frac{1}{2ik} \sum_{l=0}^{\infty} (2l+1)(e^{2i\eta_l}-1) P_l(\cos\theta). \tag{1}$$

If a certain function $f(\theta)$ fits the experimental cross section, $d\sigma_{exp} = |f(\theta)|^2 \, d\Omega$, the same will be true of $-f^*(\theta)$. In other words, if a set of phase shifts $\eta_0, \eta_1 \ldots$ agrees with the experimental data, so also will $-\eta_0, -\eta_1 \ldots$ The search for ways of resolving this ambiguity seems to have been the main incentive for the renewed interest recently displayed by physicists in the dispersion relations of scattering theory.

In other fields of physics, dispersion relations have been known for a long time. In the optics of absorbing media, which is based on the use of a complex refractive index $n(\omega)$, a function of the frequency ω, the integral relationship

$$\mathrm{Re}\,[n(\omega)-1] = \frac{2\omega^2}{\pi} \mathrm{P} \int_0^{\infty} \frac{\mathrm{Im}\, n(\omega')}{\omega'(\omega'^2-\omega^2)} \, d\omega' \tag{2}$$

was established by Kramers and Kronig [1, 2]. Similar relations exist between the resistive and capacitive parts of the impedance of an absorbing condenser [3]; also in the theory of linear networks [4]. The case of the absorptive condenser will be treated in sect. 2,

† This is the appropriate formula for the scattering of a spinless particle by a central potential.

in order to show how dispersion relations come about. Because of its straightforwardness, this example may be preferable to the better known optical one, which is lucidly described in the recent work by Jauch and Rohrlich [5]).

In the theory of scattering, dispersion relations can be established which connect the real and imaginary parts of the forward scattering amplitude $f(0)$. The imaginary part, on the other hand, is expressed in terms of the total cross section σ by the optical theorem [6])

$$\sigma = \frac{4\pi}{k} \operatorname{Im} f(0). \tag{3}$$

Thus, if the imaginary part of $f(0)$, i.e. the total cross section, is known for all energies, the real part of $f(0)$ can be calculated by integration with respect to the energy, as in eq. (2), and the ambiguity affecting the analysis of the experimental data can, at least in principle, be removed in this fashion.

Dispersion relations for the scattering amplitude in any direction can be derived in wave mechanics with no greater effort than is necessary in order to establish those for the forward direction. What is lost, however, is the possibility of attaching a direct physical meaning to the imaginary part. The non-relativistic theory of scattering, on the other hand, fails to do that in any case, since the scattering amplitude which satisfies the dispersion relations is not $f(\theta)$ given by eq. (1), but rather refers to a formulation of the problem in which the scattering due to a given interaction of radius r_0 is compared with that due to a perfectly reflecting sphere of the same radius. Complications arise if the particles taking part in a collision are capable of arranging themselves in bound states. In this case, additional terms due to the bound states occur besides those which are suggested by the optical analogy.

The connection of the dispersion relations with causality has been stressed by several authors in varying degrees. That causality requirements might determine some of the properties of the S-matrix was suggested by Kronig [7]). On the other hand, how such requirements are to be expressed depends on the particular theory in question. In the non-relativistic theory of scattering by a short range potential which we develop in sects. 3 and 4, causality must roughly mean that there cannot be a scattered wave until the impinging wave packet has reached the scatterer [8, 9]). The behaviour of the S-matrix in the upper half of the complex k-plane,

and in addition a kind of elementary dispersion relations for the phase shift [9]), are deduced from this principle in sect. 5 for s-scattering by a short range potential. The derivation from causality is made to follow one more direct based on the completeness of the system of eigenfunctions of the Schroedinger equation for the potential in question, as suggested by Gell-Mann and his co-workers [10]). The purpose of this is to show that the imposition of causality is not the only way in which dispersion relations can be deduced. But then, the completeness relation is merely what is left of a causal propagation function when the time-dependent theory of collisions is supplanted by the less intuitive stationary treatment.

Going back to sects. 3 and 4, we might mention that the dispersion relations for the forward scattering amplitude are established at the end of sect. 4 from those for s-scattering (sect. 3) and their extension to arbitrary angular momentum (sect. 4). This inductive approach is not followed in sect. 6, which deals with the relativistic scattering of spin zero particles by a short range potential [10]). Here the dispersion relations for the forward scattering amplitude are derived from the requirement that the relativistic Green function $G(\mathbf{x}, x_0; \mathbf{x}', x_0')$ for the particles in the given field of force must vanish when $\mathbf{x}$, x_0 and $\mathbf{x}'$, x_0' lie on a space-like surface. Formally the Green function can be exhibited as the vacuum expectation value of the commutator of two field operators at different space-time points, if only one-particle states are considered. This remark paves the way for the construction of dispersion relations in a theory with second quantization, which are the object of contemporary studies [11, 12, 13, 14]).

2. Dispersion Relations in the Theory of Dielectric Loss [3])

The voltage $U(t)$ applied to an absorptive condenser having a leakage resistance $R = 1/G_0$, a capacitance C_0 and a relaxation function $g(t)$ produces the current

$$I(t) = G_0 U + C_0 \frac{\mathrm{d}U}{\mathrm{d}t} + \int_{-\infty}^{\infty} g(t-\tau) \frac{\mathrm{d}U(\tau)}{\mathrm{d}\tau} \mathrm{d}\tau. \qquad (1)\,\dagger$$

The function $g(t)$ is zero for negative values of t. For positive values it is bounded, has always the same sign and its absolute

† Equations are numbered separately in each section and are quoted by their number preceded by the number of the section. The latter is omitted if the equation appears in the same section in which the reference is made.

value is continuously decreasing ($g(\infty) = 0$). For physical reasons it seems appropriate to assume the convergence of the integral

$$\int_0^\infty |g(t)|\mathrm{d}t = Q. \tag{2}$$

In fact, Q is the total anomalous charge of the condenser after application of a unit voltage for an infinitely long time.

The steady state current produced by the voltage $U(t) = U(\omega)\mathrm{e}^{i\omega t}$ is expressed by $I(t) = I(\omega)\mathrm{e}^{i\omega t}$ with

$$I(\omega) = [G(\omega)+i\omega C(\omega)]U(\omega) \tag{3}$$

and

$$\begin{cases} G(\omega) = G_0 = +\omega \int_{-\infty}^{\infty} g(t) \sin \omega t \, \mathrm{d}t, \\ C(\omega) = C_0 + \int_{-\infty}^{\infty} g(t) \cos \omega t \, \mathrm{d}t. \end{cases} \tag{4}$$

It is convenient to introduce the function

$$F(\omega) = D(\omega)+iA(\omega) \tag{5}$$

with

$$D(\omega) = C(\omega)-C_0, \qquad A(\omega) = \frac{G(\omega)-G_0}{\omega}. \tag{6}$$

Then

$$F(\omega) = \int_{-\infty}^{\infty} g(t)\, \mathrm{e}^{i\omega t}\, \mathrm{d}t, \tag{7}$$

and $D(\omega)$ and $A(\omega)$ can be regarded as the real and imaginary parts of a function whose Fourier transform is $g(t)$.

The theory of Fourier integrals has much to say about the properties of $F(\omega)$ arising from

a) the square integrability of $g(t)$; this descends from (2) and the postulated boundedness of $g(t)$;

b) the vanishing of $g(t)$ for $t < 0$.

It is enough for us to state that, according to a theorem by Titchmarsh [5, 15]), a function $F(\omega)$ defined by (7) with $g(t)$ satisfying the properties a) and b) mentioned above, has a regular analytic continuation $F(\omega_1+i\omega_2)$ in the upper complex plane $\omega_2 > 0$, and that the dispersion relations

$$D(\omega) = \frac{1}{\pi} \mathrm{P} \int_{-\infty}^{\infty} \frac{A(\omega')\, \mathrm{d}\omega'}{\omega'-\omega}, \tag{8a}$$

$$A(\omega) = \frac{1}{\pi} \mathrm{P} \int_{-\infty}^{\infty} \frac{D(\omega')\, \mathrm{d}\omega'}{\omega-\omega'} \tag{8b}$$

hold on the real axis. Here, and in the following, P$\int$ denotes the principal value.

Notice now that in our case $F(-\omega) = F^*(\omega)$, so that $D(-\omega) = D(\omega)$ and $A(-\omega) = -A(\omega)$. This enables us to write the dispersion relations in the more usual form

$$D(\omega) = \frac{2}{\pi} \mathrm{P} \int_0^\infty \frac{A(\omega')\omega' \, \mathrm{d}\omega'}{\omega'^2 - \omega^2}, \tag{9a}$$

$$A(\omega) = \frac{2}{\pi} \mathrm{P} \int_0^\infty \frac{D(\omega')\omega \, \mathrm{d}\omega'}{\omega^2 - \omega'^2}. \tag{9b}$$

The theorem enunciated above will in general prove not directly applicable to scattering theory on account of the existence of bound states. In fact, these would cause the analogue of our function to possess poles on the real axis †, so that a generalization of the theorem would be necessary. We shall therefore prefer to establish the dispersion relations of scattering by direct calculation, though making reference to Titchmarsh's theorem whenever possible. We might mention in this respect that our equations (8) and (9) could also be verified directly. Expressing $A(\omega')$ in the right member of (9a) by means of (4), (5) and (6), and interchanging the order of the ω' and t integrations (which is allowed by the square integrability of $g(t)$) we obtain

$$\begin{aligned} \mathrm{P} \int_0^\infty \frac{A(\omega')\omega' \, \mathrm{d}\omega'}{\omega'^2 - \omega^2} &= \frac{1}{2} \int_{-\infty}^\infty g(t) \, \mathrm{d}t \, \mathrm{P} \int_{-\infty}^\infty \frac{\omega' \sin \omega' t \, \mathrm{d}\omega'}{\omega'^2 - \omega^2} \\ &= \frac{\pi}{2} \int_{-\infty}^\infty g(t) \cos \omega t \, \mathrm{d}t = \frac{\pi}{2} D(\omega). \end{aligned} \tag{10}$$

Similarly we can verify the second dispersion relation (9b).

3. Dispersion Relations in the Non-relativistic Theory of s-scattering

3.1. PROPERTIES OF THE FUNCTION $S(k)$.

This section is devoted to the theory of s-scattering by a central potential of short range. As customary, it is convenient to define a new function $\varphi(r) = r\psi(r)$ from the Schroedinger wave function $\psi(r)$. For zero angular momentum, and in suitable units, φ obeys the equation

† If the energy is used as a variable.

$$\varphi''-V\varphi = -i\frac{\partial\varphi}{\partial t}, \tag{1}$$

where the potential $V(r)$ will be assumed to vanish for $r > r_0$. All physically meaningful solutions must be zero for $r = 0$. We are particularly interested in solutions of definite energy which, for $r > r_0$, can always be written in the form

$$\varphi = C\,(e^{-ikr}-S(k)\,e^{-ikr})\,e^{-iEt} \qquad (r > r_0). \tag{2}$$

In this expression $E = k^2$ is the energy, k the momentum and $S(k)$ is the "S-matrix" (here an ordinary function of k) with the property

$$S(k)S(-k) = 1. \tag{3}$$

Whenever k and E are real quantities, (2) represents a scattering wave function. In this case, $S(-k) = S^*(k)$ and therefore

$$S(k)S^*(k) = 1 \qquad (k \text{ real}), \tag{4}$$

which establishes the unitarity of the S-matrix.

Eq. (2) can be taken to hold when k and E are complex numbers. We write $k = k_1 + ik_2$, $k^* = k_1 - ik_2$, $E = (k_1^2 - k_2^2) + 2ik_1k_2$. In this case eq. (3) is still valid while eq. (4) must be changed into

$$\frac{1}{S(k)} = [S(k^*)]^* \tag{4'}$$

reducing to (4) when k is real. We see from (4') that the unitary property of the S-matrix holds only for real k.

As for the physical interpretation of complex momenta, we note first that, if the momentum is purely imaginary ($k_1 = 0$), the energy is real and negative. Thus the wave function (2) would be that of a bound state if it were square integrable. This is the case if $S(k)$ has a zero on the negative imaginary axis. Then, for $r > r_0$, φ consists only of the first term $\exp(-ikr) = \exp(k_2r)$, which is indeed square integrable for $k_2 < 0$. Note also that, by virtue of (4'), there is a pole on the positive imaginary axis for every zero on the negative imaginary axis.

If k is not a point of either the real or the imaginary axis, the energy E is a complex quantity. Complex energies are invariably met with in physics whenever one attempts to describe emission or capture processes. The theory of α-decay is a striking example of their occurrence. We shall write $E = E_0 - \frac{1}{2}i\lambda$, where the "decay" constant λ may be positive or negative. The two alternative cases

correspond to an amplitude which decreases or increases with time.

It is remarkable that the equation of continuity alone is sufficient to exclude the existence of zeros and poles of $S(k)$ in certain regions of the complex plane [16]). For example, it can be seen by inspection that $S(k)$ cannot have any zeros in the lower half of the complex plane (except on the negative imaginary axis), nor, according to (4'), any poles in the upper half (except on the positive imaginary axis). In fact, assume that $S(k)$ has a zero, say, in the fourth quadrant. This would mean a non-vanishing ingoing current $-k_1 \exp(2k_2 R)$ through a sphere of radius R from the first term of (2), while the amplitude of the wave function inside the sphere would decrease with time on account of the factor $\exp(-\frac{1}{2}\lambda t)$ ($\lambda > 0$ for $k_1 > 0$ and $k_2 < 0$). For a similar reason, zeros of $S(k)$ cannot exist in the third quadrant, nor poles in the first and second.

On the other hand, zeros in the first quadrant describe capture processes compatible with the continuity equation, and in the second quadrant radioactive decay. To these correspond poles in the third and fourth quadrants. The situation is as shown in fig. 1.

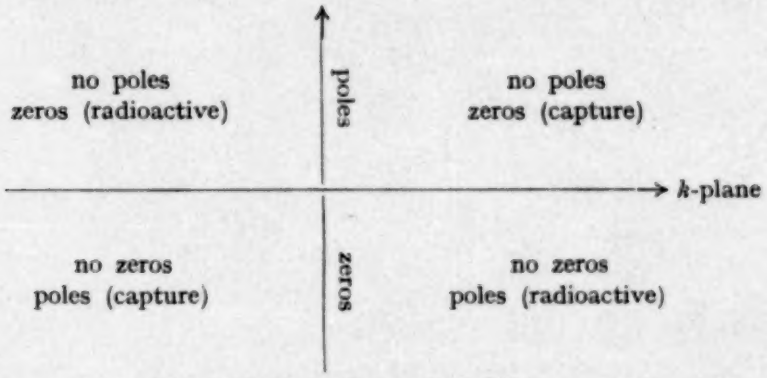

Fig. 1. Poles and zeros of $S(k)$

3.2 GENERAL FORM OF THE S-MATRIX

Following the early work of Heisenberg [17]), Hu [18]) and others, we shall now establish the general form of $S(k)$ from the completeness relation.

We consider the scattering and bound state wave functions for $r > r_0$,

$$r\psi_k(r) \equiv \varphi_k(r) = e^{-ikr} - S(k)\, e^{ikr}, \tag{5a}$$

$$r\psi_\alpha(r) \equiv \varphi_\alpha(r) = \sqrt{N_\alpha}\, e^{-\varkappa_\alpha r} \quad (\varkappa_\alpha = \sqrt{-E_\alpha}), \tag{5b}$$

where the normalization constants $\sqrt{N_\alpha}$ can be chosen to be real.

For $(r, r') \geqq r_0$, (5a) and (5b) can be substituted in the completeness relation

$$\delta(r-r') = \frac{1}{2\pi}\int_0^\infty \varphi_k(r)\,\varphi_k^*(r')\,\mathrm{d}k + \sum_\alpha \varphi_\alpha(r)\varphi_\alpha(r'), \tag{6}$$

which then reads

$$\int_0^\infty [S(k)\,\mathrm{e}^{ik(r+r')} + S^*(k)\,\mathrm{e}^{-ik(r+r')}]\,\mathrm{d}k = \sum_\alpha N_\alpha\,\mathrm{e}^{-\varkappa_\alpha(r+r')}. \tag{7}$$

Making use of the properties of $S(k)$ we can also write

$$\int_{-\infty}^\infty S(k)\,\mathrm{e}^{ik(r+r')}\,\mathrm{d}k = \sum_\alpha N_\alpha\,\mathrm{e}^{-\varkappa_\alpha(r+r')}. \tag{8}$$

We now transform the integration path into a semicircle Γ of infinite radius in the upper half plane, which gives

$$\sum_\alpha \oint_{k=k_\alpha} S(k)\,\mathrm{e}^{ik(r+r')}\,\mathrm{d}k + \int_\Gamma S(k)\,\mathrm{e}^{ik(r+r')}\,\mathrm{d}k = \sum_\alpha N_\alpha\,\mathrm{e}^{-\varkappa_\alpha(r+r')}. \tag{9}$$

This must hold for any value of $r+r' \geqq 2r_0$, so that the coefficients of $\exp[-\varkappa_\alpha(r+r')]$ on both sides must be equal. Thus we have

$$\oint_{k=\varkappa_\alpha} S(k)\,\mathrm{d}k = N_\alpha, \tag{9a}$$

$$\int_\Gamma S(k)\,\mathrm{e}^{ik(r+r')}\,\mathrm{d}k = 0 \qquad (r+r' \geqq 2r_0). \tag{9b}$$

The second of eqs. (9) determines the singularity of $S(k)$ at infinity. Hu[18]) was able to show that the $S(k)$ function must be of the general form

$$S(k) = \pm\mathrm{e}^{ick}\prod_\gamma \frac{(k-k_\lambda^*)}{(k-k_\lambda)}\prod_s \frac{(k-k_s^*)\,(k+k_s)}{(k-k_s)\,(k+k_s^*)}. \tag{10}$$

In this expression, c is a negative constant of the order of $2r_0$. Greek indices denote poles and zeros on the imaginary axis, Latin indices those elsewhere. Zeros and poles not on the imaginary axis occur in pairs, symmetrical with respect to the imaginary axis. The general form of the function $S(k)$ is essentially as dictated by the conditions (3) and (4′). As an example we quote the case of a square well potential of range r_0 and depth $-V_0$. We have

$$S(k) = \frac{1+i\dfrac{k}{\sqrt{k^2+V_0}}\,\mathrm{tg}\,(r_0\sqrt{k^2+V_0})}{1-i\dfrac{k}{\sqrt{k^2+V_0}}\,\mathrm{tg}\,(r_0\sqrt{k^2+V_0})}\,\mathrm{e}^{-2ir_0k}, \tag{11}$$

which can be written in the form of a product, as in eq. (10), by finding the roots of the algebraic equation

$$1+i\frac{k}{\sqrt{k^2+V_0}}\,\mathrm{tg}\,(r_0\sqrt{k^2+V_0}) = 0. \tag{12}$$

Incidentally we might mention the implications of the general form (10). For simplicity's sake take $c = 0$ and only one factor corresponding to a certain k_s. The cross section has then the form

$$Q = \frac{\pi}{k^2}|1-S(k)|^2 = \frac{\pi}{k^2}\left|\frac{2k(k_s-k_s^*)}{k^2-k_s^2}\right|^2 . \tag{13}$$

With $E = k^2$, $E_s = k_s^2$, $E_s = W_s - \frac{1}{2}i\gamma_s$ we have

$$Q = \frac{\pi}{k^2}\left|\frac{2k(k_s-k_s^*)}{E-E_s}\right|^2 = \frac{\pi}{(k_s+k_s^*)^2}\cdot\frac{\gamma_s^2}{(E-W_s)^2+\frac{1}{4}\gamma_s^2}, \tag{14}$$

which becomes the one level formula of the theory of nuclear reactions if $(k_s+k_s^*)^2$ is replaced by $4k^2$.

3.3. DISPERSION RELATIONS

Consider now the function $S(k)\exp(2ir_0 k)/(k^2-k_0^2)$, where k_0 is an arbitrary real constant. If k denotes a point in the upper half of the complex plane, we have

$$\frac{1}{k^2-k_0^2}S(k)\,e^{2ir_0 k} = \frac{1}{2\pi i}\oint\frac{S(k')\,e^{2ir_0 k'}}{(k'-k)(k'^2-k_0^2)}\,dk', \tag{15}$$

the integration being along the path shown in fig. 2. The small

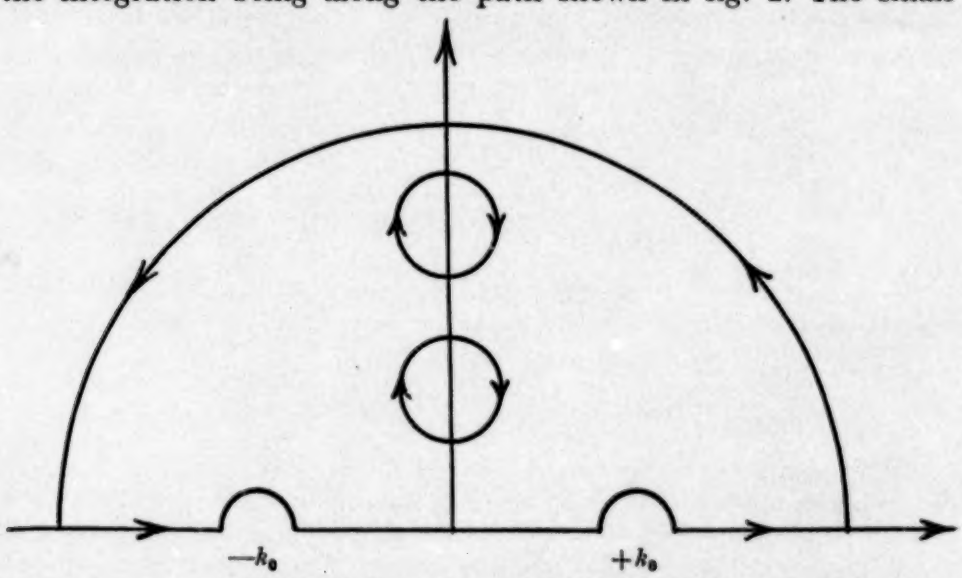

Fig. 2. Integration path for eq. (3.15)

circles enclose the poles on the imaginary axis, and the radius of the semicircle is infinite. By virtue of the convergence factor $1/(k^2-k_0^2)$ and of eq. (9b), the semicircle of infinite radius gives a vanishing contribution and we are left with

$$\frac{S(k)\,e^{2ir_0 k}}{k^2-k_0^2} = \frac{1}{2\pi i}P\int_{-\infty}^{\infty}\frac{S(k')e^{2ir_0 k'}}{(k'-k)(k'^2-k_0^2)}\,dk'$$
$$+\frac{1}{4k_0}\left[\frac{S(k_0)\,e^{2ir_0 k_0}}{k-k_0} - \frac{S(-k_0)\,e^{-2ir_0 k_0}}{k+k_0}\right] - \sum_\alpha\frac{b_\alpha}{k_\alpha(k_\alpha-k)(k_\alpha-k_0^2)}. \tag{16}$$

The principal value of the integral refers to the singularities at k_0 and $-k_0$, while $k_\alpha = i\varkappa_\alpha$ are poles on the imaginary axis (bound states) and

$$b_\alpha = \operatorname{Res}\left[kS(k)\,\mathrm{e}^{2ir_0k}\right]_{k=k_\alpha} \tag{17}$$

are real quantities by virtue of (9a).

If k is on the real axis, (16) must be modified into

$$\begin{aligned}\frac{S(k)\,\mathrm{e}^{2ir_0k}}{2(k^2-k_0^2)} &= \frac{1}{2\pi i}\,\mathrm{P}\int_{-\infty}^{\infty}\frac{S(k')\,\mathrm{e}^{2ir_0k'}}{(k'-k)(k'^2-k_0^2)}\,\mathrm{d}k' \\ &+\frac{1}{4k_0}\left[\frac{S(k_0)\mathrm{e}^{2ir_0k_0}}{k-k_0}-\frac{S(-k_0)\mathrm{e}^{-2ir_0k_0}}{k+k_0}\right]-\sum_\alpha\frac{b_\alpha}{k_\alpha(k_\alpha-k)(k_\alpha^2-k_0^2)},\end{aligned} \tag{18}$$

where the principal value now refers also to the singularity at $k'=k$.

To eq. (18) we add its complex conjugate. Making use of the fact that, if k' is real, $\operatorname{Im}\left[S(-k')\,\exp\left(-2ir_0k'\right)\right] = -\operatorname{Im}\left[S(k')\exp\left(2ir_0k'\right)\right]$, we get

$$\begin{aligned}&\frac{1}{k^2-k_0^2}\operatorname{Re}\left[S(k)\,\mathrm{e}^{2ir_0k}-S(k_0)\,\mathrm{e}^{2ir_0k_0}\right] \\ &=\frac{2}{\pi}\,\mathrm{P}\int_0^\infty\frac{k'\,\operatorname{Im}\left[S(k')\,\mathrm{e}^{2ir_0k'}\right]\mathrm{d}\,k'}{(k'^2-k^2)(k'^2-k_0^2)}-2\sum_\alpha\frac{b_\alpha}{(k_\alpha^2-k^2)(k_\alpha^2-k_0^2)},\end{aligned} \tag{19}$$

which is already a dispersion relation. A similar one is obtained by subtracting from (18) its complex conjugate,

$$\begin{aligned}&\frac{1}{k^2-k_0^2}\operatorname{Im}\left[S(k)\,\mathrm{e}^{2ir_0k}-\frac{k}{k_0}S(k_0)\,\mathrm{e}^{2ir_0k_0}\right] \\ &=\frac{2}{\pi}\,\mathrm{P}\int_0^\infty\frac{\operatorname{Re}\left[S(k')\,\mathrm{e}^{2ir_0k'}\right]k\,\mathrm{d}k'}{(k'^2-k_0^2)(k^2-k'^2)}+\frac{2k}{i}\sum_\alpha\frac{b_\alpha}{k_\alpha(k_\alpha^2-k_0^2)(k^2-k_\alpha^2)}.\end{aligned} \tag{20}$$

For the applications it is convenient to have the limit of eqs. (19) and (20) when k_0 tends to zero. It is also advantageous to define the quantities

$$\begin{aligned}D_0(k) &= \frac{1}{2k}\operatorname{Im}\left[S(k)\,\mathrm{e}^{2ir_0k}\right] = \operatorname{Re}\left[\frac{1}{2ik}S(k)\,\mathrm{e}^{2ir_0k}\right], \\ A_0(k) &= -\frac{1}{2k}\operatorname{Re}\left[S(k)\,\mathrm{e}^{2ir_0k}\right] = \operatorname{Im}\left[\frac{1}{2ik}S(k)\,\mathrm{e}^{2ir_0k}\right].\end{aligned} \tag{21}$$

It is easy to perform the limit $k_0 \to 0$ in (19). In fact, $\operatorname{Im} S(0)=0$ ($S(0) = \pm 1$) so that the integral is convergent for $k_0 = 0$, and

we obtain

$$A_0(k) = -\frac{S(0)}{2k} + \frac{2}{\pi} \mathrm{P} \int_0^\infty \frac{k D_0(k')}{k^2 - k'^2} \, \mathrm{d}k' + \sum_\alpha \frac{k b_\alpha}{k_\alpha^2 (k_\alpha^2 - k^2)} . \quad (22)$$

To perform the limit $k_0 \to 0$ in eq. (20) is less straightforward. Since

$$\lim_{k_0 \to 0} \frac{1}{k_0} [S(k_0) \, \mathrm{e}^{2ir_0 k_0} - \dot{S}(0)] = \dot{S}(0) + 2ir_0 S(0) ,$$

where a dot denotes derivative with respect to k, we get

$$D_0(k) = \frac{1}{2i} \dot{S}(0) + r_0 S(0) + \frac{2}{\pi} k^2 \lim_{k_0 \to 0} \mathrm{P} \int_0^\infty \frac{A_0(k') k' \, \mathrm{d}k'}{(k'^2 - k^2)(k'^2 - k_0^2)} - ik^2 \sum_\alpha \frac{b_\alpha}{k_\alpha^3 (k^2 - k_\alpha^2)} . \quad (23)$$

It would not be correct to put $k_0 = 0$ in the integral, as we would thus produce a divergent expression. Proceeding more cautiously, we may write

$$\frac{2}{\pi} k^2 \lim_{k_0 \to 0} \mathrm{P} \int_0^\infty \frac{A_0(k') k' \, \mathrm{d}k'}{(k'^2 - k^2)(k'^2 - k_0^2)} = \frac{2}{\pi} \mathrm{P} \int_0^\infty \frac{A_0(k') k' \, \mathrm{d}k'}{k'^2 - k^2} - \frac{2}{\pi} \lim_{k_0 \to 0} \mathrm{P} \int_0^\infty \frac{A_0(k') k' \, \mathrm{d}k'}{k'^2 - k_0^2} . \quad (24)$$

On the other hand

$$-\frac{2}{\pi} \lim_{k_0 \to 0} \mathrm{P} \int_0^\infty \frac{A_0(k') k' \, \mathrm{d}k'}{k'^2 - k_0^2} = \frac{1}{2\pi} \lim_{k_0 \to 0} \mathrm{P} \int_{-\infty}^\infty \frac{S(k') \mathrm{e}^{2ir_0 k'}}{k'^2 - k_0^2} \, \mathrm{d}k' = \frac{i}{2} [\dot{S}(0) + 2ir_0 S(0)] + i \sum_\alpha (b_\alpha / k_\alpha^3) . \quad (25)$$

Employing (24) and (25), (23) can be written

$$D_0(k) = \frac{2}{\pi} \mathrm{P} \int_0^\infty \frac{A_0(k') k' \, \mathrm{d}k'}{k'^2 - k^2} - i \sum_\alpha \frac{b_\alpha}{k_\alpha (k^2 - k_\alpha^2)} . \quad (23')$$

4. Extension to Higher Angular Momenta. Dispersion Relations for the Scattering Amplitude

If the angular momentum is larger than zero, we must generalize the discussion given in sect. 3 for the s-scattering and study the properties of the function

$$S_l(k) = (-1)^l \, e^{2i\eta_l(k)}, \tag{1}$$

which is defined by the asymptotic behaviour

$$\varphi_k^{(l)} \approx C(e^{-ikr} - S_l(k) \, e^{ikr}) \tag{2}$$

of the solution of the Schroedinger equation which vanishes for $r = 0$. In the present notation, the function $S(k)$ of sect. 3 would be $S_0(k)$, and $\varphi(r) \equiv \varphi_k^{(0)}(r)$. It is worth mentioning that (2) is not an exact solution of the Schroedinger equation outside the range of the potential $V(r)$ on account of the centrifugal potential. The functions

$$r\varphi_k^{(l)} \equiv \varphi_k^{(l)}(r) = f_l(+k, r) - S_l(k) f_l(-k, r) \tag{3}$$

with

$$f_l(+k, r) = e^{-ikr} q_l^*(kr) \tag{4}$$

and

$$q_l(kr) = \sum_{m=0}^{l} i^m \frac{\Gamma(l+1+m)}{m!\Gamma(l+1-m)(2kr)^m} \tag{5}$$

are exact solutions for $r \geqq r_0$, and, in the absence of bound states, can be chosen as a complete set of eigenfunctions. For simplicity's sake the assumption that there are no bound states will be made from now on.

For r and r' both larger than r_0 the completeness relation now reads

$$\begin{aligned} \delta(r-r') = \frac{1}{2\pi}\int_0^\infty \varphi_k^{(l)}(r)\varphi_k^{(l)*}(r')\mathrm{d}k = \frac{1}{2\pi}\int_0^\infty [f_l(+k, r)f_l(-k, r') \\ -(S_l(k)f_l(-k, r)f_l(-k, r') + S_l^*(k)f_l(+k, r)f_l(+k, r')) \\ +S_l(k)S_l^*(k)f_l(-k, r)f_l(+k, r')]\mathrm{d}k. \end{aligned} \tag{6}$$

Using the properties of $S_l(k)$ and of the functions $f_l(\pm k, r)$ we get

$$\int_{-\infty}^{\infty} e^{ik(r+r')} S_l(k) q_l(kr) q_l(kr')\mathrm{d}k = 0, \qquad (r, r') \geqq r_0. \tag{7}$$

From this it is easy to infer that

$$\int_{-\infty}^{\infty} S_l(k) \frac{f_l(-k\ r_0)}{f_l(+k, r_0)}\mathrm{d}k = 0. \tag{8}$$

In fact, the left member of (7) ($r = r' = r_0$) can be transformed into an integral along a semicircle of infinite radius in the upper half plane, on which $q_l(kr_0)q_l(kr_0)$ is equal to one and can be

replaced by $q_l(kr_0)/q_l^*(kr_0)$ which has the same value. This latter function, on the other hand, has no poles in the upper half plane, as the zeros of $q_l(kr_0)$ are in the lower half, so that the integration path can once more be deformed and made to coincide with the real axis, leading to (8). Note that, on the real axis (but not elsewhere) we can write $q_l^*(kr_0) = q_l(-kr_0)$.

Thus

$$S_l(k)\frac{f_l(-k, r_0)}{f_l(+k, r_0)} = S_l(k)\ e^{2ikr_0}\frac{q_l(kr_0)}{q_l^*(kr_0)}$$

is the generalization of the function $S(k)\exp(2ikr_0)$ of sect. 3 †, with which it shares all the properties which are necessary for the establishment of the dispersion relations between the "dispersive" and "absorptive" parts

$$\begin{aligned} D_l(k) &= \mathrm{Re}\left[\frac{1}{2ik}S_l(k)\frac{f_l(-k, r_0)}{f_l(+k, r_0)}\right], \\ A_l(k) &= \mathrm{Im}\left[\frac{1}{2ik}S_l(k)\frac{f_l(-k, r_0)}{f_l(+k, r_0)}\right] \end{aligned} \tag{9}$$

in the form

$$\begin{aligned} A_l(k) &= -\frac{(-1)^l S_l(0)}{2k} + \frac{2}{\pi}\mathrm{P}\int\frac{kD_l(k')\,\mathrm{d}k'}{k^2-k'^2} \\ D_l(k) &= \qquad\qquad \frac{2}{\pi}\mathrm{P}\int\frac{k'A_l(k')\,\mathrm{d}k'}{k'^2-k^2}. \end{aligned} \tag{10}$$

We now assume that $S_l(0) = (-1)^l$, i.e. $\eta_l(0) = 0$. This amounts to excluding the existence of bound states of zero energy [19]). The first term in the right member of (10) can then be brought over to the left member, and the vanishing of the integral $\int_0^\infty \mathrm{d}\omega'/(\omega'^2-\omega^2)$ can be employed to establish dispersion relations between the real and the imaginary parts of the scattering amplitude

$$\begin{aligned} F(\theta) &= \sum_{l=0}^{\infty}(2l+1)\left[D_l(k)+i\left(A_l(k)+\frac{1}{2k}\right)\right]P_l(\cos\theta) \\ &= \frac{1}{2ik}\sum_{l=0}^{\infty}(2l+1)\left[e^{2i\eta_l}(-1)^l\frac{f_l(-k, r_0)}{f_l(+k, r_0)}-1\right]P_l(\cos\theta). \end{aligned} \tag{11}$$

These are

† Eq. (8) would hold even if the factor $q_l(kr_0)/q_l^*(kr_0)$ were replaced by one. The choice of a slightly more complicated form is suggested by physical reasons.

$$\begin{cases} \mathrm{Re}\, F(k,\,\theta) = \dfrac{2}{\pi}\mathrm{P}\displaystyle\int_0^\infty \frac{\mathrm{Im}\, F(k',\,\theta)k'\,\mathrm{d}k'}{k'^2-k^2}, \\ \mathrm{Im}\, F(k,\,\theta) = \dfrac{2}{\pi}\mathrm{P}\displaystyle\int_0^\infty \frac{\mathrm{Re}\, F(k',\,\theta)k\,\mathrm{d}k'}{k^2-k'^2}. \end{cases} \tag{12}$$

In order to clarify the physical meaning of $F(\theta)$, it is convenient to write

$$F(\theta) = \frac{1}{2ik}\sum_{l=0}^{\infty}(2l+1)\left[(-1)^l\frac{f_l(-k,\,r_0)}{f_l(+k,\,r_0)}(\mathrm{e}^{2i\eta_l}-1) + \left((-1)^l\frac{f_l(-k,\,r_0)}{f_l(+k,\,r_0)}-1\right)\right]P_l\,(\cos\theta). \tag{13}$$

The scattering amplitude originating from the first term in the square bracket can be interpreted as an "internal" scattering amplitude, while the second term is the characteristic amplitude for scattering by a "hard sphere" of radius r_0 [20]).

More precisely (11) is the scattering amplitude as defined by a solution of the Schroedinger equation consisting asymptotically of an outgoing wave and a distorted plane wave. This latter is taken to be a solution of the Schroedinger equation for a hard sphere potential of range r_0, which at large distance is the superposition of an ordinary plane wave and an ingoing wave.

In order to see this we consider the s-scattering term only. If $\exp(-ikr)-\exp(2i\eta)\exp(ikr)$ $(r \geqq r_0)$ is a solution of a certain Schroedinger equation vanishing at the origin, multiplying by $-\exp(2ikr_0)$ we obtain a solution also having this property. Rearranging terms we get

$$[2i\sin kr - (\mathrm{e}^{2ikr_0}-1)\,\mathrm{e}^{-ikr}]+[(\mathrm{e}^{2i(\eta+kr_0)}-1)\mathrm{e}^{ikr}],$$

where the first square bracket is the distorted incident wave (it vanishes at the surface of the hard sphere) and the second square bracket the scattered wave (i.e. the $l=0$ term of $F(\theta)\exp(ikr)$).

The optical theorem quoted in the introduction could be written for the imaginary part of the forward scattering amplitude $F(0)$, so that

$$\mathrm{Im}\, F(0) = \frac{k}{4\pi}\int |F(\theta)|^2\,\mathrm{d}\Omega. \tag{14}$$

This is merely an identity arising from the orthogonality of the Legendre polynomials and from the fact that $f_l(-k, r_0)/f_l(+k, r_0)$ is a complex quantity of modulus one. However the integral differs

from the total cross section $\sigma = \int |f(\theta)|^2 d\Omega$ (with $f(\theta)$ given by eq. (1) of the Introduction) by a factor which depends on the phase shifts. It therefore appears that the optical theorem can be of real use only if the scattering is formulated in terms of incident plane waves. It does not enhance the value of the non-relativistic dispersion relations, so that in practical applications one should try rather to exploit the fact that they hold for the amplitude in any direction.

5. Causality and Dispersion Relations

We now wish to show how eq. (3.9b), which was the starting point for the derivation of the dispersion relations, could be established from the causality requirements in the time-dependent scattering theory [8]). For brevity's sake we assume that there are no bound states, and confine ourselves to s-scattering.

If the wave function $\varphi(r', t')$ is known at a time t', that at a time t is given by [21])

$$\varphi(r, t) = \int_0^\infty K(r, t;\ r', t')\varphi(r', t')\, dr', \tag{1}$$

where the propagation function $K(r, t; r', t')$ has the following properties:

$$\begin{cases} 1) \quad K(r, t; r', t) = \delta(r-r'), \\ 2) \quad K(r, t; r', t') = 0 \quad \text{for } t < t', \\ 3) \quad \left(i\dfrac{\partial}{\partial t} + \dfrac{\partial^2}{\partial r^2} - V\right) K(r, t; r', t') = 0 \text{ for } t > t'. \end{cases} \tag{2}$$

Thus

$$\left(i\frac{\partial}{\partial t} + \frac{\partial^2}{\partial r^2} - V\right) K(r, t; r', t') = i\delta(r-r')\delta(t-t'). \tag{3}$$

Since there are no bound states, the function K is explicitly given by

$$K(r, t; r', t') = \frac{1}{2\pi}\eta(t-t') \int_0^\infty \varphi_k(r)\, \varphi_k^*(r') e^{-iE_k(t-t')}\, dk, \tag{4}$$

where $\eta(t) = (1, t > 0; 0, t < 0)$ and the functions $\varphi_k(r)$ are defined as in subsect. 3.2. We then have for $t > t'$ and $(r, r') > r_0$

$$K(r, t; r', t') = \frac{1}{2\pi}\int_{-\infty}^\infty [e^{-ik(r-r')} - S(k)\, e^{ik(r+r')}] e^{-iE_k(t-t')}\, dk. \tag{5}$$

In the absence of scattering ($V = 0$) $\varphi_k(r) = \exp(-ikr) - \exp(ikr)$ and the propagation function for $t > t'$ is

$$K_0(r, t; r', t') = \frac{1}{2\pi}\int_{-\infty}^{\infty} [e^{-ik(r-r')} - e^{ik(r+r')}]\, e^{-iE_k(t-t')}\, dk. \quad (6)$$

Assume now that for $t < 0$ the incident wave packet $\varphi_i(r, t)$ has not yet reached the scatterer. Our causality requirement is that there must not be any scattered wave until the impinging wave has reached the scatterer. Thus, for $t < 0$, $\varphi(r, t) \equiv \varphi_i(r, t)$ and therefore

$$\varphi(r,t) = \varphi_i(r,t) + \varphi_s(r,t) = \int_0^{\infty} K(r,t;r',t')\varphi_i(r',t')\,dr' \quad (t' < t < 0). \quad (7)$$

On the other hand,

$$\varphi_i(r, t) = \int_0^{\infty} K_0(r, t; r', t')\varphi_i(r', t')\, dr'. \quad (8)$$

Subtracting (8) from (7) we obtain $(t' < t < 0)$

$$\begin{aligned} \varphi_s(r, t) &= \int_0^{\infty} [K(r, t; r', t') - K_0(r, t; r', t')]\varphi_i(r', t')\, dr' \\ &= \frac{1}{2\pi}\int_0^{\infty} dr' \left[\int_{-\infty}^{\infty} (1 - S(k))\, e^{ik(r+r')}\, e^{-iE_k(t-t')}\, dk\right] \varphi_i(r', t'), \end{aligned} \quad (9)$$

and making use once more of the requirement that the scattered wave $\varphi_s(r, t)$ must vanish for $r > r_0$ and $t' < t < 0$ we infer from (9) that

$$\int_{-\infty}^{\infty} (1 - S(k))\, e^{ik(r+r_0)}\, e^{-iE_k t}\, dk = 0 \quad (t > 0,\ r > r_0). \quad (10)$$

Employing the properties of the S-matrix, the complex conjugate of this equation can be written

$$\int_{-\infty}^{\infty} (1 - S(k))\, e^{ik(r+r_0)}\, e^{iE_k t}\, dk = 0 \quad (t > 0,\ r > r_0). \quad (10')$$

We conclude therefore that the convergence of the integrals (10) and (10′) cannot be due to the time exponential, so that (10) holds also for $t = 0$,

$$\int_{-\infty}^{\infty} (1 - S(k))\, e^{ik(r+r_0)}\, dk = 0 \quad (r > r_0). \quad (11)$$

This coincides with (3.8) if there are no bound states, and it would not be difficult to carry out the same argument if allowance were made for these.

We might mention at this point that van Kampen [9]) has criticized this way of postulating the causality requirements, which is due to Schutzer and Tiomno [8]). He remarks that a wave packet which vanishes rigorously outside a certain region at all times $t < 0$, say, cannot be constructed in non-relativistic wave mechanics on account of the positive value of the energy. By postulating that "if the ingoing wave packet is so normalized as to represent at $t = -\infty$ one incident particle, the total probability at $t = t_1$ of finding a particle outside of any sphere of radius $r_1 \geqq r_0$ cannot be greater than 1", van Kampen reaches the same conclusions as described here and in the previous sections, including the "elementary" dispersion relations.

The connection with the general approach of sect. 2 can easily be established. Eq. (11) can be written

$$\int_{-\infty}^{\infty} S(k)\, e^{2ir_0 k}\, e^{-ikz}\, dk = 0 \qquad \text{for } z = r_0 - r < 0, \tag{12}$$

so that $S(k) \exp(2ir_0 k)$ is the Fourier transform of a function of z which vanishes for negative values of its argument. This function, however, is not square integrable, so that Titchmarsh's theorem cannot as yet be invoked. In order to remedy this, by subtracting a zero quantity we first transform (12) into

$$\int_{-\infty}^{\infty} [S(k)e^{2ir_0 k} - S(0)]\, e^{-ikz}\, dk = 0 \qquad \text{for } z = r_0 - r < 0. \tag{12'}$$

As the function $[S(k) \exp(2ir_0 k) - S(0)]/k$ is square integrable, we may now integrate (12') with respect to z from $-\infty$ to $z < 0$ and interchange the order of the k and z integrations, by which we obtain

$$\int_{-\infty}^{\infty} \frac{S(k)e^{2ir_0 k} - S(0)}{k}\, e^{-ikz} dk = 0 \qquad \text{for } z < 0. \tag{13}$$

The general arguments of sect. 2 can now be used. The dispersion relations are given by eqs. (2.9a) and (2.9b), and agree with (3.22) and (3.23') in the absence of bound states.

6. Relativistic Theory of Scattering of Spin Zero Particles by a Short Range Potential [10])†

Our approach to this case will be based exclusively on the causality requirements, and has the purpose of introducing the

† No second quantization!

reader to the more complex collision problems of field theory, the study of which is the ultimate aim.

As the relativistic equation is of the second order in the time, it will not be possible to construct the wave function $\varphi(\mathbf{r}, t)$ from its values at a previous time without knowing also the time derivative. The analogue of eq. (5.1) will be $(t > t')$

$$\varphi(\mathbf{r}, t) = \int_{t''=t'} \left[\varphi(x'') \frac{\partial G(x, x'')}{\partial t''} - \frac{\partial \varphi(x'')}{\partial t''} G(x, x'')\right] \mathrm{d}^3 x''. \quad (1)$$

We denote by $x \equiv (\mathbf{r}, t)$ a space-time point, while $G(x, x')$ is a function which can be constructed from any complete set of eigenfunctions of the relativistic equation for spinless particles in a field of force of short range r_0.

The scattering wave functions

$$U_{\mathbf{k}}(\mathbf{r}) = \mathrm{e}^{i\mathbf{k}\cdot\mathbf{r}} + \sum_{l=0}^{\infty} \frac{(2l+1)}{2kri} (\mathrm{e}^{2i\eta_l} - 1) f_l(-k, r) P_l(\mathbf{k}\cdot\mathbf{r}) \quad (r \geqq r_0) \quad (2)$$

with $f_l(-k, r)$ defined as in sect. 4, form a complete set in the absence of bound states, and can be used to express $G(x, x')$ in the form

$$G(x, x') = \frac{1}{i} \int \frac{\mathrm{d}^3 k}{(2\pi)^3} \cdot \frac{1}{2\omega_k} \{U_{\mathbf{k}}(\mathbf{r}) U^*_{\mathbf{k}}(\mathbf{r}') \mathrm{e}^{-i\omega_k(t-t')} - U_{\mathbf{k}}(\mathbf{r}') U^*_{\mathbf{k}}(\mathbf{r}) \mathrm{e}^{i\omega_k(t-t')}\} \quad (3)$$

$(\omega_k = \sqrt{\mathbf{k}^2 + \mu^2}$, μ = particle mass).

Note that

$$\left[\frac{\partial G}{\partial t}\right]_{t=t'} = -\delta(\mathbf{r} - \mathbf{r}'). \quad (4)$$

For comparison with the case of field theory, we remark also that G is essentially the vacuum expectation value of the commutator $[\varphi(x), \varphi(x')]$ when only one-particle states are considered. This can be seen by writing

$$G(x, x') = -i \langle 0|[\varphi(x), \varphi(x')]|0\rangle \quad (5)$$

and

$$\langle 0|\varphi(x)|\mathbf{k}\rangle = \frac{1}{\sqrt{2\omega_k}} U_{\mathbf{k}}(\mathbf{r}) \mathrm{e}^{-i\omega_k t}. \quad (6)$$

The requirements of causality will be formulated by stating that

$$G(x, x') = 0 \quad \text{for} \quad (x - x')^2 > 0, \quad (7)$$

i.e. if x and x' lie outside each other's light cone. Thus signals cannot propagate with a speed greater than the speed of light.

Inserting (2) into (3), and denoting by $T = t-t'$ the time difference of the world points x and x', whose space components are the vectors $\mathbf{r}$ and $\mathbf{r}'$ assumed to be of equal length, we obtain

$$G(\mathbf{r}, \mathbf{r}', T) = \Delta(x-x')$$
$$-\frac{1}{(2\pi r)^2}\int_{-\infty}^{\infty}\frac{k\mathrm{d}k}{2\omega_k}\left[\sum_{l=0}^{\infty}\frac{(2l+1)}{2ik}(-1)^l(\mathrm{e}^{2i\eta_l}-1)q_l^2\left(\frac{kR}{2}\right)P_l(\mathbf{r}\cdot\mathbf{r}')\right]$$
$$\mathrm{e}^{ikR}\,(\mathrm{e}^{-i\omega_k T}-\mathrm{e}^{-i\omega_k T}). \quad (8)$$

In this formula $|\mathbf{r}| = |\mathbf{r}'| = r > r_0$, $R = 2r$, and $\Delta(x)$ is the well known singular function for free spinless particles.

The causality condition (7) is greatly simplified if $\mathbf{r} = -\mathbf{r}'$, and reads simply

$$G(x, x') = 0 \quad \text{for} \quad R > T. \quad (7')$$

As $\Delta(x-x')$ is already known to satisfy this condition, the second term on the right hand side of (8) must also vanish. Making use of $P_l(\mathbf{r}\cdot\mathbf{r}') = (-1)^l$ for $\mathbf{r}' = -\mathbf{r}$, we therefore have

$$\int_{-\infty}^{+\infty}\frac{k\mathrm{d}k}{2\omega_k}\left[\frac{1}{2ik}\sum_{l=0}^{\infty}(2l+1)(\mathrm{e}^{2i\eta_l}-1)q_l^2\left(\frac{kR}{2}\right)\right]\mathrm{e}^{ikR}(\mathrm{e}^{-i\omega_k T}-\mathrm{e}^{i\omega_k T})=0$$
$$\text{for } R > T \text{ and } R \geqq 2r_0. \quad (9)$$

Proceeding as in sect. 4, we now first notice that (9) will hold also when $q_l(kR/2)$ is replaced by one, which is the leading term of its expansion in powers of $1/R$. (In the following we assume that R is very large). One quick way of getting at the final result consists in remarking that the above integral can be written

$$\int_c \frac{k\mathrm{d}k}{\sqrt{k^2+\mu^2}}\left[\frac{1}{2ik}\sum_{l=0}^{\infty}(2l+1)(\mathrm{e}^{2i\eta_l}-1)\right]\mathrm{e}^{ikR}\;\mathrm{e}^{-i\sqrt{k^2+\mu^2}\,T} = 0$$
$$(R > T \text{ and } R \geqq 2r_0) \quad (10)$$

where $c = c_+ + c_-$, and c_+ and c_- are the real axes for the two Riemann surfaces corresponding to the two branches of $\sqrt{k^2+\mu^2}$. It is also convenient to differentiate (10) with respect to T and integrate with respect to the variable $z = T-R$ from $-\infty$ to a value $z < 0$ as in sect. 5. This yields

$$\int_c\left[\frac{1}{2ik}\sum_{l=0}^{\infty}(2l+1)(\mathrm{e}^{2i\eta_s}-1)\right]\mathrm{e}^{-i(\sqrt{k^2+\mu^2}-k)T}\,\mathrm{e}^{-ikz}\mathrm{d}k=0 \quad (z<0). \quad (11)$$

It is then easy to see that the negative branch gives, in the

limit of large R, a vanishing contributions as compared with the positive branch, so that eq. (11) will still be true if c is replaced by c_+. Moreover, the equation must hold also if we write $T = 0$, as the first exponential cannot be responsible for the convergence of the integral. In fact, the difference $(\sqrt{k^2+\mu^2}-k)$ tends to zero for $k \to \pm\infty$ on c_+. Thus finally we get

$$\int_{-\infty}^{\infty} \frac{1}{2ik} \sum_{l=0}^{\infty} (2l+1)(e^{2i\eta_l}-1)e^{-ik}\, dk = 0 \qquad (z<0) \qquad (12)$$

from which the dispersion relations readily follow, if the square integrability of the integrand is also taken into account.

Eq. (11) has a very simple connection with the non-relativistic eq. (5.13). This latter results from replacing $\sqrt{k^2+\mu^2}$ by $\mu+E_k$, where E_k is the non-relativistic kinetic energy. This gives an integral with the factors $e^{-iE_kT}e^{2ikr_0}e^{-ikz}$, which vanishes for

$$z = 2r_0 - R < 0.$$

This review contains part of the material covered in a series of lectures delivered by the author in the Theoretical Physics Seminar at Glasgow University. To Prof. J. G. Gunn and Dr. R. G. Moorhouse, who assigned him this task, and to other theorists, he is indebted for interest and encouragement.

References

1) R. Kronig, J. Opt. Soc. America **12** (1926) 547
2) H. A. Kramers, Atti Congresso Internazionale dei Fisici, Como **2** (1927) 545
3) B. Gross, Phys. Rev. **59** (1941) 748
4) H. W. Bode, Network Analysis and Feedback Amplifier Design (D. van Nostrand and Co., New York, 1945)
5) J. M. Jauch and F. Rohrlich, Electrons and Photons (Addison Wesley, 1955). Here and elsewhere J. S. Toll's Princeton thesis is frequently quoted.
6) Cf., e.g., M. Lax, Phys. Rev. **78** (1950) 306
7) R. Kronig, Physica **12** (1946) 543
8) W. Schutzer and J. Tiomno, Phys. Rev. **83** (1951) 249
9) N. G. van Kampen, Phys. Rev. **89** (1953) 1072 and **91** (1953) 1267
10) M. Gell-Mann, M. L. Goldberger and W. E. Thirring, Phys. Rev. **95** (1954) 1612
11) R. Karplus and M. Ruderman, Phys. Rev. **98** (1955) 771
12) M. L. Goldberger, Phys. Rev. **97** (1955) 508
13) M. L. Goldberger, Phys. Rev. **99** (1955) 979
14) M. L. Goldberger, H. Miyazawa and R. Oehme, Phys. Rev. **99** (1955) 986
15) E. C. Titchmarsh, Fourier Integrals (Oxford University Press, 1937) p. 119
16) C. Møller, Dan. Mat. fys. Medd. **23** (1945) No. 1

17) W. Heisenberg, Zeits. f. Physik **120** (1943) 513 and 673
18) N. Hu, Phys. Rev. **74** (1948) 131
19) V. Bargmann, Proc. Nat. Acad. of Sciences **38** (1952) 961
20) J. M. Blatt and V. F. Weisskopf, Theoretical Nuclear Physics, (J. Wiley and Sons, 1952) p. 328
21) R. P. Feynman, Phys. Rev. **76** (1949) 749

Nuclear Physics **2** (1956/57) 441—449; *North-Holland Publishing Co., Amsterdam*

SHELL EFFECTS IN NUCLEAR COULOMB ENERGY DIFFERENCES

O. KOFOED-HANSEN

Institute for Theoretical Physics, University of Copenhagen †

Received 23 April 1956

Abstract: In the present discussion, the classical formula for nuclear Coulomb energies eq. (3) is abandoned and the Coulomb energies are instead calculated, using simple nuclear models. In agreement with empirical findings, the calculated curves show definite effects of nuclear shell structure. The evaluation of the nuclear radius (defined as $R = [5/3\langle r^2\rangle_{Av}]^{1/2}$) from the data shows that for medium heavy nuclei ($20 < A < 40$) $R = r_0 A^{1/3} = 1.24 A^{1/3}$, whereas for the very light nuclei r_0 becomes somewhat larger.

The increasing accuracy in the experimentally determined energy differences between analogous states of an isobaric spin multiplet makes it possible to observe effects from nuclear shell structures in the differences. The experimental data from recent compilations [1]) of β-decay energies of mirror nuclei and $A = 4n+2$, $0 \to 0$ transitions and of relevant nuclear level schemes are given in table I. In order to obtain the corresponding Coulomb energies, one may use the formula

$$E_c = (E^{max} + 1.804)\ \text{MeV} \tag{1}$$

for β^+ transitions and the formula

$$E_c = (E^{max} - 0.782)\ \text{MeV} \tag{2}$$

for β^- transitions. In this manner, the E_c values given in table I are obtained.

It is customary to use the Coulomb energy differences for an evaluation of the nuclear radius for light nuclei [2]). Using the very simple picture of the nucleus as a homogeneously electrically charged sphere of total charge Ze, we find the Coulomb energy difference from the well known formula

$$\begin{aligned} E_c(Z+1, Z) &= 0.6\,\frac{(2Z+1)}{R}\,e^2 - E_c\,(1, 0) \\ &= 0.6\,\frac{(2Z+1)e^2}{r_0 A^{1/3}} - E_c(1, 0) = \frac{Z^1}{A^{1/3}}\left(1.2\,\frac{e^2}{r_0}\right) - E_c(1, 0) \end{aligned} \tag{3}$$

† Now with the Danish Atomic Energy Commission, Copenhagen.

where Z^1 is the average charge of the partners of the isobaric pair. Consequently, in order to find r_0, one usually plots the Coulomb energy differences as a function of $Z^1/A^{1/3}$ and expects a straight

TABLE I

Coulomb Energy Differences.

Transitions	A	Z^1	Decay	Energy MeV	E_c MeV
n → p	1	0.5	−	0.782	0.000
H → He	3	1.5	−	0.018	0.764±0.001
He → Li	6	2.5	−	3.55	0.80 ±0.05
Li($T=1 \rightarrow T=0$)				3.572	
Be → Li	7	3.5	K	0.864	1.646±0.002
Be → B	10	4.5	−	0.556	1.965±0.006
B($T=1 \rightarrow T=0$)				1.739	
B → C	10	5.5	(p, n)	−4.42	2.68 ±0.06
B($T=1 \rightarrow T=0$)				1.739	
C → B	11	5.5	+	0.959	2.763±0.003
N → C	13	6.5	+	1.202	3.006±0.005
C → N	14	6.5	−	0.155	2.940±0.005
N($T=1 \rightarrow T=0$)				2.313	
O → N	14	7.5	+	1.835	3.639±0.008
O → N	15	7.5	+	1.735	3.539±0.006
F → O	17	8.5	+	1.746	3.550±0.006
F → O	18		+	0.644	
Ne → F	18	9	+	3.2	3.72 ±0.10
Ne → F	19	9.5	+	2.223	4.027±0.008
Na → Ne	21	10.5	+	2.50	4.30 ±0.03
Na → Ne*			+	0.540	
Ne* → Ne	22	10.5		1.277	4.214±0.006
Na($T=1 \rightarrow T=0$)				0.593	
Mg → Na	23	11.5	+	3.037	4.841±0.010
Al → Mg	25	12.5	+	3.280	5.084±0.025
Al → Mg	26	12.5	+	3.202	5.006±0.008
Si → Al	27	13.5	+	3.780	5.584±0.010
P → Si	29	14.5	+	3.945	5.749±0.010
S → P	31	15.5	+	4.42	6.22 ±0.06
Cl → S	33	16.5	+	4.2	6.0 ±0.2
Cl → S	34	16.5	+	4.50	6.30 ±0.03
A → Cl	35	17.5	+	4.95	6.75 ±0.04
K → A	38	18.5	+	5.06	6.86 ±0.11
Ca → K	39	19.5	+	5.58	7.38 ±0.08
Sc → Ca	41	20.5	+	4.94	6.74 ±0.05
V → Ti	46	22.5	+	6	7.8 ±1.0
Mn → Cr	50	24.5	+	6.3	8.1 ±0.3
Co → Fe	54	26.5	+	7.4	9.2 ±0.3

line cutting the abscissa in the point $Z^1/A^{1/3} = 0.5$, corresponding to the neutron-proton Coulomb energy difference zero as chosen by the definitions (1) and (2).

This plot was constructed using the data given in table I. The result is shown in fig. 1. From this diagram it is apparent that a better fit to the experimental points is obtained by drawing the individual lines than by using one common line. Furthermore, it is

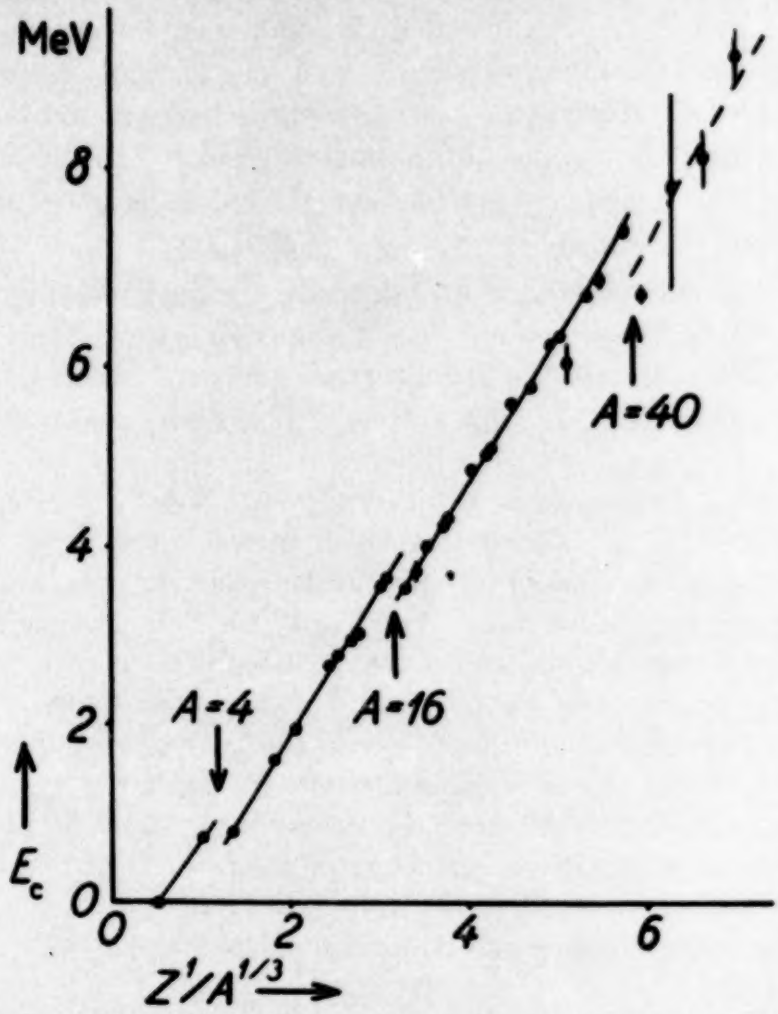

Fig. 1. Empirical Coulomb energy differences as a function of $Z^1/A^{1/3}$.

seen that each line contains all data from nuclei between successive double closed shells. Thus, it is seen that the precision with which Coulomb energy differences are now known permits the observation of closed shell effects in the sequence of these energies.

As a consequence of this effect it is natural to return to the question of the nuclear radius determination from Coulomb energy differences. It is evident that eq. (3) represents a too crude approximation and it is desirable to apply a formula that will reproduce the shell model features.

In the following, two rather extreme models have been used, viz. the infinite square well potential and the harmonic oscillator potential. Similar calculations have been performed by several authors. Jancovici [3]) calculated the Coulomb energy differences for the mirror pairs of $A = 15$ and 17 using a finite square well. Cooper and Henley [4]) calculated Coulomb energies for closed shell configurations using the infinite well model, and Carlson and Talmi [5]) have studied the pairing energy effects in mirror nuclei Coulomb energies using the harmonic oscillator model together with detailed coupling schemes for the nucleons and they also suggested the possibility of closed shell effects.

Both models to be used here depend on a single parameter only which can be interpreted in terms of some radius connected with the model. For both cases the radius of the equivalent uniform spherical nucleus defined as $R = [5/3\langle r^2\rangle_{\mathrm{Av}}]^{1/2}$ has been used as a parameter.

Since we are interested in the average behaviour of nuclear radii rather than in detailed deviations from the rough average lines drawn in fig. 1, we adopt a simplified method for calculating the Coulomb energy differences. We identify the Coulomb energy of a single proton in the l-th shell as the mean value per proton obtained from calculating the Coulomb energy of the entire closed l-th shell. Explicit expressions for these quantities can be found in textbooks [6]). Furthermore, we consider the filling of the 1s, 2p, and 3d shells only, thus omitting the 2s states for simplicity and not carrying the calculations further than to $A = 36$. Effects of spin orbit forces and Coulomb forces on the wave functions are neglected. For the energy difference of nuclei of $Z = 1$ and 2 we find

$$E_c(1, 2) = F^0\,(10, 10), \tag{4}$$

and for nuclei of $A \leqq 4$

$$R = \left[\tfrac{5}{3}\int r^2\, R_{10}^2\, \mathrm{d}r\right]^{1/2}. \tag{5}$$

For the energy difference of nuclei of $Z = 2+n$ and $3+n$ with $0 \leqq n \leqq 5$ we find

$$\begin{aligned} E_c(2+n, 3+n) = {} & 2\{F^0(10, 21) - \tfrac{1}{6} G^1(10, 21)\} \\ & + n\{F^0(21, 21) - \tfrac{2}{25} F^2(21, 21)\} \end{aligned} \tag{6}$$

and for nuclei of $4 < A = 4+m \leqq 16$

$$R = \left[\frac{5}{3A}\left(4\int r^2 R_{10}^2\,\mathrm{d}r + m\int r^2 R_{21}^2\,\mathrm{d}r\right)\right]^{1/2}. \tag{7}$$

Finally, for the energy differences of nuclei of $Z = 8+\nu$ and $9+\nu$ with $0 \leqq \nu \leqq 9$, we obtain

$$\begin{aligned} E_c(8+\nu, 9+\nu) &= 2\{F^0(10,32) - \tfrac{1}{10}G^2(10,32)\} \\ &+ 6\{F^0(21,32) - \tfrac{2}{15}G^1(21,32) - \tfrac{3}{70}G^3(21,32)\} \\ &+ \nu\{F^0(32,32) - \tfrac{2}{63}F^2(32,32) - \tfrac{1}{124}F^4(32,32)\} \end{aligned} \tag{8}$$

and for $16 < A = 16+\mu \leqq 36$

$$R = \left[\frac{5}{3A}\left(4\int r^2 R_{10}^2\,\mathrm{d}r + 12\int r^2 R_{21}^2\,\mathrm{d}r + \mu\int r^2 R_{31}^2\,\mathrm{d}r\right)\right]^{1/2}. \tag{9}$$

In eqs. (4), (6) and (8) the direct integrals F^k are given by

$$\begin{aligned} F^k(nl, n'l') &= e^2\int_0^\infty \frac{1}{r_2^{k+1}} R_{nl}^2(r_2)\int_0^{r_2} r_1^k R_{n'l'}^2(r_1)\mathrm{d}r_1\,\mathrm{d}r_2 \\ &+ e^2\int_0^\infty \frac{1}{r_2^{k+1}} R_{n'l'}^2(r_2)\int_0^{r_2} r_1^k R_{nl}^2(r_1)\,\mathrm{d}r_1\,\mathrm{d}r_2 \end{aligned} \tag{10}$$

and the exchange integrals are given by

$$\begin{aligned} &G^k(nl, n'l') \\ &= 2e^2\int_0^\infty \frac{1}{r_2^{k+1}} R_{nl}(r_2)R_{n'l'}(r_2)\int_0^{r_2} r_1^k R_{nl}(r_1)R_{n'l'}(r_1)\,\mathrm{d}r_1\,\mathrm{d}r_2 \end{aligned} \tag{11}$$

where R_{nl} is the normalized solution of the radial equation, i.e. r times the normalized radial wave function.

In both models, the calculation is straightforward but tedious. For the square well all Coulomb integrals are proportional to e^2/ϱ where ϱ is the radius of the well and all R-integrals are proportional to ϱ. Putting $R = r_0 A^{1/3}$ it is natural to express E_c in units of e^2/r_0. The results from this procedure for mirror transitions are shown in fig. 2 as a function of $Z^1/A^{1/3}$.

For the harmonic oscillator the Coulomb integrals are proportional to $\beta^{\frac{1}{2}}$, where $\beta = M\omega/h$; $\omega/2\pi$ is the classical frequency of the oscillator and all R-integrals are proportional to $\beta^{-\frac{1}{2}}$. Thus putting $R = r_0 A^{1/3}$ we can plot the energies in units e^2/r_0 as a function of $Z^1/A^{1/3}$ for mirror transitions. This is done in fig. 3.

It is evident that the empirical feature of fig. 1 is reproduced qualitatively both in fig. 2 and fig. 3. The calculated curves are

not exactly straight lines, but the deviation from a straight line is so small that it cannot be seen in the plots in figs. 2 and 3. The breaks at magic numbers reappear. For other than mirror nuclei

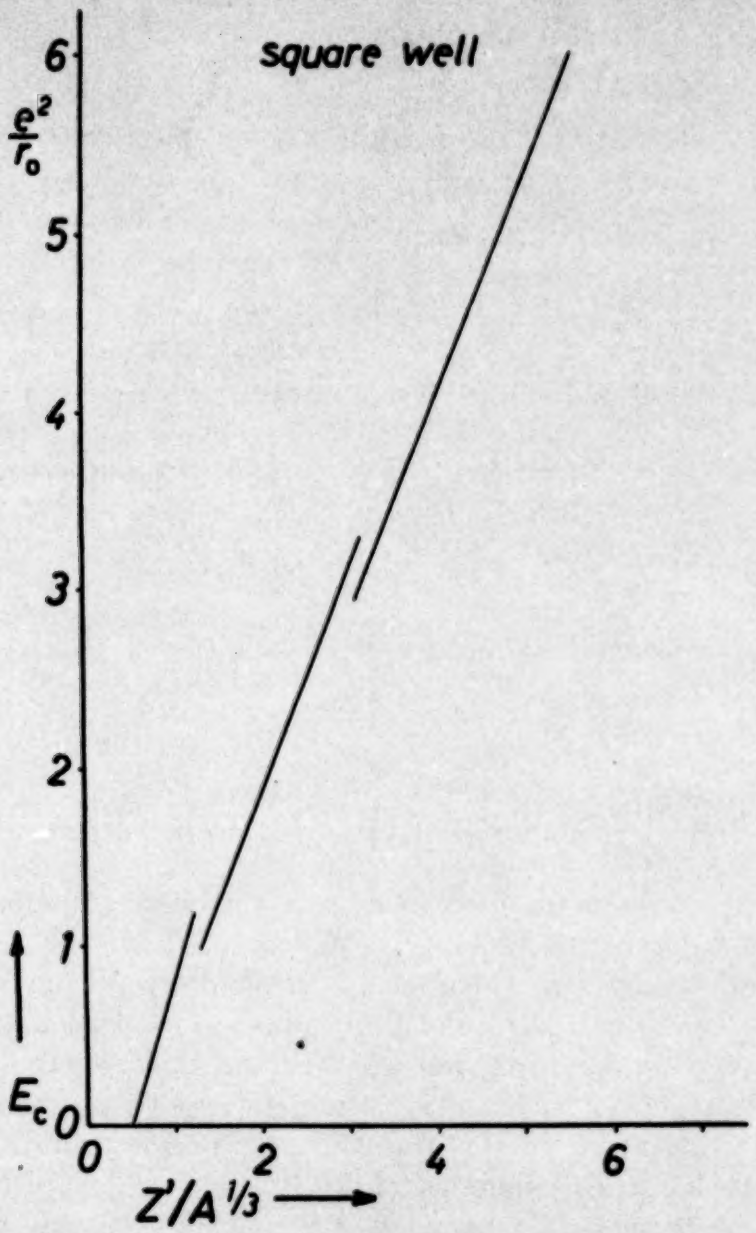

Fig. 2. Calculated Coulomb energy differences for the infinite square well potential in units e^2/r_0 as a function of $Z^1/A^{1/3}$.

the proper point in the diagram lies on the correct $Z^1/A^{1/3}$ abscissa and on a line through the point on the mirror nucleus line for $Z = Z^1$ and the point (0, 0). Since only small changes in $Z^1/A^{1/3}$ occur when we go to the $4n+2$ nuclei, and since the latter line lies

close to the Coulomb energy lines, no significant effect occurs and we are justified in including the $4n+2$ nuclei in fig. 1.

Values for r_0 were now determined from each point on fig. 1

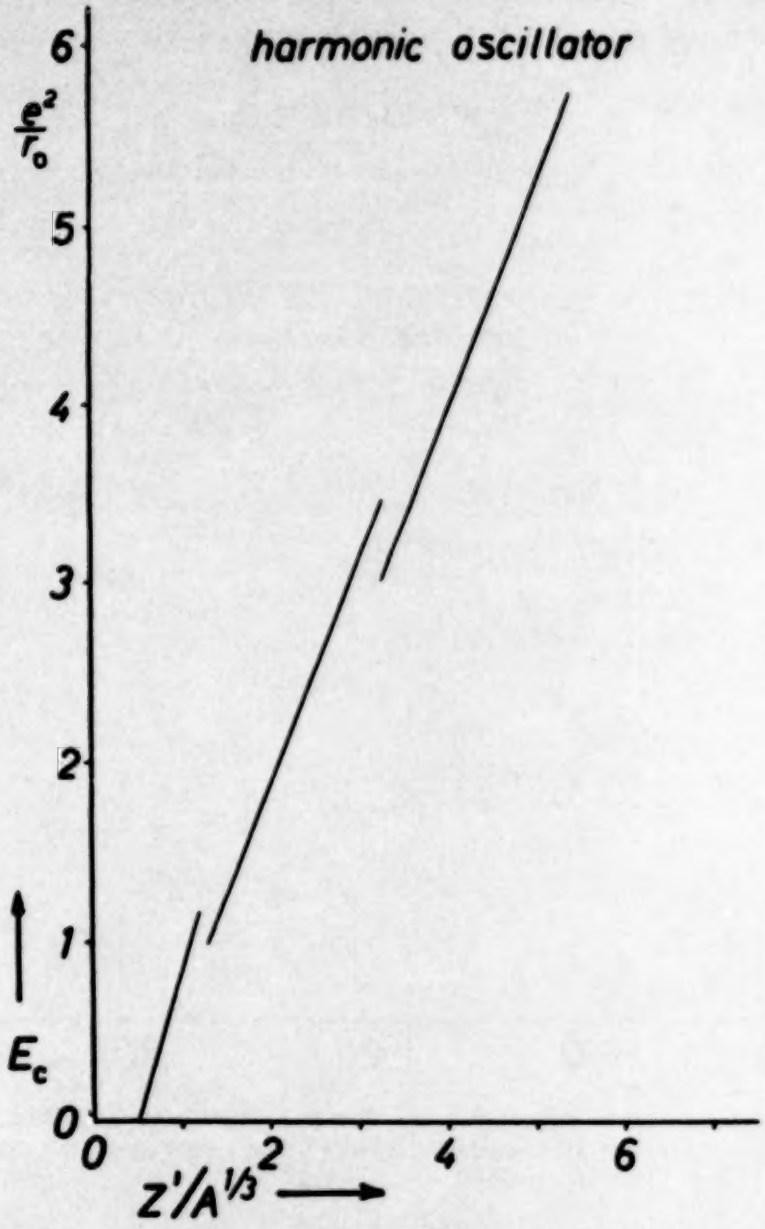

Fig. 3. Calculated Coulomb energy differences for the harmonic oscillator potential in units e^2/r_0 as a function of $Z^1/A^{1/3}$.

and the calculated integrals. The results for r_0 are shown in fig. 4 as a function of A. For the very light nuclei there is no reason to believe that the radius should vary smoothly with A. The point very much off the average lines is due to the He^6—Li^6 Coulomb

energy difference. For the heavier nuclei the behaviour of r_0 is quite smooth but not entirely constant with A. It is seen that the value of r_0 is relatively insensitive to the model used and also the calculations on the finite well [3]) fit into the curve using the new experimental data. For the heavier nuclei the r_0 values tend towards

$$r_0 = 1.24 \times 10^{-13} \text{ cm}$$

where we have taken an average value between the two determinations in fig. 4.

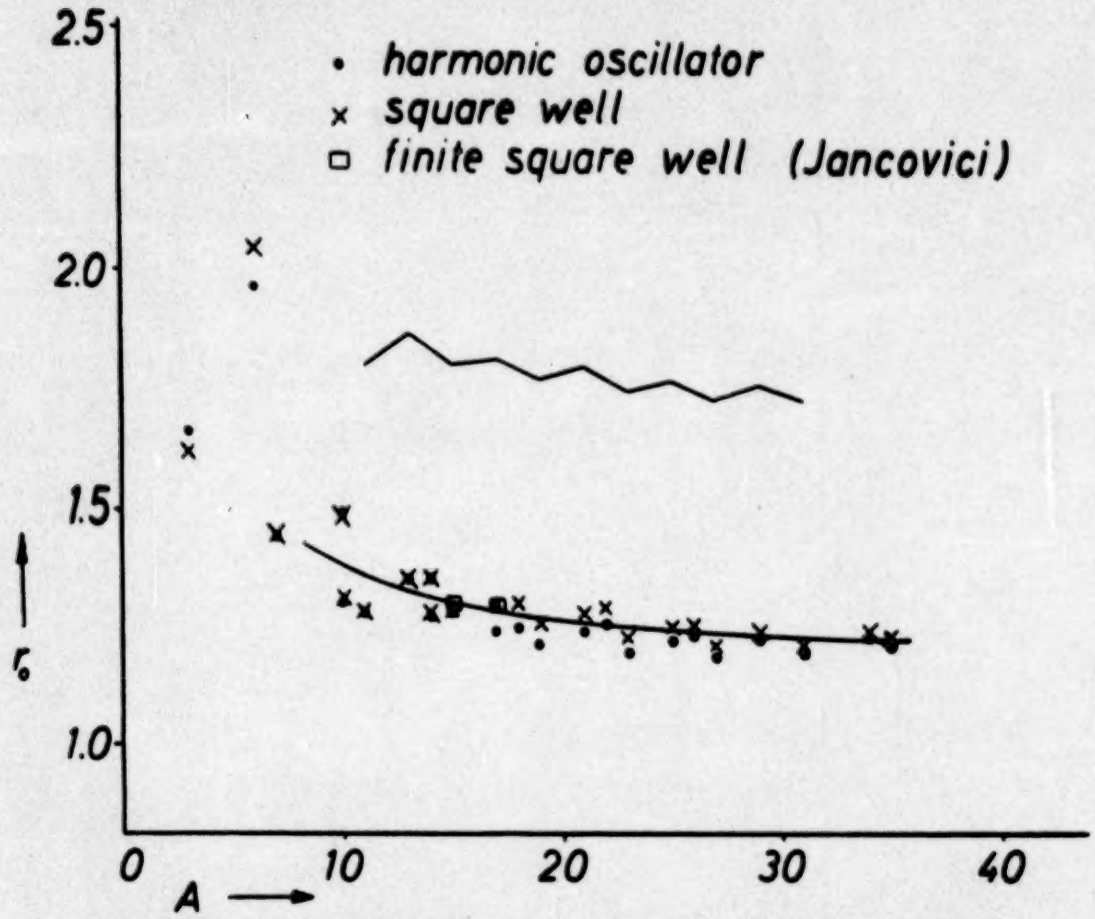

Fig. 4. Nuclear radius constant r_0 as a function of A. Also the values obtained from the finite well [3]) are included using the present definitions of radii and the present experimental data.

It should be noted that the determination of ϱ (the well radius) is not very important since its determination is directly connected with the unrealistic model of an infinite well. For a finite well ϱ becomes significantly smaller [3]) and it has been shown by Rotenberg [7]) that the well shape for the self-consistent field is approximately equal to the shape of the density distribution. However,

since the r_0 values are relatively insensitive to the model applied, they may be compared with other radius determinations like those obtained from μ-mesic atoms ($r_0 = 1.20$ for $A = 50$) [8]) and electron scattering ($r_0^S = 1.30$ for $A = 50$) [9]).

Thus, the light nuclei Coulomb energy differences give radii in reasonably good agreement with other radius determinations.

References

1) O. Kofoed-Hansen, Handbuch der Physik, vol. 42 (in the press)
F. Ajzenberg and T. Lauritsen, Rev. Mod. Phys. **27** (1955) 77
P. M. Endt and J. C. Kluyver, Rev. Mod. Phys. **26** (1954) 95
2) H. A. Bethe, Phys. Rev. **54** (1938) 436
E. P. Wigner, Phys. Rev. **56** (1939) 519
White, Creutz, Delsasso, and Wilson, Phys. Rev. **59** (1941) 63
E. Feenberg and G. Goertzel, Phys. Rev. **70** (1946) 597
R. R. Wilson, Phys. Rev. **88** (1952) 350
D. C. Peaslee, Phys. Rev. **95** (1954) 717
3) B. G. Jancovici, Phys. Rev. **95** (1954) 389
4) L. N. Cooper and E. M. Henley, Phys. Rev. **92** (1953) 801
5) B. C. Carlson and I. Talmi, Phys. Rev. **96** (1954) 436
6) E. U. Condon and G. H. Shortley, The Theory of Atomic Spectra (Cambridge 1935) p. 177 ff
7) M. Rotenberg, M.I.T. Technical Report (1955) No. 6
8) V. L. Fitch and J. Rainwater, Phys. Rev. **92** (1953) 789
9) Hahn, Revenhall and Hofstadter, Phys. Rev. **101** (1956) 1131; see also A. R. Bodmer, Proc. Phys. Soc. A **66** (1953) 1041

Nuclear Physics **2** (1956/57) 450—453; *North-Holland Publishing Co., Amsterdam*

REMARKS ON THE CHARGE DISTRIBUTION IN NUCLEI

L. ROSENFELD

Dept. of Theoretical Physics, University of Manchester

Received 21 July 1956

The renewed discussion of the evidence from mirror nuclei on the nuclear charge distribution presented in the preceding paper by Dr. Kofoed-Hansen [1]) leads to interesting conclusions. Previous attempts to analyse this evidence in terms of a uniform charge distribution of radius $R = r_0 A^{1/3}$ had led to an estimate of the parameter r_0 considerably higher than that derived from the first measurements on the scattering of fast electrons by heavy nuclei. (The latter experiments yield in fact, if the nuclear density distribution is $\varrho(r)$, in the first instance [2]) the quantity $\int \varrho(r) r^2 \mathrm{d}V$, from which one obtains the radius of the equivalent uniform distribution as defined in Kofoed-Hansen's paper.) The existence of this discrepancy was pointed out in my report at the Copenhagen Conference in 1952 and it was suggested that such a difference, if real, would indicate that the density of nuclei is not strictly constant but increases with the number of constituent nucleons.†

At the time, however it was not known how sensitively the Coulomb energy differences of mirror nuclei might depend on the details of the nuclear model assumed in their estimation. From subsequent calculations by Cooper and Henley [3]), Carlson and Talmi [4]) and Jancovici [5]) it appeared that the values of r_0 were insensitive to the model and, apart from fluctuations reflecting shell structure, remained on the whole appreciably higher than that derived for heavier nuclei from electron scattering data.††

The situation in this respect is now completely elucidated by Dr. Kofoed-Hansen's analysis. He shows how by taking account

† The proceedings of the Copenhagen Conference were not published, but attention was brought to this point in A. R. Bodmer's paper [2]) of 1953.

†† There were apparent discrepancies between some results of Cooper and Henley and those of Jancovici, but according to what the latter told me, these were only due to numerical slips in the former authors' calculations and could be removed by a check of those calculations.

more carefully of the shell structure effects the latest data lead to a determination of the r_0 value for each pair of isobars which is practically independent of the model used. Besides, a very interesting feature appears: the parameter r_0 is not constant but shows a definite decrease as the nucleon number increases.

Now, the more recent data from fast electron scattering, extended to light nuclei also, exhibit a quite similar variation of the para-

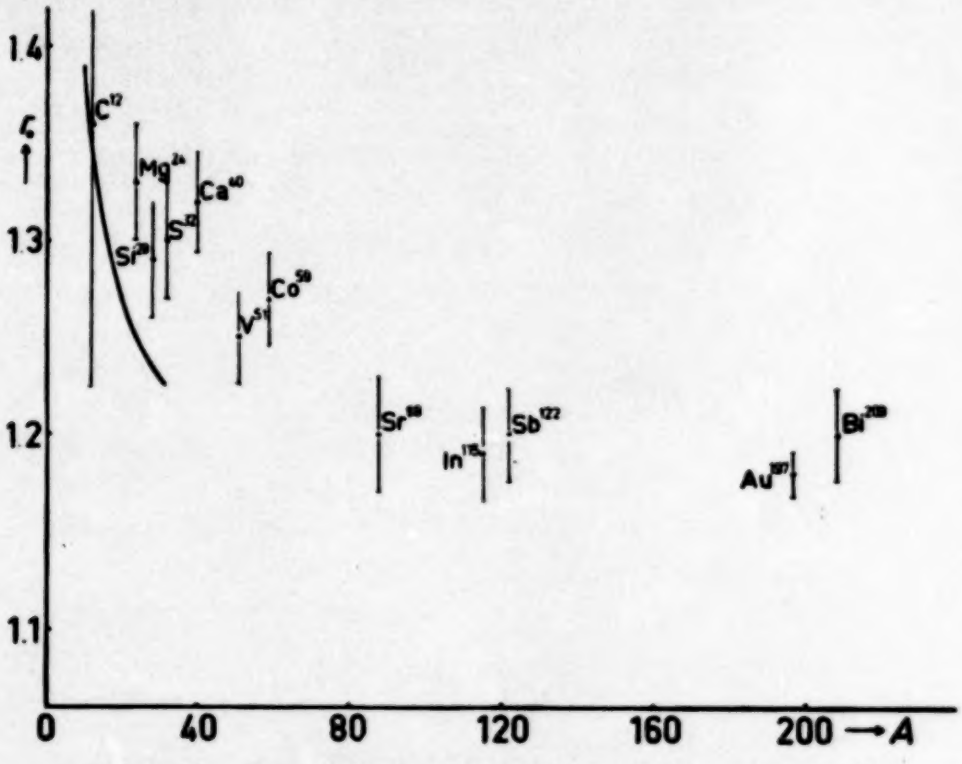

Values of r_0 from electron scattering data and from mirror nuclei. The full-drawn line shows the variation of r_0 derived from mirror nuclei data according to Kofoed-Hansen [1]). References for electron scattering data: C^{12} ref. [10]), Mg^{24}, Si^{28}, S^{32}, Sr^{88} ref. [11]), all others ref. [12]).

meter r_0 with nucleon number. The accompanying figure shows how far the two sets of data are in agreement on this point. It is true that the r_0 values derived from the study of μ-mesic atoms [6]) do not clearly show a similar trend, but within the limits of their accuracy they do not contradict it.

It would seem, therefore, that the apparent discrepancy mentioned above between the evidence from mirror nuclei and electron scattering data has now been eliminated and replaced by a definite statement of the existence of an increase of nuclear density as the number of constituent nucleons increases; this density increase

occurs for light nuclei up to about $A = 70-80$, when the density further stays constant. With a view to a possible interpretation of this behaviour it must be recalled in the first place that the Coulomb interactions and the part of the nuclear interactions depending on the neutron excess are expected to give rise to a decrease of density with increase of the nucleon number; the effect of surface interactions goes in the opposite direction, but would not seem to be sufficient to reverse this trend[7]). The empirical indication of constant density would therefore suggest that the volume interactions have a tendency to increase the density as the number of nucleons increases in contrast with the requirement of strict saturation.

I might use the opportunity to call attention to the analytical treatment of the problem of fast electron scattering by nuclei, initiated by A. R. Bodmer [2]) and completed by G. N. Fowler [8]) and more recently by J. Reignier [9]). This treatment is based on the consideration of a certain parameter determining the phase shifts of the partial waves, and for which an analytical expression can be obtained in terms of an arbitrary, centrally symmetrical charge distribution. It is then possible to assess very simply how far the angular distribution of the scattered electrons may be expected to be sensitive to the density distribution. In this connection J. Reignier has derived a very general "equivalence condition" for two density distributions: he shows that they will give rise to the same angular distribution if they lead to the same value for the quantities

$$\int_0^{r_1} V(r)[J^2_{|k|-\frac{1}{2}}(\varkappa r)+J^2_{|k|+\frac{1}{2}}(\varkappa r)]r\mathrm{d}r$$

referring to the successive partial waves of quantum number $k(k = \pm(j+\frac{1}{2})$ according as $j = l\mp\frac{1}{2})$. In these expressions, $V(r)$ is the Coulomb potential of the charge distribution considered, and $\varkappa$ may be taken to be the wave number of the incoming particles; for the upper limit r_1 one has to take some value for which the two density distributions compared are both negligible. From this condition it results in particular, as already pointed out by Fowler [8]), that at very high energies the angular distribution becomes quite insensitive to the charge distribution. If, therefore, the scattering experiments are used to derive as detailed a picture as possible of the density distribution, the electron energy ought not to be taken too large; according to Fowler's estimate the greatest sensitivity would be obtained with energies of about 70 MeV.

References

1) O. Kofoed-Hansen, Nuclear Physics **2** (1956/57) 441
2) A. Bodmer, Proc. Phys. Soc. A **66** (1953) 1041
3) L. N. Cooper and E. M. Henley, Phys. Rev. **92** (1953) 801
4) B. C. Carlson and I. Talmi, Phys. Rev. **96** (1954) 436
5) B. G. Jancovici, Phys. Rev. **95** (1954) 389
6) V. L. Fitch and J. Rainwater, Phys. Rev. **92** (1953) 789
7) E. Feenberg, Rev. Mod. Phys. **19** (1947) 239
8) G. N. Fowler, Proc. Phys. Soc. A **68** (1955) 559
9) J. Reignier, Bull. Acad. Roy. Belg., Cl. Sc. **41** (1955) 151; **42** (1956) 173
10) J. H. Fregeau and R. Hofstadter, Phys. Rev. **99** (1955) 1503
11) R. H. Helm, HEPL Report No. 40 (1956)
12) B. Hahn, D. G. Ravenhall and R. Hofstadter, Phys. Rev. **101** (1956) 1131

Nuclear Physics **2** (1956/57) 454—475; *North-Holland Publishing Co., Amsterdam*

ANALYSIS OF NUCLEAR QUADRUPOLE MOMENTS ON THE BASIS OF A KINEMATICAL MODEL

R. K. OSBORN AND E. D. KLEMA †

Oak Ridge National Laboratory Oak Ridge, Tennessee

Received 7 July 1956

Abstract: The kinematical model used previously in the correlation of nuclear magnetic moments has been applied to the analysis of nuclear quadrupole moments. The empirical rules found in the previous work are in general confirmed; however, the $d_{3/2}$ nuclei form an exceptional group and are discussed in detail. A possible explanation of the anomalous magnetic moment of W^{183} is given. Shape factors are obtained for a number of odd mass nuclei on the basis of the present model.

1. The Kinematical Model

In a previous paper [1]), referred to as I, it was shown that primarily upon the basis of kinematical considerations the concept of a rotating core plus odd nucleon adequately correlates practically all nuclear magnetic moments. The correlation is essentially expressed in a set of empirical rules which distinguish fundamentally among various core-plus-particle configurations depending upon whether the single particle in question is characterized by $j = l+\frac{1}{2}$ or $j = l-\frac{1}{2}$. The present investigation is an extension of the kinematical model to a consideration of nuclear quadrupole moments and shapes.

The crux of the model, discussed in detail in I, may be briefly summarized. The system (a given nucleus) is to be regarded as being primarily defined by a limited set of dynamical variables and the data-selected components of the state vector they generate. However, for concreteness as well as for the purpose of enabling comparatively straightforward and exact calculations of relevant quantities, a simple physical system is conceived which is compatible with our choice of defining dynamical variables. But it is to be emphasized that the conceptual physical system is itself far less general than the dynamical variables, and hence literal inferences drawn essentially from the nature of the conceptual system must be interpreted with caution. In fact, our intent is precisely the converse; namely, to attempt to determine whether nuclear data taken

† Now at the University of Michigan, Ann Arbor, Michigan.

in conjunction with a relatively simple model can be employed in the determination of the nature of the model itself.

Accordingly, we assume that a given nucleus may be regarded as consisting of a rigid core if A and Z are even; a rigid core plus one nucleon if A is odd; a rigid core plus two nucleons if A is even and Z odd. For reasons discussed in I, nuclei with even A and odd Z will be given no further consideration in the present work; and since we are concerned here with the implications for the model of data on nuclear quadrupole moments, we shall restrict our attention in the following exclusively to odd mass nuclei.

The rigid core is presumed to be characterized by an axially-symmetric spheroidal deformation. The dynamical variables appropriate to such a system of deformed-core-plus-nucleon are:

1) $\mathbf{S}^2$, the square of the intrinsic spin moment of the extra-core nucleon;
2) $\mathbf{L}^2$, the square of the orbital angular momentum of the nucleon;
3) $\mathbf{J}^2 = (\mathbf{L}+\mathbf{S})^2$, the square of the total nucleon angular momentum;
4) $\mathscr{L}^2$, the square of the core angular momentum;
5) $\mathscr{J}^2 = (\mathscr{L}+\mathbf{J})^2$, the square of the total angular momentum of the system;
6) $\mathscr{J}_z$, the projection of the system angular momentum on the z-axis of a space-fixed coordinate system;
7) $\mathscr{L}'_z$, the projection of the core angular momentum on the body symmetry axis (taken to be along the z-axis of a coordinate system fixed in the body);
8) J'_z, the projection of the total nucleon angular momentum along the body-symmetry axis;
9) $\mathscr{J}'_z$, the projection of the total angular momentum of the system along the body-symmetry axis; and
10) Π, the parity of the total system.

Not all of these operators correspond to constants of motion for the system. In fact, the only ones which may be presumed to be constants of the motion are $\mathscr{J}^2$, $\mathscr{J}_z$, $\mathscr{L}'_z$, and Π; the first two because of the invariance of the system as a whole under arbitrary rotations of the space coordinate system; $\mathscr{L}'_z$ because of the invariance of the core configuration under rotations about the body-symmetry axis; and Π because of system reflection symmetry. It should be pointed out perhaps that although J'_z would be a constant

of the motion for a single nucleon moving in a *static* axially symmetric potential [2]), it cannot in general be expected to be so if the well is rotating [3, 4, 5]). In fact, both the hydrodynamical model and the rigid rotator model lead to a kinetic coupling of the particle motion to that of the core of the form $\mathcal{J}' \cdot \mathbf{J}'$ (with which neither $\mathcal{J}'_z$ nor J'_z commutes) if it is assumed that the unconstrained degrees of freedom of the system are those for collective core rotation and single particle motion relative to the body coordinate system. Furthermore, if the particle and core degrees of freedom cannot be regarded as unconstrained, it is probable that it is precisely this kinetic coupling which will be most influenced by the constraints. It is for this reason, as well as for others elucidated in I, that we have chosen to construct our base vectors with which to construct nuclear ground states as follows:

Since the kinematical properties of the system will be independent of whether the particle coordinates are expressed in a body — or space-fixed coordinate system, we choose a representation for the nucleon which diagonalizes $\mathbf{L}^2$, $\mathbf{S}^2$, $\mathbf{J}^2$, and J_z; i.e.,

$$\chi^m_{jl} = \sum_\tau C(\tfrac{1}{2}lj;\ \tau,\ m-\tau)\chi^\tau_{\frac{1}{2}} Y^{m-\tau}_l. \tag{1}$$

To this is adjoined the core representation $D^{\lambda*}_{\mu,K}$, which diagonalizes $\mathcal{L}^2$, $\mathcal{L}_z$, and $\mathcal{L}'_z$ with eigenvalues $\lambda(\lambda+1)$, μ, and K, respectively, to form the base vectors

$$\Psi^M_{I\lambda jl} = \left(\frac{2\lambda+1}{8\pi^2}\right)^{\frac{1}{2}} \sum_m C(j\lambda I;\ m,\ M-m)\,\chi^m_{jl}\, D^{\lambda*}_{M-m,0},\ \lambda \text{ even}. \tag{2}$$

This representation diagonalizes the following operators with corresponding eigenvalues:

$$\mathcal{J}^2 \approx I(I+1) \tag{3a}$$
$$\mathcal{L}^2 \approx \lambda(\lambda+1) \tag{3b}$$
$$\mathbf{J}^2 \approx j(j+1) \tag{3c}$$
$$\mathbf{L}^2 \approx l(l+1) \tag{3d}$$
$$\mathbf{S}^2 \approx 3/4 \tag{3e}$$
$$\mathcal{J}_z \approx M \tag{3f}$$
$$\mathcal{L}'_z \approx 0 \tag{3g}$$
$$\Pi \approx (-1)^l. \tag{3h}$$

A discussion of the significance of the restriction on the representation characterized by (3g) is presented below.

Thus, in general, the ground state of a given nucleus, characterized by the parity of the extra-core nucleon and a specified total angular momentum I, would be

$$\Psi_I^M = \sum_{\lambda j l} a_{\lambda j l} \Psi_{I\lambda j l}^M, \tag{4}$$

all even l's if parity even and all odd l's if parity odd. In accordance with the intent to determine whether nuclear data might delineate some simple regularity in the description of the ground states, and hence provide implications for the model itself, it was assumed that two of the components of the state vector (4) were dominant and that the ground state might be represented by

$$\Psi_I^M = (1-a^2)^{\frac{1}{2}} \Psi_{I\lambda j l}^M + a \Psi_{I\lambda' j' l'}^M. \tag{5}$$

It was found from the analysis of magnetic moment data in I that a simple set of rules might be postulated for the prescription of the quantum numbers appropriate to a given nuclear ground state; i.e.,

1) $I = \frac{1}{2}$ nuclei; the state consists of the components

$$\Psi_{\frac{1}{2}0 j l} \text{ and } \Psi_{\frac{1}{2}2 j' l'}$$

where (jl) are taken from the single-nucleon shell model and $(j'l')$ are nearby single-particle states of the same parity;

2) $I > \frac{1}{2}$ nuclei for which $j = l + \frac{1}{2}$; the components are either

$$\Psi_{I0 j l} \text{ and } \Psi_{I2 j l} \text{ or}$$
$$\Psi_{I2 j l} \text{ and } \Psi_{I4 j l},$$

where again the particle quantum numbers are dictated by the single-nucleon shell model; and

3) $I > \frac{1}{2}$ nuclei for which $j = l - \frac{1}{2}$; the components are

$$\Psi_{I2 j l} \text{ and } \Psi_{I2 j' l'},$$

where $(j'l')$ are nearby proper parity states. In all cases it is presumed that the mixing states lie in the same major shell. It is observed below that the application of rule (3) to $d_{3/2}$ single-particle configurations must be modified.

It is to be noted that the core configuration characterized by $\lambda = 2$ appears to be of predominant importance in the description of nuclear ground states. This predominance is peculiar neither to the rigid rotator model nor to the present choice of representation, but rather appears to be common to collective models in general. For example, if in the strong-coupling limit of the hydrodynamical

model [3]) one assumes that the total angular momentum = the total single-particle angular momentum = the projection of the single-particle angular momentum along the body-symmetry axis in the ground state; then for an $I = 3/2$ nucleus the corresponding core states are $\lambda = 0$ and 2 in equal amounts.

It is clear at the outset that if we are to avoid the question of dynamics, one or more parameters must be introduced in order to characterize the shape of the core. Furthermore, these parameters must be treated empirically. This proliferation of empirical parameters is actually less objectionable than it might seem at first sight, since the results of many quite different types of experiments are expected to depend more or less sensitively upon nuclear shape; for example, quadrupole moments, rotational energy levels, and scattering cross sections.

Here also we shall extend our considerations to light as well as heavy nuclei, in spite of the rapidly growing success of sophisticated applications of the shell model in the region $A \leqq 40$. We feel justified in this extension on the ground that overlapping success or failure of apparently dissimilar points of view can be meaningful in its own right.

Since in the following, nuclear shapes are to be considered only in a most elementary sense, it is both feasible and desirable to introduce easily defined shape parameters and to treat them exactly throughout. Thus, at the risk of oversimplification, the burden of successful correlation is placed upon the relevance of the basic tenets of the model itself, rather than upon the resolution of ambiguities of approximation. Consequently, subsequent considerations rest upon the following:

a) The assumptions in I summarized above which provide a prescription for two-component wave functions consistent with observed nuclear magnetic moments.

b) The assumption that the nuclear core is characterizable in terms of the static moments of inertia of a spheroid; i.e.

$$\Lambda'_x = \Lambda'_y \neq \Lambda'_z$$

where the primes imply that these quantities are defined in the principal axis system of the body.

The actual computational parameters of assumption (b) are the semi-axes of the spheroid, which are related to the moments of inertia as follows:

$$\Lambda_x' = \Lambda_y' = \tfrac{1}{5} M R_0^2(\gamma^2+\alpha^2) \tag{6a}$$

and

$$\Lambda_z' = \tfrac{2}{5} M R_0^2 \alpha^2, \tag{6b}$$

where γ and α are the semi-axes in units of R_0 along and perpendicular to the symmetry axis, respectively, and M is the mass of the core. If now the wave function is taken to be (5), the expression for the quadrupole moment of the nucleus is

$$\begin{aligned} Q = {} & (1-a^2)(I\lambda jl|Q_{\text{op}}^0|I\lambda jl) \\ & +2a(1-a^2)^{\frac{1}{2}}(I\lambda jl|Q_{\text{op}}^0|I\lambda' j' l') \\ & +a^2(I\lambda' j' l'|Q_{\text{op}}^0|I\lambda' j' l'), \qquad M = I. \end{aligned} \tag{7}$$

An appropriate expression for Q_{op} may be derived from the definition

$$Q_{\text{op}}^m \equiv \left(\frac{16\pi}{5}\right)^{\frac{1}{2}} \sum_{i=1}^{z} e_i r_i^2 Y_2^m(\hat{r}_i), \tag{8}$$

by assuming that all nucleons but the last odd one belong to the rotating core. Then

$$\begin{aligned} Q_{\text{op}}^m &= \left(\frac{16\pi}{5}\right)^{\frac{1}{2}} \sum_{\text{core}} e_i r_i^2 Y_2^m(\hat{r}_i) + \left(\frac{16\pi}{5}\right)^{\frac{1}{2}} e_{\text{p}} r_{\text{p}}^2 Y_2^m(\hat{r}_{\text{p}}) \\ &= \left(\frac{16\pi}{5}\right)^{\frac{1}{2}} \int_{\text{core}} \varrho(\text{e}) r^2 Y_2^m(\hat{r}) \text{d}^3\text{r} + \left(\frac{16\pi}{5}\right)^{\frac{1}{2}} \text{e}_{\text{p}} r_{\text{p}}^2 Y_2^m(\hat{r}_{\text{p}}) \\ &= \left(\frac{16\pi}{5}\right)^{\frac{1}{2}} \sum_{m'} D_{mm'}^{2*}(\Theta) \int_{\text{core}} \varrho(\text{e}) r'^2 Y_2^{m'}(\hat{r}') \text{d}^3\text{r}' + \left(\frac{16\pi}{5}\right)^{\frac{1}{2}} \text{e}_{\text{p}} r_{\text{p}}^2 Y_2^m(\hat{r}_{\text{p}}). \end{aligned} \tag{9}$$

The symbol Θ stands for the Euler angles of a rotation from the space to the body-fixed principal axis coordinate system. Hence the primed integration runs over the static shape of the core.

If we define a shape factor Q_0 by

$$Q_0 = \left(\frac{16\pi}{5}\right)^{\frac{1}{2}} \int_{\text{core}} \varrho(\text{e}) r'^2 Y_2^0(\hat{r}') \text{d}^3 r',$$

then in terms of the shape parameter defined above we have for a uniform charge distribution

$$Q_0 = \tfrac{2}{5} Z e R_0^2(\gamma^2-\alpha^2). \tag{10}$$

The expectation value for the quadrupole moment may now be expressed as

$$Q = Q_0[(1-a^2)P_s(Ij;\lambda\lambda)+a^2P_s(Ij';\lambda'\lambda')+2a(1-a^2)^{\frac{1}{2}}P_s(Ij;\lambda\lambda')\delta_{jj'}]$$
$$+\langle er_p^2\rangle[(1-a^2)P_p(I\lambda;jljl)+a^2P_p(I\lambda';j'l'j'l')$$
$$+2a(1-a^2)^{\frac{1}{2}}P_p(I\lambda;jlj'l')\delta_{\lambda\lambda'}] = Q_s+Q_p\,.$$

The expression $\langle er_p^2\rangle$ implies that an appropriate radial function for the last odd nucleon has been adjoined to the kinematical wave function. The quantities P_s and P_p are the core and particle projection factors, respectively, and essentially measure the distortion of the charge distribution due to the core rotation. They are defined by

$$P_s(Ij;\lambda\lambda') = (I\lambda jl|D^{2*}_{00}|I\lambda' jl)$$
$$= (-1)^{j-I-\lambda}\left[\frac{I(2I-1)(2I+1)}{(I+1)(2I+3)}\right]^{\frac{1}{2}}(2\lambda'+1)^{\frac{1}{2}}\,C(\lambda' 2\lambda;0,0)W(\lambda'\lambda II;2j) \tag{12a}$$

and

$$P_p(I\lambda;jlj'l') = \left(I\lambda j\,l\left|\left(\frac{16\pi}{5}\right)^{\frac{1}{2}}Y^0_2(\vartheta_p)\right|I\lambda j'\,l'\right)$$
$$=(-1)^{j'+I-\lambda}\left(\frac{16\pi}{5}\right)^{\frac{1}{2}}(lj||2||l'j')\left[\frac{I(2I-1)(2I+1)}{(I+1)(2I+3)}\right]^{\frac{1}{2}} \tag{12b}$$
$$(2j+1)^{\frac{1}{2}}W(jj'II;2\lambda),$$

where

$$(lj||2||l'j') =$$
$$\left(\frac{5}{4\pi}\right)^{\frac{1}{2}}(-1)^{j'+l'-\frac{1}{2}}[(2l'+1)(2j'+1)]^{\frac{1}{2}}C(l'2l;0,0)\,W(ljl'j';\tfrac{1}{2}2). \tag{12c}$$

Since $\gamma/\alpha > 1$ for prolate nuclei and $\gamma/\alpha < 1$ for oblate nuclei, it is clear that Q_0 is positive for prolate and negative for oblate nuclei. In order to evaluate the particle contribution to the quadrupole moment, we have taken $\langle er_p^2\rangle = 3/5eR_0^2$ and have used the value $R_0 = 1.44\times10^{-13}A^{\frac{1}{3}}$ cm. In general it is found that, as expected, the core contribution predominates in the determination of the sign and magnitude of the moment.

The fact that the core contribution does indeed generally determine the moment raises the interesting and not entirely trivial question of the distinction between the static and dynamic nuclear shapes; i.e. between the shape seen by an observer in the rotating principal axis system and that seen by an observer in a space-fixed coordinate system †. As the momental tensor is not irre-

† The authors are indebted to Dr. L. C. Biedenharn for helpful discussions on this point.

ducible, but in fact includes an important scalar component, it is not to be expected that its expectation value as computed by the space-fixed observer will be simply proportional to the quadrupole expectation value. However, the *sign* of the dynamic shape does exhibit such a simple relationship. Explicitly, if the momental tensor, $J_{\mu\nu}$, is expressed in that system of coordinates in which the components of the position vector are $r_{\pm 1} = \mp (2)^{-\frac{1}{2}}(x \pm iy)$; $r_0 = z$, then the relation between the momental tensor in the space-fixed and rotating coordinate systems is

$$J_{\mu\nu}(\mathrm{e}) = \sum_{L\mu'\nu'} C(11L; \mu, \nu)\, C(11L; \mu', \nu')\, D^{L*}_{\mu+\nu,\, \mu'+\nu'}\, J_{\mu'\nu'}(\mathrm{e}'). \quad (13)$$

Since J is a symmetric tensor and since

$$C(11L; \mu, \nu) = (-1)^L C(11L; \nu, \mu),$$

we see that the irreducible components of J rotate according to D^0 and D^2, respectively. If now we define the expectation value of a space Cartesian component of J in a pure state to be $\langle J_{ij}\rangle = (Ij\lambda l|J_{ij}(\mathrm{e})|I\lambda jl)$, we find that for $\lambda = 0$ and axial symmetry in the body-fixed system of coordinates,

$$\langle J_{xx}\rangle = \langle J_{yy}\rangle = \langle J_{zz}\rangle = \frac{2\Lambda'_x + \Lambda'_z}{3}, \quad (14)$$

and for arbitrary λ,

$$\langle J_{xx}\rangle - \langle J_{zz}\rangle = P_s(Ij; \lambda\lambda)[\Lambda'_x - \Lambda'_z]. \quad (15)$$

Thus for positive core projection factors the sign of the dynamic shape and of the static shape will be the same. A further point of interest here is the question of the axis of core rotation. The assumption that the projection of the core angular momentum, K, in the body system is zero requires the core to rotate about an axis perpendicular to the axis of symmetry. The above expression for the dynamic shape factor is based upon that assumption. The converse assumption that the core rotate about the body symmetry axis would imply $\lambda = K$. In this case the dynamic shape factor would be

$$\langle J_{xx}\rangle_{\lambda=K} - \langle J_{zz}\rangle_{\lambda=K} = -\frac{2\lambda - 1}{\lambda + 1} P_s(Ij; \lambda\lambda)[\Lambda'_x - \Lambda'_z]. \quad (16)$$

Thus for a given λ the dynamic shape will be of opposite sign for $K = \lambda$ and $K = 0$.

If now the very considerable correlation between the signs of

observed quadrupole moments and the state of fullness of corresponding subshells [6]) is not to be completely destroyed by the concept of the rotating core, it is clear that the dynamic shape must be of the same sign as the static shape — as it is the latter which is presumably determined by the number of particles in unfilled subshells. At least this must be the case whenever the core contribution to the quadrupole moment dominates the particle contribution.

If it is assumed that the core deformations in the ground state are volume preserving, then a simple relationship exists between the semi-axes; viz. $\gamma = 1/\alpha^2$. Accordingly, the expression for the quadrupole moment shape factor becomes

$$Q_0 = \frac{2}{5} ZeR_0^2 \left(\gamma^2 - \frac{1}{\gamma}\right). \tag{17}$$

Since the cubic

$$\gamma^3 - h\gamma - 1 = 0, \qquad h = \frac{5Q_0}{2ZeR_0^2}, \tag{18}$$

has only one positive root, we see that assumptions (a) and (b) plus knowledge of nuclear magnetic and quadrupole moments suffice to determine a nuclear shape parameter, γ.

2. Application of Model

2.1 THE $j = l + \frac{1}{2}$ NUCLEI

The signs and magnitudes of the distortions computed on the basis of the present model for the 39 $j = l + \frac{1}{2}$ nuclei which have measured quadrupole moments are in the main quite reasonable and consistent. The situation relative to Li^7 is quite unsatisfactory, but also probably not very meaningful. The measured quadrupole moment for Pr^{141} is so closely accounted for by the odd proton that the computed core shape is spherical — which might be regarded as an anomalously small distortion. Conversely, the enormous distortions computed for Lu^{175} and Ta^{181} seem anomalously large.

The single-particle configuration assumed in I for the nucleus Yb^{173} seems to require modification. It was taken to be $f_{5/2}$, which presumably admixed with the $f_{7/2}$ state, $\lambda = 2$ being a good quantum number. So far as the magnetic moment is concerned, this admixture is quite satisfactory. Here there are two possible values for the mixing ratio a (since this is a case of spin-orbit partner mixing) — one near unity and the other very small. The

state with the small ratio, however, predicts an anomalously large distortion whereas the large ratio implies that the single-particle configuration is more nearly $f_{7/2}$ than $f_{5/2}$. If this implication is exploited, as suggested by Moszkowski and Townes [6]), then we would assign Yb^{173} the ground-state admixture $(f_{7/2}, \lambda = 2, I = 5/2) + (f_{7/2}, \lambda = 4, I = 5/2)$. As seen in table I, such a configuration correlates the magnetic moment quite satisfactorily and leads to a prediction of an entirely reasonable value of the distortion.

The quadrupole and magnetic moments and nuclear shapes of the remaining nuclei in this class all seem consistently correlated within the context of the model. Further, there is some reinforcement of the conclusion previously drawn that the appropriate core state admixture is always λ and $\lambda+2$. Among the $d_{5/2}$, $f_{7/2}$, and $g_{9/2}$ nuclei there were magnetic moments which required the $\lambda = 4$ core component. But whether the basic core component was to be that with $\lambda = 0$ or that with $\lambda = 2$ was ambiguous so far as the magnetic moments alone were concerned — although the concept of interacting core states was invoked to provide a justification for $\lambda = 2$ rather than $\lambda = 0$.

However, the necessity for the presence of a large $\lambda = 2$ component in the core configurations for these nuclei can be inferred from consideration of the core contribution to their quadrupole moments. The assumption of the (0, 4) admixture leads to the contribution

$$Q_s = Q_0 a^2 P_s(II; 44) \tag{19}$$

whereas the admixture (2, 4) provides

$$Q_s = Q_0 [(1-a^2) P_s(II; 22) + 2a(1-a^2)^{\frac{1}{2}} P_s(II; 24) + a^2 P_s(II; 44)]. \tag{20}$$

Now

$$\begin{aligned} P_s(II; 44) &= -0.1012, \quad I = 5/2 \\ &= +0.0173, \quad I = 7/2 \\ &= +0.0826, \quad I = 9/2. \end{aligned}$$

Thus the (0, 4) admixture leads to opposite-signed static and dynamic shapes for $I = 5/2$; and for $I = 7/2$ and $9/2$ to such a severe decrease in the dynamic asymmetry that only abnormally large static deformations could account for the observed quadrupole moments. Conversely, an examination of table I reveals that the (2, 4) admixture predicts signs of the distortions of these nuclei

which are quite consistent with expectation [6]), and magnitudes which are in general reasonable.

2.2 THE $j = l - \frac{1}{2}$, $I > 3/2$ NUCLEI

In the case of $j = l - \frac{1}{2}$ nuclei, which according to I admix single-particle states, one is led immediately to reinforcement of the conclusion that λ tends to be a constant of the motion-provided that $I > 3/2$. In accordance with the discussion in I it is expected that a two-state description of the $f_{5/2}$, $g_{7/2}$, and $h_{9/2}$ nuclei (except for Eu^{153}, which will be discussed later) would consist of one or the other of two alternative admixtures; either

$$(I, j=I, \lambda=0)+(I, j=I-1, \lambda=2) \text{ or } (I, j=I, \lambda=2)+(I, j=I-1, \lambda=2).$$

In the first instance the core contribution to the quadrupole moment is

$$Q_s = Q_0 a^2 \frac{I-5}{7(I+1)}, \tag{21}$$

and in the second instance it is

$$Q_s = Q_0 \frac{4I(I+1)-15}{7(I+1)(2I+3)} \left[1 - a^2 \frac{(2I+5)(I+3)-15}{4I(I+1)-15}\right]. \tag{22}$$

Thus the former configuration is characterized by opposite-signed static and dynamic shapes whereas the latter is not; hence it is expected that the latter configuration should predominate in the ground state in accordance with the previous remarks. Furthermore, it is to be noted that the core contribution to the quadrupole moment for these nuclei is independent of the sign of a, the mixing coefficient determined by the magnetic moments.

The nucleus Eu^{153} was assigned in I the ground state of a $d_{5/2}$ odd particle with core states $\lambda = 2$ and 4 admixed. This configuration, however, contains an unusually large amount of the $\lambda = 4$ component, and also predicts a very large distortion. For this nucleus Moszkowski and Townes [6]) have suggested the shell configuration $(g_{7/2})^5_{5/2}(d_{5/2})^6(h_{11/2})^2$. In accordance with this suggestion, we would regard Eu^{153} as a $g_{7/2}$ odd particle coupled to a core in the state $\lambda = 2$ to give a total spin $I = 5/2$, and admixing the state ($d_{5/2}$, $\lambda = 2$, $I = 5/2$). This latter assignment does indeed seem quite preferable in that only a small amount of the ($d_{5/2}$, $\lambda = 2$) component is required to correlate the magnetic moment. Furthermore, though the distortion remains large ($\gamma/\alpha = 1.57$, see table I), it

is considerably less than that predicted by the previous configuration ($\gamma/\alpha = 1.73$).

2.3. THE $j = l-\frac{1}{2}$, $I = 3/2$ NUCLEI

The situation relative to the $d_{3/2}$ nuclei is, however, no longer satisfactory if the rules advocated in I are strictly enforced. For purposes of magnetic moment correlation the $d_{3/2}$ nuclei were classed with all other $j = l-\frac{1}{2}$ nuclei and presumed therefore to be characterized by mixed single-particle configurations rather than mixed core configurations. It was found that all of the $d_{3/2}$ magnetic moments, with the exception of those for Cl^{35}, Cl^{37}, S^{33}, and Xe^{131}, which apparently required admixture of the $d_{5/2}$ state, could be accounted for by admixture of the nearby $s_{1/2}$ state with λ a constant of the motion and equal to 2. But for such a state the core contribution to the quadrupole moment is

$$\begin{aligned} Q_s &= Q_0 a^2 P_s(\tfrac{3}{2}\,\tfrac{1}{2}\,2\,2) \\ &= -0.2\, Q_0 a^2. \end{aligned} \tag{23}$$

Thus in accordance with the suggestion above that the static and dynamic shapes should be of the same character (both oblate or both prolate), we feel that these configurations for the $d_{3/2}$ nuclei are unacceptable.

Now it is perhaps significant that only for this group of $j = l-\frac{1}{2}$ nuclei is it possible to account for magnetic moments on the assumption of core state mixing alone, with the same exceptions as mentioned above for the $d_{3/2}$—$s_{1/2}$ configuration. The admixed core states would be those characterized by $\lambda = 0$ and 2; hence the core contribution to the quadrupole moment would be

$$\begin{aligned} Q_s &= 2Q_0 a(1-a^2)^{\frac{1}{2}} P_s(\tfrac{3}{2}\,\tfrac{3}{2};\ 0\,2) \\ &= 0.4\, Q_0 a(1-a^2)^{\frac{1}{2}}. \end{aligned} \tag{24}$$

This is the same as the corresponding quantity for $p_{3/2}$ cases, and in general leads to a reasonable description of the shape of the $d_{3/2}$ (when applicable) and $p_{3/2}$ nuclei.

The magnetic moments of Cl^{35}, Cl^{37}, S^{33}, and Xe^{131} require admixture of the ($d_{5/2}$, $\lambda = 2$) state. The apparent difference between the confiuration assigned to these cases and that assigned to the other members of their class is probably mainly a consequence of the oversimplification inherent in the assumption of only two components in the wave function. In actuality, one would expect that

the $d_{5/2}$ state is slightly admixed in all of the $d_{3/2}$ configurations, but to such a small extent that only for the four cases above is it impossible to ignore it completely so far as magnetic and quadrupole moments are concerned. There is some further justification for this point of view in that even with the admixture of the $d_{5/2}$ state, λ does not appear to be a good quantum number. That is, if one assumes a configuration consisting of the states $(d_{3/2}, \lambda = 2)$ and $(d_{5/2}, \lambda = 2)$, one finds, because of the cross term in the expression for the magnetic moment, that two possibilities exist for the mixing ratio a, one close to unity and the other extremely small. Neither of these admixtures is satisfactory in that the former suggests that the appropriate single-particle configuration should be $d_{5/2}$ instead of $d_{3/2}$, whereas the latter implies that the static deformations are so nearly averaged out by the core motion that only for unreasonable deformations could the core contribute significantly to the quadrupole moment.

Conversely, the two-component state $(d_{3/2}, \lambda = 0)+(d_{5/2}, \lambda = 2)$ correlates the magnetic moments for relatively small amounts of admixed state while at the same time predicting reasonable distortions. Thus it appears that λ is not a good quantum number for the $d_{3/2}$ nuclei, although j may be so considered except for these four cases. In table I the mixing coefficients and nuclear distortions are presented for these four nuclei on the assumption of the $(d_{3/2}, \lambda = 0)+(d_{5/2}, \lambda = 2)$ configuration.

3. Discussion

It would appear that the experimental information on nuclear quadrupole moments is not only consistent with the basic assumptions of the kinematical model developed in I, but actually provides additional support in several instances. In particular it seems to strengthen the basic assumption that $j = l+\frac{1}{2}$ and $j = l-\frac{1}{2}$ nuclei are fundamentally differentiated with respect to the nature of the core-particle degrees of freedom which are more nearly constants of the motion in the ground state. Actually, of course, consistent correlation of both magnetic and quadrupole moments within the context of the model has largely destroyed this differentiation so far as the $d_{3/2}$ nuclei are concerned. But the fact that it is for only these $j = l-\frac{1}{2}$ nuclei that the distinction disappears merely suggests the possibility that the distinguishing mechanism is significantly less operative if $I = 3/2$ than otherwise. It is clear that to a large

extent this differentiation is an assumed consequence of the shell model, in that the $j = l+\frac{1}{2}$ levels frequently seem to be more isolated from other favorable parity single-particle levels than is the case for the $j = l-\frac{1}{2}$ levels. Thus the factor of foremost importance here is the same one that has led to the gross level ordering scheme on the $j-j$ coupling model which provides a reasonable accounting for the magic numbers and for most nuclear spins and parities. A second mechanism which quite consistently operates to favor this differentiation is the pairing energy. It is observed that the $j = l-\frac{1}{2}$ single-particle states $f_{5/2}$, $g_{7/2}$, and $h_{9/2}$ appear to admix predominantly the nearby $p_{3/2}$, $d_{5/2}$, and $f_{7/2}$ states, respectively. Thus whenever the admixed level is non-empty, the change in the pairing energy favors the admixture. If the admixed level is empty, there is, of course, no pairing energy change. Conversely, exactly the same effect tends to oppose the inverse admixture.

However, these considerations are considerably weakened in their application to the $I = 3/2$ nuclei, since both the $p_{3/2}$ and $d_{3/2}$ states are characterized by nearby lower spin states of favorable parity; i.e. $p_{1/2}$ and $s_{1/2}$, respectively. But in spite of this fact, practically all nuclei characterized by the single-particle assignments $p_{3/2}$ or $d_{3/2}$ are observed (see table I) to admix core states rather than single-particle states. This apparent preference for core-state admixture stems directly from the assumption that the static and dynamic core shapes should be of the same sign.

Since $P_s(II-1;2\,2) = (I-5)/7(I+1)$, it is clear that the contribution to the core shape from the $j' = I-1$, $\lambda' = 2$ state that is admixed in the case of $f_{5/2}$, $g_{7/2}$ and $h_{9/2}$ nuclei is always negative; i.e., such admixtures invariably tend to change the character of the dynamic shape. But inspection of table I shows that in these cases the favorable shape contribution from the $j = I$, $\lambda = 2$ state considerably exceeds the unfavorable contribution without exception; so that the sign of the resultant dynamic shape is always the same as that of the static one. Hence the net result of this type of admixture for $I > 3/2$ nuclei is simply to reduce somewhat the dynamic asymmetry of the configuration.

This situation for the $I = 3/2$ nuclei is, however, completely altered by the fact that the pure states $j = I = 3/2$, $\lambda = 0$ or 2 are spherically symmetric. Thus here the unfavorable shape contribution from the $j' = I-1$, $\lambda' = 2$ configuration is the total contribution; and if the assumption concerning the correspondance

between static and dynamic shapes remains valid, such admixtures must be regarded as unlikely. Conversely, it is seen from eq. (24) that the static and dynamic shapes are of the same sign for core state admixtures with $j' = j = I = 3/2$. Furthermore, the four $d_{3/2}$ nuclei discussed above which require the $d_{5/2}$, $\lambda = 2$ state to account for their magnetic moments are also characterized by proper shape correspondence since

$$P_s(I, I+1; 2\ 2) = \frac{(2I-1)(I+6)}{7(I+1)(2I+3)} > 0, \qquad I > \tfrac{1}{2}. \qquad (25)$$

The significance of this seems to be that the configurations of the $I = 3/2$ nuclei are more sensitive to core dynamics than are those of the $I > 3/2$ cases.

Finally, it is to be pointed out that the correlation of the quadrupole moment data provides some corroboration of the assumption that the core rotation is such that its angular momentum has zero projection upon the body symmetry axis; i.e., the assumption that $K = 0$. From the kinematical point of view, and so far as magnetic moments are concerned, this assumption is largely arbitrary — its only effect being to restrict λ to even values if the parity of the nucleus is to be that of the single particle. The assumption receives some justification from the analysis by Bohr and Mottelson [7]) of the hydrodynamical model of the core, but it would be desirable to establish it empirically.

First of all it is to be expected that for the axially symmetric system the magnitude of K would be a good quantum number. That is, axial symmetry implies that the state of the system should be invariant under an infinitesmal rotation about the body z'-axis, and hence an eigenfunction of $\mathscr{L}_{z'}$. But the further invariance of the system under rotations of 180° about the axis perpendicular to the symmetry axis defines an operator which does not commute with $\mathscr{L}_{z'}$, but does with $\mathscr{L}^2_{z'}$; and hence if the state is chosen to be an eigenfunction of this operator, then it is the magnitude of K which is expected to be a good quantum number. Therefore, those nuclear states which contain a core component characterized by $\lambda = 0$ and consequently $K = 0$ should have other core components with $K = 0$ and even values of λ only [1]). It is to be noted that K need not be restricted to even values, but rather that $\lambda + K$ must be even.

Since the magnetic moments are independent of K (except

insofar as the evenness or oddness of K determines the evenness or oddness of λ), one finds that a consistent scheme for the correlation of magnetic moments can largely be worked out employing odd values of λ. However, one finds further that the dynamic shapes computed from these core-plus-particle configurations are either of the wrong sign, as is almost invariably the case for the $I = 3/2$ nuclei, or so much more spherically symmetric than those computed from the $K = 0$ configurations that the consequent distortions are considerably larger — often unreasonably so. Hence we feel that the data, taken in conjunction with the assumptions of the model, provide adequate justification for continuing with the assignment of $K = 0$ to nuclear ground-state configurations.

It is clear from the above that the empirical determination of the $K = 0$ assignment for odd-mass nuclei is deduced primarily from the evidence on quadrupole moments. However, one finds that the assignement $K \neq 0$ for $I = 1/2$ nuclei is actually ruled out on the basis of magnetic moment evidence alone; except for the cases [8]) W^{183} and Os^{187}, whose moments are ≈ 0.12 and cannot be correlated by any $K = 0$ configuration. These are satisfactorily accounted for by the core-plus-particle configuration $(p_{1/2},\ \lambda = 1,\ K = 1) + (f_{5/2},\ \lambda = 3,\ K = 1)$.

The results of the analysis discussed above are presented in table I. The odd-particle configurations listed are those given by Mayer and Jensen [9]) unless indicated by an asterisk. The cases so indicated are discussed in detail in the text. The quantum numbers which define the ground states are given in accordance with the convention $(1-a^2)^{\frac{1}{2}}(lj\lambda I) + a(l'j'\lambda' I)$. The magnetic moments used in calculating the a's are taken from the recent compilation of Walchli [10]). The observed quadrupole moments are taken from Ramsey [11]) or from Gordy, Smith and Trambarulo [12]), unless noted by a letter. In these cases the literature references are cited. In each case the value used in the computation and listed as Q_{obs} is a weighted average of the data indicated above.

It is interesting to compare the deformations calculated in the present work with those presented in Blatt and Weisskopf [13]), calculated for a static, axially symmetric spheroid. It is found, as is to be expected, that the shape parameters in table I lead to deformations which are in general of the order of five times as great as those obtained for non-rotating nuclei. Large static deformations were also predicted within the context of the hydrodynamical

model [3]). Such large deformations tend to strengthen the requirement employed above that the character of the static and dynamic shapes be the same [6]).

References

1) R. K. Osborn and E. D. Klema, Phys. Rev. **100** (1955) 822
2) S. G. Nilsson, Dan. Mat.-fys. Medd. **29** (1955) No. 16
3) A. Bohr, Dan. Mat.-fys. Medd. **26** (1952) No. 14
4) Kenneth W. Ford, Phys. Rev. **90** (1953) 29
5) A. K. Kerman, Dan. Mat.-fys. Medd. **30** (1956) No. 15
6) S. A. Moszkowski and C. H. Townes, Phys. Rev. **93** (1954) 306
7) A. Bohr and B. R. Mottelson, Dan. Mat.-fys. Medd. **27** (1953) No. 16
8) K. Murakawa, Phys. Rev. **98** 1285 (1955)
9) Maria Goeppert Mayer and J. Hans D. Jensen, Elementary Theory of Nuclear Shell Structure (John Wiley and Sons, New York, 1955)
10) H. E. Walchli, A Table of Nuclear Moment Data, ORNL-1469 (Supplement II)
11) Norman F. Ramsey, Nuclear Moments (John Wiley and Sons, New York, 1953)
12) Walter F. Gordy, William V. Smith, and Ralph F. Trambarulo, Microwave Spectroscopy (John Wiley and Sons, New York, 1953)
13) John M. Blatt and Victor F. Weisskopf, Theoretical Nuclear Physics (John Wiley and Sons, New York, 1952)

TABLE I

Analysis of nuclear quadrupole moment data. The odd-particle configurations are given in the second column and the assumed ground states in the third. The mixing coefficients are given in the fourth column. The experimental values of the quadrupole moments are listed in the fifth column. The calculated shape parameters are given in the last three columns.

Spin 3/2 Nuclei

Nucleus	Odd Particle Configuration	Assumed Ground State Quantum Numbers, $(lj\lambda I)$	a	Q_{obs}	γ	α	γ/α
		$P_{3/2}$ Odd Proton					
$_3Li_4$	$(1s_{1/2})^2(1p_{3/2})^1$	(1 3/2 0 3/2) (1 3/2 2 3/2)	0.463	0.02	1.656	0.777	2.13
$_5B_6$	$(1s_{1/2})^2(1p_{3/2})^3$	(1 3/2 0 3/2) (1 3/2 2 3/2)	0.665	0.040[a])	1.373	0.853	1.61
$_{29}Cu_{34}$	$(2p_{3/2})^1$	(1 3/2 0 3/2) (1 3/2 2 3/2)	0.792	—0.15[b,c])	0.932	1.036	0.90
$_{29}CU_{36}$	$(2p_{3/2})^1$	(1 3/2 0 3/2) (1 3/2 2 3/2)	0.751	—0.15[b])	0.939	1.032	0.91
$_{31}Ga_{38}$	$(2p_{3/2})^3$	(1 3/2 0 3/2) (1 3/2 2 3/2)	0.844	0.2318	1.093	0.956	1.14
$_{31}Ga_{40}$	$(2p_{3/2})^3$	(1 3/2 0 3/2) (1 3/2 2 3/2)	0.702	0.1461	1.062	0.970	1.09
$_{33}As_{42}$	$(2p_{3/2})^3(1f_{5/2})^2$	(1 3/2 0 3/2) (1 3/2 2 3/2)	0.972	0.3	1.188	0.917	1.30
$_{35}Br_{44}$	$(2p_{3/2})^3(1f_{5/2})^4$	(1 3/2 0 3/2) (1 3/2 2 3/2)	0.822	0.33[d])	1.107	0.950	1.16
$_{35}Br_{46}$	$(2p_{3/2})^3(1f_{5/2})^4$	(1 3/2 0 3/2) (1 3/2 2 3/2)	0.781	0.28[d])	1.088	0.958	1.14
$_{37}Rb_{50}$	$(2p_{3/2})^3(1f_{5/2})^6$	(1 3/2 0 3/2) (1 3/2 2 3/2)	0.646	0.15[e])	1.051	0.975	1.08
		Odd Neutron					
$_4Be_5$	$(1s_{1/2})^2(1p_{3/2})^3$	(1 3/2 0 3/2) (1 3/2 2 3/2)	0.595	0.02[f])	1.241	0.898	1.38
$_{80}Hg_{121}$	$(2f_{7/2})^8(1h_{9/2})^{10}(3p_{3/2})^3$ $(2f_{5/2})^6(1i_{13/2})^{12}$	(1 3/2 0 3/2) (1 3/2 2 3/2)	0.792	0.50[g])	1.038	0.982	1.06

a) G. Wessel, Phys. Rev. **92** (1953) 1581
H. D. Dehmelt, Z. Physik **133** (1952) 528; **134** (1953) 642
A. Bassompierre, C. R. Acad. Sci. **237** (1953) 1224

b) B. Bleaney, K. D. Bowers and M. H. L. Pryce, Proc. Roy. Soc. A **228** (1955) 166
B. Bleaney, K. D. Bowers and R. S. Trenam, Proc. Phys. Soc. A **66** (1953) 410

c) H. Kopfermann, A. Steudel, S. Wagner and W. Walcher, Nachr. Akad. Wiss. Göttingen, Math-Physik Kl IIa No. 1 (1953) 1

d) J. G. King and V. Jaccarino, Phys. Rev. **94** (1954) 1610; **91** (1953) 209A
W. Gordy, J. Chem. Phys. **19** (1951) 792
H. G. Dehmelt, Z. Physik **130** (1951) 480

e) B. Senitzky, I. I. Rabi and M. L. Perl, Phys. Rev. **98** (1955) 1537A
H. Krüger and U. Meyer-Berkhout, Naturwissenschaften **42** (1955) 94

f) W. D. Knight, Phys. Rev. **92** (1953) 539A

g) K. Murakawa, Phys. Rev. **98** (1955) 1285
H. G. Dehmelt, H. G. Robinson and W. Gordy, Phys. Rev. **93** (1954) 480

TABLE I (continued)

Spin 3/2 Nuclei

Nucleus	Odd Particle Configuration	Assumed Ground State Quantum Numbers, $(lj\lambda I)$	a	Q_{obs}	γ	α	γ/α
		$d_{3/2}$					
		Odd Proton					
$_{17}Cl_{18}$	$(1d_{5/2})^6(2s_{1/2})^2(1d_{3/2})^1$	(2 3/2 0 3/2) (2 5/2 2 3/2)	0.534	—0.0789[k])	0.774	1.136	0.68
$_{17}Cl_{20}$	$(1d_{5/2})^6(2s_{1/2})^2(1d_{3/2})^1$	(2 3/2 0 3/2) (2 5/2 2 3/2)	0.479	—0.0620[k])	0.865	1.075	0.80
$_{77}Ir_{114}$	$(1g_{7/2})^8(2d_{5/2})^6(1h_{11/2})^{10}(2d_{3/2})^3$	(2 3/2 0 3/2) (2 3/2 2 3/2)	0.426	1.25[l])	1.139	0.937	1.22
$_{77}Ir_{116}$	$(1g_{7/2})^8(2d_{5/2})^6(1h_{11/2})^{10}(2d_{3/2})^3$	(2 3/2 0 3/2) (2 3/2 2 3/2)	0.337	1.2[l])	1.164	0.927	1.26
$_{79}Au_{118}$	$(1g_{7/2})^8(2d_{5/2})^6(1h_{11/2})^{12}(2d_{3/2})^3$	(2 3/2 0 3/2) (2 3/2 2 3/2)	0.213	0.56[m])	1.129	0.941	1.20
		Odd Neutron					
$_{16}S_{17}$	$(1d_{5/2})^6(2s_{1/2})^2(1d_{3/2})^1$	(2 3/2 0 3/2) (2 5/2 2 3/2)	0.497	—0.065[n,o])	0.589	1.303	0.45
$_{16}S_{19}$	$(1d_{5/2})^6(2s_{1/2})^2(1d_{3/2})^3$	(2 3/2 0 3/2) (2 3/2 2 3/2)	0.628	0.045[o])	1.054	0.974	1.08
$_{54}Xe_{77}$	$(2d_{5/2})^6(1g_{7/2})^8(3s_{1/2})^2(1h_{11/2})^{10}(2d_{3/2})^1$	(2 3/2 0 3/2) (2 5/2 2 3/2)	0.473	—0.14[p])	0.875	1.069	0.82

k) G. F. Koster, Phys. Rev. **86** (1952) 148

l) W. v. Siemens, Ann. Phys. **13** (1953) 136
K. Murakawa and S. Suwa, Phys. Rev. **87** (1952) 1048

m) W. v. Siemens, Ann. Phys. **13** (1953) 158
W. v. Siemens, Naturwissenschaften **38** (1951) 455

n) G. R. Bird and C. H. Townes, Phys. Rev. **94** (1954) 1203

o) C. A. Burrus, Jr. and W. Gordy, Phys. Rev. **92** (1953) 274
H. G. Dehmelt, Phys. Rev. **91** (1953) 313

p) E. Brun, J. Oeser, H. H. Staub and C. G. Telschow, Phys. Rev. **93** (1954) 904
A. Bohr, J. Koch and E. Rasmussen, Ark. Fys. **4** (1952) 455

TABLE I (continued)

Spin 5/2 Nuclei

Nucleus	Odd Particle Configuration	Assumed Ground State Quantum Numbers, $(lj\lambda I)$	a	Q_{obs}	γ	α	γ/α
		$d_{5/2}$ Odd Proton					
$_{11}Na_{12}$	$(1d_{5/2})^3$	(2 5/2 2 3/2) (2 5/2 4 3/2)	0.297	0.11 [q]	1.241	0.898	1.38
$_{13}Al_{14}$	$(1d_{5/2})^5$	(2 5/2 0 5/2) (2 5/2 2 5/2)	0.959	0.153 [r]	1.232	0.901	1.37
$_{51}Sb_{70}$	$(2d_{5/2})^1$	(2 5/2 2 5/2) (2 5/2 4 5/2)	0.248	—0.65 [s]	0.877	1.068	0.82
$_{53}I_{74}$	$(1g_{7/2})^2(2d_{5/2})^1$	(2 5/2 2 5/2) (2 5/2 4 5/2)	0.499	—0.819 [t]	0.869	1.072	0.81
$_{59}Pr_{82}$	$(1g_{7/2})^3(2d_{5/2})^1$	(2 5/2 0 5/2) (2 5/2 2 5/2)	0.844	—0.054 [u]	1.001	0.999	1.00
$_{63}Eu_{88}$	$(1g_{7/2})^3(2d_{5/2})^5$	(2 5/2 0 5/2) (2 5/2 2 5/2)	0.976	1.2	1.130	0.941	1.20
$_{75}Re_{112}$	$(1g_{7/2})^3(2d_{5/2})^5(1h_{11/2})^{12}$	(2 5/2 2 5/2) (2 5/2 4 5/2)	0.352	2.6	1.232	0.901	1.37
		Odd neutron					
$_8O_9$	$(1d_{5/2})^1$	(2 5/2 0 5/2) (2 5/2 2 5/2)	0.124	—0.004 [v]	0.955	1.023	0.93
		$f_{5/2}$ Odd Proton					
$_{37}Rb_{48}$	$(2p_{3/2})^4(1f_{5/2})^5$	(3 5/2 2 5/2) (1 3/2 2 5/2)	0.438	0.30 [w]	1.302	0.876	1.48

q) M. L. Perl, I. I. Rabi and B. Senitzky, Phys. Rev. **98** (1955) 611; **97** (1955) 388
P. L. Sagalyn, Phys. Rev. **94** (1954) 885

r) H. Lew and G. Wessel, Phys. Rev. **90** (1953) 1
G. F. Koster, Phys. Rev. **86** (1952) 148

s) A. W. Jache, G. S. Blevins and W. Gordy, Phys. Rev. **97** (1955) 680
K. Murakawa, Phys. Rev. **93** (1954) 1232
G. Sprague and D. H. Tomboulian, Phys. Rev. **92** (1953) 105

t) K. Murakawa and S. Suwa, Z. Phys. **137** (1954) 575
V. Jaccarino, J. G. King and H. H. Stroke, quoted by R. Livingston, B. M. Benjamin, J. T. Cox and W. Gordy, Phys. Rev. **92** (1953) 1271
T. Kamei, J. Phys. Soc. Japan **7** (1952) 649

u) H. Lew, Phys. Rev. **91** (1953) 619

v) G. R. Bird and C. H. Townes, Phys. Rev. **94** (1954) 1203 calculated from data of S. Geschwind, G. R. Gunther-Mohr and G. Silvey, Phys. Rev. **85** (1952) 474

w) H. Krüger and U. Meyer-Berkhout, Naturwissenschaften **42** (1955) 94
B. Senitzky, I. I. Rabi and M. L. Perl, Phys. Rev. **98** (1955) 1537A

TABLE I (continued)

Spin 7/2 Nuclei

Nucleus	Odd Particle Configuration	Assumed Ground State Quantum Numbers, $(lj\lambda I)$	a	Q_{obs}	γ	α	γ/α
		$f_{7/2}$					
		Odd Proton					
$_{23}V_{28}$	$(1f_{7/2})^3$	(3 7/2 0 7/2) (3 7/2 2 7/2)	0.897	0.3[z])	1.126	0.942	1.20
$_{25}Mn_{30}$	$(1f_{7/2})^5$	(3 7/2 2 5/2) (3 7/2 4 5/2)	0.591	0.55[y,z])	1.177	0.922	1.28
$_{27}Co_{32}$	$(1f_{7/2})^7$	(3 7/2 2 7/2) (3 7/2 4 7/2)	0.427	0.5[z])	1.177	0.922	1.28
		Odd Neutron					
$_{70}Yb_{103}$	$(2f_{7/2})^7(1h_{9/2})^{10}(2p_{3/2})^{4*}$	(3 7/2 2 5/2) (3 7/2 4 5/2)	0.657	3.9	1.206	0.911	1.32
		$g_{7/2}$					
		Odd Proton					
$_{51}Sb_{72}$	$(1g_{7/2})^1$	(4 7/2 2 7/2) (2 5/2 2 7/2)	0.543	—1.0[aa])	0.715	1.182	0.60
$_{53}I_{76}$	$(1g_{7/2})^3$	(4 7/2 2 7/2) (2 5/2 2 7/2)	0.565	—0.47[ab])	0.890	1.060	0.84
$_{55}Cs_{78}$	$(1g_{7/2})^5$	(4 7/2 2 7/2) (2 5/2 2 7/2)	0.554	—0.003[ac])	1.043	0.979	1.06
$_{57}La_{82}$	$(1g_{7/2})^7$	(4 7/2 2 7/2) (2 5/2 2 7/2)	0.612	0.8[ad])	1.314	0.872	1.51
$_{63}Eu_{90}$	$(1g_{7/2})^7(2d_{5/2})^{6*}$	(4 7/2 2 5/2) (2 5/2 2 5/2)	0.400	2.5	1.350	0.861	1.57
$_{71}Lu_{104}$	$(1g_{7/2})^7(2d_{5/2})^6(1h_{11/2})^8$	(4 7/2 2 7/2) (2 5/2 2 7/2)	0.646	5.9	2.287	0.661	3.46
$_{73}Ta_{108}$	$(1g_{7/2})^7(2d_{5/2})^6(1h_{11/2})^{10}$	(4 7/2 2 7/2) (2 5/2 2 7/2)	0.376	6.2[ae])	1.791	0.747	2.40

y) A. Javan and A. Engelbrecht, Phys. Rev. **96** (1954) 649
A. Javan, G. Silvey, C. H. Townes and A. V. Grosse, Phys. Rev. **91** (1953) 222A

z) K. Murakawa and T. Kamei, Phys. Rev. **92** (1953) 325

aa) A. W. Jache, G. S. Blevins and W. Gordy, Phys. Rev. **97** (1955) 680
K. Murakawa, Phys. Rev. **93** (1954) 1232
G. Sprague and D. H. Tomboulian, Phys. Rev. **92** (1953) 105

ab) W. Gordy, J. Chem. Phys. **19** (1951) 792 calculated from data of R. Livingston, O. R. Gilliam and W. Gordy, Phys. Rev. **76** (1949) 149

ac) K. H. Althoff and H. Krüger, Naturwissenschaften **41** (1954) 368

ad) K. Murakawa, Phys. Rev. **98** (1955) 1285
K. Murakawa, J. Phys. Soc. Japan **9** (1954) 391
K. Murakawa and T. Kamei, Phys. Rev. **92** (1953) 325

ae) B. M. Brown and D. H. Tomboulian, Phys. Rev. **88** (1952) 1158

TABLE I (continued)

Spin 9/2 Nuclei

Nucleus	Odd Particle Configuration	Assumed Ground State Quantum Numbers, $(lj\lambda I)$	a	Q_{obs}	γ	a	γ/a
		$g_{9/2}$					
		Odd Proton					
$_{41}Nb_{52}$	$(2p_{3/2})^4(1f_{5/2})^6(2p_{1/2})^2(1g_{9/2})^1$	(4 9/2 2 9/2) (4 9/2 4 9/2)	0.179	—0.2 [af])	0.985	1.008	0.98
$_{43}Tc_{56}$	$(2p_{3/2})^4(1f_{5/2})^6(2p_{1/2})^2(1g_{9/2})^3$	(4 9/2 2 9/2) (4 9/2 4 9/2)	0.629	0.34 [ag])	1.046	0.978	1.09
$_{49}In_{64}$	$(2p_{3/2})^4(1f_{5/2})^6(2p_{1/2})^2(1g_{9/2})^9$	(4 9/2 2 9/2) (4 9/2 4 9/2)	0.716	0.98 [ah])	1.096	0.955	1.15
$_{49}In_{66}$	$(2p_{3/2})^4(1f_{5/2})^6(2p_{1/2})^2(1g_{9/2})^9$	(4 9/2 2 9/2) (4 9/2 4 9/2)	0.710	1.0[ah])	1.096	0.955	1.15
		Odd Neutron					
$_{32}Ge_{41}$	$(2p_{3/2})^4(1f_{5/2})^6(2p_{1/2})^2(1g_{9/2})^1$	(4 9/2 2 9/2) (4 9/2 4 9/2)	0.720	—0.21	0.961	1.020	0.94
$_{34}Se_{45}$	$(2p_{3/2})^4(1f_{5/2})^6(1g_{9/2})^7$	(4 9/2 2 7/2) (4 9/2 4 7/2)	0.748	1.05 [ai])	1.160	0.928	1.25
$_{36}Kr_{47}$	$(2p_{3/2})^4(1f_{5/2})^6(2p_{1/2})^2(1g_{9/2})^7$	(4 9/2 2 9/2) (4 9/2 4 9/2)	0.664	0.15	1.022	0.989	1.03
		$h_{9/2}$					
		Odd Proton					
$_{83}Bi_{126}$	$(1h_{9/2})^1$	(5 9/2 2 9/2) (3 7/2 2 9/2)	0.686	—0.4	0.978	1.011	0.97

af) K. Murakawa, Phys. Rev. **98** (1955) 1285

ag) K. G. Kessler and R. E. Trees, Phys. Rev. **92** (1953) 303

ah) G. F. Koster, Phys. Rev. **86** (1952) 148

ai) G. R. Bird and C. H. Townes, Phys. Rev. **94** (1954) 1203 calculated from data of W. A. Hardy, G. Silvey, C. H. Townes, B. F. Burke, M. W. P. Strandberg, G. W. Parker and V. W. Cohen, Phys. Rev. **92** (1953) 1532

Nuclear Physics **2** (1956/57) 476—484; *North-Holland Publishing Co., Amsterdam*

INTERNAL CONVERSION COEFFICIENTS FOR M1 TRANSITIONS IN $_{83}Bi^{214}$, $_{84}Po^{214}$ AND $_{83}Bi^{212}$

K. O. NIELSEN, O. B. NIELSEN and M. A. WAGGONER †

Institute for Theoretical Physics, Copenhagen, Denmark

Received 23 July 1956

Abstract: Measurements on internal conversion lines of Bi^{214} confirm that the experimental M1 internal conversion coefficients for heavy elements are considerably smaller than the values calculated for a point nucleus. The results are in approximate agreement with the finite size corrected values of Sliv and Band [1]).

A number of transitions in Po^{214} with $\Delta I = 0$ or 1 were found to be mainly M1 according to conversion coefficients corrected for finite size effects. The tables of uncorrected conversion coefficients [2, 3]) would have indicated the systematic occurrence of large E2 admixtures.

The K/L ratio for the 115 keV M1 transition in Bi^{212} was found to agree with the theoretical value, which is not sensitive to the finite size effect. This ratio was earlier thought to be abnormally low [4]).

1. Introduction

Sliv [5]) has pointed out, that the approximations made in the calculation of internal conversion coefficients by neglecting the finite size of the nucleus give rise to serious errors for heavy elements, especially for magnetic transitions. Recently, Wapstra and Nijgh [4]) have demonstrated that the tables of internal conversion coefficients calculated by Rose *et al.* [2, 3]) in the point nucleus approximation disagree with experimental values in the region of heavy elements, whereas good agreement is obtained when a finite size correction of the order of magnitude indicated by Sliv and Listengarten [6]) is applied.

During an extensive investigation [7]) of the $_{82}Pb^{214} \rightarrow {}_{83}Bi^{214} \rightarrow {}_{84}Po^{214}$ decay, i.e., RaB → C → C′, we have obtained some additional evidence regarding the magnitude of M1 internal conversion coefficients. A summary of the experimental results is presented here. The observed values are compared with the tables of finite size corrected K conversion coefficients of Sliv and Band [1]), which are now available for Z values above 65 and for five electric and

† On leave from Vassar College, Poughkeepsie, New York.

five magnetic multipole orders. We have also included a measurement of the K/L ratio of the 115 keV M1 transition in Bi^{212} (ThC). Earlier measurements [9]) had indicated that this ratio was much lower than the theoretical value for M1 transitions.

2. Spectrometers and Sources

A six gap β-ray spectrometer [9]) and an intermediate-image lens spectrometer were used in the measurements. Sources of very high quality were prepared by bombarding 150 $\mu g/cm^2$ aluminum foil with an ionized beam of 3.8 day $_{86}Em^{222}$ in an isotope separator[10, 11]). Activities of the order of 1 millicurie on 3 mm^2 were obtained in this manner. The two α-decays preceding the formation of the Pb^{214} have no effect on the β-decay investigation.

3. The Transition $_{82}Pb^{214} \rightarrow {}_{83}Bi^{214}$

The decay of Pb^{214} provides favourable conditions for a comparison of experimental and theoretical conversion coefficients. The case has been discussed by Wapstra and Nijgh [4]) using old measurements of the internal conversion lines [12, 13, 14]).

The majority of the decays (fig. 1) proceed through one of three strong γ-transitions of 242, 295 and 352 keV (the F, G, and H transitions, respectively, in Ellis' notation [14]). From their $L_I : L_{II} : L_{III}$ ratios [15]) these lines are known to be almost pure M1. Since E2 radiation is strongly converted in the L_{III} subshell, the absence of observable L_{III} conversion lines excludes E2 admixtures of more than 10 percent.

The experimental and theoretical K/L ratios for these three transitions are given in table I.

Since tables of corrected L conversion coefficients are at present not available, the theoretical ratios are the point nucleus values of Rose *et al.* [3]). The experimental K/L ratios seem to be systematically a few percent lower than this calculation. This is the expected effect of the finite size correction [16]). The observed K/L ratios also exclude E2 admixtures of more than 10 percent.

We have preferred to base the comparison of experimental and theoretical conversion coefficients on the total intensity of these three strong γ-rays, since this can be determined experimentally more accurately than their separate intensities. The measured intensities of the K-conversion lines of the 242, 295 and 352 keV transitions are given in table II. The intensities of the last two are

considerably stronger than had been reported earlier [12, 13]). The last two columns of table II, obtained by dividing the K-con-

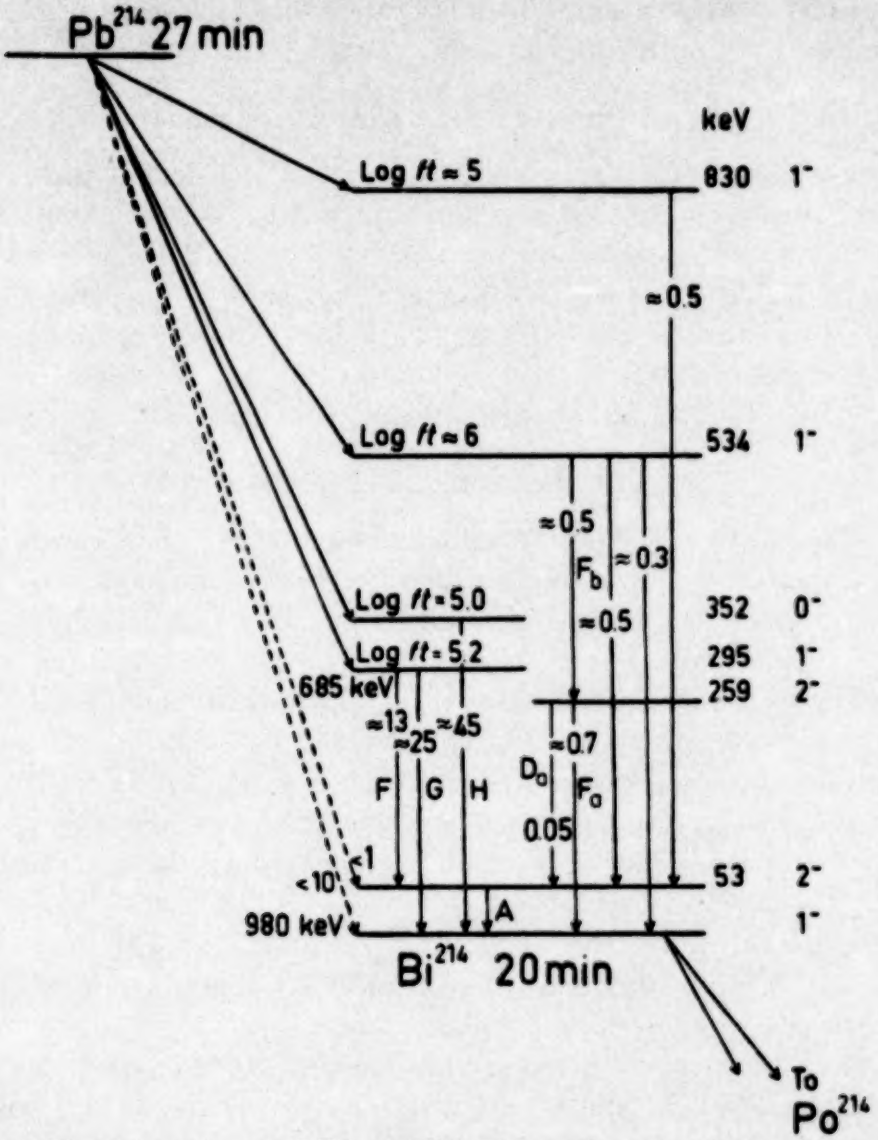

Fig. 1. The decay scheme $_{82}Pb^{214} \rightarrow {}_{83}Bi^{214}$. The angular momentum assignments are tentative.

version line intensities with the uncorrected and corrected conversion coefficients, respectively, represent the γ-intensities consistent with each of these two calculations. The relative values calculated in this way agree well with the measurements of Muller *et al.* [17]).

The actual intensities of these transitions can be obtained by considering the strength of the branches in the decay which do not proceed through one of these rays. 23 ± 2 percent of all decays

take place through the K, L, M and N conversion lines of the three strong transitions. All other modes of decay must therefore account for the remaining 77±2 percent.

TABLE I

K/L Ratios.

Line in Ellis' notation	γ-ray energy (keV)	K/L ratios observed	K/L ratios theoretical (ref. [2, 3])	
			M1	E2
F	242	5.30±0.15	5.65	0.9
G	295	5.55±0.15	5.70	1.4
H	352	5.65±0.15	5.70	1.9

TABLE II

K Conversion Lines.

γ-ray energy (keV)	Intensity of K conversion line		M1 conversion coefficients		γ-ray intensity	
	Relative	Absolute (percent)	Rose	Sliv	Rose	Sliv
242	0.570±0.015	4.5±0.4	0.92	0.67	4.9	6.7
295	0.785±0.020	6.2±0.5	0.55	0.39	11.2	15.9
352	1	7.9±0.6	0.34	0.25	23.2	31.6
	Total	18.6±1.5			39.3±2.9	54.2±4.1

The total absolute intensity of the K, L, M and N internal conversion lines of these three transitions is 23±2 percent.

We have found the six weak transitions shown in the decay scheme in fig. 1. They amount together to about 2 percent of all decays. In addition, four weaker conversion lines totalling 0.2 percent of all decays, corresponding to γ-rays of 196, 272, 279 and 549 keV, have been observed, but not placed in the decay scheme. We are from this able to place an upper limit of 5 percent on γ-transitions parallel to the 242, 295 and 352 keV transitions.

Other possible by-pass routes are through β-decay of Pb^{214} to the 53 keV or ground level of Bi^{214}. The spectrum of β-particles coincident with the internal conversion lines of the 53 keV transition shows no high energy tail corresponding to a 927 keV β-transition directly to the 53 keV level. On the possible intensity of such a β-decay we would place an upper limit of 7 percent of the 53 keV transition or 1 percent of all decays.

A β-transition to the ground state of Bi^{214} would have an energy

of 980 keV. We have observed a knee in the continuous β-spectrum, indicating the presence of one or more β-rays with endpoints in this energy region with a total intensity about 10 percent. It is known [7]) that there is a β-ray ending in this neighbourhood, namely a transition from Bi^{214} to the 2204 keV level in Po^{214} with an intensity between 6 and 10 percent. Thus, even if we have not proved the existence of a 980 keV β-ray, cautious interpretation of the experimental data does not permit us to fix an upper limit on the intensity of such a transition lower than 10 percent. Further, it should be noted that a transition of this order is not unlikely from the decay scheme. The angular momentum assignments shown in fig. 1, which represent merely a set of values consistent with the observed transition probabilities, allow a transition to the ground state†, and in the neighbouring Bi^{212} (ThC) isotope the β-transition to the ground state is similarly depressed relative to transitions to excited states.

When these possible by-pass transitions are taken into account, the result indicates that the intensity of the three strong γ-rays may be as low as $75-(5+1+10) = 59$ percent and not higher than $79-2 = 77$ percent ††.

This result suggests that the experimental conversion coefficients may be even somewhat lower than the values of Sliv and Band. There need be no definite disagreement, as the admixture of E2 radiation, which is allowed by the K/L ratios, would bring the theoretical values just within the experimental limits.

The conversion coefficients of Rose *et al.* would demand an E2 admixture of at least 40 percent, which is excluded by the $L_I : L_{II} : L_{III}$ and K/L ratios.

The conversion coefficient for the 242 keV transtion can be estimated independently in still another way since it is in cascade with the 53 keV transition. The total intensity of the L, M and N conversion lines of this latter transition was found to be ††† 2.8 times

† *Note added in proof:* This transition has now been observed by H. Daniel, the intensity being 6.3 $\pm$ 2 percent.

†† *Note added in proof:* These limits are now 61 and 73 percent.

††† We give no uncertainty assignment to this value owing to difficulties in the measurement of intensities at low energies. Scattering in the source backing causes a considerable anisotropy in the low energy radiation. The stated value is obtained as an average by using the six gaps of the spectrometer displaced 60° relative to each other. We have in a similar manner measured the conversion lines for the 40 keV transition in $_{81}Tl^{208}$ and obtained an intensity which agreed with that which can be calculated from the known α-branching ratio.

the intensity of the line K_{242}. Due to the low energy there is no K conversion, and the γ-ray contributes only 7 ± 2 percent to the intensity, so the total intensity of the 53 keV transition is 3.0 times K_{242}.

The total intensity of all conversion lines for the 242 keV transition is 1.24 times K_{242}. We have studied the spectrum of γ-rays coincident with the 53 keV lines by means of a NaI crystal placed behind the source and a 35 channel pulse analyzer. In addition to the 242 keV line, two γ-rays (see fig. 1) of 480 and 780 keV were observed, with intensities about 4 and 7 percent of the 242 keV γ-ray. This results in a K conversion coefficient for the 242 keV transition of

$$\alpha_K = \frac{N_e}{N_\gamma} = \frac{1.11\,K_{242}}{(3.0-1.24)K_{242}} = 0.63.$$

If we consider the possibility of a β-ray to the 53 keV level with a maximum intensity of 7 percent, the conversion coefficient might be as high as 0.71. These values of the conversion coefficient thus agree with the previous determination.

We were able to estimate the ratio between the three L conversion lines of the 53 keV transition. The $L_I : L_{II}$ ratio was 10 ± 3, in agreement with the uncorrected theoretical value [3]) of 11 for M1 radiation. The $L_I : L_{III}$ ratio 85 ± 15 disagrees with the theoretical value of 165. The deviation is in the direction expected from the finite size effect [16]), but it can also be explained by an admixture of less than 0.2 percent of E2 radiation.

4. The Transition $_{83}Bi^{214} \rightarrow {}_{84}Po^{214}$

In the $Bi^{214} \rightarrow Po^{214}$ decay, several of the excited levels of Po^{214} de-excite by γ-transitions to the 0^+ ground state and to the 2^+, 609 keV first excited level. For these transitions to the 609 keV level, ΔI must be 0 or 1. A 807 keV γ-ray from the 0^+, 1416 keV level must be pure E2. The predominantly M1 nature of a 935 keV γ-ray from a 1544 keV level can be inferred from the K/L ratio and the approximate strength of the γ-ray [18]). The internal conversion lines for six of these transitions, which represent the major part of the excitation of the 609 keV level, could be measured relative to the 609 keV K conversion line.

According to the tables of Sliv and Band, the finite size correction to the E2 conversion coefficient of the 609 keV transition is only 6 %. We are thus able from the observed intensity of the

609 keV K conversion line to calculate with only small ambiguity the total intensity of the transitions passing the 609 keV level.

TABLE III

Transitions feeding the 609 keV level in Po^{214}.

γ-ray energy (keV)	Intensity of K-line	Assignment	$\alpha_k \times 10^2$ (ref. [1]))	Intensity of γ-ray	K/L ratios observed	K/L ratios theor. (ref. [2, 3]))	
						M1	E2
768	9.3±0.4	M1	3.40	4.1	4.6±1.2	5.8	3.9
807	1.6±0.4	E2	0.86	2.8	3.0±1.5	5.8	4.1
935	8.8±0.4	M1	2.05	6.5	5.4±0.3	5.8	4.3
1120	28.0±1.0	M1	1.27	33.1	5.6±0.2	5.8	
1155	3.2±0.3	M1	1.18	4.1			
1238	10.3±0.5	M1	0.98	15.7	5.7±0.3	5.8	
γ-rays with energy above 1238 keV				22 ±7			
β-ray directly to the 609 keV level				1.0±0.5			
Total				89 ±11			

The K conversion line intensities and the γ-ray intensities are given relative to the intensity of the 609 keV conversion line and γ-ray. The calculation of the intensity of the 609 keV γ-ray is based on an E2 conversion coefficient of 1.50×10^{-2} (ref. [1])).

We have not been able to resolve the conversion lines for γ-rays with energy above 1238 keV which are coincident with the 609 keV transition. The γ-intensities are obtained from the $\gamma-\gamma$ coincidence measurements of Rowland [20]). We have repeated his measurements with a similar result. The intensity of the β-decay directly to the 609 keV level is found from a study of γ-rays coincident with the high energy part of the continuous β-spectrum.

Table III gives the pertinent data on the transitions known to feed this level. In column two of this table the experimental values of the relative intensities of the conversion lines mentioned above are given. The fifth column contains the corresponding γ-intensities calculated from these conversion line intensities and Sliv and Band's theoretical conversion coefficients. The γ-intensities are expressed in percent of the total excitation of the 609 keV level, since this procedure demands knowledge of only the relative intensities of the conversion lines.

As can be seen, if pure or almost pure M1 radiation is assumed for these $\Delta I = 0$ or 1 transitions, use of the corrected conversion coefficients results almost in a balance between excitations and de-excitations of the 609 keV level. The result would seem to indicate conversion coefficients somewhat smaller than those given by Sliv

and Band, but the experiment is no real test of the theoretical values, since E2 admixtures are not excluded experimentally. We even have reason to believe that the E2 contribution is not entirely negligible for some of the transitions in table III.

The uncorrected conversion coefficients would have demanded a considerable admixture of E2 radiation.

5. The 115 keV Transition in $_{83}Bi^{212}$

Earlier measurements of the K/L ratio for this transition (among others by Ellis [8]) indicated a K line much weaker than would be expected from the theoretical values for Ml transitions, though this multipole nature is clearly indicated by the $L_I : L_{II} : L_{III}$ ratio. The case, which seemed to indicate the possibility of a strong deviation from the theoretical conversion coefficients, has been discussed in detail by Wapstra and Nijgh [4]).

The measurement of the K conversion line is difficult, since it is situated between the L_I and L_{II} lines of the strong 40 keV transition in $_{81}Tl^{208}$ (ThC''), which is formed by the α-decay of Bi^{212}. However, we have been able to measure the intensity by utilizing the fact that it is coincident with the 299 keV γ-ray [18]), whereas the 40 keV transition is coincident with only a few very weak γ-rays [19]).

A NaI crystal was placed immediately behind a source of Th-active deposit, and the coincident efficiency, ζ, i.e., the ratio between the peak heights of the line in the coincident spectrum and in the total spectrum, was measured for the composite line made up of the K_{115} and L_{40} conversion lines, for the L_{115} line and for the M_{40} line. Calling these three efficiencies ζ_c, ζ_{115}, and ζ_{40}, respectively, we have

$$\zeta_c(K_{115}+L_{40}) = \zeta_{115}K_{115}+\zeta_{40}L_{40},$$

giving

$$\frac{K_{115}}{K_{115}+L_{40}} = \frac{(\zeta_c-\zeta_{40})}{(\zeta_{115}-\zeta_{40})}.$$

In this manner it was found that 19 ± 3 percent of the composite line had to be ascribed to the K conversion line of the 115 keV γ-ray. This gives a K/L ratio for the 115 keV transition of 5 ± 1, which is in agreement with the theory. The basis for the suggestion of an anomaly in the conversion coefficients at low energies is thus removed.

The experimental intensity of the L+M+N conversion lines of

the 40 keV transition agreed with the intensity calculated from the known α-branching ratio.

6. Discussion

Although we have not obtained very accurate values of the internal conversion coefficients, our measurements on the pure M1 transitions in Bi^{214} deviate significantly from the point nucleus calculation. The tables of Sliv and Band indicate that these should be corrected by a factor about 0.7 for $Z = 83$ or 84. Our results, covering a wide energy range, agree within the limits of uncertainty with the tables of Sliv and Band, but suggest a slightly greater deviation from the point nucleus calculation, corresponding to a correction factor between 0.6 and 0.7. This result seems to be in accord with the trend from neighbouring isotopes [4]).

We wish to express our gratitude to Professor N. Bohr for continuous encouragement and support. We are indebted to Professor L. Sliv for stimulating discussions and for kind permission to use his tables prior to publication. Dr. A. H. Wapstra has communicated the results of his work at an early stage.

The multichannel analyzer has been constructed and placed at our disposal by Mr. B. Madsen.

References

1) L. Sliv and J. Band, privately distributed tables
2) M. E. Rose, G. H. Goertzel and C. L. Perry, ORNL—1923 (1953)
3) M. E. Rose, G. H. Goertzel and C. Swift, L-shell internal conversion coefficients, privately distributed
4) A. H. Wapstra and G. J. Nijgh, Nuclear Physics **1** (1956) 245
5) L. Sliv, Zh. Eksp. Theor. Fiz. **21** (1951) 770
6) L. Sliv and M. A. Listengarten, Zh. Eksp. Theor. Fiz. **22** (1952) 29
7) K. O. Nielsen, O. B. Nielsen and M. A. Waggoner, to be published
8) C. D. Ellis, Proc. Roy. Soc. A **138** (1932) 318
9) O. B. Nielsen and O. Kofoed-Hansen, Dan. Mat. Fys. Medd. **29** (1955) No. 6
10) K. O. Nielsen, Proc. 1955 Harwell Isotope Conf., Ch. 9
11) J. Koch, Proc. 1955 Harwell Isotope Conf., Ch. 25
12) R. W. Gurney, Proc. Roy. Soc. **109** (1925) 540
13) C. D. Ellis and G. H. Aston, Proc. Roy. Soc. **129** (1930) 180
14) C. D. Ellis, Proc. Roy. Soc. A **143** (1933) 350
15) M. Mladjenovic and H. Slätis, Ark. f. Fys. **8** (1954) 65
16) L. Sliv, private communication
17) D. E. Muller, H. C. Hoyt, D. J. Klein and J. W. M. DuMond, Phys. Rev. **88** (1952) 775
18) M. Mladjenovic and A. Hedgran, Ark. f. Fys. **8** (1954) 49
19) O. B. Nielsen, Dan. Mat. Fys. Medd. **30** (1955) No. 11
20) R. E. Rowland, Phys. Rev. **99** (1955) 757

Nuclear Physics **2** (1956/57) 485—495; *North-Holland Publishing Co., Amsterdam*

THE (γ, n) REACTION IN Be^9 AT INTERMEDIATE ENERGIES

R. D. EDGE

Research School of Physical Sciences, Australian National University, Canberra

Received 11 September 1956

Abstract: Cross sections for the reaction $Be^9(\gamma, n)Be^8$ for monochromatic gamma rays in the energy range 2.6 to 8.1 MeV have been obtained using a large Szilard-Chalmers neutron detector. At energies of 2.61, 4.4, 6.2 and 8.1 MeV they are $(3.77 \pm 0.2) \times 10^{-28}$ cm^2, $(1.86 \pm 3.6) \times 10^{-28}$ cm^2, $(11.4 \pm 1.0) \times 10^{-28}$ cm^2 and $(13.8 \pm 1.6) \times 10^{-28}$ cm^2 respectively. The implications of these results for current theories of the reaction are discussed.

1. Introduction

Low energy measurements of the $Be^9(\gamma, n)$ reaction, performed using radioactive gamma ray sources, indicate a sharp peak in the cross section just above threshold [1, 2]). Because there are no sources yielding gamma rays of energy greater than 2.8 MeV and because bremsstrahlung data at energies below 10 MeV are difficult to interpret, this energy region, which is of considerable theoretical interest, has been investigated only tentatively. The most promising approach would be to use monochromatic gamma rays produced by the proton bombardment of light elements but, because of the low intensities available, this necessitates the development of a sensitive neutron detector.

The method which proved most successful, in that it was sensitive to neutrons and at the same time insensitive to gamma rays in the medium energy range, employed the Szilard-Chalmers reaction in a large volume, water acting as a moderating medium. The development of the method has been described in a previous paper [3]), and is mentioned but briefly here. Solutions of sodium and potassium permanganate were used. The active $Mn^{56}O_2$ precipitated from the solution on neutron capture in manganese, was filtered off and counted by wrapping the filter paper, after it had been dried and protected by a cellophane sheath, round a cylindrical thin-walled Geiger counter.

2. Gamma Ray Sources

It was necessary to select the gamma ray source carefully, since many (p, γ) reactions in light elements suffer from the disadvantages of a poor yield of gamma rays, and of not being monochromatic. The sources chosen were from the interaction of protons with Li^7, C^{13}, N^{15} and F^{19}. Of these the last is by far the most prolific and can yield nearly monochromatic gamma radiation; for these reasons it was the first to be studied.

Preliminary investigations indicated that the neutron background from a thick target of CaF_2 bombarded by 900 keV protons [4, 5, 6]) was $(4.9 \pm 0.5) \times 10^{-12}$ neutrons per proton of the ion beam. The sources of neutrons were:

1) Two consecutive reactions in which the alpha particle from the reaction $F^{19}(p, \alpha)O^{16}$ yielded a neutron through the process $F^{19}(\alpha, n)Na^{22}$.

2) The D(d, n) reaction taking place in the target tube and in the vacuum box of the resolving magnet of the High Tension Set, produced by the deuteron component of the proton beam, owing to its natural abundance in the gas admitted to the ion source.

Attempts to reduce the first of these sources, by using a thin target, and the second by using a longer target tube and wax shielding between the target and the magnet box, were only moderately successful.

Investigations using other proton targets as sources of gamma-rays indicated that the neutron background, both from the target and the H.T. set used as the source of protons, would make the detection of photoneutrons difficult. Of the possible targets considered, namely Li^7, C^{13} and N^{15}, a lithium target was found to give $\approx 10^{-10}$ neutrons per proton, which was an order of magnitude too large to allow its use.

Using a C^{13} target, in the same experimental arrangement as for fluorine the background was approximately 90 % of the total neutron yield from the samples, and the gamma ray yield per proton from the best N^{15} targets was down by a factor of two on the C^{13} targets, although the neutron background per proton was approximately the same.

3. Experimental Procedure for Irradiations

The experimental arrangement for irradiations using the fluorine target is shown in fig. 1. The tube B in the diagram was made of

soft glass to reduce neutron absorption and passed through a polythene coated rubber bung, C. After filling the fifty litre carboy with a saturated potassium permanganate solution, which was used as the Szilard-Chalmers neutron detector, the bung was

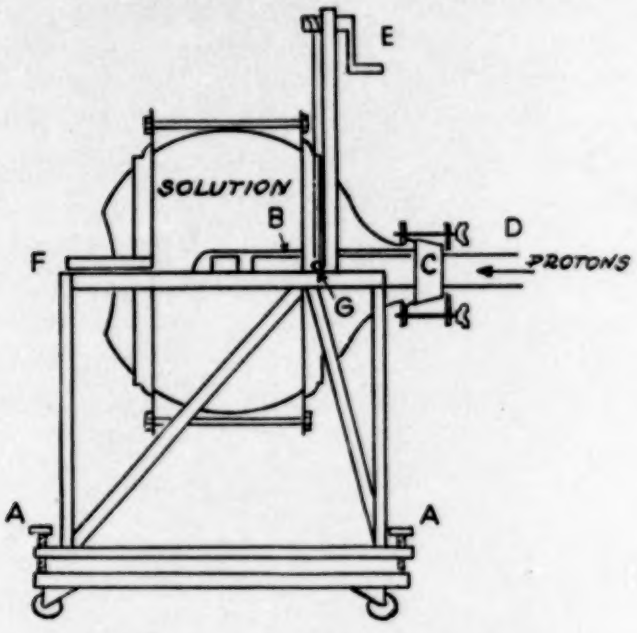

Fig. 1. Neutron detector and framework in position. A, Height adjustment; B, Glass tube holding the block containing D_2O or Be; C, Rubber bung; D, Target tube; E, Hoist to raise the flask for filtration process; F, Removable bar to allow the flask to rotate to the vertical about the pivot G.

inserted in the neck of the flask, the carboy tilted until the tube was horizontal and then run over the target tube. A frame located the carboy exactly, and sylphon bellows, supported in gimbals, allowed free angular, vertical and lateral motions of the target tube.

The first series of experiments was performed using a thick calcium fluoride target, because of the advantages of simplicity and slow deterioration.

Three identical hollow copper cylinders were constructed, each $1\frac{1}{2}$ inches long by $1\frac{1}{2}$ inches in diameter. One was left empty, one filled with heavy water and the last filled with beryllium. Runs were performed in series of three, one with beryllium, one with heavy water and one, for background, with the empty cylinder. In each case the cylinder was placed at the end of the glass tube, so that there was a gap of 3.2 cm between the cylinder and the CaF_2 target. This reduced the error due to the wandering of the ion beam over the target.

Two and a half hour irradiations using a proton beam of from one to two hundred microamperes were made and were monitored by a calibrated thick-walled Geiger counter, placed 199 cm from the target centre. Counter readings were taken every ten minutes, the ion source being adjusted to keep the counting rate as uniform as possible. After irradiation, the solution was filtered through a 9 cm filter paper to remove the active $Mn^{56}O_2$ which had been precipitated by the Szilard-Chalmers reaction [7]). After washing and drying, the precipitate was counted as described above.

A second series of experiments, performed several months later with a slightly different experimental arrangement and a thin CaF_2 target, gave results agreeing to better than 10 % with the thick target experiments.

The ratio of the number of neutrons emitted by the D to the Be sample per gamma ray was given by the ratio of the $Mn^{56}O_2$ activity for the two samples allowing for decay, for a fixed number of counts of the gamma ray monitor. Hence, assuming a value for the D photodisintegration cross section [8, 9]), that for beryllium could be found after making the corrections discussed below. Six major corrections were required, namely for

1) the differential absorption of gamma-rays in beryllium and heavy water [10]),

2) the slight difference in geometry of the samples,

3) the (n, 2n) reaction occurring in beryllium, produced by the photoneutrons [11]),

4) the differential escape of neutrons from the detector,

5) the collision of neutrons and Be^9, with loss of neutron energy, inside the blocks,

6) the Be-Al alloy used in place of beryllium for one experiment.

The escape correction was by far the largest ($\approx$ 30 % of the neutrons escaped the tank) and experiments were performed to provide an empirical correction [3]). A value for the deuteron photo-cross section of 21.2×10^{-28} cm^2 was taken, assuming the mixture of gamma rays found in the $F^{19}(p, \alpha, \gamma)$ reaction [8, 9]).

From these results, the value of the photoneutron cross section for Be^9 at 6.2 MeV was found to be $(11.3 \pm 1) \times 10^{-28}$ cm^2.

Experiments involving the use of N^{15} and C^{13} targets were performed in a similar manner to the fluorine runs, but much greater care was necessary to ascertain the background. To increase the neutron yield per gamma ray, larger quantities of D_2O and Be

were used, blocks of Be-Al alloy being arranged symmetrically round the proton target [12]). The more sensitive sodium permanganate solution replaced the potassium as detector. It was essential to maintain constant the ratio of the number of protons striking the target to those striking the magnet box, because of the D(d, n) neutrons emitted by the latter, and this was achieved by using two current integrators, one recording the resolved, the other the total beam, and keeping the ratio between the two constant.

Contamination of the targets arose from C^{12} deposited from pump oil vapour and from F^{19} which, though present in minute quantity, had an intense gamma ray yield, as well as from other sources. The gamma ray spectrum from the targets was investigated using a sodium iodide crystal-photomultiplier detector. Comparison with known spectra indicated a fluorine contamination of the C^{13} target amounting to some $(5\pm2)\%$ of the total number of gamma rays. For the N^{15} target, the number of gamma rays from N^{15}: C^{12}: F^{19} was in the ratio of 100: 74: 40 respectively. A correction had to be applied using the known cross section for fluorine gamma rays.

After applying appropriate corrections of the type discussed above and also corrections for extraneous gamma rays, the cross sections obtained were:

$$\sigma_{Be^9(\gamma,n)} \text{ at } 8.06 \text{ MeV} = (13.8\pm1.6)\times10^{-28} \text{ cm}^2,$$
$$\sigma_{Be^9(\gamma,n)} \text{ at } 4.43 \text{ MeV} = (1.86\pm3.2)\times10^{-28} \text{ cm}^2.$$

4. Experiments Using Thorium Gamma Rays

In order to relate the experiments at the intermediate energies reported above with experiments at low energies performed by other workers, a determination of the cross section using the 2.61 MeV gamma rays from thorium was made.

The thorium source, a cylinder 0.5 cm long and 0.2 cm diameter, was placed centrally between the end faces of two beryllium cylinders each 4 cm long and 4 cm diameter encased in copper, the whole being enclosed in a soft glass vessel, and totally submerged at the centre of the fifty litre tank of sodium permanganate solution. After a known time the solution was filtered and the activity of the precipitate measured as described earlier. The experiment was repeated using cylinders of identical shape filled with heavy water, and then with empty cylinders. After corrections had been applied, the cross section for beryllium was found to be

$$\sigma_{Be^9(\gamma,n)} \ 2.61 \text{ MeV} = (3.9\pm0.2)\times10^{-28} \text{ cm}^2.$$

5. Discussion of the Reaction $Be^9(\gamma, n)$

Szilard and Chalmers discovered the reaction $Be^9(\gamma, n)^7$) which is now much used as a basis for neutron standards [13]). Early determinations gave a threshold of 1.63 MeV [14, 15, 16]) but more recent techniques yielded a value of (1.664 ± 0.002) MeV [17]).

The results of measurements of the cross section using radioactive gamma ray sources are tabulated below.

Source	Energy of gamma ray MeV	$Be^9(\gamma, n)$ Cross section $\times 10^{-28}$ cm^2	Reference
Ra(B C)	Mixture	2.0	41
		19.75 ± 5.0	42
		19.5	43
		10.8 ± 2.2	44
		8.69 8.83 8.83	45
Th C†	2.61		45
		9.0 ± 2.3	42
		3.0	22
		4.4	46
		4.0	2
		4.1	35
Na^{24}	2.76	7.0	2
		6.6	35
		6.74	35
Mn^{56}	(2.06)1.77	5.9	2
Sb^{121}	1.67	19.0	2
		10.0	1
La^{140}	2.50	4.5	1
Pr^{144}	2.185	3.9	47
Ga^{72}††	2.51		2
In^{116}†††	1.8, 2.1		2

† Yield ratio Ra/Th = 1.15 [43]).
†† Ratio Be/D yield = 0.86 [2]).
††† Yield per curie = 0.82×10^4 [2]).

The main sources of error in these results arose from inaccurate measurement of the gamma ray and neutron fluxes. The gamma ray

yields from the radium and thorium sources have been accurately measured in other connections [18]), but those from the new isotopes produced in nuclear reactions were determined by the neutron activation cross sections, using the pile neutron flux, and the results could have been in error by as much as 15 %. Gamma ray yield determinations by coincidence measurements, pair spectrometry or NaI (Tl) crystal spectrometry are more accurate. In general the largest inaccuracy lay in the neutron measurements, which could not be better than 5 % this being the accuracy of the

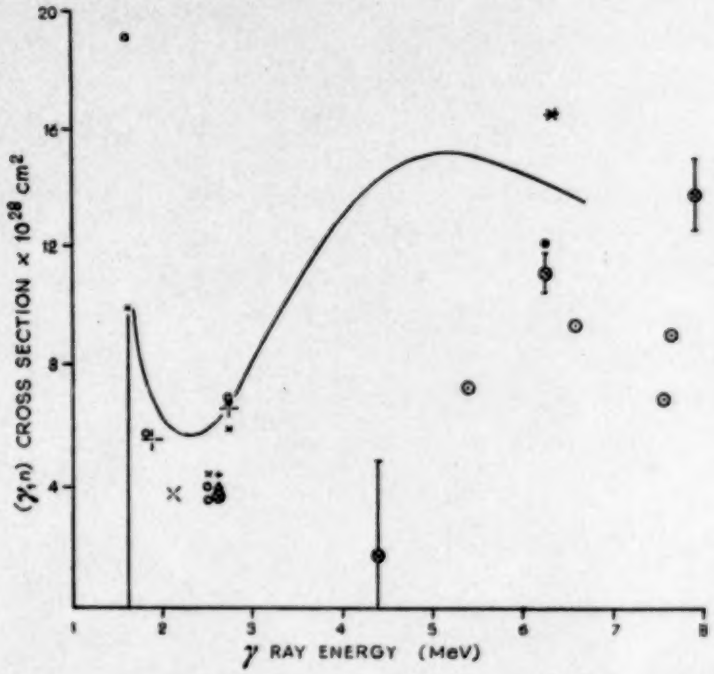

Fig. 2 Experimental and theoretical. results at low and intermediate energies for the photoneutron cross section for Be^9. The curve follows the theory of Guth and Mullin. The points have been obtained experimentally as follows: O Wattenberg *et al.* [2]), X Snell *et al.* [1]), Δ Elliot [35]), + Segre [35]), ⊗ Edge, ⊙ Eriksen and Zaleski [40]), ⚹ Arakatsu [39]), ● Carver *et al.* [23]), ⁜ Hamermesh *et al.* [47]), + Allan and Poole [48]).

standards [19]). For measurements above 2.3 MeV, the ratio of the Be photodisintegration cross section to D has been obtained, reducing this error, since the deuteron cross section is known from proton measurements to better than 5 % [8, 9]). Most comparisons between the standard source and the neutron flux from the reaction were performed using "long" BF_3 counters [20]) or the Amaldi-Fermi method [21]).

The low energy results are plotted in fig. 2 and are consistent

with the exception of the large value of the cross section using the gamma rays from Sb^{124} at 1.67 MeV energy. They indicate a definite peak in the yield curve just above threshold, followed by a minimum between 2.1 and 2.5 MeV gamma ray energy and a rapid increase in cross section between 2.5 and 2.8 MeV. The agreement between the present results for thorium and those of other workers [22]) is good and effectively relates the higher energy results of the present experiments using the same neutron detector to the low energy results obtained by many other workers. The resonance level at 1.7 MeV has been predicted theoretically by Guth and Mullin on the basis of a model involving an orbital neutron. A resonance at approximately 1.7 MeV has been discovered by Allen [6]) using the reaction $Li^7(He^3, p)Be^9$.

The stable nature of the alpha particle, the long life of Be^8, and the low threshold for the reaction $Be^9(\gamma, n)$ suggested that a model in which a central core of two alpha particles or a Be^8 nucleus was encircled by an orbital neutron might prove useful to explain these features of the yield curve. It now seems that Be^8 may be left in an excited state following the (γ, n) reaction at energies above about 5 MeV, in which case this model could only be valid at low energies [23]).

The earliest workers [14, 15, 24, 25, 26, 27, 28]) used "ordinary" nuclear forces which gave a reasonable order of magnitude for the cross section ($\approx 4 \times 10^{-28}$ cm^2), but not the sharp peak found experimentally just above threshold [29, 30, 31, 32, 33]). Guth and Mullin [34, 35, 36]) by including exchange forces, obtained quite a reasonable fit to the low energy results (fig. 2). However, their predicted maximum at 5 MeV is not found experimentally, although a maximum of about the same cross section is found at 10 MeV [37]). A considerable increase in nuclear well depth is required to bring their maximum up to 10 MeV, and it seems most likely that the peak here is due to some other mode of interaction, possibly followed by a break up to $He^4 + He^5$ [23]).

Nathans and Halpern [37]) used bremsstrahlung radiation filtered through 30 cm of carbon absorber to reduce the relative number of low energy gamma rays, although this also makes their results less reliable. Their results indicate a cross section peak at ten million volts of about 1.8 mb. They are in agreement with the present experiment in showing a slow rise up to this energy, but their cross section (fig. 3) rises more rapidly towards 10 MeV than at

lower energies. This may be due to inadequate allowance for the bremsstrahlung spectrum since the sharp peak, which is definitely known to be present above threshold, is missing in their excitation function. Their excitation function shows a drop to 0.8 mb at 18 MeV and rises to a second maximum of 3 mb which they state is the so-called "giant resonance" centered at 23 MeV. In this they differ from Jones and Terwilliger [38]) who obtained a peak of 4 mb at 19 MeV falling to 1.8 mb at 200 MeV and rising to 2 mb at 320 MeV.

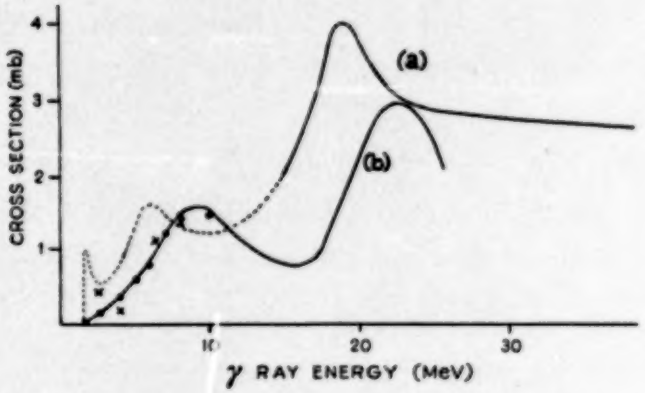

Fig. 3. A comparison of bremsstrahlung results with the results of this experiment. Curve (a) follows the results obtained by Jones and Terwilliger [38]).
(b) follows the results obtained by Nathans and Halpern [37]).
X Author, O Nathans and Halpern [37]).

Guth and Mullin predict a peak at 5 MeV, which is not in agreement with the above, although the value of the cross section at 8 MeV is approximately the same as at their peak. The known decay through another level, however, would make agreement between this theory and experiment at such energies somewhat fortuitous.

Other results above the energy limit for radioactive gamma ray sources indicate a slowly increasing cross section towards 8—10 MeV. Carver *et al.* [23]) obtained a cross section of 12.5×10^{-28} cm² at 6.2 MeV by a method similar to the above. Japanese workers [39]) obtained values for the cross section at 6.13 and 17.6 MeV, using methane filled counters, with a BeO wall coating. Their measurements at 6.13 MeV of 16.2×10^{-28} cm² is in very rough agreement with this work, whereas their value at 17.6 MeV of 53×10^{-28} cm² is far too large, if experiments using bremsstrahlung are to be believed [37, 38]). They state that transitions occur to the 7 MeV but not the 3 and 4.8 MeV states of Be^8.

Eriksen and Zaleski [40]) have used gamma rays from the (n, γ) reaction produced by pile neutrons on various elements. Their values for the $Be^9(\gamma, n)$ cross section are given below. The results agree with the bremsstrahlung results within the experimental error:

7.6 MeV gamma rays from	Fe give $\sigma_{Be^9(\gamma, n)}$	of 0.7 mb
6.6	Ti	0.94
5.4	S	0.74
7.7	Cu	0.91.

The error is stated to be of the order of 20 % but these values are considerably lower than those of the present experiments, as can be seen from figure 2.

6. Conclusion

Figures 2 and 3 show that there are three interesting features of the photoneutron excitation function, namely the sharp resonance just above threshold, and the broad resonances at 10 MeV and 18 MeV.

The low energy resonance has been explained on the basis of the "orbital neutron" model, which, however, predicts a second resonance much below the experimental peak at 10 MeV. The so-called "giant resonance", thought to occur at 18 MeV, has been explained by Goldhaber and Teller as a mass dipole vibration of nuclear matter. Thus it seems that the peak at 10 MeV indicated by bremsstrahlung data which agrees with the present and other experiments just below the resonance still requires explanation, and might repay further experimental investigation.

References

1) A. H. Snell, E. C. Barker and R. L. Sternberg, Phys. Rev. **80** (1950) 637
2) A. Wattenberg, R. Russell, D. Sachs and R. Fields, Phys. Rev. **73** (1948) 545
3) R. D. Edge, Aust. Jrnl. Phys., in press.
4) C. Y. Chao, A. V. Tollestrup, W. A. Fowler and C. C. Lauritsen, Phys. Rev. **79** (1950) 108
5) F. Ajzenberg and T. Lauritsen, Rev. Mod. Phys. **24** (1952) 321
6) F. Ajzenberg and T. Lauritsen, Rev. Mod. Phys. **27** (1955) 77
7) L. Szilard and T. A. Chalmers, Nature **134** (1934) 494
8) C. A. Barnes, J. H. Carver, G. H. Stafford and D. H. Wilkinson, Phys. Rev. **86** (1952) 359
9) J. H. Carver and D. H. Wilkinson, Nature **167** (1951) 154
10) W. Heitler, The Quantum Theory of Radiation (Oxford, 1944)
11) R. D. Edge, Ph. D. Thesis, Cambridge, 1956

12) D. H. Wilkinson, Proc. Roy. Soc. A **195** (1948) 116, 123
13) M. Goldhaber, Klaiber and Scharf-Goldhaber, Phys. Rev. **65** (1944) 61)
14) G. B. Collins, B. Waldman and W. R. Polye, Phys. Rev. **55** (1939) 412
15) G. B. Collins, B. Waldman and E. Guth, Phys. Rev. **56** (1939) 876
16) F. E. Myers and L. C. van Atten, Phys. Rev. **61** (1942) 19
17) J. C. Noyes, J. E. van Hoomissen, W. C. Miller and B. Waldman, Phys. Rev. **85** (1952) 727
18) C. D. Ellis and G. H. Aston, Proc. Roy. Soc. A **129** (1930) 180
19) D. J. Hughes, Pile Neutron Research (Addison Wesley, 1953)
20) A. O. Hanson and J. L. McKibben, Phys. Rev. **72** (1947) 673
21) E. Amaldi, L. R. Hafstad and N. A. Tuve, Phys. Rev. **51** (1937) 896
22) H. von Halban, C. R. **206** (1938) 1170
23) J. H. Carver, E. Kondaiah and B. D. McDaniel, Phil. Mag. (7) **45** (1954) 948
24) V. I. Mamasachlisov, Phys. Zeits. Zowjetunion **9** (1936)
25) V. I. Mamasachlisov, Jrnl. Phys. U.S.S.R. **7** (1943) 239
26) G. Wick, Ricerca Scient. **11** (1940) 49
27) P. Caldirola, Jrnl. de Phys. et Rad. **8** (1947) 155
28) E. Guth, Phys. Rev. **55** (1939) 411
29) F. Schlögl, Zeit. Naturf. **3***a* (1948) 229
30) A. Borsellino, Nuovo Cimento **5** (1948) 263
31) C. K. Jen and Y. C. Hsieh, Sci. Rep. Nat. Tsing Hua Univ. **4** (1947) 278
32) T. Sexl, Acta Phys. Aust. **2** (1949) 377
33) V. de Sabata, Nuovo Cimento **6** (1949) 368
34) E. Guth and C. J. Mullin, Phys. Rev. **74** (1948) 832, 833, 834
35) E. Guth and C. J. Mullin, Phys. Rev. **76** (1949) 234
36) C. J. Mullin and E. Guth, Phys. Rev. **76** (1949) 682
37) R. Nathans and J. Halpern, Phys. Rev. **92** (1953) 940
38) L. W. Jones and K. M. Terwilliger, Phys. Rev. **91** (1953) 699
39) D. Arakatsu, M. Sonada, Y. Uemura, S. Yasumi and Y. Saji, Jrnl. Phys. Soc. Jap. **66** (1951) 66
40) V. D. Eriksen and C. P. Zaleski, Jrnl. Phys. Rad. **15** (1954) 492
41) W. Gentner, C. R. **200** (1935) 310
42) L. I. Rusinov, Phys. Zeits. Zowjetunion **10** (1936) 203, 219
43) D. H. Frisch, H. Halban and J. Koch, Dan. Mat. Fys. Medd. **15** (1938) nr. 10
44) Z. Ollano, Nuovo Cimento **15** (1938) 604
45) F. G. Houtermans and I. Bartz, Phys. Zeit. **44** (1943) 167
46) D. L. Allan and M. J. Poole, Nature **162** (1950) 373
47) B. Hamermesh and C. Kimbull, Phys. Rev. **90** (1953) 1063

NEWS ITEM

ON THE NOMENCLATURE OF NUCLEAR FAMILIES

Beware the Jubjub bird . . .
LEWIS CARROLL, *Jabberwocky*

The slight innovation in the nomenclature for nuclear families, adopted in this journal, has met with some resistance. No objection is raised against the designations of the *odd mass nuclei*; the trouble concerns the names *even nuclei* and *odd nuclei*, from which the logically unnecessary repetition of the adjective is eliminated. A most interesting paper by R. K. Sheline, published in this issue, has brought the matter to a crisis. The author has in fact requested the Editor to retain the "old" nomenclature (a request, needless to say, most willingly granted), with the following motivation:

> "When I originally wrote this article the convention, even, odd, and odd mass nuclei was used throughout as suggested in *Nuclear Physics*. However, since, in some parts, this paper deals rather exclusively with comparisons between even, odd and odd mass nuclei and since the four people who read the paper here at the Institute were not able to understand it with the new nomenclature, I felt it was necessary to change" even" to "even-even" and "odd" to "odd-odd"."

This curious observation forcefully reminds us of the importance of non-logical components of language even in the process of rational communication. It casts some light, perhaps, on the frequent occurrence of words consisting of repeated syllables, like "dukduk" or "beri-beri", in primitive languages; after all, the Greeks, to denote peoples speaking what sounded to them a strange lingo, coined a repetitive word, *βάρβαρος*.

However, what are we to do about it? The Editor would welcome expressions of opinion sufficiently representative to afford a guidance as to the proper course to take.

E. CORINALDESI, Causality and dispersion relations in wave mechanics 420

O. KOFOED-HANSEN, Shell effects in nuclear Coulomb energy differences 441

L. ROSENFELD, Remarks on the charge distribution in nuclei 450

R. K. OSBORN and E. D. KLEMA, Analysis of nuclear quadrupole moments on the basis of a kinematical model 454

K. O. NIELSEN, O. B. NIELSEN and M. A. WAGGONER, Internal conversion coefficients for M1 transitions in $_{83}Bi^{214}$, $_{84}Po^{214}$ and $_{83}Bi^{212}$ 476

R. D. EDGE, The (γ, n) reaction in Be^9 at intermediate energies 485

News item 496

Pu^{242} Resonances $Pu^{241}(n, f)$ $E_n = 0.01$ to 9 ev
94 148 0.255 *20* $\Gamma = 103$ *20* mev cryst,
$\sigma_0 = 1420$ *150* chopper
4.45 *10* $\Gamma = 470$ mev (double?)
5 to 7.5 3 resonances

R. Richmond, B. T. Price, J. Nuclear Energy 2, 177 (1956).

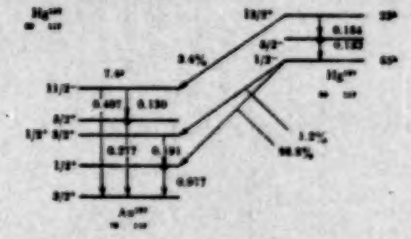

R. Joly, J. Brunner, J. Halter, O. Huber, Helv. Phys. Acta 28, 403 (1955); 26, 591A (1953).

Sm^{148} τ 8.3^m *3* $Sm^{(144)}$ ($\leq$30-Mev n,2n)
62 81 β^+ 2.3 *3* a
$_8^m$ No γ with $E\gamma > 0.15$ scin

M. Mirnik, A. H. W. Aten, Jr., Physica 22, 14 (1956).

N^{15} Capture γ's $N^{(14)}$ (th n,γ) $s\pi$ pr
7 8

15†	3.520	*20*	17†	6.323	*8*
17†	3.669	*16*	9†	7.305	*12*
16†	4.497	*11*	4†	8.313	*13*
22†	5.259	*8*	0.2†	8.54	*4*
35†	5.288	*7*	0.2†	9.03	*3*
18†	5.534	*8*	1†	9.145	*10*
14†	5.543	*8*	12†	10.833	*8*

No 7.164 γ (< 0.8†)
†Photons/100 N radiative captures

P. J. Campion, G. A. Bartholomew, Bull. Am. Phys. Soc. 1, No. 1, 28, GA2 (1956); verbal report.

NEW
LOW
COST

made possible by widespread response to this service.

Subscriptions
(for calendar year only)

United States and Canada

$ 15 1st Class Postage

Elsewhere

$ 15 Printed Matter Postage or **$ 19** 1st Class Postage

Airmail rates on request.
Formerly $ 20 U.S. and Canada (1st class postage), $ 30 elsewhere (airmail postage).

NUCLEAR DATA CARDS

Prepared by the Nuclear Data Group, National Research Council; K. Way, director, C. L. McGinnis, editor, G. H. Fuller, D. N. Kundu, M. Yamada

with the cooperation of an international group of nuclear scientists.

The Nuclear Data Cards give in a prompt and convenient form new experimental results on the energies, spins, and moments of nuclear levels as found from the study of nuclear reactions and of the decay of radioactive nuclei.

Monthly card sets consist of about 150 3-by-5 inch cards ordered first by *Z* and then by *A*.

A limited number of 1956 card sets is available at the above prices. The supply of the 1954 and 1955 card sets is exhausted.

Order from: Publications Office, National Academy of Sciences-National Research Council, 2101 Constitution Ave., Washington 25, D. C. Payment should accompany order (check, money order, international draft, international money order, or UNESCO book coupons).

Editorial Board

K. B. Adams
E. Amaldi
H. L. Anderson
K. T. Bainbridge
C. J. Bakker
P. R. Bell
R. E. Bell
S. de Benedetti
A. Berthelot
H. Brinkman
G. von Dardel
M. Deutsch
W. Gentner
P. C. Gugelot
H. Halban
O. Haxel
M. de Hemptinne
P. Huber
D. J. Hughes
S. Kikuchi
J. Koch
S. Livingston
E. M. McMillan
P. B. Moon
M. L. Oliphant
W. Paul
A. S. Rao
G. Salvini
P. Savic
P. Scherrer
C. Schmelzer
A. de Shalit
H. W. B. Skinner
R. Tangen
D. Taylor
S. du Toit
O. Wernholm
R. R. Wilson
S. D. Winter

A NEW JOURNAL

NUCLEAR INSTRUMENTS

A journal on accelerators, instrumentation and techniques in nuclear physics

EDITOR: K. SIEGBAHN
UPPSALA

It will contain

- **Original papers**
- **Short notes**
- **Survey articles**
- **Progress reports**
- **News items**
- **Book reviews**

Nuclear Instruments will be published in bi-monthly issues. It is planned to publish annually one volume of approx. 350 pages, but this may be increased to more volumes if required. Subscription price 130 sh; $ 17.00, postage free.

NORTH-HOLLAND PUBLISHING COMPANY AMSTERDAM

Subscriptions for USA are to be sent exclusively to
INTERSCIENCE PUBLISHERS, INC. - NEW YORK, N.Y.